Safety Regulation Group

Civil Aviation Authority

CAA PAPER 2008/02

Offshore Helideck Environmental Research

Part 1 – Validation of the Helicopter Turbulence Criterion for Operations to Offshore Platforms

Part 2 – Review of 0.9 m/s Vertical Wind Component Criterion for Helicopters Operating to Offshore Platforms

www.caa.co.uk

Safety Regulation Group

Civil Aviation Authority

CAA PAPER 2008/02

Offshore Helideck Environmental Research

Part 1 – Validation of the Helicopter Turbulence Criterion for Operations to Offshore Platforms

May 2009

ISBN 978 0 11792 051 4

Published May 2009

Enquiries regarding the content of this publication should be addressed to:
Research and Strategic Analysis Department, Safety Regulation Group, Civil Aviation Authority, Aviation House, Gatwick Airport South, West Sussex, RH6 0YR.

The latest version of this document is available in electronic format at www.caa.co.uk, where you may also register for e-mail notification of amendments.

Published by TSO (The Stationery Office) on behalf of the UK Civil Aviation Authority.

Printed copy available from:
TSO, PO Box 29, Norwich NR3 1GN
Telephone orders/General enquiries: 0870 600 5522
Fax orders: 0870 600 5533
www.tso.co.uk/bookshop
E-mail: book.orders@tso.co.uk
Textphone: 0870 240 3701

List of Effective Pages

Part	Section	Page	Date
		iii	May 2009
		iv	May 2009
Contents		1	May 2009
Contents		2	May 2009
Foreword		1	May 2009
Part 1	Executive Summary	1	May 2009
Part 1		1	May 2009
Part 1		2	May 2009
Part 1		3	May 2009
Part 1		4	May 2009
Part 1		5	May 2009
Part 1		6	May 2009
Part 1		7	May 2009
Part 1		8	May 2009
Part 1		9	May 2009
Part 1		10	May 2009
Part 1		11	May 2009
Part 1		12	May 2009
Part 1		13	May 2009
Part 1		14	May 2009
Part 1		15	May 2009
Part 1		16	May 2009
Part 1		17	May 2009
Part 1		18	May 2009
Part 1		19	May 2009
Part 1		20	May 2009
Part 1		21	May 2009
Part 1		22	May 2009
Part 1		23	May 2009
Part 1		24	May 2009
Part 1		25	May 2009
Part 1		26	May 2009
Part 1		27	May 2009
Part 1		28	May 2009
Part 1		29	May 2009
Part 1		30	May 2009
Part 1		31	May 2009
Part 1		32	May 2009
Part 1		33	May 2009
Part 1		34	May 2009
Part 1		35	May 2009
Part 1		36	May 2009
Part 1		37	May 2009
Part 1		38	May 2009
Part 1		39	May 2009
Part 1		40	May 2009
Part 1		41	May 2009
Part 1		42	May 2009
Part 1		43	May 2009
Part 1		44	May 2009
Part 1		45	May 2009
Part 1		46	May 2009
Part 1		47	May 2009
Part 1		48	May 2009
Part 1		49	May 2009
Part 1		50	May 2009
Part 1		51	May 2009
Part 1		52	May 2009
Part 1		53	May 2009
Part 1		54	May 2009
Part 1		55	May 2009
Part 1		56	May 2009
Part 1		57	May 2009
Part 1		58	May 2009
Part 1		59	May 2009
Part 1		60	May 2009
Part 1		61	May 2009
Part 1		62	May 2009
Part 1		63	May 2009
Part 1		64	May 2009
Part 1		65	May 2009
Part 1		66	May 2009
Part 1		67	May 2009
Part 1		68	May 2009
Part 1	Appendix A	1	May 2009
Part 1	Appendix B	1	May 2009
Part 1	Appendix C	1	May 2009
Part 1	Appendix C	2	May 2009
Part 1	Appendix C	3	May 2009
Part 1	Appendix C	4	May 2009
Part 1	Appendix C	5	May 2009
Part 1	Appendix C	6	May 2009
Part 1	Appendix C	7	May 2009
Part 1	Appendix D	1	May 2009
Part 1	Appendix D	2	May 2009
Part 1	Appendix D	3	May 2009
Part 1	Appendix D	4	May 2009
Part 1	Appendix D	5	May 2009
Part 1	Appendix D	6	May 2009
Part 1	Appendix D	7	May 2009
Part 1	Appendix D	8	May 2009
Part 1	Appendix D	9	May 2009

Part	Section	Page	Date
Part 1	Appendix D	10	May 2009
Part 1	Appendix D	11	May 2009
Part 1	Appendix D	12	May 2009
Part 1	Appendix D	13	May 2009
Part 1	Appendix D	14	May 2009
Part 1	Appendix D	15	May 2009
Part 1	Appendix D	16	May 2009
Part 1	Appendix D	17	May 2009
Part 1	Appendix D	18	May 2009
Part 1	Appendix D	19	May 2009
Part 1	Appendix D	20	May 2009
Part 1	Appendix D	21	May 2009
Part 1	Appendix D	22	May 2009
Part 1	Appendix D	23	May 2009
Part 1	Appendix D	24	May 2009
Part 1	Appendix D	25	May 2009
Part 1	Appendix D	26	May 2009
Part 1	Appendix D	27	May 2009
Part 1	Appendix D	28	May 2009
Part 1	Appendix D	29	May 2009
Part 1	Appendix D	30	May 2009
Part 2	Executive Summary	1	May 2009
Part 2		1	May 2009
Part 2		2	May 2009
Part 2		3	May 2009
Part 2		4	May 2009
Part 2		5	May 2009
Part 2		6	May 2009
Part 2		7	May 2009
Part 2		8	May 2009
Part 2		9	May 2009
Part 2		10	May 2009
Part 2		11	May 2009
Part 2		12	May 2009
Part 2		13	May 2009
Part 2		14	May 2009
Part 2		15	May 2009
Part 2		16	May 2009
Part 2		17	May 2009
Part 2		18	May 2009
Part 2		19	May 2009
Part 2		20	May 2009
Part 2		21	May 2009
Part 2		22	May 2009
Part 2		23	May 2009
Part 2		24	May 2009
Part 2		25	May 2009
Part 2		26	May 2009
Part 2		27	May 2009
Part 2		28	May 2009
Part 2		29	May 2009
Part 2		30	May 2009
Part 2		31	May 2009
Part 2		32	May 2009
Part 2		33	May 2009
Part 2		34	May 2009
Part 2		35	May 2009
Part 2		36	May 2009
Part 2		37	May 2009
Part 2		38	May 2009
Part 2		39	May 2009
Part 2		40	May 2009
Part 2		41	May 2009
Part 2		42	May 2009
Part 2		43	May 2009
Part 2		44	May 2009
Part 2		45	May 2009
Part 2		46	May 2009
Part 2		47	May 2009
Part 2		48	May 2009
Part 2		49	May 2009
Part 2		50	May 2009
Part 2		51	May 2009
Part 2		52	May 2009
Part 2		53	May 2009
Part 2		54	May 2009
Part 2		55	May 2009
Part 2		56	May 2009
Part 2		57	May 2009
Part 2		58	May 2009
Part 2		59	May 2009
Part 2		60	May 2009
Part 2	Appendix A	1	May 2009
Part 2	Appendix A	2	May 2009

Contents

Part 2 – Review of 0.9 m/s Vertical Wind Component Criterion for Helicopters Operating to Offshore Platforms

Executive Summary

Foreword

The research reported in this paper was funded by the Safety Regulation Group of the UK Civil Aviation Authority and the Offshore Safety Division of the Health and Safety Executive, and was performed by BMT Fluid Mechanics Limited with support from QinetiQ Bedford and GE Aviation. The work follows on from the research to develop a helicopter turbulence criterion for operations to offshore platforms reported in CAA Paper 2004/03, itself commissioned in response to a recommendation (10.2 (i)) that resulted from earlier research into offshore helideck environmental issues reported in CAA Paper 99004.

Part 1 of this paper covers the validation of the turbulence criterion as recommended in CAA Paper 2004/03 (Recommendation 3). The main outcome of the exercise was that the turbulence criterion is considered to have been validated, albeit at a lower value than that originally determined (1.75 m/s Std. Dev. of the vertical component, versus the initial value of 2.4 m/s). Accordingly, the criterion was added to CAP 437 in the 6th Edition published in December 2008. A secondary outcome was the development of a turbulence mapping capability for implementation in helicopter operations monitoring programmes (HOMP). This was fully briefed to the helicopter operators at the 16th April 2008 meeting of the Helicopter Management Liaison Committee (HMLC), and CAA is actively encouraging its implementation and use. This facility will enable helicopter operators to validate and refine existing operating restrictions, and to monitor for changes on a continuous basis. An incident early in 2008 at a North Sea platform illustrated the potential hazards of unannounced modifications to platform topsides which continuous monitoring via HOMP would likely have detected at lower wind speeds where helicopters would not have been exposed to excessive turbulence. This would enable the early implementation of mitigating actions, helping to avoid serious incidents or accidents.

Regarding Part 2 of this paper, the review of the 0.9 m/s vertical flow criterion in CAP 437 found no evidence of any link between vertical flow and helicopter performance or handling hazards. As recommended in Part 2 of this paper, the industry has been consulted with a view to removing the criterion from the CAP 437 guidance material. Specifically, this work was presented to the industry Helideck Certification Agency (HCA) NNS Helideck Steering Committee meeting held on 05 December 2007, where it was agreed that the 0.9 m/s criterion be removed once the turbulence criterion was in place. This change was implemented when CAP 437 was updated to the 6th Edition, published in December 2008.

Safety Regulation Group
May 2009

INTENTIONALLY LEFT BLANK

Part 1 – Validation of the Helicopter Turbulence Criterion for Operations to Offshore Platforms

Executive Summary

This report describes a two-phase project conducted in response to recommendations contained in the final report on the development of a turbulence criterion for safe helicopter operations to offshore helidecks [1]. The overall objective of the work was to use data from the Helicopter Operations Monitoring Programme (HOMP) to seek operational validation of the turbulence criterion developed in [1].

The development of the turbulence criterion was based on a pilot workload predictor that estimates a handling qualities rating (HQR) using pilot control actions as input. The predictor had been developed using relatively high sample rate data, and was based on a flying task of maintaining a fixed position hover. Phase 1 of the work designed the filtering and windowing required to adapt the predictor to cope with complete approaches, and verified that the resulting algorithm would work satisfactorily at the lower sampling rate of the HOMP data. Data from the earlier flight simulator trials and example data from HOMP were used in the design and specification of the revised pilot workload algorithm.

In Phase 2, the adapted algorithm was implemented and tested in the HOMP data analysis system. A 16 month archive of HOMP data containing some 13,000 helideck landings was then analysed, and the statistics of maximum pilot workload experienced during each approach and landing were analysed and interpreted. The plots of maximum workload for each platform were compared with operational experience as evidenced by turbulence warnings in the Helideck Limitations List [2]. For five platforms it was also possible to compare the pilot workload plots with measurements of vertical turbulence made in wind tunnel tests.

It was found that in most cases the wind speed and direction causing high pilot workload compared well with the warnings of turbulent conditions found in the HLL. In the case of two platforms where no turbulent sectors have hitherto been defined, it is recommended that consideration be given to adding turbulent sectors to the HLL entries based on the workload patterns seen in the HOMP data. The HOMP workload data also agreed well with the wind tunnel aerodynamic data for the five platforms for which the comparison was possible, and this represents the most direct validation of the turbulence criterion.

The provisional turbulence criterion specified in the guidance was set at 2.4 m/s based on the pilot workload boundary between safe and unsafe flight of HQR=6.5. The criterion made no allowance for flight in reduced visual cueing conditions, or for the less able or less experienced pilot. When the HOMP database was analysed it was found that only one of the 13,000 helideck landings had violated the HQR=6.5 criterion. It is recommended, therefore, that the turbulence criterion of standard deviation of the vertical component of airflow be reduced to 1.75 m/s (equivalent to a pilot workload of HQR=5.5), and that the guidance material [3] should be amended accordingly.

It is also recommended that routine analysis of HOMP data should include the monitoring of pilot workload, and that this should be used to continuously inform and enhance the quality of the HLL entries for each platform. It is recommended that a pilot workload event threshold lower than HQR=5.5 should be set in order to capture a range of higher workload events. This process should also alert helicopter operators to any unexpected changes in the helideck environment caused, for example, by modifications to platform topsides or combined operations. Operators should also look for turbulence reports from pilots that occur at low workload values, because these might indicate that the turbulence criterion has been set too high.

INTENTIONALLY LEFT BLANK

Part 1 – Validation of the Helicopter Turbulence Criterion for Operations to Offshore Platforms

1 Introduction

The scope of work described in this report was conducted in response to recommendations contained in the final report on the development of a turbulence criterion for safe helicopter operations to offshore helidecks [1][1]. The previous work of [1] is briefly summarised in Section 2.

The relevant parts of the recommendations of [1] were as follows (numbering as per original):

> 2. *Reanalyse the predictors used to estimate HQR from pilot control activity using all the data available from the BRAE02 trial in order to derive coefficients of improved reliability for future general use.*
>
> 3. *Seek validation of the entire modelling process and the limiting turbulence criterion against operational experience by means of:*
>
> b. *Implement the optimised HQR predictors (see recommendation 2 above) in the Helicopter Operations Monitoring Programme (HOMP) analysis, apply the analysis to the HOMP data archive and compare the resulting turbulence mapped around offshore installations with turbulent sectors.*
>
> c. *Use the analysis performed in (b) above to identify specific severe turbulence events in the HOMP data archive, establish the turbulence levels likely to have been experienced from the associated wind conditions and wind tunnel data for the platforms concerned, and correlate this with the workload values obtained from the HOMP analysis.*
>
> 5. *In the longer term, use data collected from the full-scale implementation of HOMP and optimised HQR predictors (see recommendation 2 above) to routinely map HQR around offshore installations, and make this information available to BHAB Helidecks[1] to help improve and maintain the quality of the IVLL[2] [2].*

1. Now Helideck Certification Agency (HCA)
2. Now the Helideck Limitations List (HLL)

A two-phase programme of work was defined in order to address these recommendations. The work was performed by BMT Fluid Mechanics (BMT) supported by subcontractors QinetiQ, and Smiths Aerospace[2].

2 Background

A turbulence criterion for safe helicopter operations to offshore helidecks has been developed and reported in [1]. The work arose as a result of a wide-ranging research project into the environment around helidecks [4], and a key recommendation from that research was that a criterion for turbulence should be developed to complement existing criteria for vertical flow and temperature rise.

1. References are listed in Section 17.
2. Now GE Aviation.

Piloted flight simulation trials using three qualified and experienced test pilots were used to establish a relationship between turbulence (measured in terms of the standard deviation of the vertical velocity) and pilot workload (or handling qualities rating, HQR). Pilot workload was defined in terms of the well-known Cooper-Harper rating scale [5] shown in Figure 1.

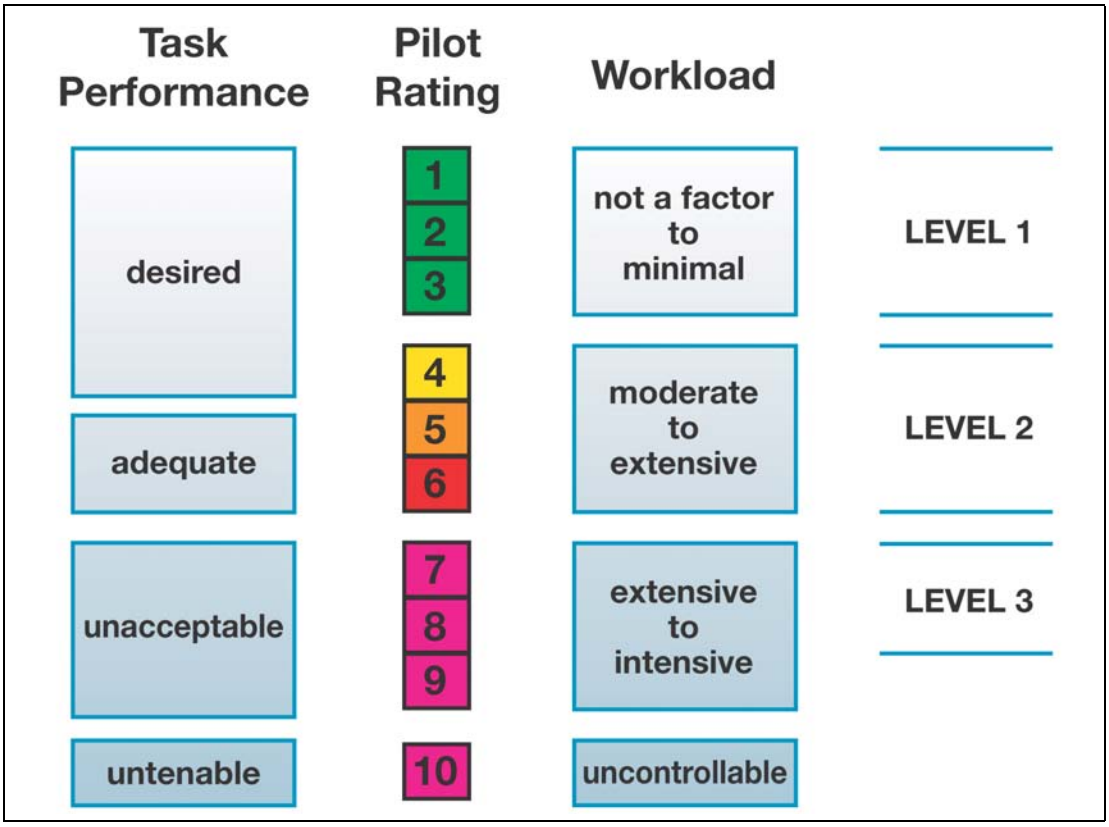

Figure 1 Cooper-Harper workload rating scale

The implicit assumption in this work was that the Cooper-Harper handling qualities rating scale could be used as an inverse measure of safety. That is, the higher the pilot workload or HQR, then the lower the margin of safety.

Due to the lack of any existing suitable data, it was necessary to conduct a series of wind tunnel tests on an offshore platform in order to generate the wind flow data required for the simulations. The tests were performed in flow conditions with a realistic representation of the atmospheric boundary layer found at sea. The BMT Fluid Mechanics Boundary Layer Wind Tunnel was used for these tests. This facility has a long working section and incorporates special features to model the variation in mean wind speed with height and the level of naturally occurring turbulence.

A 1:100 scale model of the North Sea Brae A was rotated on a turntable in the wind tunnel to generate a range of wind directions. These directions were chosen so that the flow was sampled when the helideck was upwind and unobstructed, and also when it was downwind of identifiable obstructions to the wind flow such as the drilling derricks, or gas turbine exhaust stacks.

The results from hot wire probe measurements made during the tests provided a 3-axis turbulent environment with realistic spatial variation in mean velocity and turbulence. These wind tunnel data were processed to provide time histories of both velocity and velocity gradients at the rotor hub. The distribution of vertical flows over the rotor disc was allowed to vary linearly in both longitudinal and lateral directions, thereby enabling the interaction of the helicopter with the airflow to be more accurately modelled.

Using this data, complete approaches could be flown in the simulator in a representative turbulence field. The pilots all commented that the result was the most realistic simulation of flight in turbulence in close proximity to an offshore platform that they had experienced. It did not exhibit the usual 'plank-like' characteristics evident in simulations where the entire rotor disc is subjected to the same wind flow.

The flight simulation facility was the Advanced Flight Simulator (AFS) at the QinetiQ site in Bedford, UK. For the purposes of the work a visual database representing the Brae A platform was produced with sufficient photo texturing to allow the pilot, as closely as possible, to use the same control strategies as for real world. Figure 2 shows a typical view from the visual database.

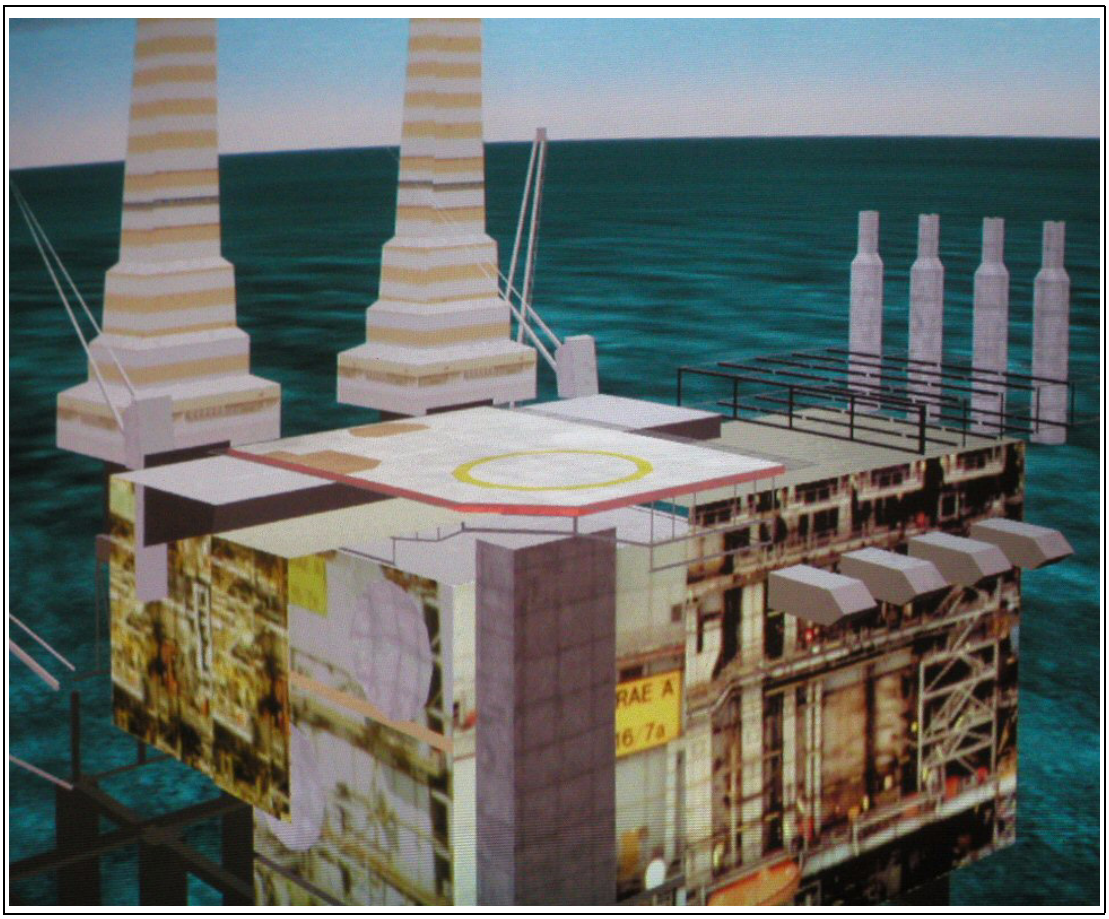

Figure 2 Platform Brae-A visual database as used for simulator trials

The helicopter used in these trials was a representation of an S-76. Sufficient design data were not available for a completely authentic model, and so a model with S-76-like features was developed (and referred to as S-76X).

Figure 3, taken from [1], shows the correlation between the test pilot awarded HQRs and the vertical component of turbulence. Using the assumption that workload is excessive and safety margins too low for cases where HQR>6.5, the turbulence criterion based on the HQR ratings from all three test pilots was that the standard deviation of vertical airflow velocity should be less than 2.4 m/s.

The report on the work [1] recommended that the turbulence criterion be validated using data from the Helicopter Operations Monitoring Programme (HOMP) prior to adoption. This report covers the validation exercise performed in response to this recommendation.

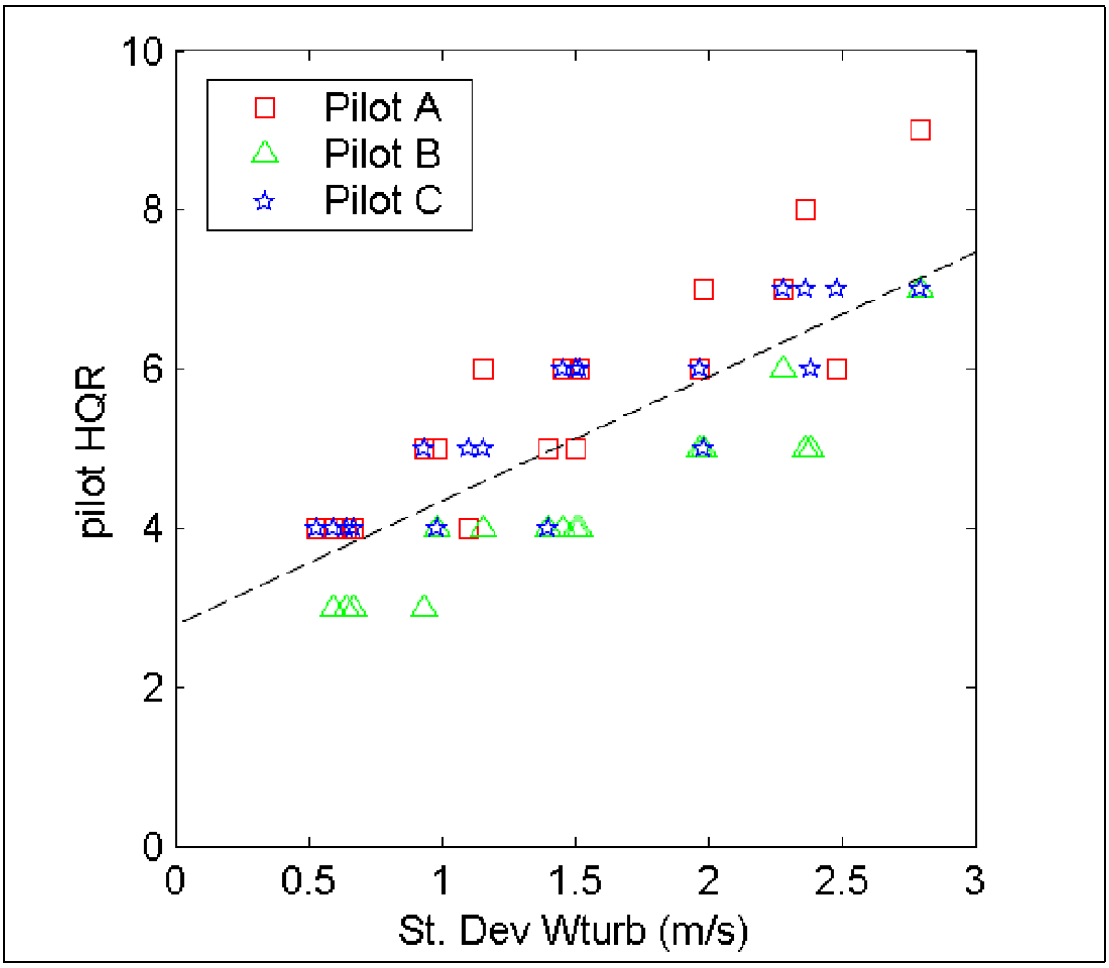

Figure 3 Pilot HQR plotted against standard deviation of vertical flow [1]

3 Objectives

The two-phase programme of work had the following objectives:

3.1 Phase 1 Objectives

a) To check that the workload predictor will function at the lower sampling rates available with HOMP data. (See Section 5)

b) To develop a modified pilot workload algorithm for application to helicopter control records for complete approaches. (See Sections 7.1 to 7.3)

c) To derive more reliable workload predictor coefficients by utilising all the available piloted flight simulation data. (See Sections 6.1 to 6.2)

d) To validate the modified workload algorithm against the original version using existing computer and flight simulation data. (See Section 7.4)

e) To specify the modified algorithm to enable it to be programmed into the HOMP system in Phase 2. (See Section 7.2 and Appendix A)

3.2 Phase 2 Objectives

a) Implement the modified workload algorithm in the HOMP data analysis system. (See Section 10)

b) Use analysis of the HOMP data archive to validate the workload algorithm. (See Sections 12 and 13)

c) Deliver the modified HOMP software to the helicopter operators. (See Recommendations in Section 15)

4 The Pilot Workload Predictor

The basic pilot workload predictor was developed in earlier work, and is fully documented in [1].

4.1 Pilot Workload

For the purposes of discussing workload, the pilot has two main tasks at any one time. The first is the guidance of the helicopter to the desired location in space and time. The second is to compensate for external influences and the inherent instability of the aircraft. The first of these two tasks is not generally considered to be a major driver of pilot workload, but the second increases workload when the helicopter experiences increasing amounts of turbulence.

The pilot workload predictor was developed around the flying task of maintaining a fixed position hover in turbulence and was thus based on control activity, and hence workload, comprising stabilisation type inputs with little or no guidance activity. In contrast, flying an approach to a helideck involves a number of changes to flight path and flight conditions and hence includes both guidance and stabilisation activity.

The fundamental hypothesis upon which workload prediction is based is that the pilot's control activity is a reliable indicator of his perceived workload. It is known that other factors impinge on the pilot's assessment of workload. For instance, a degradation of the visual environment in which the pilot is operating affects his control strategy. Some of these factors are believed to be represented in increased control activity. This has not been quantified or identified at this time and, therefore, an underlying assumption in this work is that the visual environment is good and does not affect pilot workload. However, the value set for the turbulence criterion has taken some account of this assumption (see Section 13).

Sections 4.2 to 4.4 below summarise and review the analysis of the test pilots' control movements recorded during the QinetiQ simulator-based trials, and reported in [1].

4.2 Data Summary

The Cooper-Harper Handling Qualities Rating (HQR) scale (Figure 1) was employed to quantify workload. A structured debriefing of the pilot was undertaken to arrive at an HQR on a scale of 1-10. Three test pilots (referred to as A, B and C) performed trials in the QinetiQ Advanced Flight Simulator (AFS). After each flight the test pilot provided a workload rating derived from the Cooper-Harper decision tree. Data were available from two piloted simulations trials, BRAE01 and BRAE02, reported in [1]. The data sets gathered from these trials are listed in Table 1 below.

Table 1 Data sets gathered from piloted simulation trials in the AFS

Trial	Sortie	Pilot	Manoeuvre	No. of Runs
BRAE01	01	A	Hover	29
BRAE02	14	A	Approach	07
BRAE02	15	A	Hover	26
BRAE02	16	B	Hover	18
BRAE02	18	C	Hover	23

4.3 HQR Prediction Method

This section describes the method of calculating HQR predictors from the pilot ratings and measured control time history data (see [6] for further information).

A predictor is a coefficient vector $\boldsymbol{c}$ that relates a chosen set of metrics to the HQR awarded by the pilot. In this case, the metrics used were the standard deviation of the control input and the standard deviation of the control input rate. These metrics were calculated for the lateral cyclic control, longitudinal cyclic control, and the collective lever. The relationship between the metrics and the HQR awarded by the pilot is:

$$r = c_1 + c_2\,\sigma(\xi) + c_3\,\sigma^*(\xi) + c_4\,\sigma(\eta) + c_5\,\sigma^*(\eta) + c_6\,\sigma(\theta_0) + c_7\,\sigma^*(\theta_0)$$

where,

r = HQR awarded by pilot

$c_1 - c_7$ = predictor coefficients

ξ= lateral cyclic position

η= longitudinal cyclic position

θ_0 = collective lever position

$\sigma(x)$ = function : standard deviation of x

$\sigma^*(x)$ = function : standard deviation of first derivative of x with time

Using data from multiple runs leads to the matrix equation of the form:

$$\boldsymbol{Xc=r+e},$$

where $\boldsymbol{X}$ is the m by n matrix of the n metrics from the m runs, $\boldsymbol{r}$ is the vector of pilot HQRs, and $\boldsymbol{e}$ is an error vector. The matrix $\boldsymbol{X}$ is factored using singular value decomposition into:

$$\boldsymbol{X}=USV^H$$

where U and V are unitary matrices, S is an m by n diagonal matrix containing the singular values of X, and the superscript ^{H} denotes the conjugate transpose operator. Singular value decomposition produces singular values that are ordered in reducing magnitude. Small singular values indicate a rank deficiency (occurs when the rows or columns of a matrix are not independent, in this case related to the correlation between control time histories) in the original data, and thus there is a need to avoid over-fitting to a particular data set. Small singular values also indicate an ill-conditioned system. An ill-conditioned system is overly sensitive to small perturbations in the input.

The error is minimised in a least squares sense by:

$$\boldsymbol{c}=VS^{-1}U^H\boldsymbol{r}$$

where S^{-1} is n by m and is the inverse of S, since S is diagonal this is quite simply the inverse of the diagonal elements themselves.

A full set of coefficients can be calculated corresponding to retaining 1 to 7 singular values. For each increase in the order of the solution, the number of retained singular values is increased by one. However, the composition of each singular value in terms of raw variables will change with each successive change to the solution order, and hence the coefficients cannot be expected to be similar for different orders of solution. The trade off is between using smaller singular values to better fit the current data set and compromising any future use of the coefficients as predictors. Having determined a predictor vector $\boldsymbol{c}$, a vector of control activity metrics $\boldsymbol{m}$ is converted into the predicted HQR, $\boldsymbol{\acute{r}}$, by the product:

$$\boldsymbol{\acute{r}} = c^t m$$

4.4 Predictor Coefficients derived during Validation Trials

The full set of predictor coefficients (as originally processed at Glasgow Caledonian University (GCU) [1]) is presented in Table 2. These predictor coefficients were calculated from the pilot ratings and measured control activity from the BRAE01 trial data. The order five set of predictor coefficients are highlighted in Table 2, as this set was used for the workload predictor in the validation exercise reported in [1]. For each increase in the order the number of retained singular values is increased by one. Since there are six metrics and one constant term in the workload predictor there are a total of seven singular values. There are no hard and fast criteria for determining how many orders should be selected - the choice, instead, is one requiring judgement. On the basis of quality of fit, the final choice was between orders 4 and 5. Order 5 was chosen as it gave a better fit to the higher workload cases.

Table 2 Original predictor set for trial BRAE01 (obtained from GCU analysis)

Order	1	2	3	4	5	6	7
c_1	4.1832	1.8924	1.8978	2.0971	**2.1238**	1.3434	0.7878
c_2	0.2434	1.0325	1.4531	1.5840	**0.6240**	9.7234	46.5698
c_3	1.1954	6.0130	7.4460	7.5999	**7.2237**	5.9211	-2.3776
c_4	0.1961	0.7600	0.3611	0.3568	**-0.7879**	65.4232	60.3412
c_5	0.9879	4.4560	2.5453	2.2804	**0.8214**	-12.4400	-9.6098
c_6	0.3168	-0.3030	0.1992	-1.4695	**-4.7042**	-5.2539	-5.1046
c_7	0.3875	1.1395	1.0590	0.3926	**8.8116**	16.2860	19.9755

5 Application of Pilot Workload Predictor to Low Sample Rate Data

The first objective of Phase 1 was to check that the workload predictor continued to function adequately when applied to data of a lower sampling rate than that used in its development. This was in anticipation of the application of the predictor to HOMP data, which is recorded at sample frequencies of 2 to 4 Hz as opposed to the 20Hz sample rate used in the simulator work.

As an initial step, the original predictor was applied to simulator data with a reduced sample rate to assess the effect on the predicted HQRs. The data used were those from trial BRAE02, providing control movements and pilot HQRs using three different pilots (A, B, C) conducting the hover task. Workload estimates for all pilot data were calculated using three sampling rates – 20Hz, 4Hz and 2Hz.

This part of the work addressed objective a) stated in Section 3.1.

5.1 Results

Figure 4 to Figure 6 show a comparison of predicted workloads with pilot HQRs for the three sampling rates for each pilot in turn. The 20Hz data reproduce the results given in Table O-1 of ref [1]. For all three pilots, as the sample rate reduces, so does the estimate of workload, especially where the workload is high. This is particularly noticeable in the results for pilot B in Figure 5.

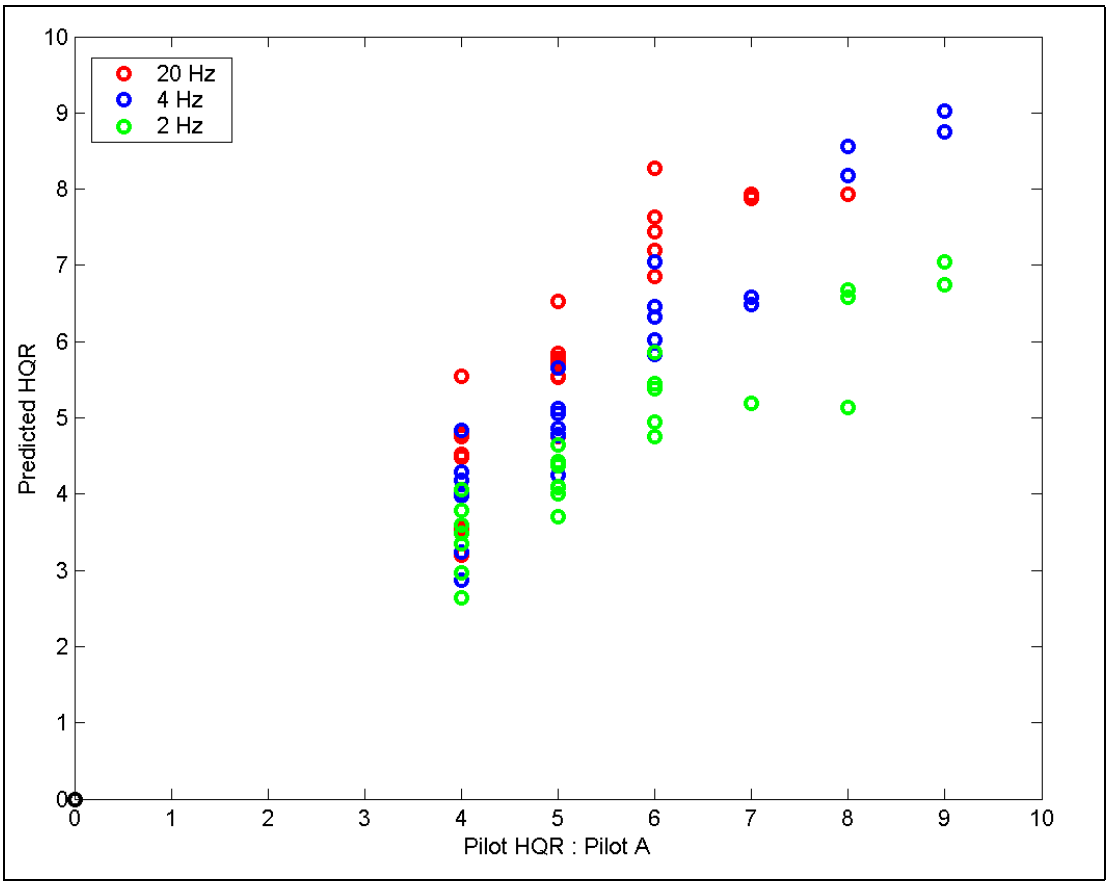

Figure 4 HQR predictions for pilot A data at 20Hz, 4Hz and 2Hz

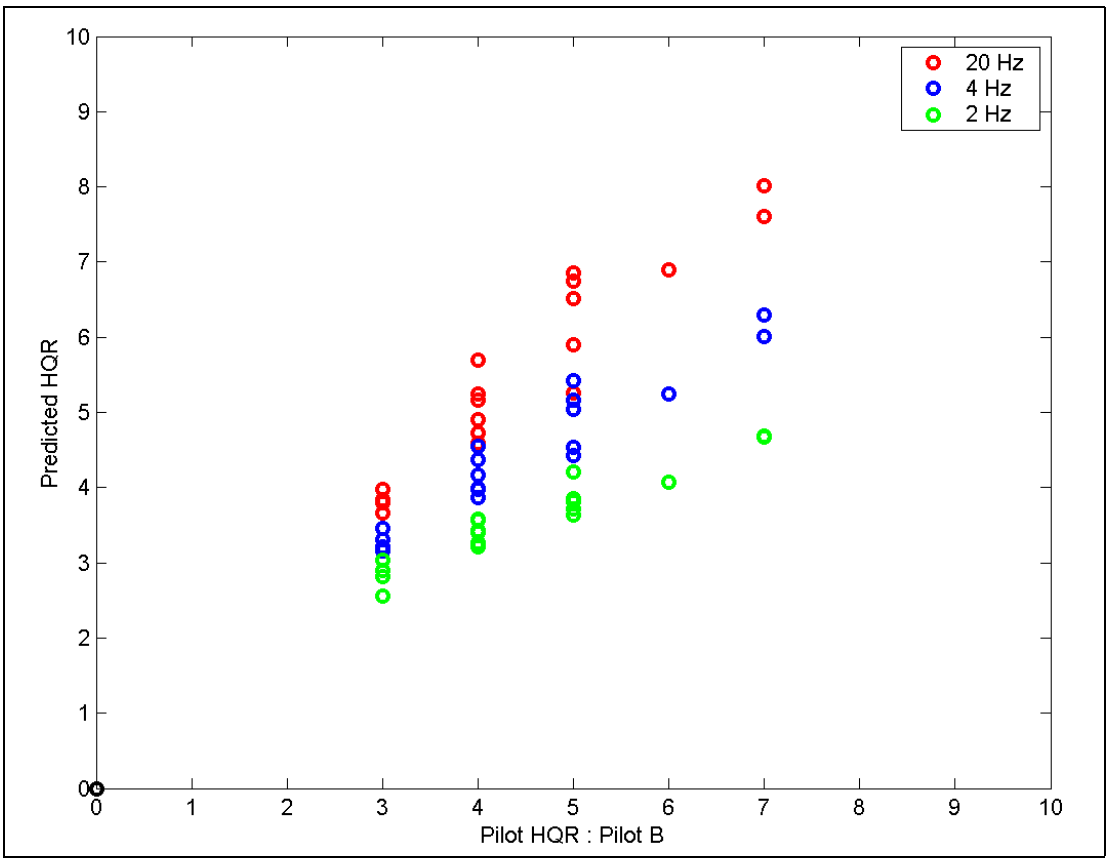

Figure 5 HQR predictions for pilot B data at 20Hz, 4Hz and 2Hz

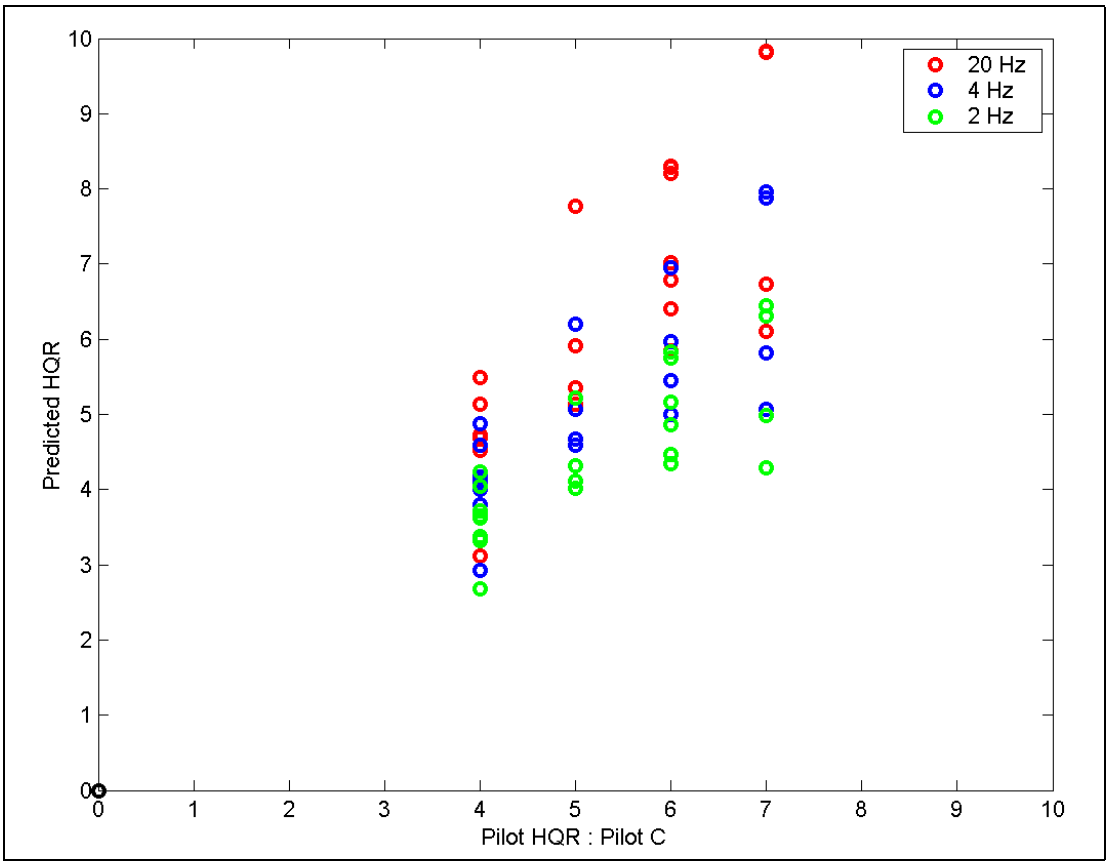

Figure 6 HQR predictions for pilot C data at 20Hz, 4Hz and 2Hz

Figure 7 to Figure 9 show how the workload predictor parameters vary between the results from 20Hz and 2Hz for pilot A, B and C respectively. Ignoring the constant offset (2.1238) there are six parameters in the workload predictor, three based on standard deviation of control positions, and three based on the standard deviation of the control rates. In each figure the left hand graph relates to control position and the right hand graph to control rate. The vertical axis gives the parameter values from the 2Hz data and the horizontal axis gives the same parameter from the 20Hz data.

Each point on each graph is generated from analysis of a single time history and is the appropriate standard deviation multiplied by the magnitude of the associated coefficient in the workload predictor. The dashed line represents a one-to-one correlation between 2Hz and 20Hz results. It is clear that the calculation of standard deviation of control position is unaffected by the reduced sampling rate whereas the standard deviation of control rate is underestimated in all cases. This is most apparent for lateral and longitudinal cyclic with the collective only marginally affected. Overall, the reduced sampling rate does have a significant effect on the calculation of standard deviation of control rate data.

The reduced sampling of the data has clearly caused some of the features of the control activity to be lost. The nature of this effect is that the gradients of control position i.e. the rates as used in the workload predictor, are more likely to be lower with a lower sampling rate.

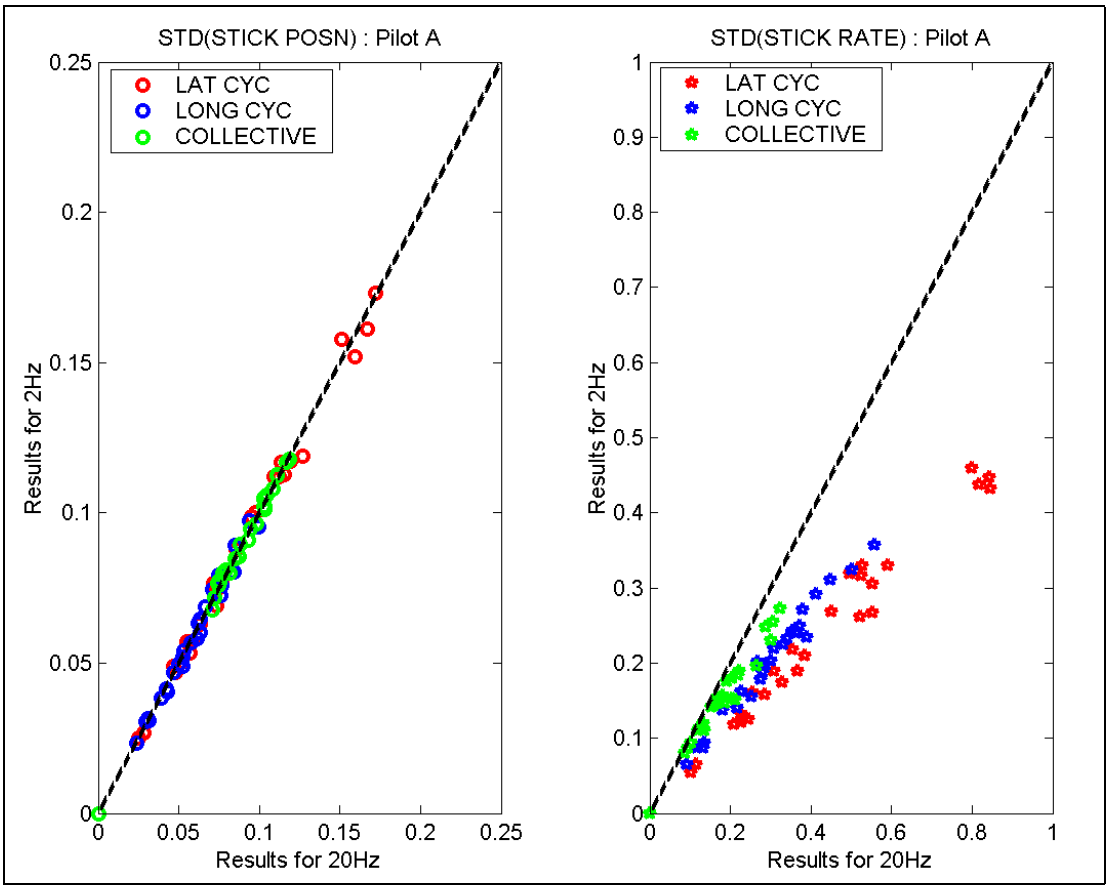

Figure 7 Comparisons of factored standard deviations from 20Hz and 2Hz - pilot A

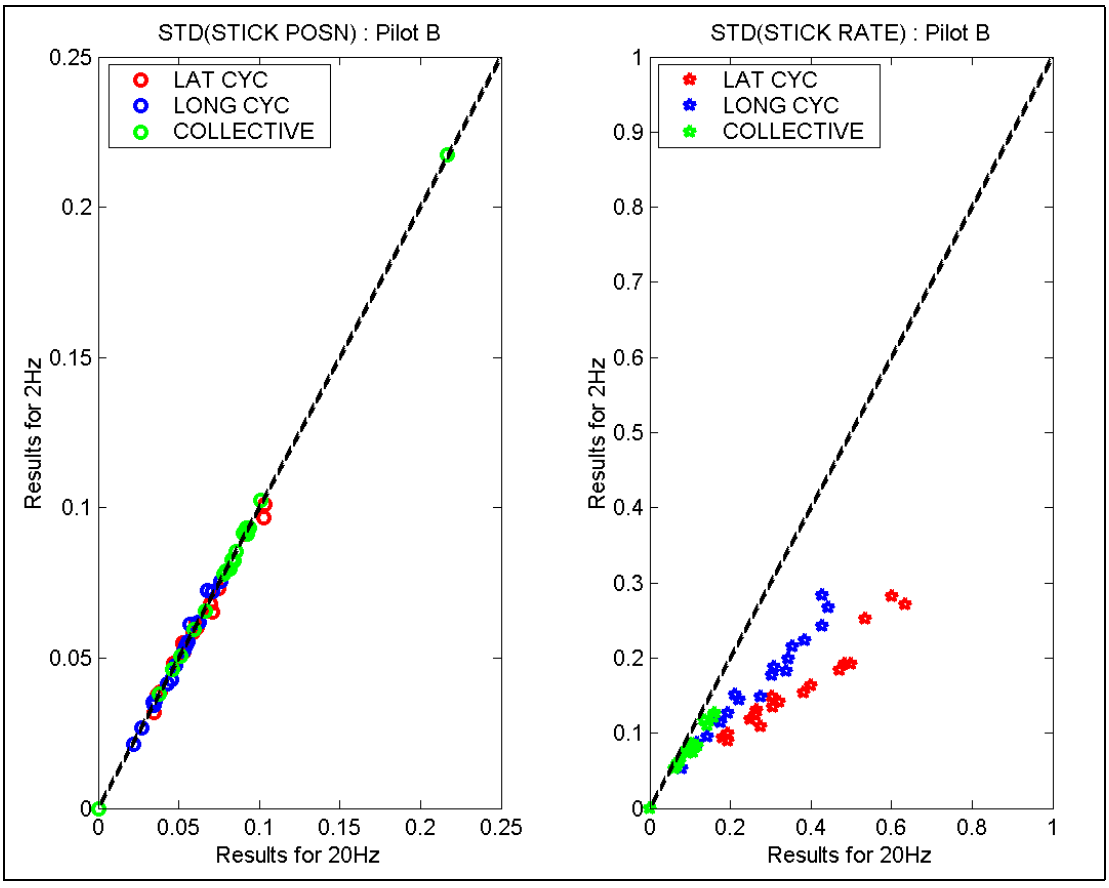

Figure 8 Comparisons of factored standard deviations from 20Hz and 2Hz - pilot B

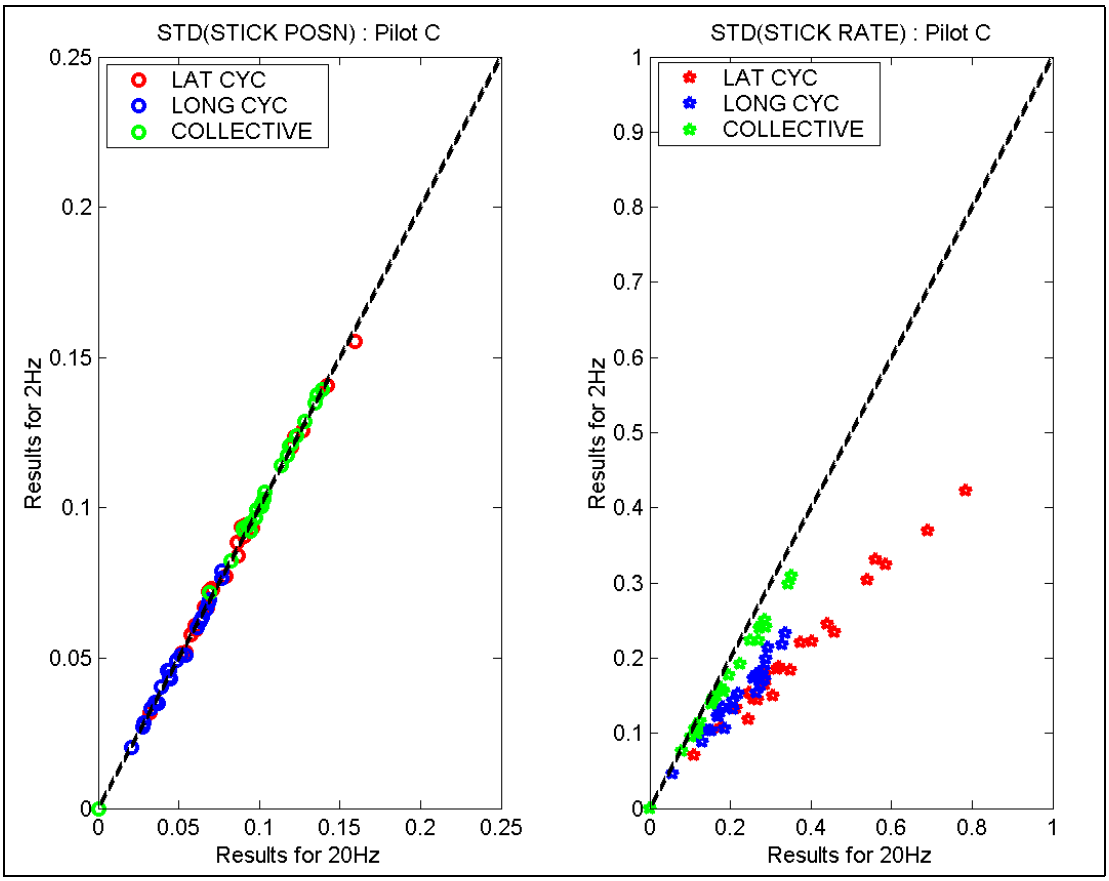

Figure 9 Comparisons of factored standard deviations from 20Hz and 2Hz - pilot C

Figure 10 shows the overall quality of the HQR predictions for all pilots using data at 20Hz, 4Hz and 2Hz. The first graph, generated with 20Hz data, is equivalent to Figure 4.4 of [1]. The second and third graphs show results for 4Hz and 2Hz data respectively.

Despite the fact that the reduced sampling has an effect on the analysis of control rate data, it does not affect the ability of the workload predictor to distinguish cases of high and low workload. In fact, the results from 4Hz data have a better match than those from 20Hz data due to the over prediction of workload when applied to 20Hz [3]data being opposed by the tendency of calculations using data sampled at 4 Hz to have a lower workload estimate. In this particular case the two opposing effects have cancelled each other.

3. This tendency to over-prediction of the 20Hz data is removed when the workload predictor coefficients are recalculated using all the data from the BRAE01 and BRAE02 trials.

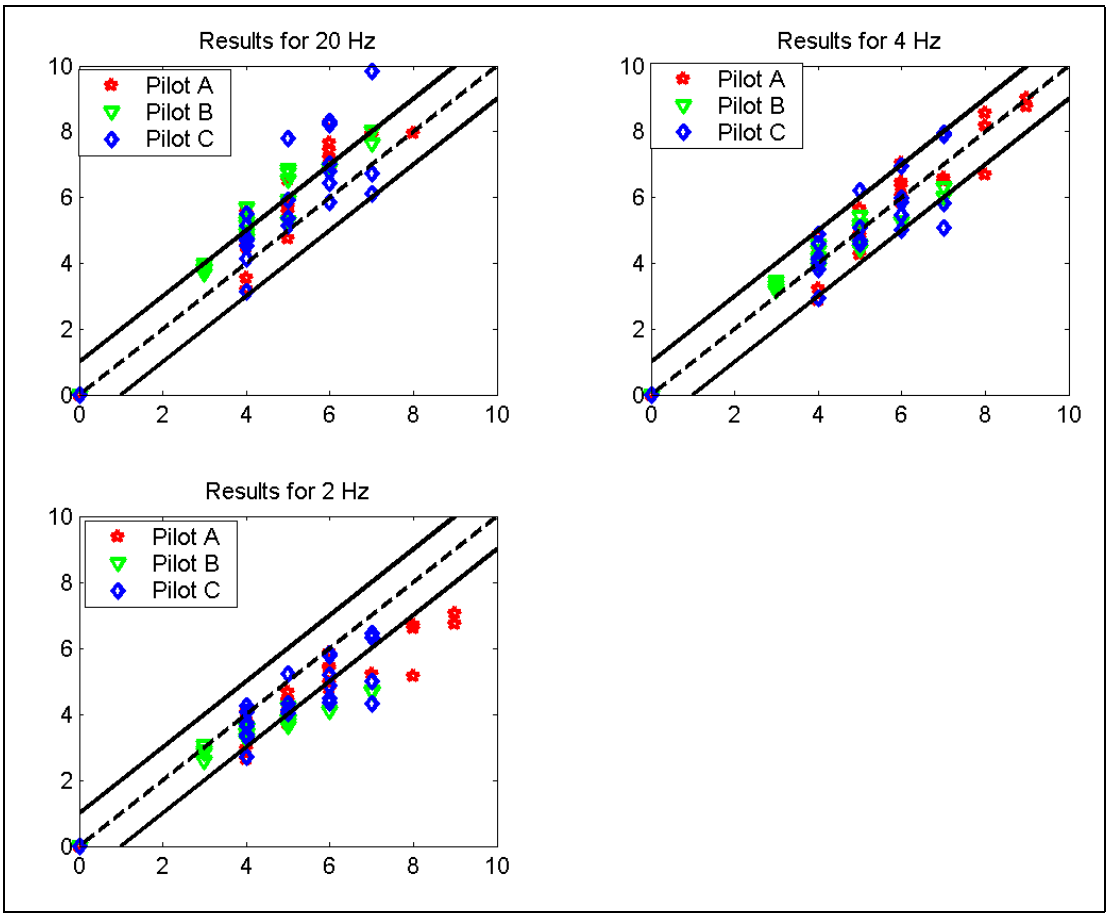

Figure 10 Overall performance of workload predictor for 20Hz, 4Hz and 2Hz

5.2 Discussion

The result of the assessment of the impact of reduced sample rate can be summarised as follows:

- The standard deviation of control position is not affected by reducing the sample rate.
- The standard deviation of control rate is significantly affected and returns lower values at reduced sample rates.
- The reduction of standard deviation of control rate is due to the aliasing of the 20Hz signal as it is reduced to a 4Hz or 2Hz signal.
- The effect on the overall performance of the workload predictor is to reduce the predicted workload.
- Despite the above, the ability of the workload predictor to distinguish between high and low workload is retained.

Given these results there were three possible courses of action:

a) Add a correction term to the workload predictor based on sampling frequency and calibrated using a number of sets of Trial BRAE02 data re-sampled at frequencies across the range 0-20Hz.

b) Produce different workload predictors based on the data sampling frequency.

c) Retain the predictor based on 20Hz data and accept that analysis of data recorded at 2-4 Hz will predict a lower workload.

The fact that the effect of sampling frequency is dependent on the exact form of the control time history may make quantifying its effect problematic, particularly for cases where either pilot or aircraft have changed. Hence action a) was not considered desirable.

The tuning of the predictor for data at specific sample frequencies, as in b), makes the predictor more complicated and introduces the potential for it to be incorrectly applied. Furthermore, it would apply a level of fine tuning that is inappropriate at this stage given that there are other more fundamental properties of the predictor (such as the effects of using it for different aircraft and control systems) which would need to be tested when the HOMP data analysis has been completed.

In view of the above, retaining the previously derived 20Hz predictor for the current study was considered to be the most appropriate way forward.

6 Update of the Workload Predictor

One of the recommendations of [1] had been that all the flight simulator data should be used to recalculate coefficients to produce an improved workload predictor. This aspect of the work was intended to address objective (c) stated in Section 3.1.

The predictors developed in [1] had been calculated by Glasgow Caledonian University (GCU), and so before recalibrating the predictor coefficients using all the data from the BRAE01 and BRAE02 trials, it was necessary to check that the original coefficients could be reproduced using QinetiQ's data and software.

6.1 Reproduction of Workload Predictor Coefficients

The predictors based on BRAE01 and re-calculated during this current work are given in Table 3.

Table 3 Full predictor set for trial BRAE01 re-calculated for current work

Order	1	2	3	4	5	6	7
c_1	4.1759	1.9158	1.9324	2.1532	**2.1792**	1.4474	1.2382
c_2	0.2455	1.0171	1.5839	1.7209	**0.7209**	10.5846	24.4932
c_3	1.2096	5.9844	7.8818	8.0511	**7.7061**	5.6636	2.5605
c_4	0.1959	0.7400	0.2311	0.2360	**-0.9217**	56.1689	53.6936
c_5	0.9865	4.3103	1.6934	1.3941	**0.0292**	-10.8481	-9.6717
c_6	0.3162	-0.2861	0.3985	-1.4381	**-4.5469**	-5.0921	-5.1356
c_7	0.3869	1.1048	1.0039	0.2671	**8.3063**	15.6116	17.0355

There are slight differences between predictors shown here in Table 3 and those given earlier in Table 2. This is due to clipping of the recorded control time history data when they were processed at GCU.

The effect on estimations of the HQR is shown in Figure 11, and seem to be quite small. The standard deviation of the error in the HQR prediction is only 0.0343 HQR points and highlights the insignificance of the effect that the small change in predictor coefficients has on workload prediction.

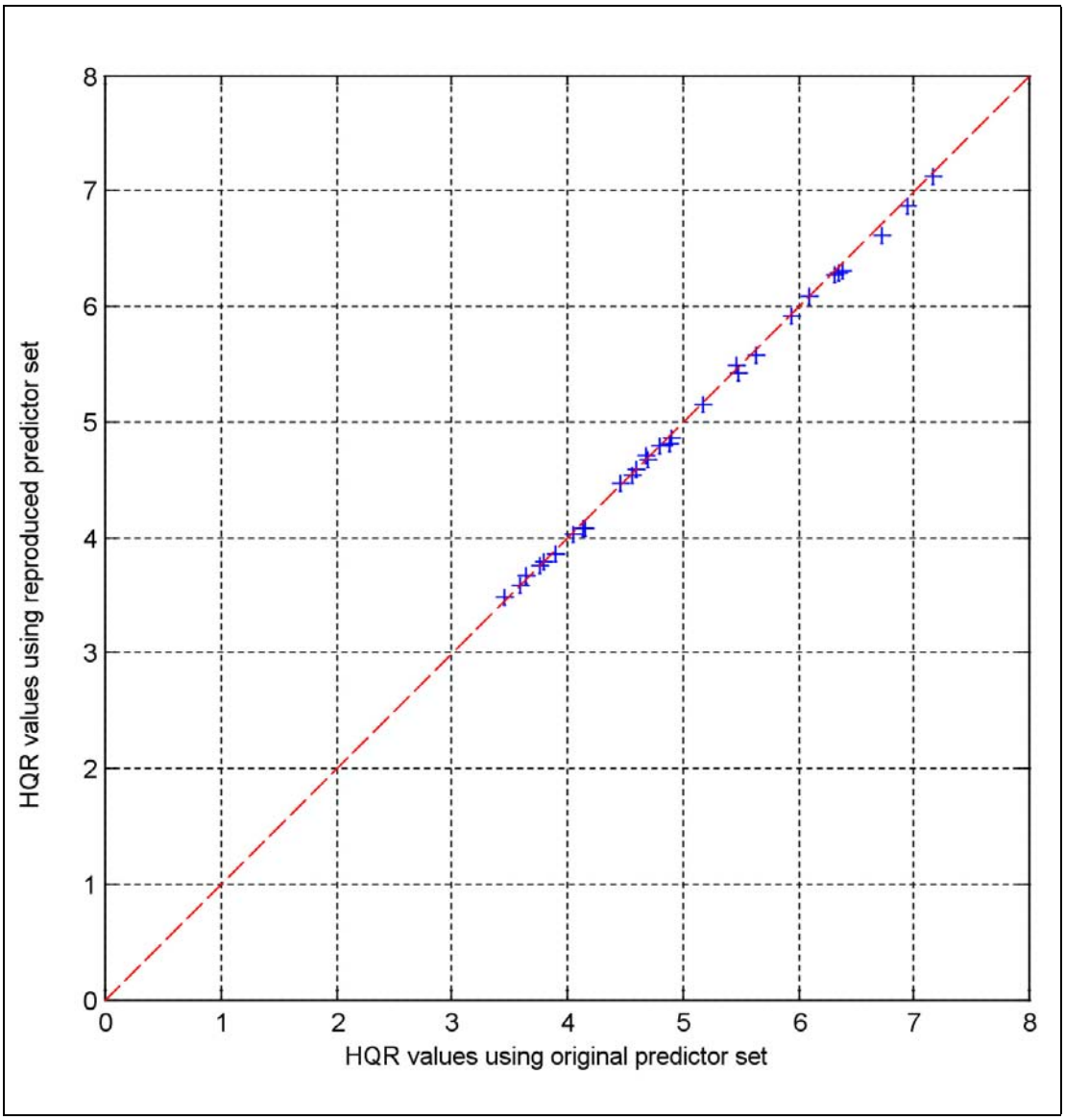

Figure 11 Workload predictions of BRAE01 using original predictor coefficients versus re-calculated predictor coefficients

6.2 Recalibration of Workload Predictor Coefficients

The workload predictor coefficients determined above were calibrated using BRAE01 data and validated using BRAE02 data. For the current work, in order to make the predictor more robust it had been recommended in [1] that the workload predictor should be recalibrated using all available data, including data from BRAE01 and the hover data from BRAE02.

Table 4 presents the resulting new predictor coefficients.

Table 4 Coefficients recalculated using both BRAE01 and BRAE02 hover data

Order	1	2	3	4	5	6	7
c_1	4.3361	2.4586	2.5070	**2.4069**	2.1231	2.0331	2.2641
c_2	0.3239	1.0041	1.2249	**1.0356**	18.5402	3.5865	-1.0695
c_3	1.4853	5.0522	4.8974	**3.9514**	0.8447	4.1494	5.0940
c_4	0.2202	0.5196	0.4390	**0.7333**	12.4763	32.6162	45.7145
c_5	1.0306	2.7132	1.5106	**2.8197**	1.8485	-2.5162	-5.1532
c_6	0.2091	0.5492	1.1153	**1.3430**	3.1070	14.8465	-12.4518
c_7	0.5901	1.8644	3.7069	**4.4501**	1.4366	-2.0655	5.8053

Order four is highlighted as the best compromise between using the highest order possible and avoiding over fitting of the data. Over fitting is indicated here by the rapid change in coefficient values between orders 4 and 5, whereas between orders 1 and 4 they follow more of a trend.

An important feature of this predictor compared to the previous ones shown in Tables 2 and 3, is that the coefficients are now all positive. This means that all of the control terms now contribute positively to the workload, which seems intuitively correct.

A further point to note is that the standard deviation of control rate coefficients are larger than those for the standard deviation of control position terms. This is consistent with general operational experience where the magnitude of control rates, and therefore the corresponding standard deviations, are greater than the magnitude of control positions. Given these two factors, it is expected that the control rate terms will contribute more to the workload prediction than the control position terms.

7 Further Development of the Workload Predictor for use with HOMP Data

7.1 Frequency Analysis

Frequency analysis was used to compare the frequency content of the hover data and approach data from the simulator trials. The difference between the sets of data is that the approach task contains guidance and stabilisation inputs and the hover task has stabilisation inputs only. The objective was therefore to remove, or at least reduce, the guidance inputs from the approach data using filters (objective 3.1(b) stated in Section 3.1).

From [7] the premise is made that guidance control movements are conducted at a relatively low rate compared to stabilisation control movements. A power spectral density (PSD) plot of control input should therefore exhibit peaks at the two frequencies corresponding to these two types of control input. The requirement, therefore, was to identify the frequency that partitioned the two peaks in the PSD plots of control time histories. Using a filter, the guidance control inputs were removed from the control time histories to leave only the stabilisation control inputs. This focused the workload predictor on the stabilisation control inputs that are the primary cause of workload for the pilot.

Figure 12 shows a PSD plot of trial BRAE02 approach data. In this figure, a peak is clearly visible in the lateral cyclic at around 0.5 Hz. At frequencies below 0.1 Hz a possible second peak is also apparent as the curve begins to rise towards lower frequencies. In contrast to the full approach spectra of Figure 12, Figure 13 shows the PSD of hover only data.

From these two plots, it is evident that there is a difference in the power of the signals below 0.1 Hz. Following on from the hypothesis that guidance control inputs are spectrally separated from stabilisation control inputs, the power in the signal below 0.1 Hz is identified as relating to guidance control inputs and the power in the signal above 0.1 Hz is identified as relating to stabilisation. From this, a cut-off frequency of 0.1 Hz was chosen to eliminate the guidance control inputs of the pilot from the control time histories.

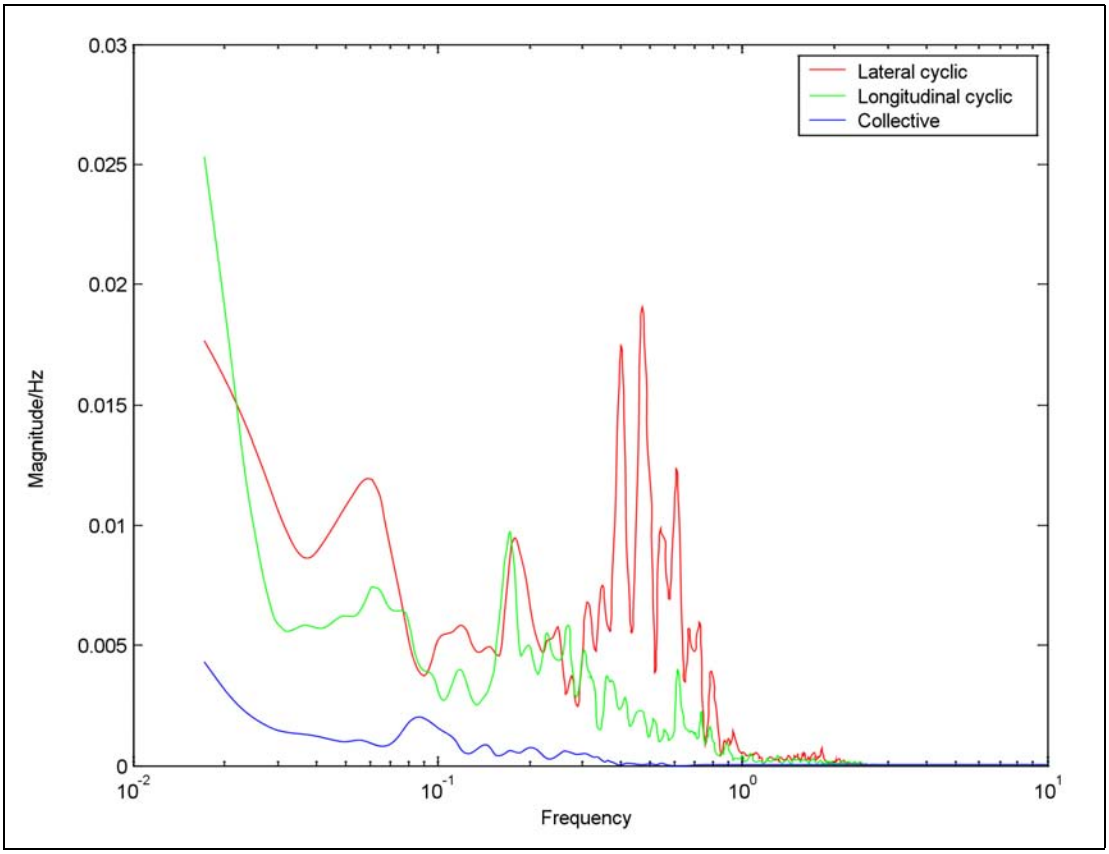

Figure 12 PSD plot of approach runs

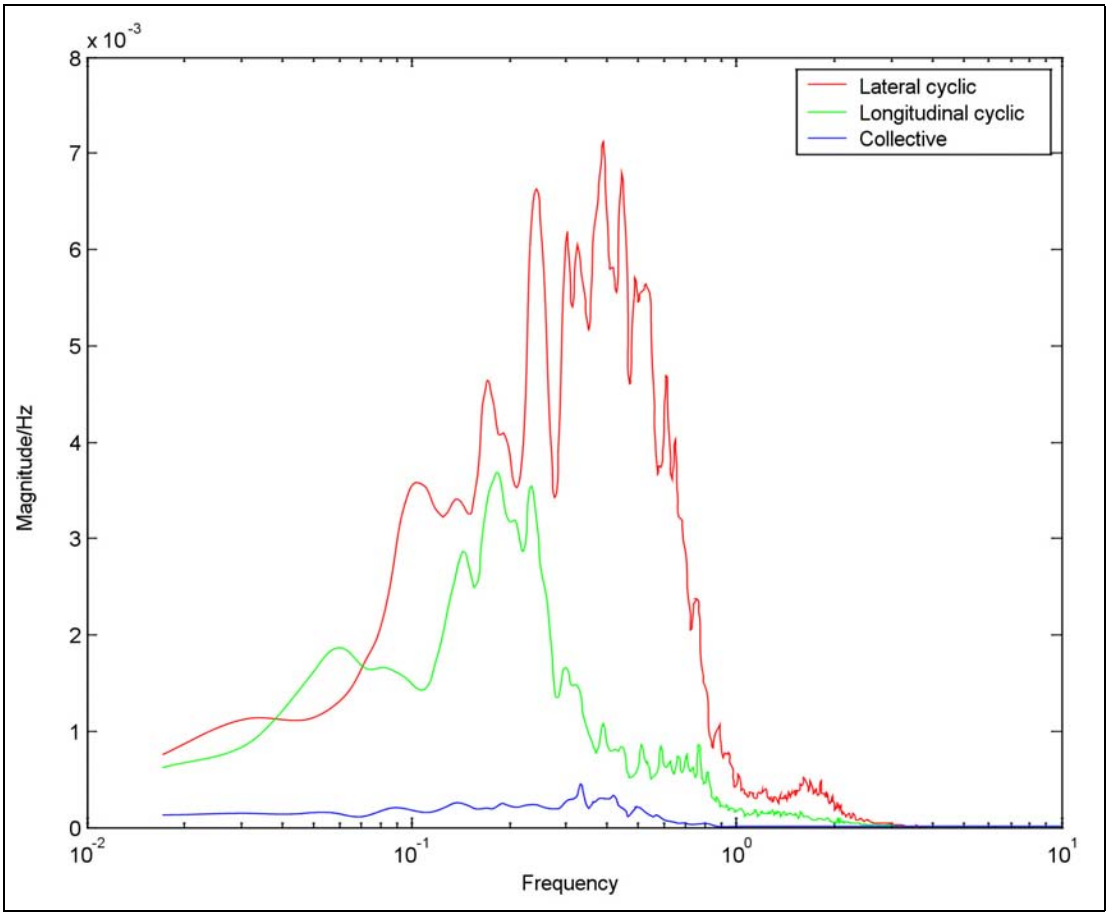

Figure 13 PSD plot of hover runs

7.2 Windowing

The re-calibrated workload coefficients of Section 6.2 were based on a statistically stationary 60-second helicopter hover over the helideck of an offshore platform. In contrast, an approach to the deck is statistically non-stationary and can last for longer (or shorter) periods than the hover task depending on, for example, the difficulty of the task, the point on the approach at which the recording is started and the wind speed. To allow the approach task to be treated as stationary, it is necessary to average the data. This requires an appropriate averaging period, or time domain window size, to be determined and applied to the control data prior to presentation to the workload predictor. By windowing the data, it is possible to equate the metrics of the approach data to the workload predictor.

The type of window implemented was a sliding 'boxcar' with the defining value calculated at the leading edge. The first values calculated were not used when the window length was longer than the available data.

Figure 14 shows the predicted HQR versus window length for windows between 0.25 seconds and 60 seconds in length, and where each line on the plot relates to a single BRAE02 trial approach run, sampled at 4Hz, with an associated HQR awarded by the pilot. From this graph, for windows of less than 10 seconds duration, the predicted HQR changes rapidly, especially for the higher HQR ratings. For window lengths of between 10 and 25 seconds, the predicted HQR has a lower rate of change. For a window length between 25 and 60 seconds, longer periods of inactivity in the control time history begin to dilute the workload prediction and the process becomes non-stationary. Further increases in window length would lead to further dilution and further decreases in the workload prediction.

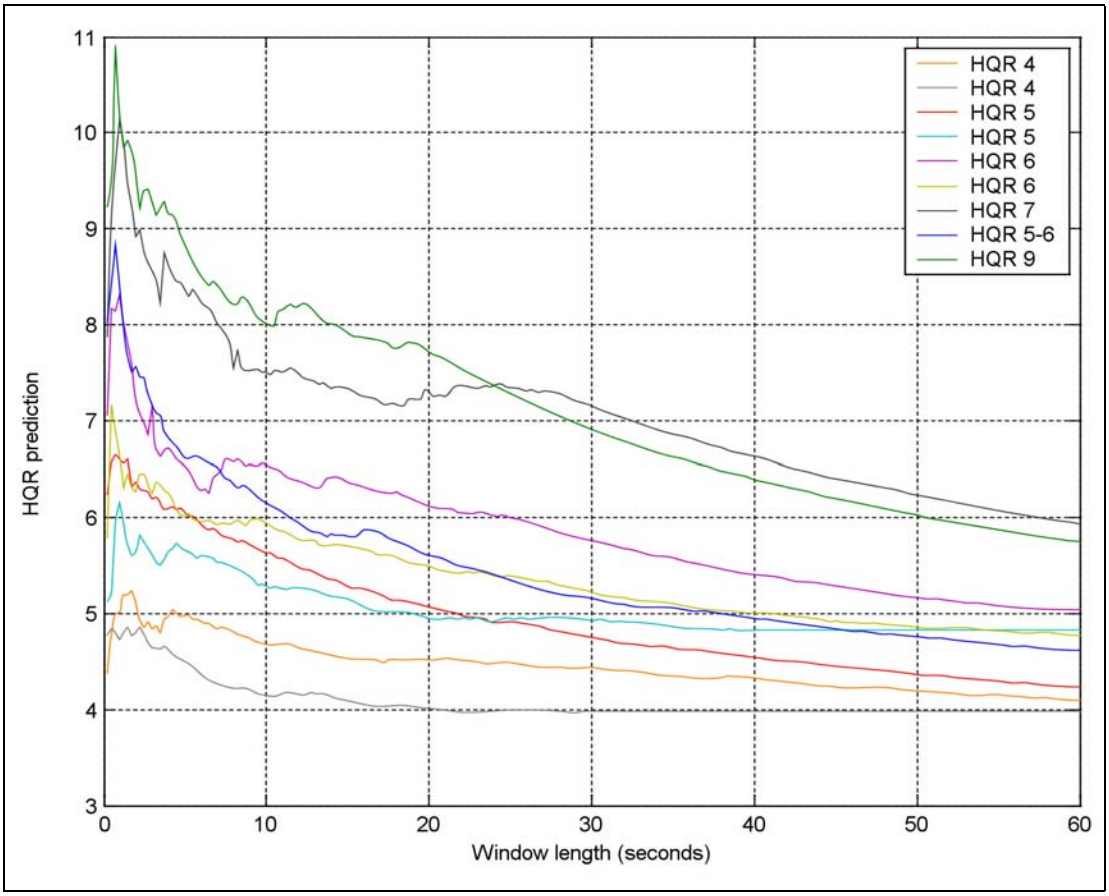

Figure 14 Workload prediction of approach data (4 Hz sample) versus window length

Figure 15 shows some statistics for the measure of fit against the window length. The characteristics on this graph are *a*, *b*, r^2, and the standard deviation of the error. These parameters arise from least squares regression. The *a* and *b* parameters are from the equation $y=ax+b$. The closer *a* is to 1 and *b* is to 0 the better the correspondence between predicted HQR and pilot derived HQR. The r^2 parameter is a measure of how well the data is represented by the associated least squares line. The closer the r^2 value is to 1 the better the data fits the least squares line. The last parameter is the standard deviation of the error. The closer this parameter is to 0 the better.

Figure 15 has three regions marked on it encompassing desired measure of fit statistics for different window lengths. Region 1 has a very good r^2 value and a low standard deviation of the error. Region 2 has *b* near 0, a good r^2 value, and the standard deviation of the error is also quite good. Region 3 has *a* near 1, a good r^2 value, and a reasonable standard deviation of the error. Both regions 2 and 3 lie in the area where the window length is greater than 25 seconds, meaning that they are affected by the non-stationary nature of the approach data. The main issue with Region 1 is the inflated value of slope, *a*. However, while not having the ideal value of 1, this will give the workload predictor an increased sensitivity to changes in control activity. Therefore, Region 1 is considered to contain the most favourable solution for the window length.

From this figure, a window length of 17 seconds was chosen on the basis that it has a high r^2 value, a low standard deviation of error. Hence, this choice of window length is in a region where the statistical parameters are insensitive to the precise choice of window length. This choice of window length has parameter values a=1.5412, b=-1.0181, r^2=0.9451, and a standard deviation of error of 0.4257 HQR points.

In calculating these statistics, the approach given an HQR of 9 in the BRAE02 trials has been omitted. The test pilot aborted this approach because he expected the flying conditions to deteriorate beyond safe flying practices. The rating of 9 was therefore given in the *expectation* that worse conditions were about to follow, and were not necessarily a true reflection of the workload actually experienced up to the point at which the approach was aborted.

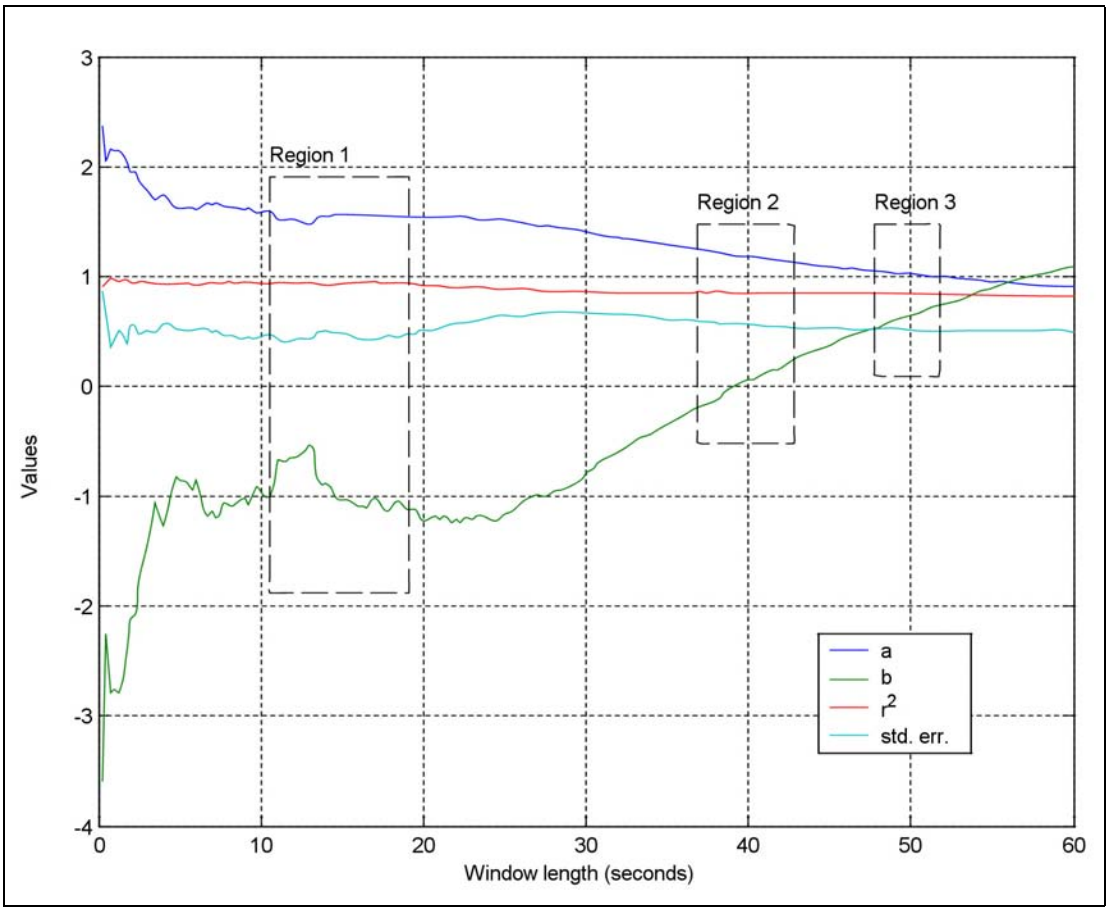

Figure 15 Measure of fit statistics versus window length

7.3 HQR predictions with Filtering and Windowing

Figure 16 shows the HQR prediction of an approach with filtering and windowing applied. The modified workload predictor has produced conservatively high predictions outside the desired limits. This is due to placing greater priority on achieving good values of r^2 and standard deviation of the error than on the fit coefficients *a* and *b*. Importantly the trend of pilot HQR against predicted HQR is well defined with little dispersion.

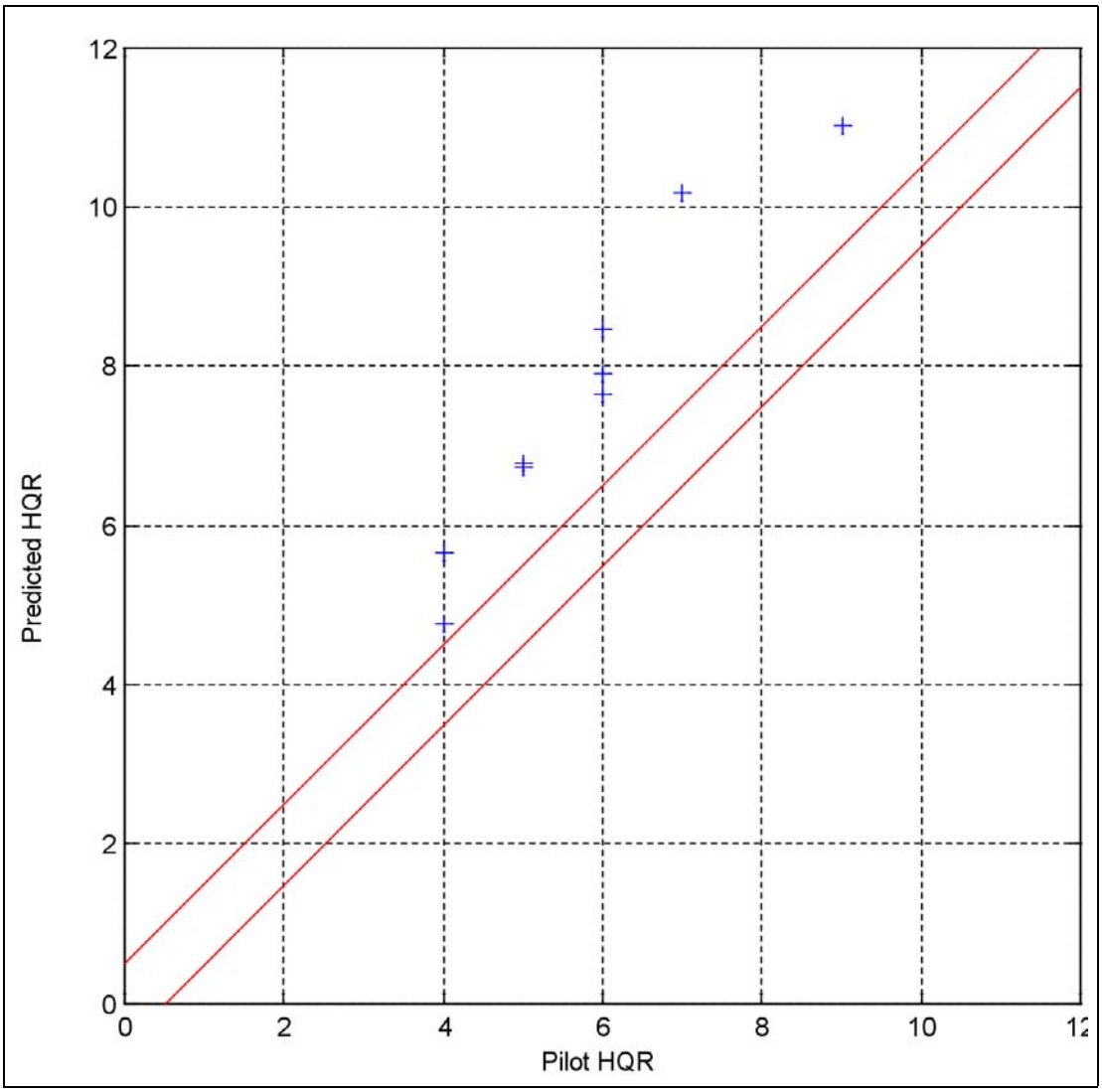

Figure 16 Approach HQR prediction with filtering and windowing versus pilot HQR with control inputs sampled at 20Hz

7.4 Hover HQR Predictions with Filtering and Windowing

The changes made by the filtering and windowing to the original predictions were examined to ensure that they did not affect the analysis (objective 3.1(d) in Section 3.1). The effect of the filtering and windowing on the hover data can be seen in Figure 17. The figure shows the filtered and windowed hover data plotted versus the original hover predictions. Differences between the two sets are evident but they are relatively small with a standard deviation of scatter of only 0.45 HQR points.

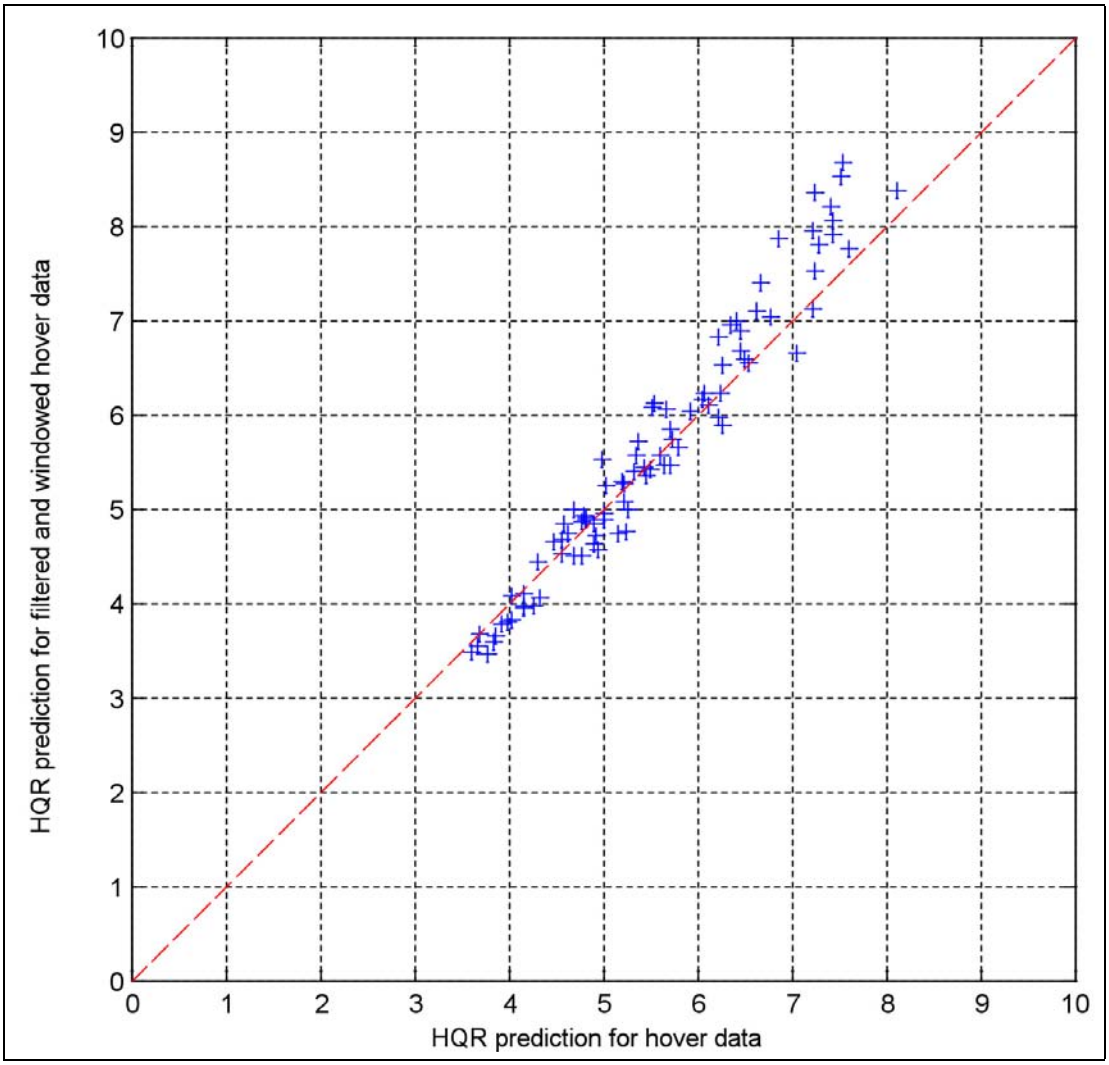

Figure 17 Hover filtered and windowed HQR predictions versus standard hover HQR predictions

8 The Significance of Automatic Flight Control Systems

8.1 Introduction

The operational data to be provided by HOMP in support of the validation of the turbulence criterion contains time histories of control activity. The control activity is measured at the helicopter swash plate, and is therefore a combination of both pilot control inputs and contributions from the Automatic Flight Control System (AFCS).

The flight simulator used to develop the pilot workload predictor also included an AFCS, but the control data comprised pilot control actions only. This inconsistency cannot be completely resolved because AFCS control inputs from the flight simulator were not recorded, and the pilot control inputs are not separately recorded in HOMP. Consequently an analysis was performed to estimate the uncertainties introduced by the AFCS.

8.2 Method

In order to gauge the significance of the additional control motions, the AFCS inputs generated during trial BRAE02 were examined. The AFCS inputs were not among the parameters logged during the trial and therefore were reconstructed using the model of the AFCS, and the appropriate states and control positions from the captured data.

The host model, FLIGHTLAB, was not the most appropriate for simulating this subsystem, and so the control system was re-implemented in MATLAB/Simulink. The pedal control movements are not used in the workload predictor and therefore were not reconstructed. The AFCS contributions to collective could not be reconstructed because they depend in part on the normal acceleration, and this acceleration was not logged during the trial. Consequently the HQR predictions given in the following are based on modified signals for longitudinal and lateral cyclic, and the 'raw' collective lever position.

8.3 Results and Discussion

Figure 18 shows the workload predictions for 12 cases taken from the hover tests conducted by pilot A during BRAE02, with and without AFCS inputs. Predictions from data without AFCS are shown in red, and with AFCS in blue, with a green line linking associated pairs of predictions.

Table 5 shows the results in tabular form where it can be seen that the AFCS inputs increase the HQR prediction by between 0.3 and 2.0 HQR points with the large changes generally occurring for the higher workload cases. Expressed as a percentage the changes are in the range 5-22%.

It is clear that the presence of AFCS inputs in the control position and control rate inputs to the workload predictor does introduce an additional uncertainty and does lead to over estimation of the pilot workload. The AFCS inputs in the longitudinal and lateral axes are calculated using both aircraft attitudes and control positions and are partly correlated to the pilot's control inputs. It would therefore be difficult to process data recorded at the swash plate to remove AFCS contributions. In particular, the design of a filter to isolate the AFCS inputs from the pilot's cyclic and collective control inputs is unlikely to be possible.

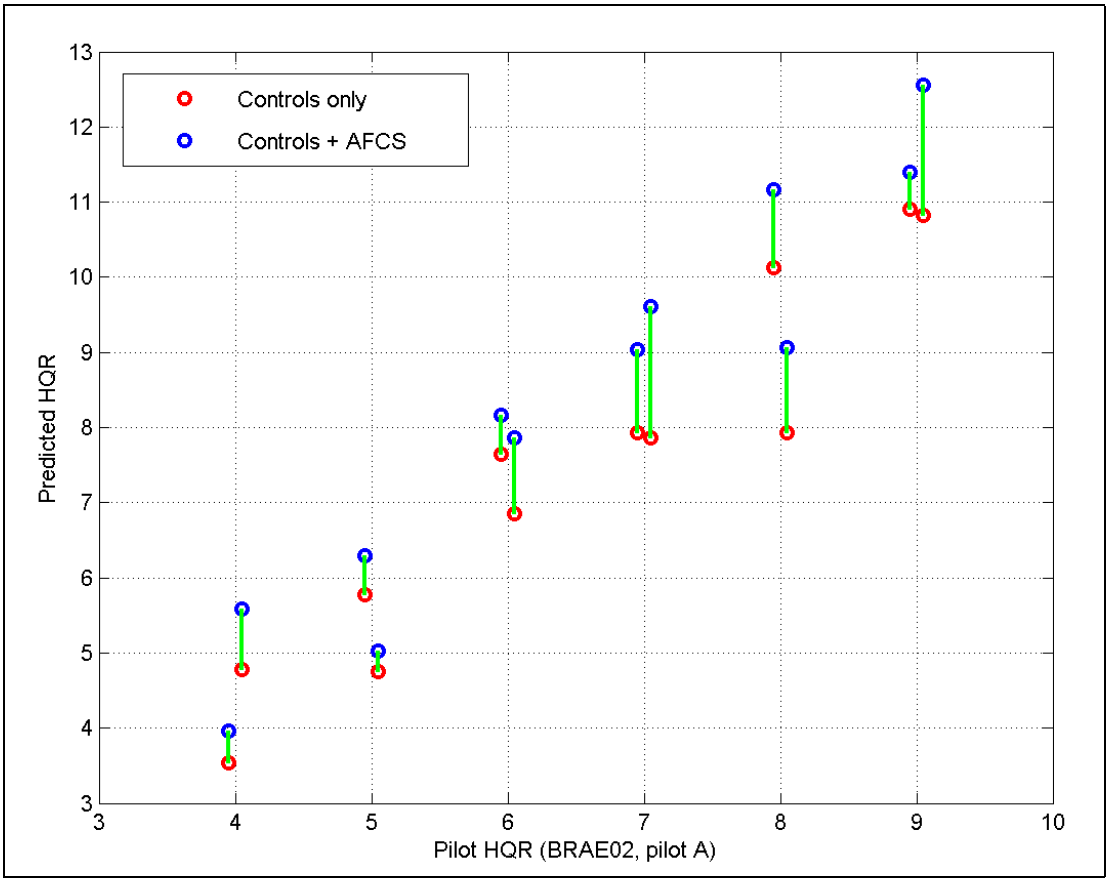

Figure 18 Predictions of HQR with and without AFCS contributions

Table 5 Predictions of HQR with and without AFCS contributions

Pilot HQR	Predicted HQR Pilot Control Only	Predicted HQR Pilot Control + AFCS	Difference (HQR pts)	Difference (Percent)
4	3.54	3.96	0.42	12%
4	4.78	5.58	0.79	17%
5	5.77	6.29	0.52	9%
5	4.75	5.02	0.27	6%
6	7.64	8.16	0.52	7%
6	6.85	7.87	1.01	15%
7	7.93	9.04	1.11	14%
7	7.87	9.61	1.73	22%
8	10.13	11.17	1.04	10%
8	7.93	9.06	1.13	14%
9	10.90	11.40	0.50	5%
9	10.83	12.56	1.73	16%

8.4 Effect of AFCS on workload estimated from HOMP data

The difference in the way control actions are measured in the simulator and in operational helicopters will affect the estimation of pilot workload from HOMP data.

On the collective (z-axis) control, although the flight simulator had the benefit of AFCS, the control activity was measured at the collective lever and so did not include AFCS input. As there is no AFCS (stability augmentation) on the Super Puma collective (or on most other UK offshore helicopters), the part of the workload predictor linking collective control activity to pilot workload remains valid in the HOMP analysis, i.e. the pilot workload on this control is estimated correctly.

On the cyclic (x/y-axis) control, the flight simulator again had the benefit of AFCS and the control activity was again measured at the cyclic control. Thus, like the collective, the workload predictor linking pilot activity to pilot workload does not include the AFCS. In contrast however, the measurement of cyclic activity in the Super Puma HOMP data *does* include AFCS control inputs. Consequently the workload predictor (which assumes all the control activity to be due to the pilot), will over-estimate the pilot workload.

The actual workload predictor, which is based both on cyclic and collective control activity, will therefore over-estimate pilot workload derived from the Super Puma HOMP data due to the cyclic AFCS control inputs. Estimates of the AFCS cyclic activity in the flight simulator have suggested that the pilot HQR may be inflated by up to 22%. Although the application of the workload predictor to HOMP data that includes AFCS inputs may be more indicative of the turbulence encountered, it will ignore the ability of the AFCS to reduce pilot workload and maintain safe flight. Subject to other overriding considerations, for future HOMP installations it would be preferable if control inputs were measured without AFCS contributions.

Table 6 summarises the involvement of AFCS in the derivation of the pilot workload predictor in the flight simulator, and in its use in the analysis of Super Puma HOMP data.

Table 6 AFCS Influence Summary

	QinetiQ Simulator		Super Puma HOMP Data	
	AFCS assistance?	**Measured control data**	**AFCS assistance?**	**Measured control data**
Collective	Yes	Pilot only	No	Pilot only
Cyclic	Yes	Pilot only	Yes	Pilot + AFCS

8.5 Effect of AFCS on the turbulence criterion

The maximum turbulence value for safe flight has been determined by correlating the rms vertical wind speed against the test pilot awarded HQR in the flight simulator. AFCS was operating on the collective control in the simulator, reducing the pilot control activity in that axis, and presumably resulting in a lower HQR than would have been the case without collective AFCS. Unfortunately the collective AFCS control activity was not recorded in the simulator, and it has not been possible to estimate the likely impact on HQR.

It is understood that most transport helicopters do not have AFCS (stability augmentation) operating on the collective axis. In general, therefore, a helicopter pilot meeting a given level of vertical axis turbulence will generate more activity on the collective control than was necessary in the simulator, and thus work somewhat harder than the simulator test pilot. The turbulence criterion developed in the simulator may therefore be non-conservative if applied to helicopters without collective AFCS.

Furthermore, the Lynx AFCS (as used in the BRAE01/02 S-76X model) may not be typical of those used in offshore helicopters in the cyclic (x/y) axes as well as in the collective (z) axis. The turbulence criterion would also be non-conservative for a helicopter with an AFCS of poorer performance and vice-versa.

9 Analysis of Sample HOMP Data

9.1 The Helicopter Operational Monitoring Programme (HOMP)

The Helicopter Operations Monitoring Programme (HOMP) started as a joint CAA, Shell Aircraft, Smiths Industries, Bristow Helicopters, CHC Scotia Helicopters and British Airways initiative to implement a Flight Data Monitoring (FDM) programme for the North Sea helicopter fleets with a view to improving operational safety [8,9,10]. FDM involves the pro-active use of flight data to identify and address operational risks before they lead to incidents and accidents.

The initial HOMP programme involved recording and downloading Flight Data Recorder (FDR) data for a limited number of aircraft on a daily basis for replay and analysis. Based on the success of the initial trial, the United Kingdom Offshore Operators Association[4] (UKOOA) has committed its members to implement HOMP on all UK offshore helicopters, and the International Civil Aviation Organisation (ICAO) has added operations monitoring to Annex 6 Part III as a Recommended Practice for flight recorder equipped helicopters.

4. The UK Offshore Operators Association (UKOOA) changed its name to Oil & Gas UK in 2007.

9.2 HQRs from Filtered and Windowed BRAE02 Approach Data

Since the HOMP data are recorded at 4 Hz, the effect of using the complete (filtered and windowed) workload algorithm was investigated using data from the BRAE02 approach cases down-sampled to 4 Hz. It has already been shown in Section 5 that a reduction of the data sampling rate reduces the workload prediction for the hover cases. Figure 19 shows HQR predictions from the BRAE02 approach data that have been down-sampled to 4 Hz.

The figure shows that applying the workload algorithm to 4 Hz sample rate data gives a very good correlation between predicted HQR and pilot HQR. The increase in predicted HQR through the filtering and windowing of the approach data is balanced by the decrease in predicted HQR caused by the reduction in the sampling rate. This is encouraging, although with only nine approach cases available it is not possible to create definitive statistics. By comparison with Figure 16, reducing the sampling rate from 20 Hz to 4 Hz has dropped the predicted HQR overall, and suggests an increased tail-off for the highest HQR values. The overall drop is consistent with the expectations reported in Section 5.

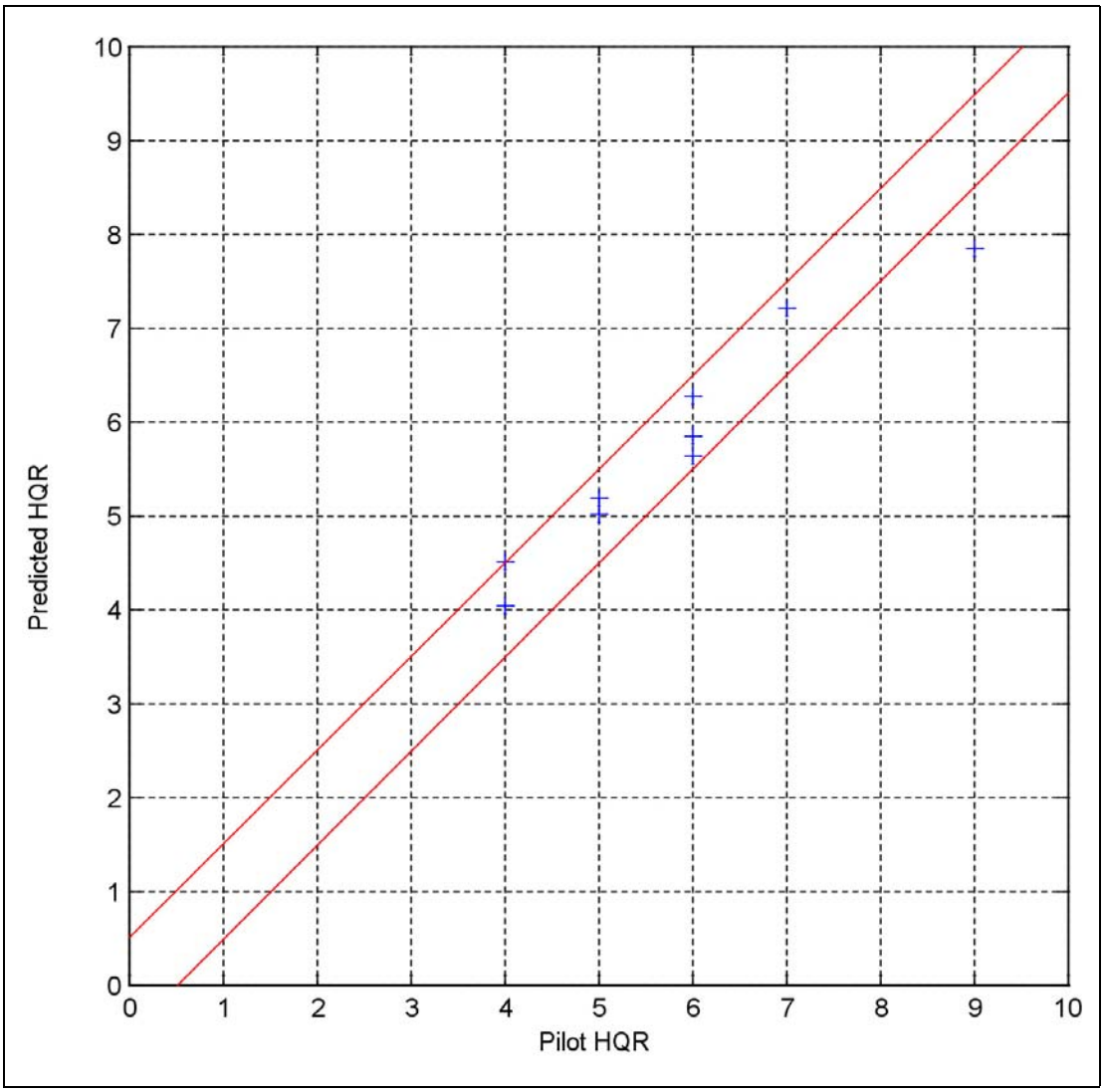

Figure 19 Approach HQR predictions with filtering and windowing versus pilot HQR, with control inputs sampled at 4 Hz

9.3 Results using Sample data from HOMP

The workload algorithm was applied to the data from 20 example records supplied from the HOMP project. For these data, there was no pilot HQR, however a so-called "Digicoll" value was supplied as a measure of turbulence. Figure 20 is a plot of predicted HQR versus "Digicoll" value. From this figure it can be seen that the HQR prediction ranges from 3.1 to 6.7 HQR points and is generally increasing with "Digicoll" value. This trend is not necessarily an indication of a robust workload algorithm as the "Digicoll" has not been the subject of a rigorous validation exercise.

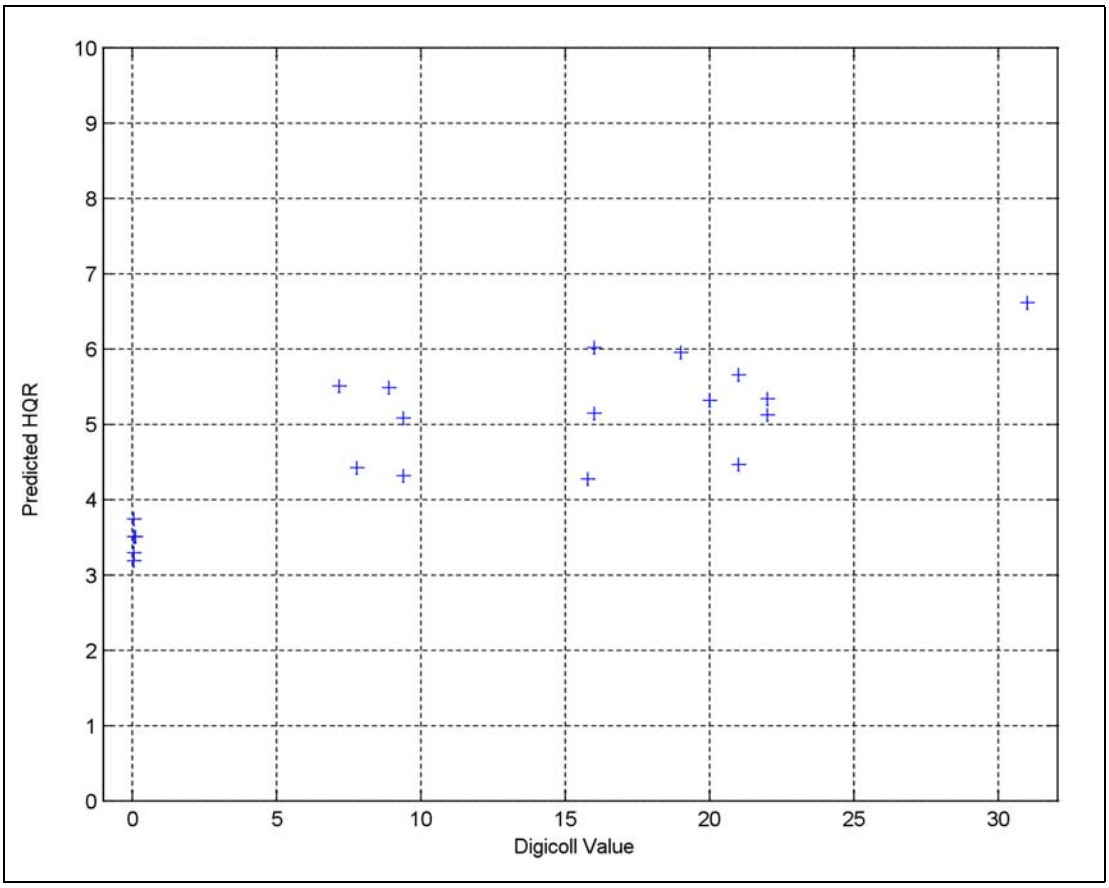

Figure 20 Predicted HQR for 20 example HOMP cases

10 Implementation of the Workload Algorithm in HOMP

Having developed the workload algorithm to operate on flight data from operational helicopters, and verified that it worked well on helideck approaches flown in the simulator (see Section 7), it was necessary to implement the workload algorithm in the HOMP analysis, and test it to demonstrate that it generated the same result as the original implementation when supplied with the same input data.

Three HOMP helideck landings were selected for checking, and the workload time series independently calculated by QinetiQ using the original Matlab code, and by Smiths within the HOMP system. Intermediate results in the workload calculation (e.g. windowed standard deviation of each control axis) were also output and compared.

This task proved to be a little more difficult than had been anticipated, with the initial implementation in the HOMP system showing a number of discrepancies in the results produced by the development analysis (which had been coded in Matlab), and the workload results produced by the HOMP system. The most important issue

proved to be the numerical precision in the 8th order Butterworth filter. The HOMP analysis environment was performing arithmetic at a lower numerical precision and, as a result, the filter characteristics proved to be significantly different from those implemented in the Matlab coding of the algorithm. When this was discovered the solution was to implement the 8th order filter as 4 x 2nd order filters, which achieved an almost identical result without requiring excessive arithmetical precision.

The final results for the three example landings are shown in Figure 21 to Figure 23. It can be seen that the results are in all cases very close. An aberration for a few seconds in the HOMP analysis shown in Figure 23 was caused by a dropout in the collective pitch data that had been filtered out by QinetiQ, but had been left in the data analysed by Smiths.

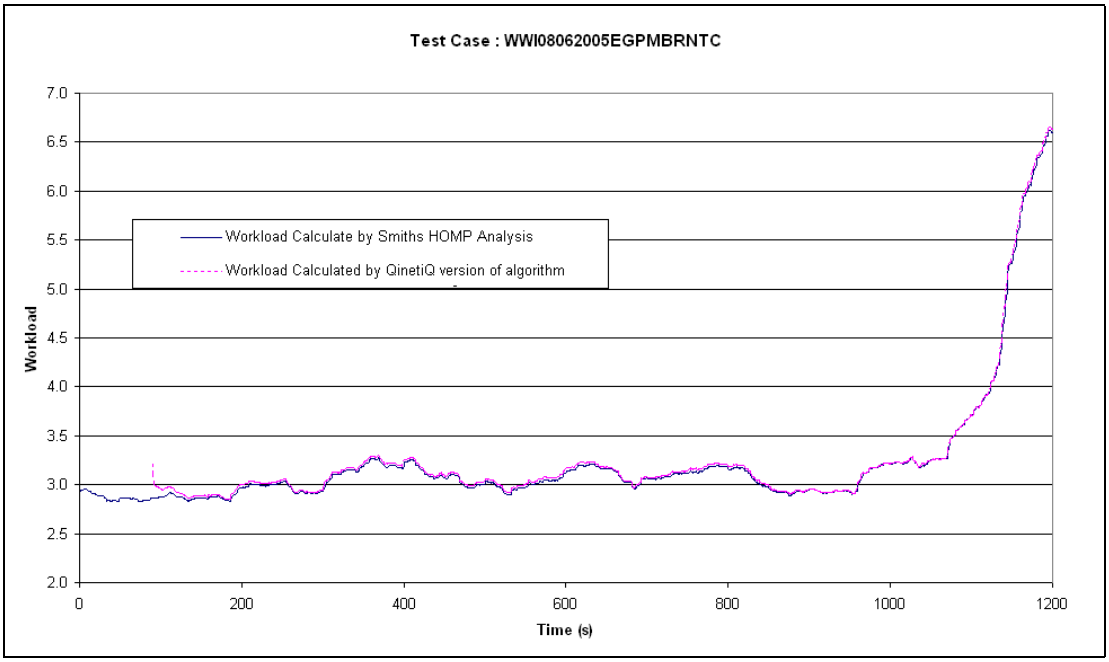

Figure 21 Workload time series checking comparison

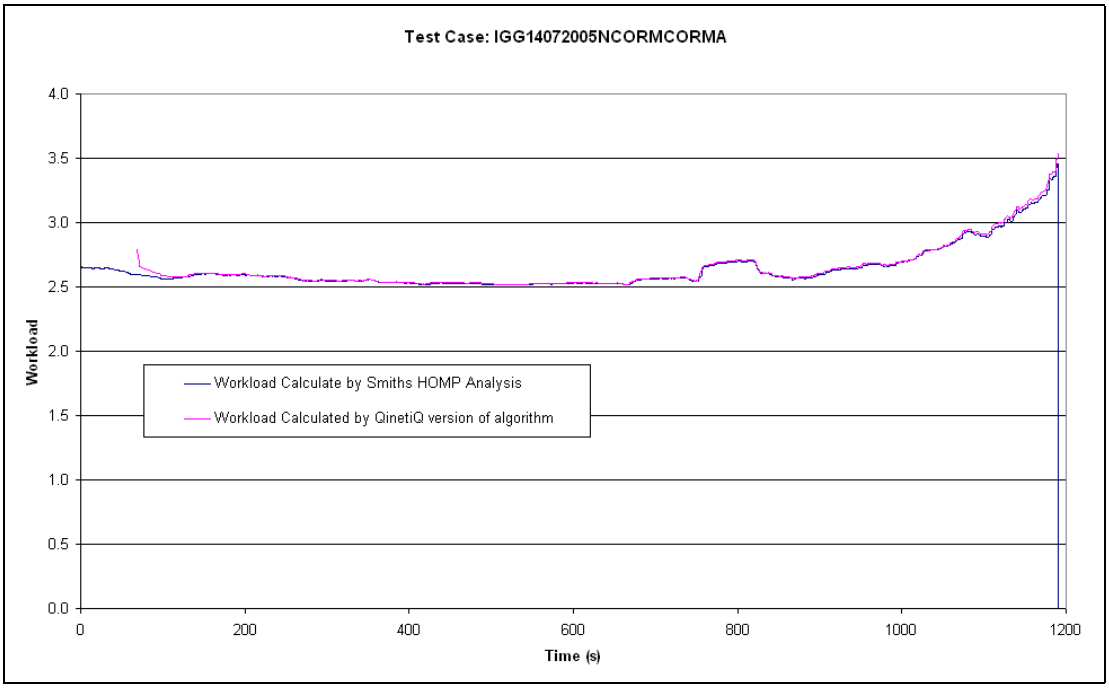

Figure 22 Workload time series checking comparison

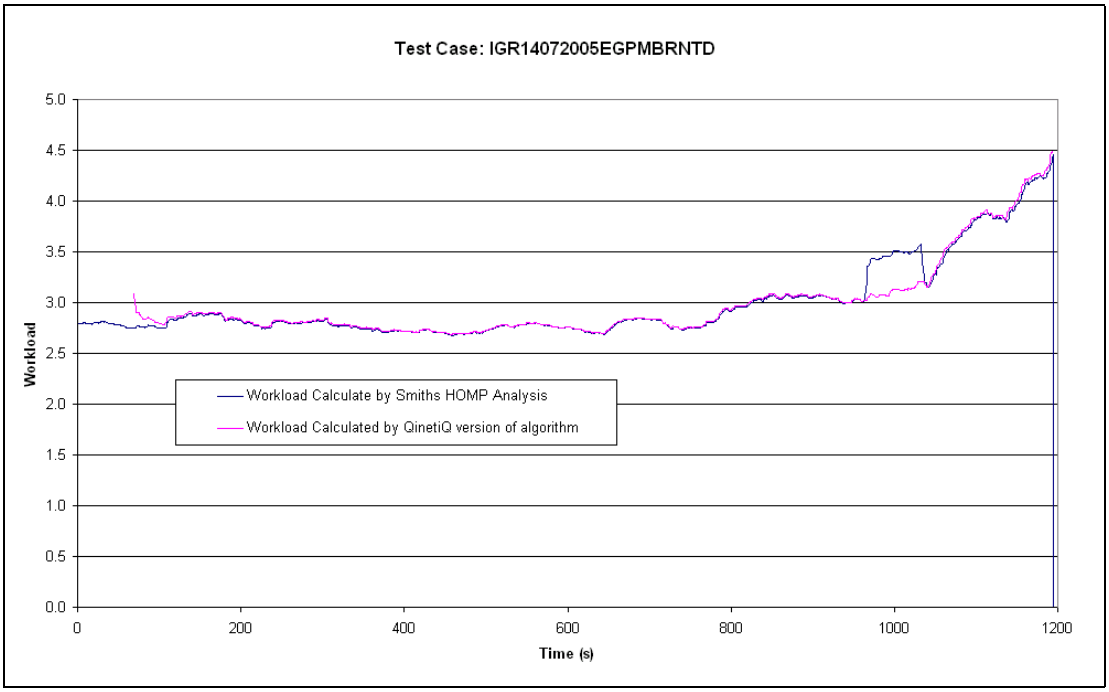

Figure 23 Workload time series checking comparison

Appendix B contains guidance on programming the pilot workload algorithm into a HOMP analysis system.

11 The HOMP Data Archive

The HOMP data used in the workload analysis was not live data from current helicopter operations, but an archive of some 32,000 flight sectors operated by Bristow Helicopters in the North Sea between the dates of 1st July 2003 and 31st October 2004. Altogether 122 different offshore helidecks had been visited by these flights. Once helideck landings had been selected, and a proportion of landings with bad data had been eliminated, there remained about 13,000 valid landings over the 16 month period that could be used in the analysis.

Of the 122 platforms visited a number had relatively few landings, which prevented any pattern being reliably presented and interpreted for that platform, but certain manipulations and presentations could be performed for the population of landings as a whole (e.g. the overall distribution of pilot workload values are presented in Figure 34 and discussed in Section 12.2).

It was decided to focus on helidecks that had received more than 20 landings, and helidecks for which platform layout sketches had been provided, this permitting interpretation of the results in terms of wind directions and the relative locations of installation structures likely to cause turbulence over the helideck. This resulted in a 'top 70' list of platforms. These platforms are listed in the table in Appendix C, which shows the number of landings in the database for each of these platforms. This table also summarises HLL entries and the main features of the workload plots (see Section 12.2).

The availability of platform sketches also enabled wind directional sectors to be defined that would be either 'open' (i.e. no significant platform structures upstream to cause turbulence), or 'turbulent' (i.e. for the wind directions where the turbulent wake of platform structures upwind would be expected to have a significant effect). This in turn enabled the ensemble data for the 'open' and 'obstructed' wind directions to be presented separately.

The HOMP parameters used in this particular pilot workload analysis are listed in Table 7:

Table 7

Variable name	Description
FlightType	Flight type (from imported ops data, 1,2,6 = revenue, 4 = training, 5 = air test)
MX_WORK_LDG	Maximum Pilot Workload Rating from 500m to landing
MXWORKTIMLDG	Number of Frames from Landing point to recorded MX_WORK_LDG (2 frames = 1 sec)
MX_WORK_XDIST	Lateral distance between MX_WORK_LDG and Landing Point (m)
MX_WORK_YDIST	Longitudinal distance between MX_WORK_LDG and Landing Point (m)
COR_MX_WSPDLDG	Wind speed in the Landing Phase at Measurement Point (1500m from Landing) (m/s)
COR_MX_WANGLDG	Wind angle in the Landing Phase at Measurement Point (1500m from Landing) (m/s)
MX_CORWSPDLDG	COR_MX_WSPDLDG corrected to helideck height (m/s)

The wind speed and direction estimated from the helicopter FDR at the 'measurement point' (COR_MX_WSPDLDG and COR_MX_WANGLDG) is derived from GPS track and heading information. The accuracy of this is dependent on the aircraft flying straight and level, and at a reasonable airspeed. If the airspeed is low, or the aircraft is turning, the GPS derived wind speed and direction will be unreliable, and so reasonably accurate data is ensured by:

1. Averaging GPS wind speed / wind angle data over a 10 s period;
2. Identifying the data as valid only if the aircraft roll angle is < 5.5 degrees;
3. Identifying the data as valid only if indicated airspeed is > 55 kt at the start and end of the 10 s averaging period;
4. Acquiring landing wind measurements when the aircraft is 1500 m from the landing point (when conditions 2, 3 and 4 are more likely to be satisfied).

The wind speed data were then corrected (MX_CORWSPDLDG) for the altitude difference between that at the helicopter 'measurement point' and the helideck height using a standard atmospheric boundary layer power law profile:

$$u_1 = u_2 (z_1 / z_2)^{1.4}$$

where:

u_1 = wind speed at height 1 [m/s]
u_2 = wind speed at height 2 [m/s]
z_1 =height 1 [m]
z_2 =height 2 [m]

With this rather complex derivation of the corrected wind speed and direction it is very difficult to know the accuracy of the resulting wind estimates, and this uncertainty needs to be taken into account in the interpretation of the results of the analyses presented in this report.

In order to obtain some guidance as to the likely repeatability of the wind data an analysis was performed, searching the database for all helideck landings made by the same aircraft, on the same day, within 30 minutes of each other. It was argued that such landings must be on platforms reasonably close to each other, and with not much time for the wind conditions to change.

In the 13,000 landings there were 424 that met this criterion, and the standard deviation of the difference in speed and direction for the two observations was calculated, and found to be 7 kt for the wind speed and 10 degrees for the wind direction. Given that wind speed and direction are usually changing with time, and are likely to be slightly different for the different platform locations, this level of variability is considered reasonable. If the variation in readings was solely caused by measurement error, and if these errors were normally distributed, then one would expect 95% of samples to lie within 2 standard deviations (i.e. within ±14 kt and ±20 degrees) of the true wind velocity.

In addition to the HOMP parameters listed above, separate but related research projects were analysing ambient temperature and rotor torque, and as some example results from these are presented here, the additional HOMP parameters are listed in Table 8:

Table 8

Variable name	Description
MX_LDGWGHT	Landing weight (lb)
MXTORQ	Maximum Total Torque from 500m to landing (%)
MXTORQTIMLDG	Number of Frames from Landing point to recorded MXTORQ (2 frames = 1 sec)
MX_TORQ_XDIST	Lateral distance between MXTORQ and Landing Point (m)
MX_TORQ_YDIST	Longitudinal distance between MXTORQ and Landing Point (m)
MXINCRTORQ	Maximum Increase in Torque from 500m to Landing Point (%)
MXINCTRQTIMLDG	Number of Frames from Landing point to recorded MXINCRTORQ (2 frames = 1 sec)
MX_INCRTQ_XDIST	Lateral distance between maximum MXINCTORQ and Landing Point (m)
MX_INCRTQ_YDIST	Longitudinal distance between maximum MXINCTORQ and Landing Point (m)
MX_INCRTQ_TORQ	Total Torque at finish point of MXINCTORQ (%)
OATMPLDG	Averaged OAT at point 500m from landing
ALTMPLDG	Radio Altitude at point 500m from landing
COROATMPLDG	Averaged OAT at point 500m from landing corrected to helideck height
MX_AVTEMPDIFFL1	Maximum Averaged Temperature Difference from COROATMPLDG from 500m to landing
MXTPL1TIMLDG	Number of Frames from Landing point to recorded MX_AVTEMPDIFFL1 (2 frames = 1 sec)
MX_TEMPL1_XDIST	Lateral distance between MX_AVTEMPDIFFL1 and Landing Point (m).
MX_TEMPL1_YDIST	Longitudinal distance between MX_AVTEMPDIFFL1 and Landing Point (m).
AVOATLDG	Averaged OAT measured at Landing point
MX_AVTEMPDIFFL2	Maximum Averaged Temperature Difference from AVOATLDG from 500m to landing
MXTPL2TIMLDG	Number of Frames from Landing point to recorded MX_AVTEMPDIFFL2 (2 frames = 1 sec)
MX_TEMPL2_XDIST	Lateral distance between MX_AVTEMPDIFFL2 and Landing Point (m).
MX_TEMPL2_YDIST	Longitudinal distance between MX_AVTEMPDIFFL2 and Landing Point (m).

12 HOMP Results

12.1 Example Platform Results

The plots in this section show the maximum pilot workload values with points colour coded according to the workload value, and with the position of the point on the plot representing the estimated wind speed and direction at the time of the landing.

Each plot includes a sketch of the platform layout correctly orientated with respect to true North, so that the relationship between wind directions and platform obstructions that might cause turbulence can be assessed. The sketches of the platforms were obtained from the 'Aerad Plates' published by European Aeronautical Group (now part of Navtech Inc). In some cases an appropriate plan view sketch of the platform was not readily available. In a few cases it was noticed that the sketches contained errors. Examples of these were; Alba Northern (unobstructed sector markings wrongly aligned on the sketch), Brae A (4^{o} to 5^{o} error in helideck orientation), K14-FA-1 (major alignment error), and K15-FA-1 (major alignment error).

Workload plots are presented here for 8 platforms, Brae A, Brent A, Brent B, Brent C, Britannia, Cormorant A, Ninian Central, and Auk A. The first 7 were selected because they all contained examples of high workload landings (> 5.5), whilst Auk A by contrast tended to exhibit lower workload landings.

In general the Heather A platform does not appear to suffer from regular severe turbulence. The single high workload landing was the only landing with a value greater than 6.5. However, as noted in Appendix C, and as can be seen from the plot of the workload values for Heather A in Figure 24, there is a cluster of higher workload events for wind directions in the range 115 to 180 degrees.

The HLL entry for Heather A (Appendix C) mentions turbulence, and requests turbulence reports, but does not define a range of wind directions in which turbulence might be expected. This is a good illustration of the benefit of the HOMP data analysed in this research project. The HLL, being largely reliant on subjective reports submitted by pilots, is an imperfect description of the helideck environment. The HOMP data provides objective evidence on which to base a turbulent sector, and offers the opportunity for a more specific warning in the HLL entry for this platform.

Figure 25 shows the data for Brae A, and it can be seen that the highest (purple) workload landing occurred when the wind was from just west of north at about 35 kt. There is a cluster of high workload landings from around this wind sector and for a range of wind speeds from 15 kt to 40 kt. This would be expected to be a wind direction that would cause significant turbulence over the helideck, as the helideck is downwind of the large clad derrick for this wind sector. There is also a small cluster of higher workload (red) points for winds from the South at about 10-20 kt. It is possible that these are due to the a relatively challenging landing manoeuvre involving poor visual cues when the helicopter is landing facing South into the Southerly wind.

Figure 26 shows similar information for the Brent A platform. For this installation the helideck is located on the Northwest end of the platform, and so highest workload events are seen in winds from the Southeast. There is one high workload event (>5.5) with wind at about 36 kt from WSW.

Data for Brent B is shown in Figure 27. Although the detailed design of the platform is quite different from Brent A, the helideck is again located on the Northwest end, and so the general pattern of the pilot workload is very similar.

The design and alignment of Brent C is somewhat similar to Brent B, and so a very similar picture is seen again in Figure 28.

Results for the Britannia platform are shown in Figure 29. The design and alignment of Britannia is quite different from the Brent platforms, and the helideck is located on the Western corner. Consequently high workload events are seen for higher wind speeds from the East and Southeast.

For Cormorant A (Figure 30) the helideck is located on the Northern corner, and most of the high workload events are seen in winds from the South. However, it is apparent that the very highest workload event (6.02) occurred with the wind at 39 kt from the Southwest. At this heading the wind is blowing across the significant accommodation block located on the West corner, and so this high value is not surprising, particularly since it occurs for the highest wind speed from this direction.

Results for Ninian C are shown in Figure 31. This platform has more high workload events than seen in the foregoing platforms, with 11 events over 5.5. The high workload events are all clustered for moderate to high wind speeds from the SE to SSW sector, which is to be expected with the helideck located on the NW corner of the platform with some significant structures directly to the South. It is known that Ninian C suffers from hot exhaust gas plumes in the helicopter flightpath [11]. Figure 32 shows a plot of maximum ambient temperature increase as measured by the OAT sensor and it can be seen that there is a cluster of high temperature events with the wind in the E to S sector. The pattern is similar to, but not the same as, the pilot workload plot and so both structure induced turbulence and temperature effects are likely to be factors in causing high workload.

Finally, Figure 33 shows workload values for the Auk A platform. This is clearly an easier platform on which to land, with only 5 well scattered events with workload above 4.5. Auk A is a relatively small platform and all structures, with the exception of an unclad drilling derrick are below the level of the helideck.

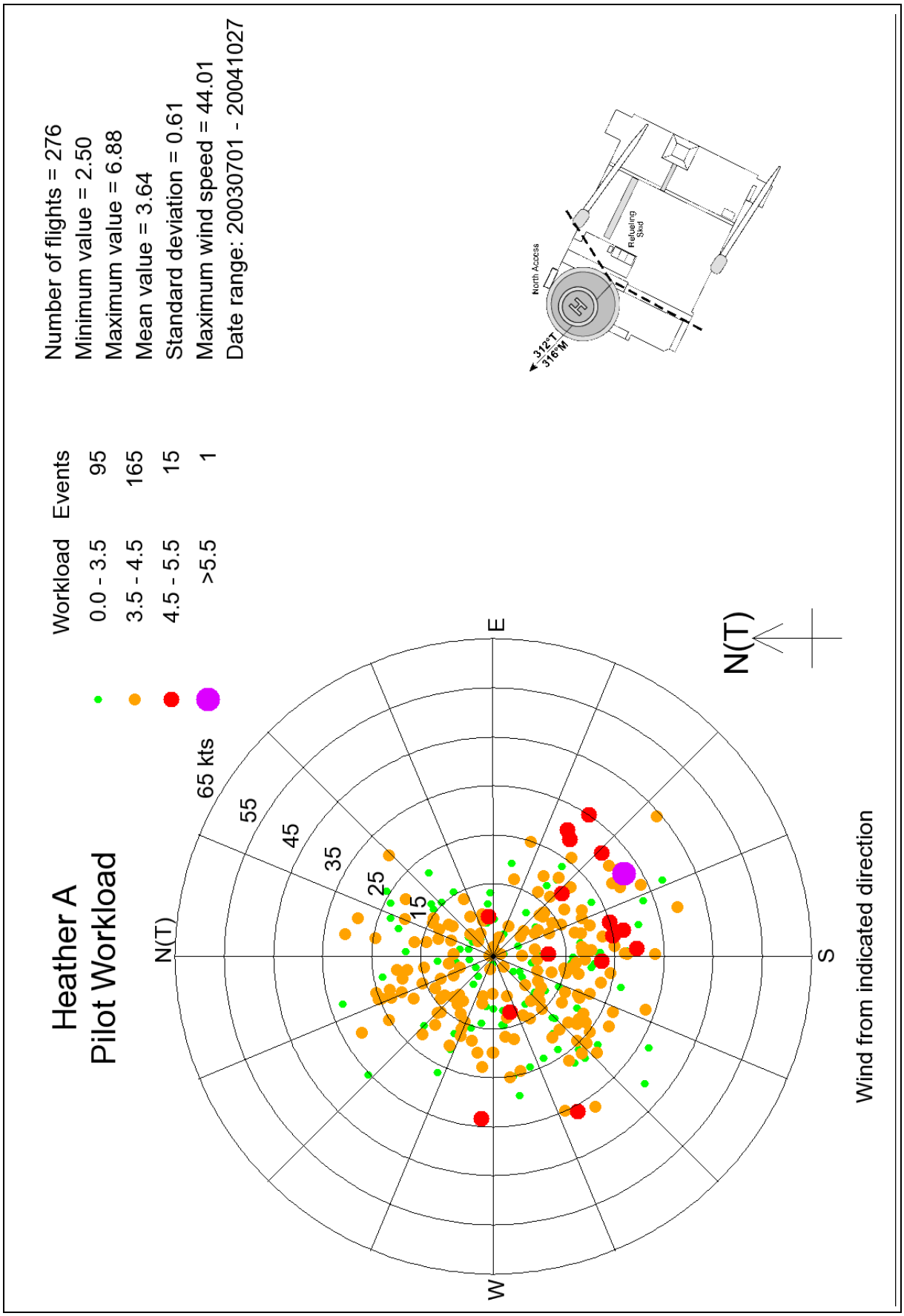

Figure 24 Pilot workload plot for Heather A showing the highest workload event (HQR=6.88) in the 16 month HOMP archive

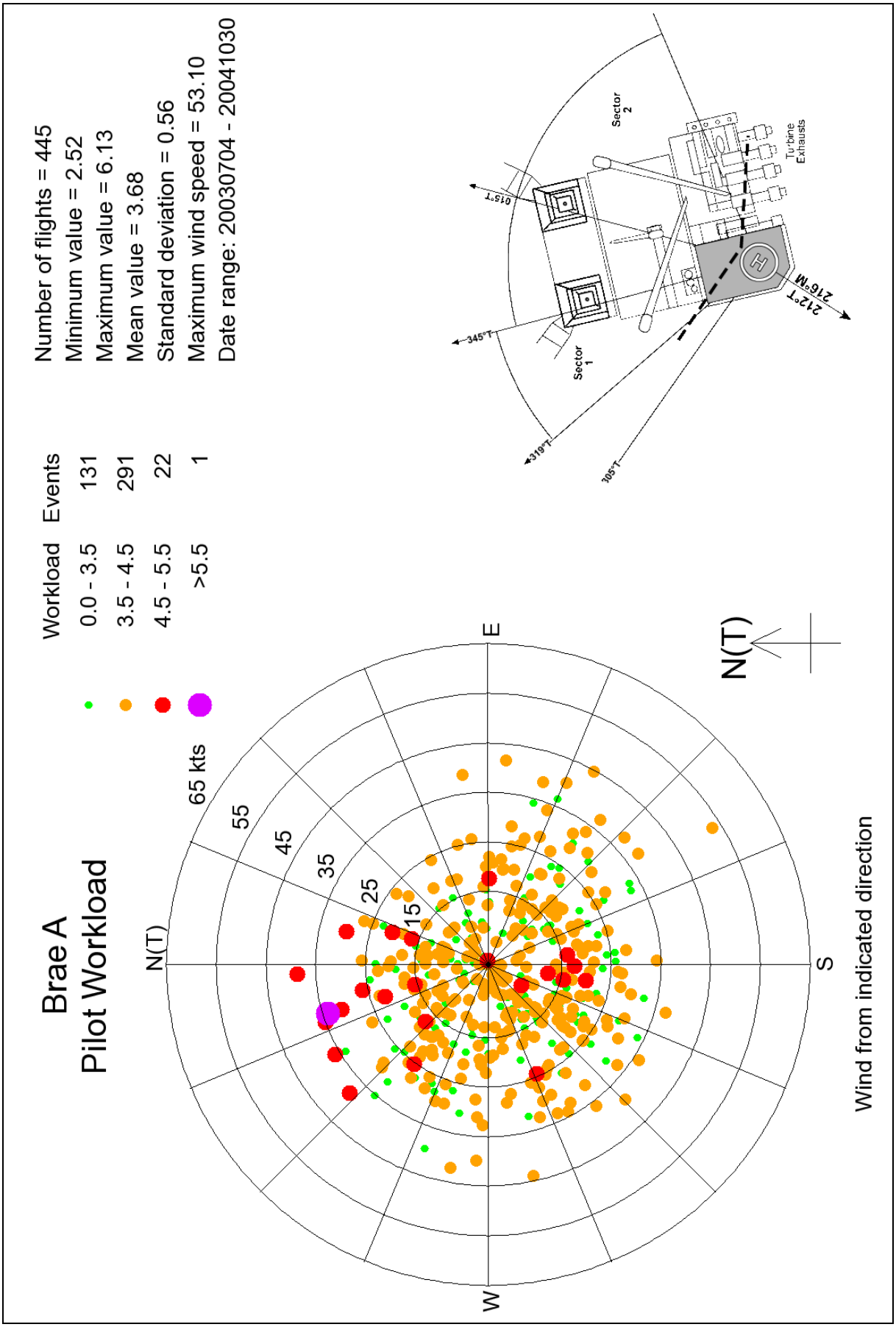

Figure 25 Pilot workload plot for Brae A

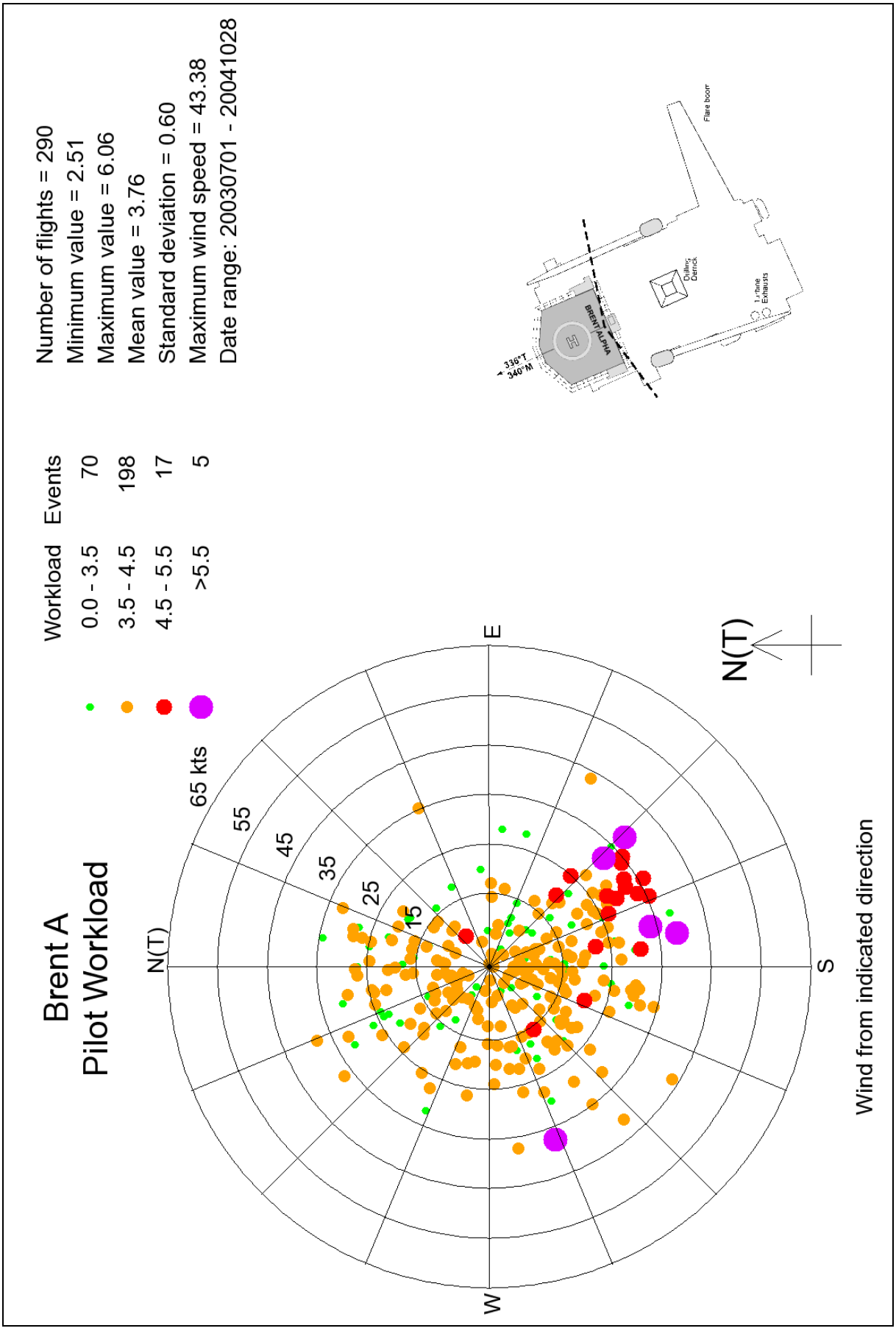

Figure 26 Pilot workload plot for Brent A

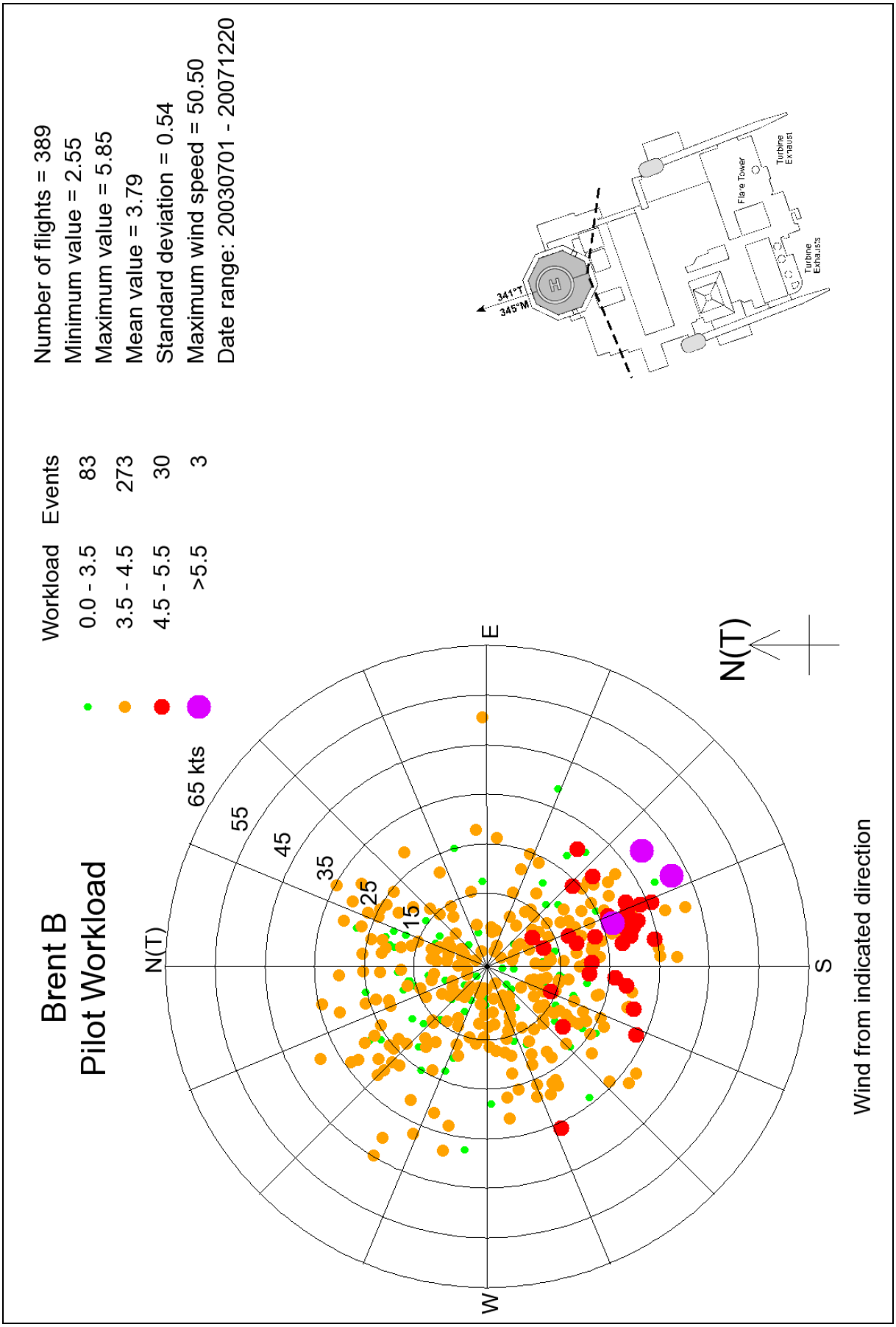

Figure 27 Pilot workload plot for Brent B

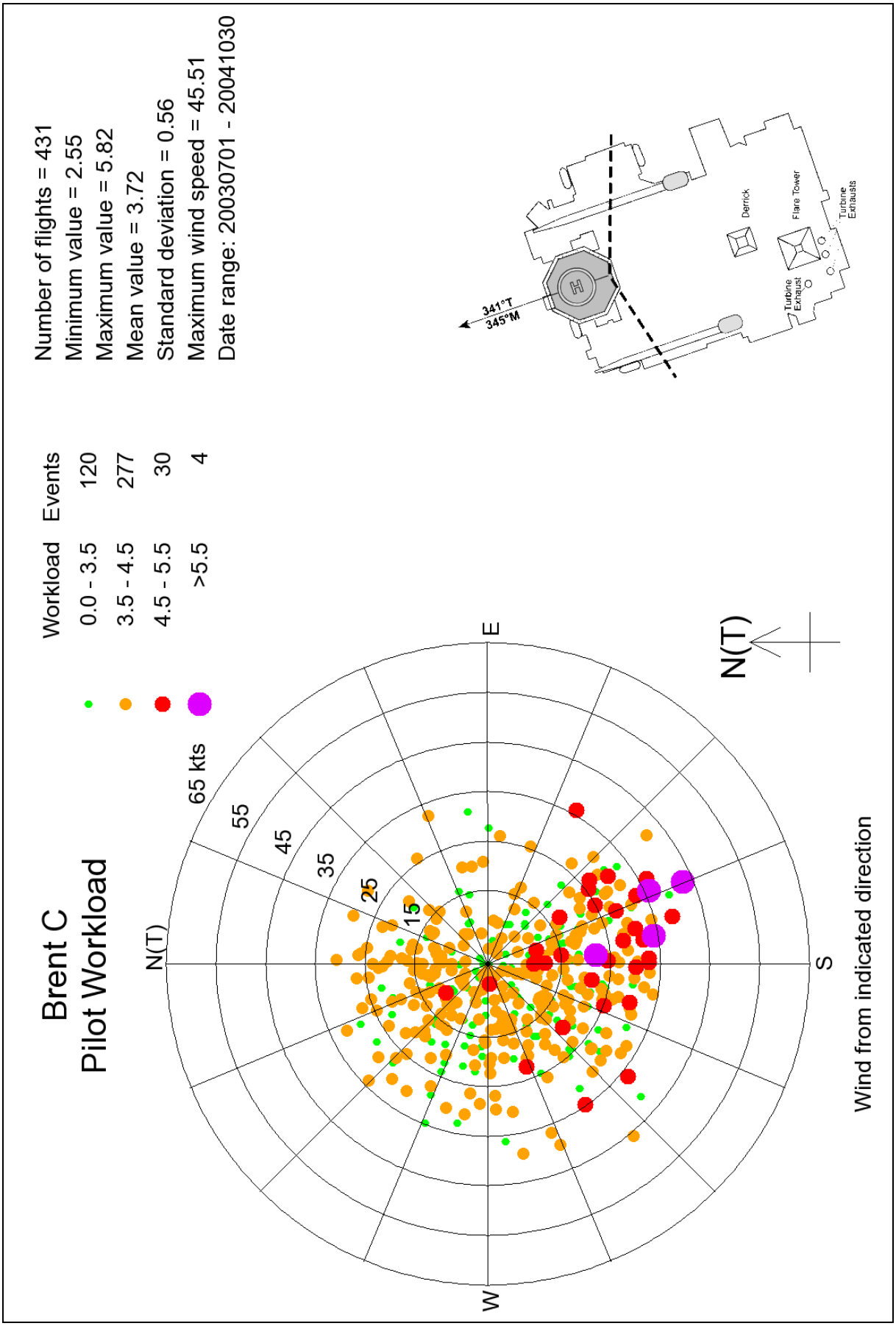

Figure 28 Pilot workload plot for Brent C

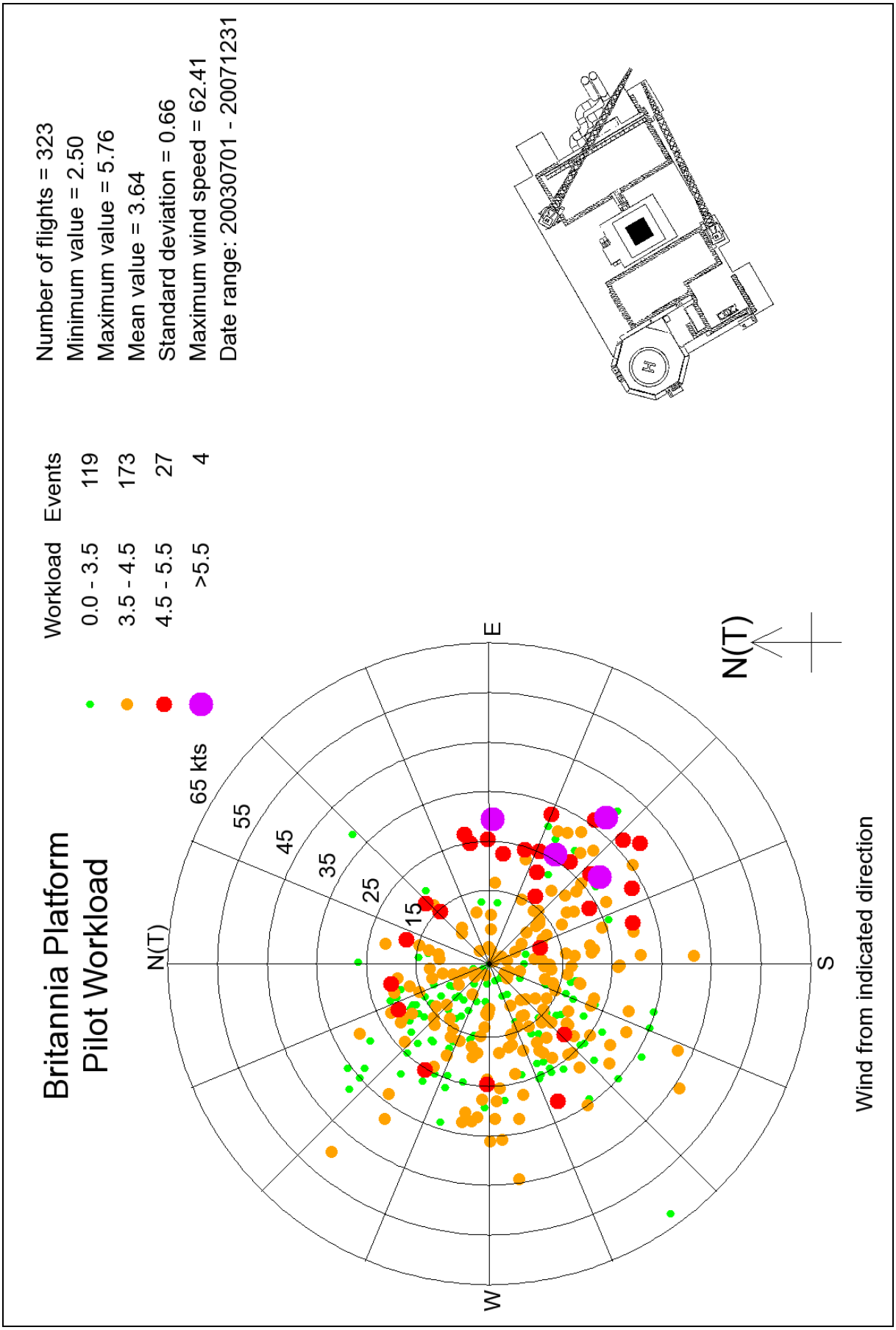

Figure 29 Pilot workload plot for Brittania

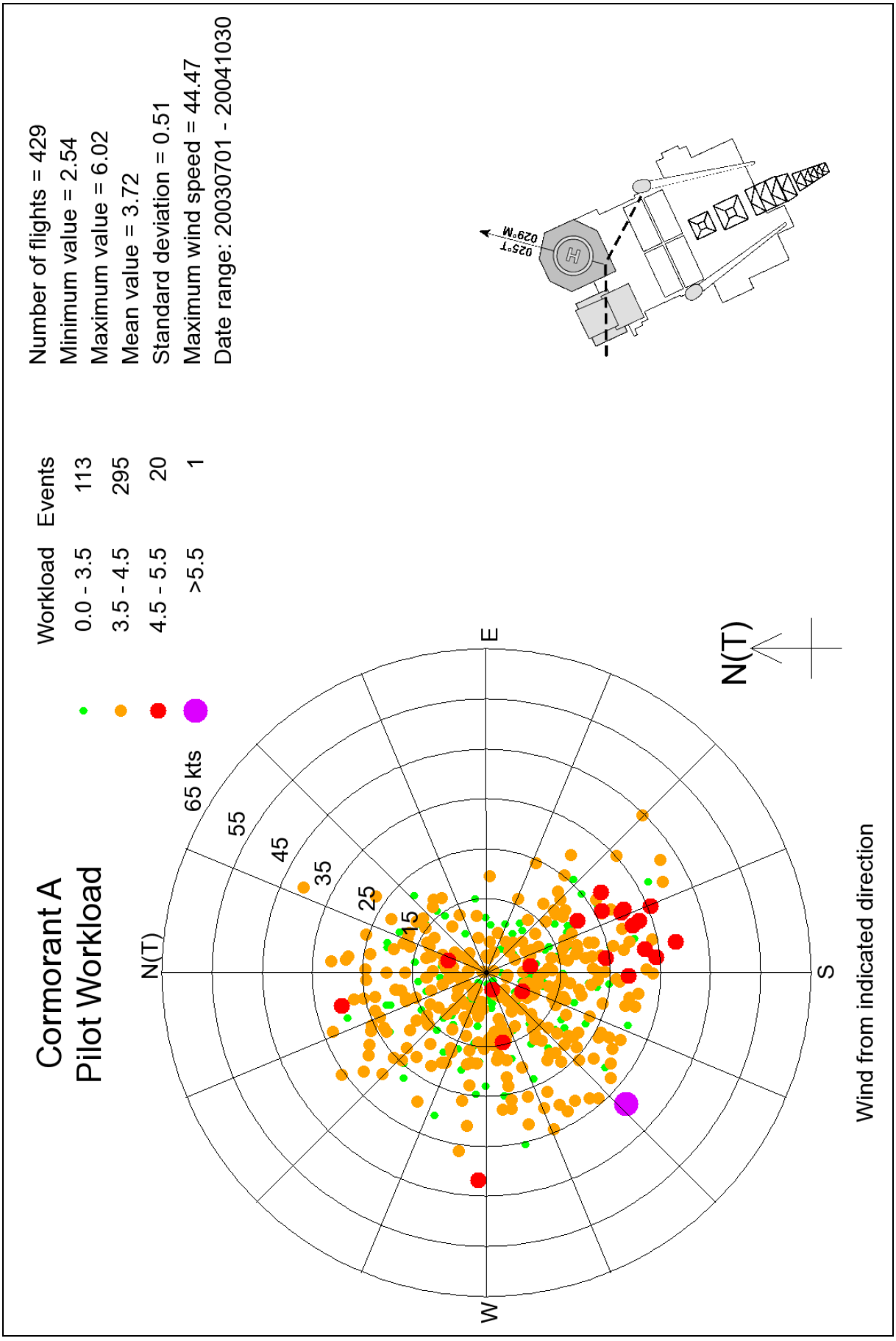

Figure 30 Pilot workload plot for Cormorant A

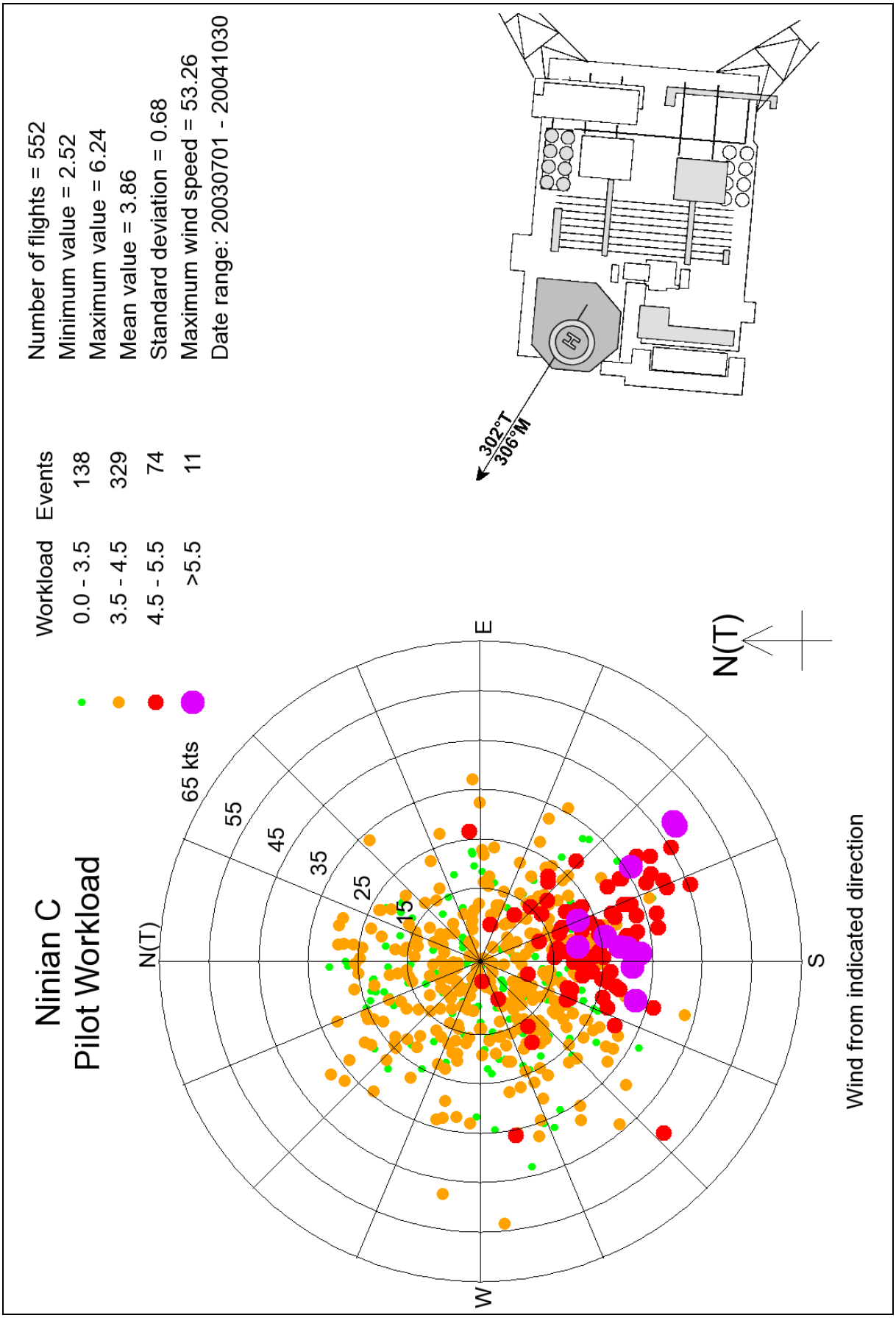

Figure 31 Pilot workload plot for Ninian C

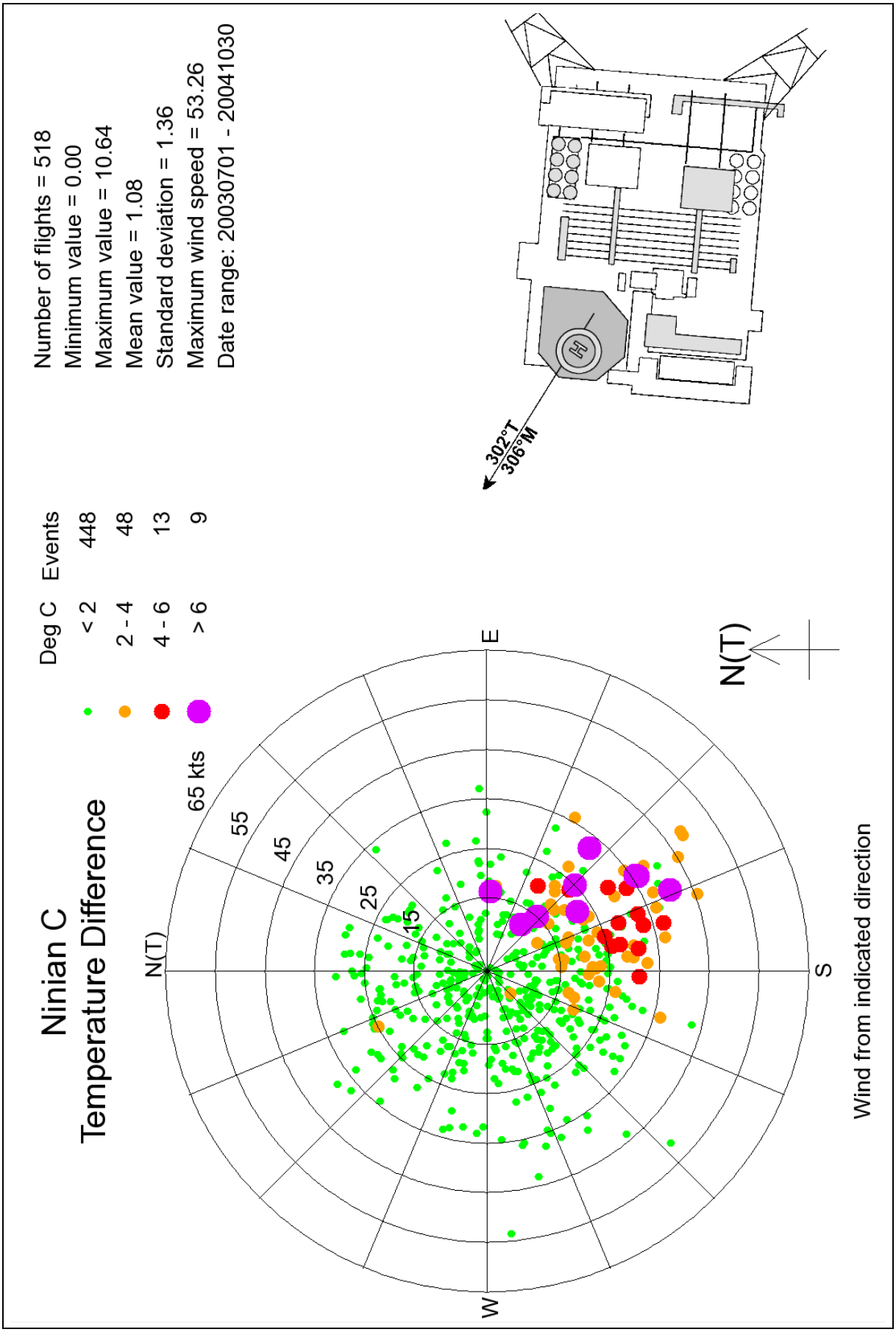

Figure 32 Air temperature difference plot for Ninian C

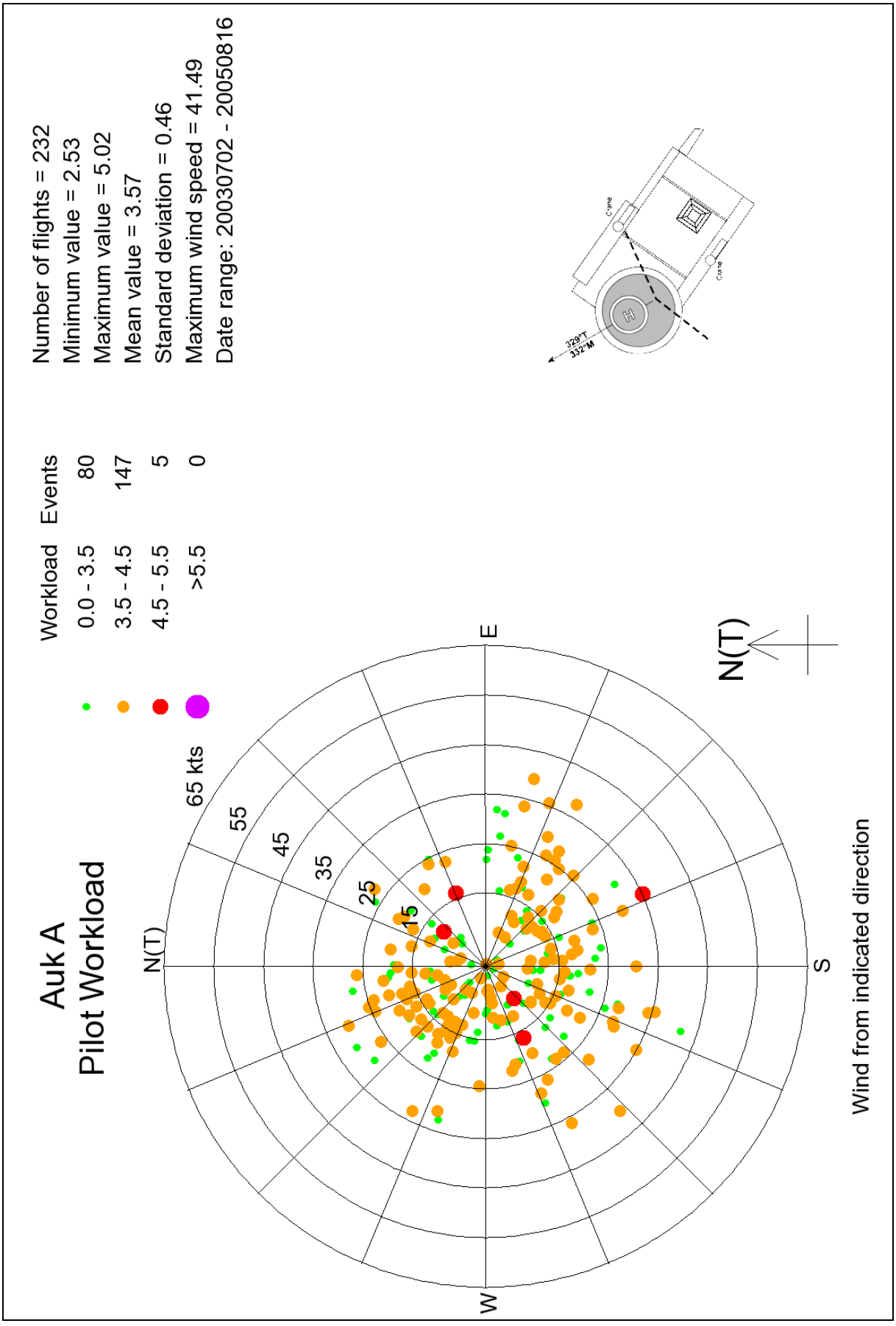

Figure 33 Pilot workload plot for Auk A

12.2 Ensemble Results

12.2.1 General

This section reviews some general properties of the pilot workload estimates made from the 12,978 landings. The mean, 95-percentile and maximum workload for the 12,978 valid landings were as shown in Table 9.

Table 9 Workload statistics

	Obstructed Wind Sectors	Open Wind Sectors	All valid landings
Mean	3.81	3.64	3.69
95 percentile	4.87	4.34	4.52
Maximum	6.88	6.37	6.88

Figure 34 presents the distribution of workload values obtained. It can be seen that the peak value of the probability density was at a workload of about 4.0. An interesting feature of Figure 34 is the secondary peak of workload that is seen to occur at about 2.7. It appears that there may be two distinct probability distributions; a main distribution with a peak at 4.0 and a smaller narrow distribution with its peak at 2.7.

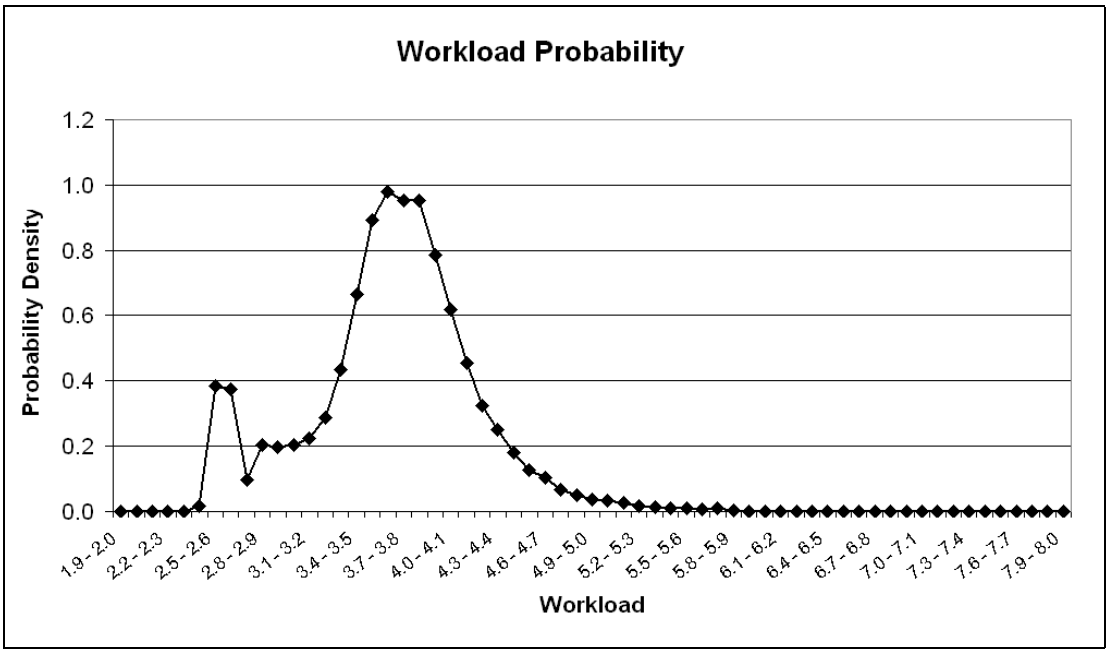

Figure 34 Workload distribution for all valid helideck landings

12.2.2 Lower Workload Peak

Clearly the workload predictor cannot give a workload less than 2.4 because this is the value of the constant offset (see Appendix A). The constant offset results from the lack of landings with HQRs less than 3 during the simulation trials.

It is speculated that the smaller secondary peak might be due to the control actions of the Automatic Flight Control System (AFCS). Although the AFCS operates at a reasonably high rate, it has only ±5% control authority and does not operate on the collective control and so would not be expected to generate high workload values by itself. It is possible to calculate the maximum workload that could be caused by the AFCS acting alone if it were to slew the full –5% to +5% range within one HOMP sample period (0.5s). Using the workload constant term and the (dominating) cyclic

rate terms a maximum workload of 3.08 was estimated. This is close to the secondary workload peak, and supports the hypothesis that the peak may be due to the AFCS control activity.

It is also plausible that the relatively high rate, but low amplitude, AFCS control inputs might dominate the workload calculation in low turbulence conditions. As part of the investigation of the secondary peak the landings were therefore split into those where the wind was seen to be coming from a direction which would involve physical wake effects from upstream platform structures ('turbulent' sectors), and those where the wind should be substantially unaffected by platform structures ('open' wind sectors). The results for these two different populations of workload values are shown in Figure 35.

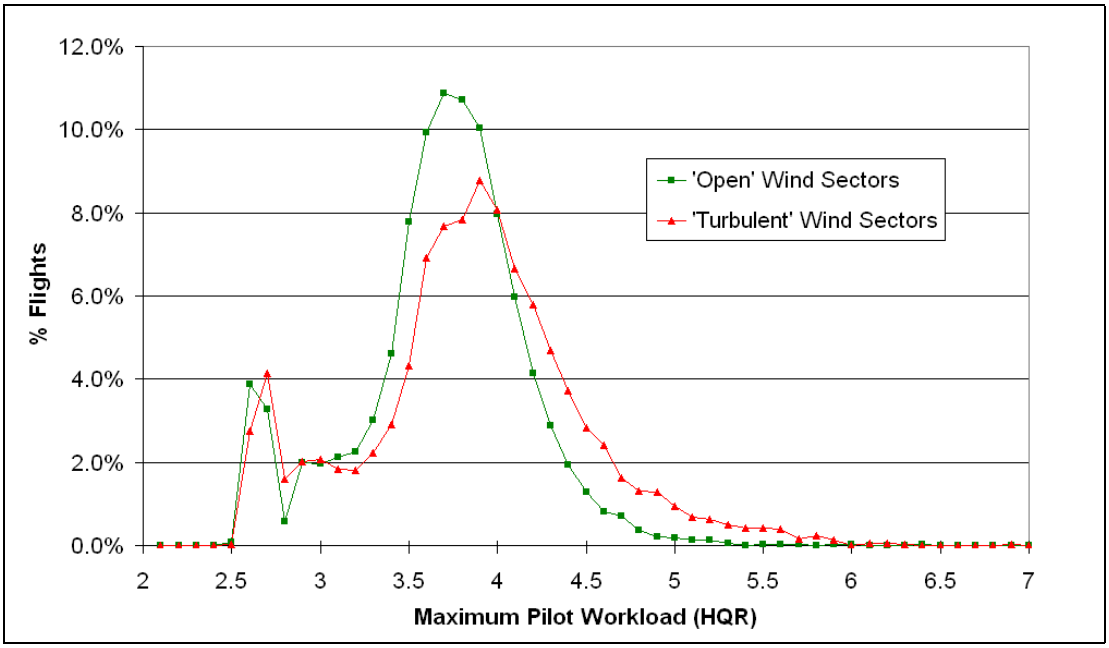

Figure 35 Workload distributions for 'open' and 'turbulent' sectors – 44 platforms

It can be seen from the figure that the general form of the distributions is similar, with the lower peak at a workload of 2.7 almost identical, but that the 'turbulent' sectors, represented by the red line, tend to give rise to higher workload values. This is as expected, with the presence of structural induced turbulence requiring more control activity and a higher pilot workload to stabilise the helicopter. However, there is no significant difference in the magnitude or shape of the secondary peak.

For comparison Figure 36 shows the same data presentation for a single platform (Ninian Central). This platform is known for moderately severe turbulence when the wind direction is such that the helideck is downwind of the platform structure. It can be seen that the workload distribution for these turbulent wind directions is shifted to the right showing higher workload values. It can also be seen that the secondary peak is not apparent in the landings from the 'turbulent' wind directions, supporting the AFCS theory. It is possible that the secondary peak appears in the 'turbulent' wind sector data for Figure 35 solely because there are a significant number of the platforms amongst the 44 that do not experience serious turbulence even when the wind is from the 'turbulent' sector directions.

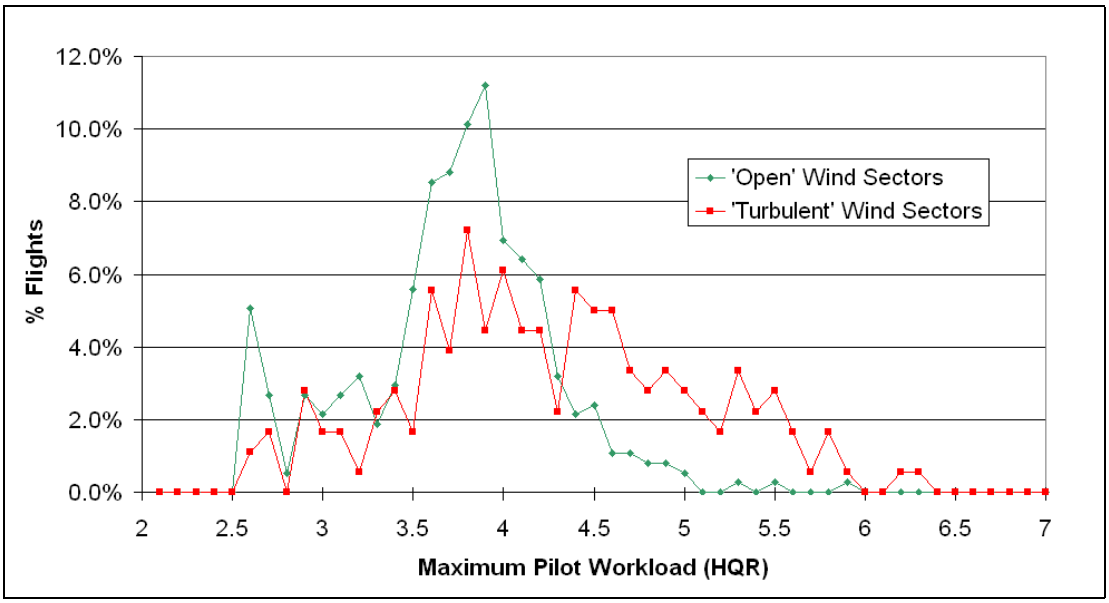

Figure 36 Workload distribution for 'open' and 'turbulent' sectors - Ninian Central

It cannot be said with certainty that the secondary peak of workload at about 2.7 is definitely due to the AFCS, but there is a certain amount of circumstantial evidence to suggest that this is the case. In any event the existence of the peak at such low workload levels would not appear to be a concern in the context of using the data to validate the turbulence criterion.

12.2.3 Location of Peak Workload

The maximum pilot workload can occur at any time during the approach and landing, and, in this analysis, data has been recorded from 500m out to the touchdown point. The workload values were plotted against the distance from touchdown at which the maximum occurred. It was found that the vast majority of maximum workload values occurred at touchdown, or very close to the touchdown point. In fact 82% of all maximum workload values were registered within 1m of the touchdown point, see Figure 37.

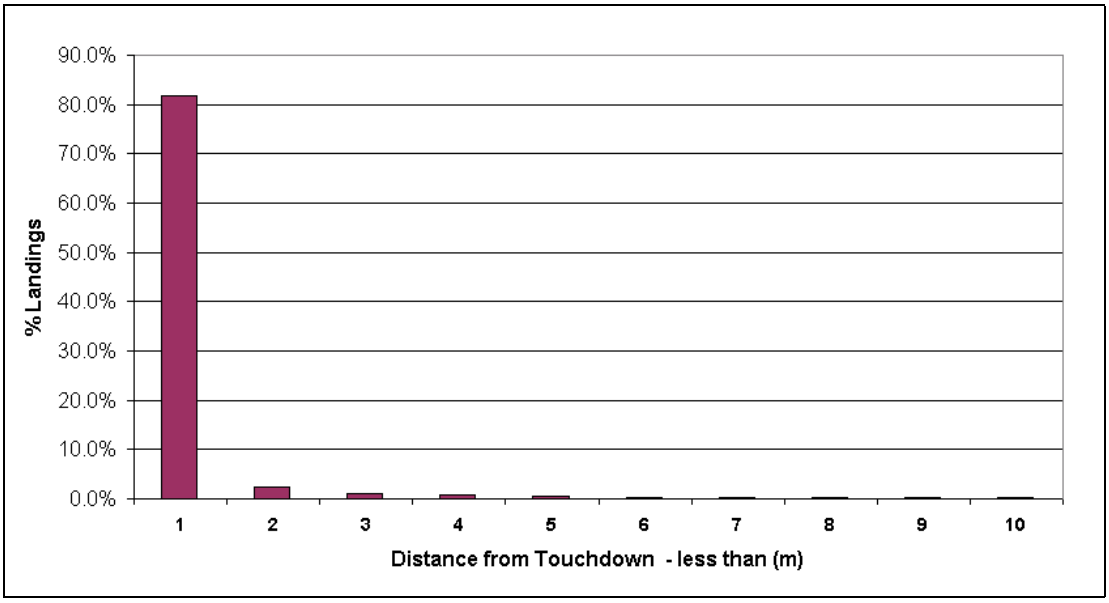

Figure 37 Location of Maximum Pilot Workload

This is not surprising for three reasons:

- Firstly, it would be expected that the worst turbulence would be experienced when the helicopter is flying at its closest proximity to the platform superstructure, and this occurs over the helideck.
- Secondly, the accuracy of flight path that the pilot is trying to achieve will be greater just before touchdown in order to hold position over the deck with good control of sink rate and no lateral motion, leading to more control activity.
- Thirdly, the workload algorithm is in part an integration of pilot control activity over a time window of 17s. Thus, the general increase in control activity observed as the helicopter approaches the helideck will take 17 seconds to achieve maximum effect on the predicted workload, placing the helicopter nearer to the touchdown point by a distance equivalent to 17 seconds of flight time.

The helicopter location at which this maximum workload is registered is therefore a little misleading. The maximum workload relates to activity over the past 17s, and does not therefore really equate to a specific point in space.

12.2.4 Correlation with Ambient Temperature and Rotor Torque Measurements

As part of other work on visualisation of hot gas plumes [11] and an investigation into the 0.9 m/s vertical wind speed component criterion [12], the HOMP database analysis included ambient temperature and rotor torque measurements. It was therefore decided to search for any significant correlations between the pilot workload and these parameters.

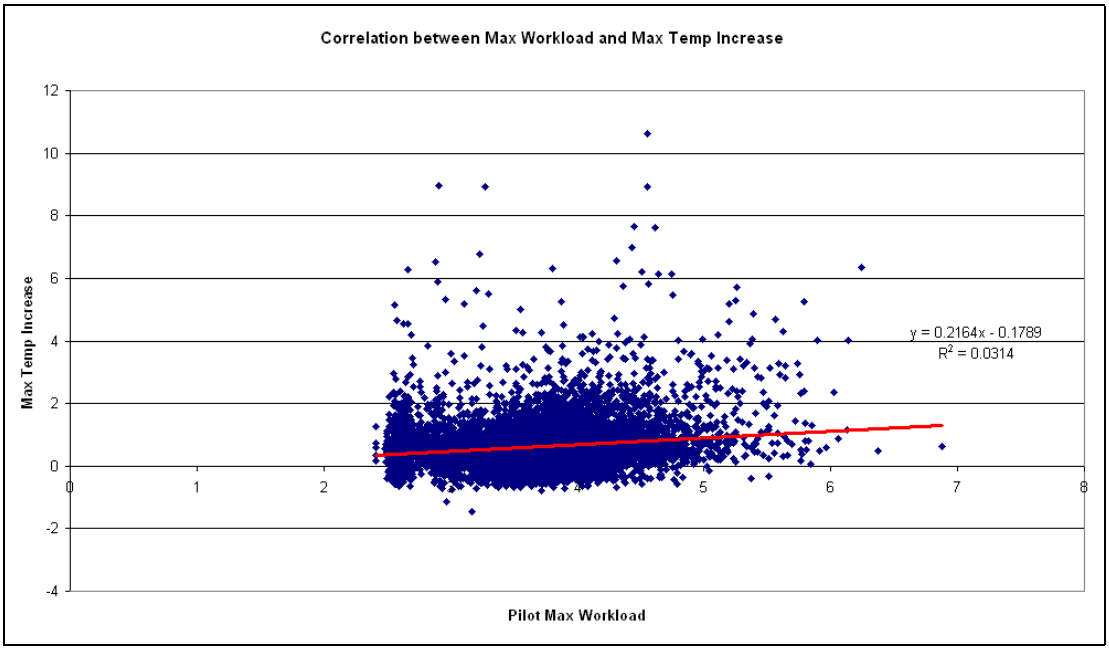

Figure 38 Correlation between maximum workload and maximum temperature increase

Figure 38 shows maximum pilot workload plotted against the maximum temperature increase for all valid landings in the database. The temperature increase was measured relative to a reference reading taken in the flight path 500m from the platform, and a small correction was included for the altitude difference assuming a standard lapse rate (2°C per 1000ft). It can be seen that there is a general trend of increasing workload with increasing maximum temperature, but the effect is not strong. This is not surprising for the overall population of workload data because, while it seems likely that disturbance to the helicopter caused by hot gas plumes will lead to increased workload, in many cases helidecks are not affected by any hot gas

hazards. In contrast, examination of the pattern of workload and temperature for individual platforms subject to hot gas effects is expected to show a stronger correlation (see for example Figure 31 and Figure 32 on pages 41 and 42 respectively, and described in Section 12.1). A similar weak correlation is seen between workload and maximum rotor torque in Figure 39. The correlation is much stronger between workload and maximum torque increase (over 2s) shown in Figure 40. This connection is not surprising given that the workload predictor is particularly sensitive to collective pitch control rate, and that a high rate of change of collective pitch will inevitably induce a rapid change in torque. (Note that the data presented in Figure 39 and Figure 40 has been limited to a helicopter landing weight range 17,000lb – 18,500lb in order to remove any major effects of weight on torque.)

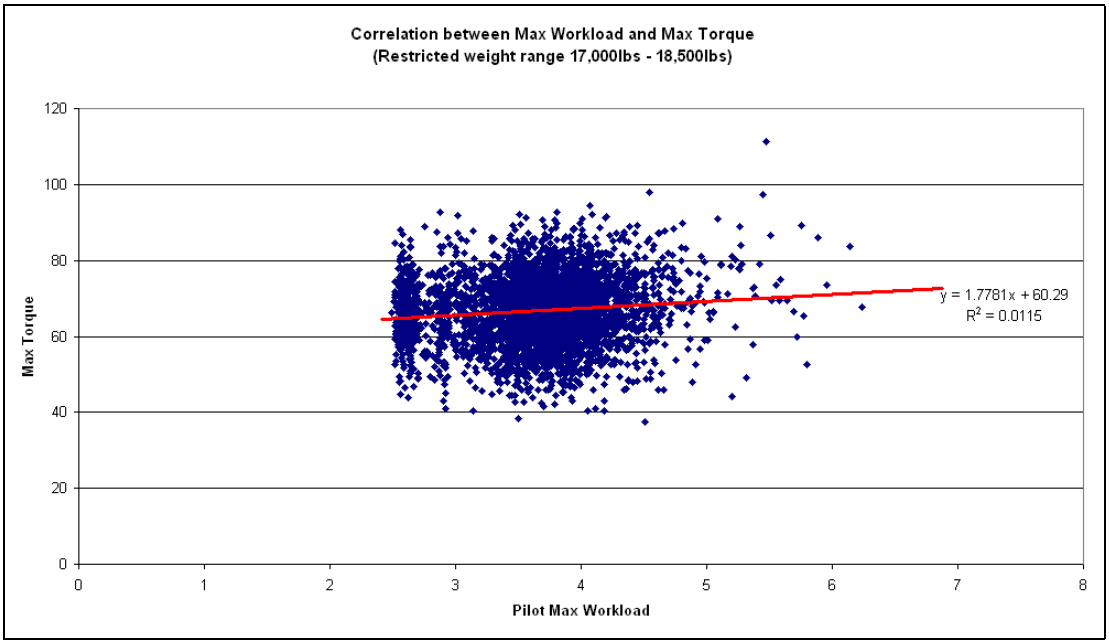

Figure 39 Correlation between maximum workload and maximum torque

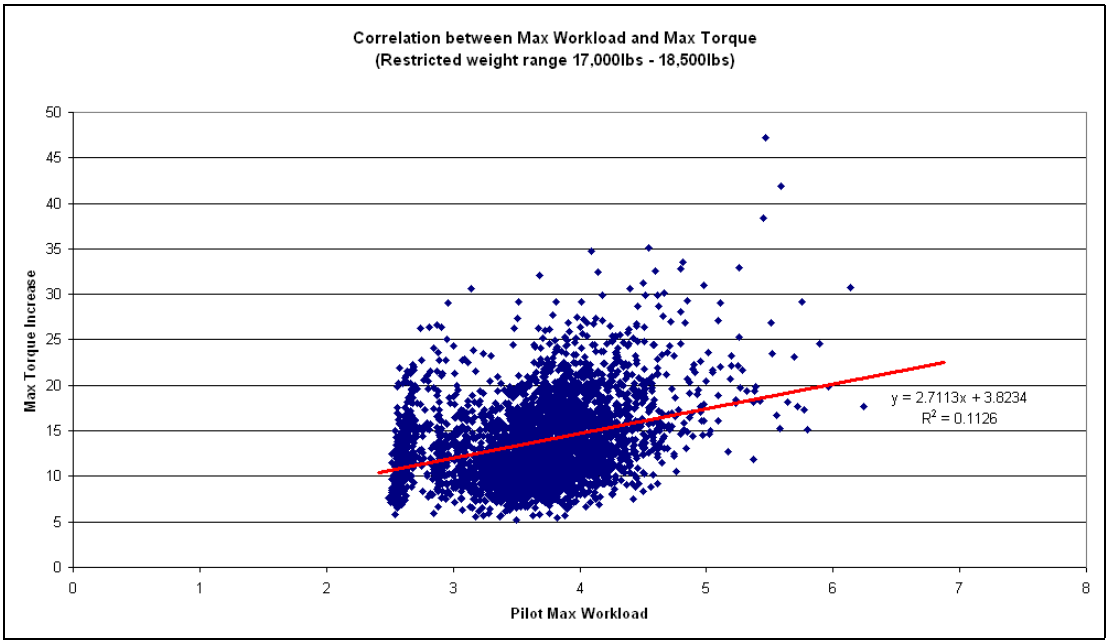

Figure 40 Correlation between maximum workload and maximum torque increase

12.2.5 **Discussion**

The analysis of the full 12,978 valid landings in the 16 month HOMP archive revealed that only one landing showed a pilot workload HQR>6.5. This was a value of HQR=6.88 recorded on a landing on the Heather A platform in a wind of 32 kt from 152 degrees.

On the presumption that the vast majority of flights are operated safely, the fact that only one landing in the archive recorded a maximum pilot workload over the HQR = 6.5 threshold (proposed as the workload limit for safe flight operations, and used to develop the turbulence criterion), may be taken as some evidence that the turbulence criterion is not set at too low a level.

The average level of pilot workload for all the landings was found to be HQR=3.69. The mean, 95-percentile and maximum values for the workload are summarised in Table 9 on page 44, which gives values for all landings, and segregated into wind from 'open' and 'turbulent' sectors where these are known.

It can be seen from Table 9 on page 44, that, taken over all the platforms for which sketches were available and for which open and turbulent wind sectors could be defined, there is a clear trend for workloads to be higher for the turbulent sectors. The 95 percentile and maximum workload values are both about 0.5 HQR greater for the obstructed wind directions. This difference between the two populations of landings is not particularly marked, but this will be due, at least in part, to 'dilution' by the large number of platforms that do not have serious turbulence issues even when the wind is blowing from a 'turbulent' direction.

When a platform known to suffer from a turbulence problem is examined, the difference between the open sector and turbulent sector populations becomes much more marked (see for example Ninian C in Figure 31 and Figure 36). In addition, the workload plots for the 8 selected platforms (presented in Figure 25 to Figure 33) show visually the clear correlation between high pilot workloads and wind directions where the helideck will be downwind of the bulk of the platform structure, and thus where the helicopter will be flying in the turbulent wake of the platform structure.

The evidence linking high pilot workload with turbulence is therefore considered to be very strong, and emphasises the need for a turbulence criterion on which helideck wind speed and direction limitations can be based.

12.3 **Comparison with the HLL**

The workload values calculated from the HOMP data can be compared with the operational experience to-date as documented in the HLL [2].The table given in Appendix C lists all the 70 installation helidecks included in the HOMP analysis that received more than 20 landings. The first 5 columns of the table contain basic HOMP data such as the platform name and the number of landings in the database. Column 6 contains a 'Y' if the heading of the installation is unknown (e.g. because it is a weather-vaning FPSO, or a mobile moored drilling unit). This prevents any useful plotting of the data on a wind direction basis. Columns 7 to 12 are taken directly from the HLL [2] and the size of the helideck and the details of any flight restrictions are added. HLL entries shaded contain no mention of turbulence or restricted wind sectors/speeds. Columns 13 to 15 briefly summarise the main features seen in the torque, temperature increase, and workload plots respectively. In many cases an entry NSF indicates 'No Significant Features', which means that the values seen are not particularly severe and/or form no discernible patterns. The final column 16 contains comments. In some cases (e.g. Alba Northern) these comments relate to apparent errors or anomalies in the helideck sketches or associated information. In other cases the comments highlight an apparent difference between the HLL and

what has been seen in the HOMP results, perhaps suggesting that the turbulent sector identified in the HLL might be extended (e.g. Britannia).

Overall, there is good consistency between the HOMP results and the turbulent sectors identified in the HLL. In the cases of Alba Northern, Britannia, Brent A, Brent B, Brent D, Magnus, Ninian C, and NW Hutton, there is the suggestion in the HOMP data that the HLL turbulent sectors might be extended or redefined slightly[5]. In the cases of Gannet and Heather A it is suggested that the HLL should include a defined turbulent sector. There appear to be errors in the helideck sketches for Alba Northern, Brae A, K14-FA-1, K15-FA-1 and North Cormorant.

Despite the good consistency of the data with the advice in the HLL, it is difficult to interpret this data, or the other comparisons with operational experience presented in this report, to verify that the turbulence criterion has not been set at too *high* a level. It was seen that only one landing out of 12,978 registered a workload higher than 6.5, which indicates that operationally such pilot workload/turbulence levels are only met very rarely. However, it is possible that the workload threshold for safe flight should in fact be set at a lower level, to offer a greater margin of safety, particularly for the less experienced pilot flying at night, in poor visibility or in otherwise challenging conditions. It is therefore considered important that pilots should continue to be strongly encouraged to submit turbulence reports, and that these reports should be correlated against HOMP pilot workload in order to look for any evidence of turbulence difficulties at lower pilot workload values. Any such evidence could be used to justify a reduction in acceptable level of pilot workload / HQR and the associated turbulence criterion. The discussion in Section 13 develops these points further.

12.4 Comparison with Wind Tunnel Data

BMT Fluid Mechanics holds an archive of wind tunnel test data for offshore installations that have been tested in its wind tunnels. However, only five of the BMT archive North Sea platforms were visited by Bristow helicopters during the period covered by the HOMP archive. These were; Clair, Britannia, Cormorant A, East Brae and Scott.[6]

HOMP data from Clair is not easy to interpret because there were only 72 landings recorded in the archive. However, these data are presented here in Figure 41 and it can be seen that the highest workload events occurred for wind directions in the range 120 to 190 degrees and speeds 20 to 35 kt.

The wind tunnel measured turbulence data for Clair is shown in Figure 42. The figure shows a blue area, the outer boundary of which indicates the wind speeds and directions at which the 2.4 m/s vertical component standard deviation turbulence criterion is violated[7]. Also shown is a green area, the outer boundary of the green area indicates wind speeds and directions at which a vertical turbulence standard deviation of over 1.75 m/s is experienced. The value of 1.75 m/s was selected here because it approximated to a HQR=5.5 in the flight simulator trials of [1] (see Figure 3 in Section 2) and is therefore more directly comparable with the higher workload values experienced in the HOMP data. For Clair it can be seen that the severest turbulence occurred for winds from headings 40-100 degrees. At these headings the turbulence limit is violated for winds of about 40 kt and above. The HOMP archive does not

5. Any such redefinition based on the HOMP data will need to take account of the likely accuracy of the HOMP wind speed and direction estimates (see Section 11).
6. There was also data for the MacCulloch FPSO, but this could not be interpreted owing to a lack of information on the vessel heading at the time of the landing in the HOMP database.
7. The notation of the figures uses the shorter abbreviation rms (root mean square). Standard deviation and rms are one and the same for a turbulence record that has already been corrected to zero mean.

include any winds of this magnitude from this direction for the Clair platform, nor does it include any pilot workload values of HQR>5.5, but it is noted that the highest workload events occur with winds from 135 to 190 degrees. [8]

In the case of Britannia there are 323 landings in the HOMP archive and so the data is easier to interpret. The HOMP data is presented in Figure 43 and the wind tunnel turbulence data in Figure 44.

It can be seen that the highest workload events (of which 4 are HQR>5.5) occur for wind directions in the range 90 to 140 degrees and speeds 25 to 40 kt. The wind tunnel data shows that turbulence in excess of 1.75 m/s and thus HQR>5.5 would be expected to occur for directions 80 to 150 degrees and wind speeds above 30 to 40 kt. The wind tunnel data and the HOMP data are therefore consistent for this platform.

For Cormorant A the HOMP data is presented in Figure 45 and the wind tunnel data in Figure 46.

It can be seen that the majority of higher pilot workload events occur for wind speeds in the heading range 135-180 degrees and speeds 25-40 kt. This is again broadly consistent with the wind tunnel data, which shows that turbulence in excess of 1.75 m/s would be experienced for wind speeds of around 35 kt at a heading of 225 degrees. This coincides with the single very high workload value that occurred with a wind speed of 40 kt at 225 degrees.

HOMP data for East Brae is presented in Figure 47, and the wind tunnel turbulence data is shown in Figure 48. It is evident from the wind tunnel data that the worst turbulence is expected to occur with wind headings in the range 340 to 80 degrees with the turbulence criterion being violated for wind speeds above about 30 to 40 kt. However there have been no landings recorded in the HOMP database for wind speeds above 25 kt for these headings. This is consistent with the HLL entry for this platform which warns of turbulence for headings in the range 335 to 035 degrees and speeds above 30 kt. The evidence from the HOMP data is that these wind conditions are indeed being avoided.

Data for the Scott platform is shown in Figure 49 and Figure 50. The wind tunnel data in Figure 50 shows that there is reasonably high turbulence for a number of wind directions, but the worst wind headings are 345-080 degrees where the turbulence criterion is violated at a wind speed of about 40 kt. The HOMP data shows no landings at wind speeds above 30 kt for these headings. There is no turbulence entry for Scott in the HLL.

The figures are evidence of validation of the turbulence criterion as defined in [1].

8. Only one landing exhibited a high workload at a 190 degree wind heading, and it is possible that this is an example of an individual poor estimate of direction from the HOMP analysis.

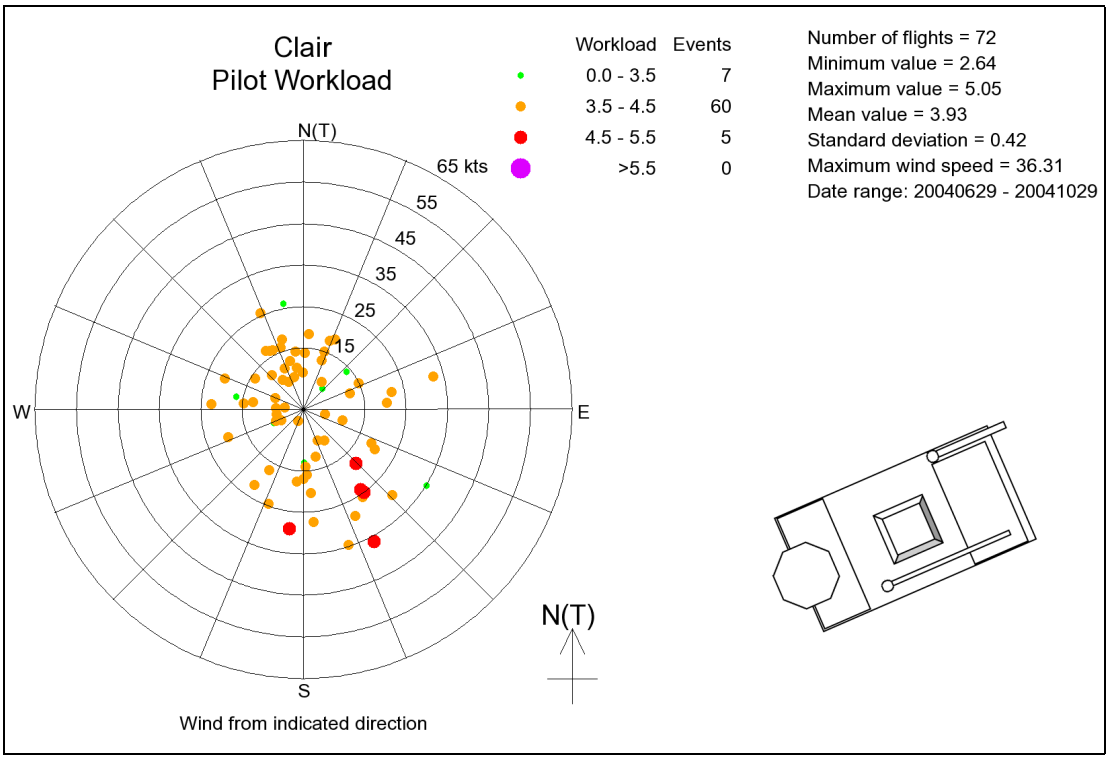

Figure 41 Clair Platform pilot workload

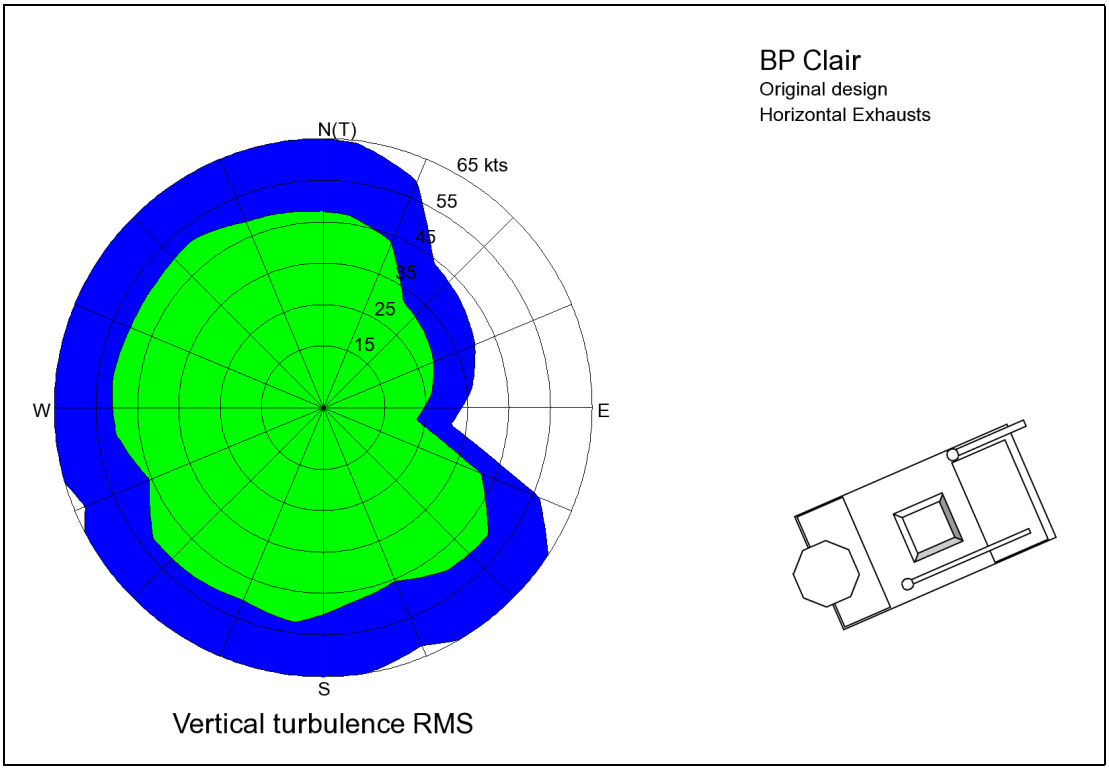

Figure 42 Clair Platform vertical turbulance – green boundary u_{rms}>1.75 m/s, blue boundary u_{rms} >2.4 m/s

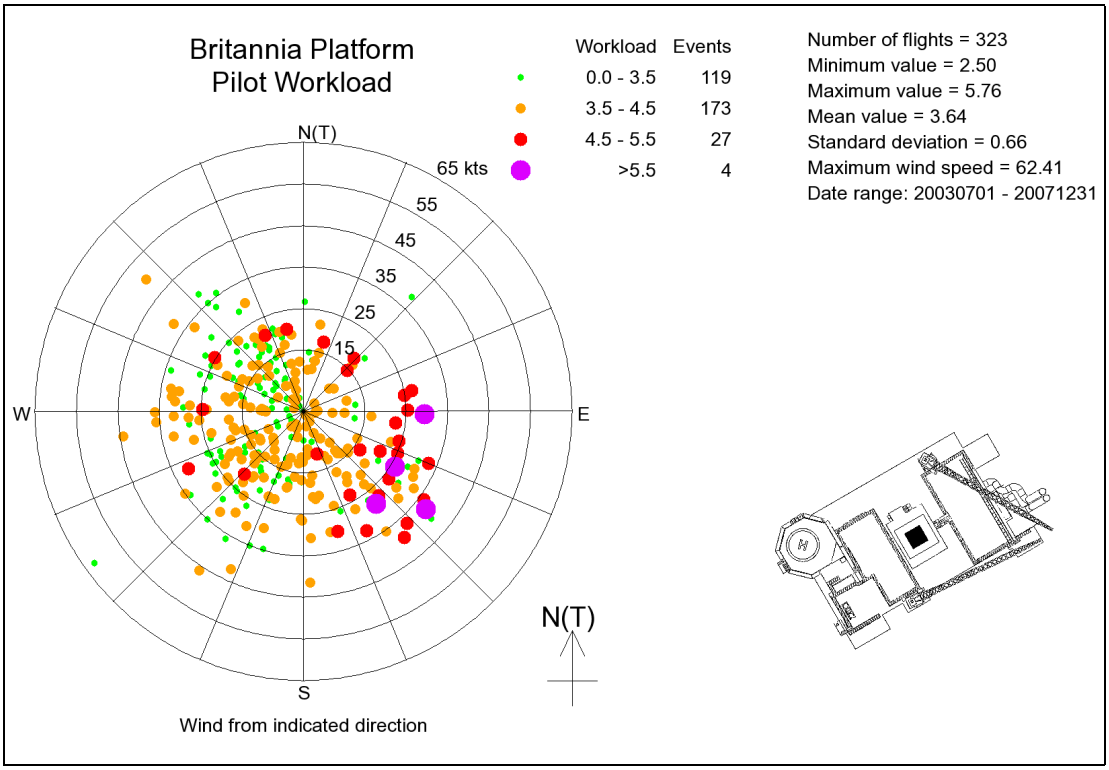

Figure 43 Brittania Platform pilot workload

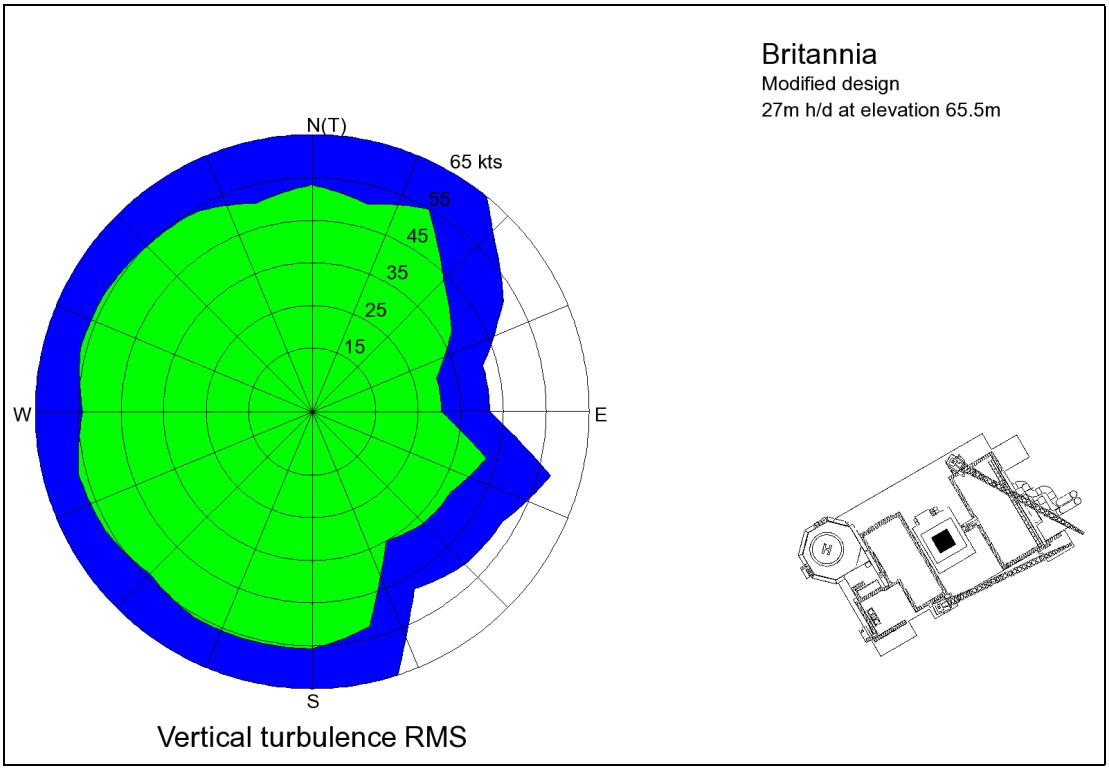

Figure 44 Britannia Platform vertical turbulance – green boundary u_{rms}>1.75 m/s, blue boundary u_{rms} >2.4 m/s

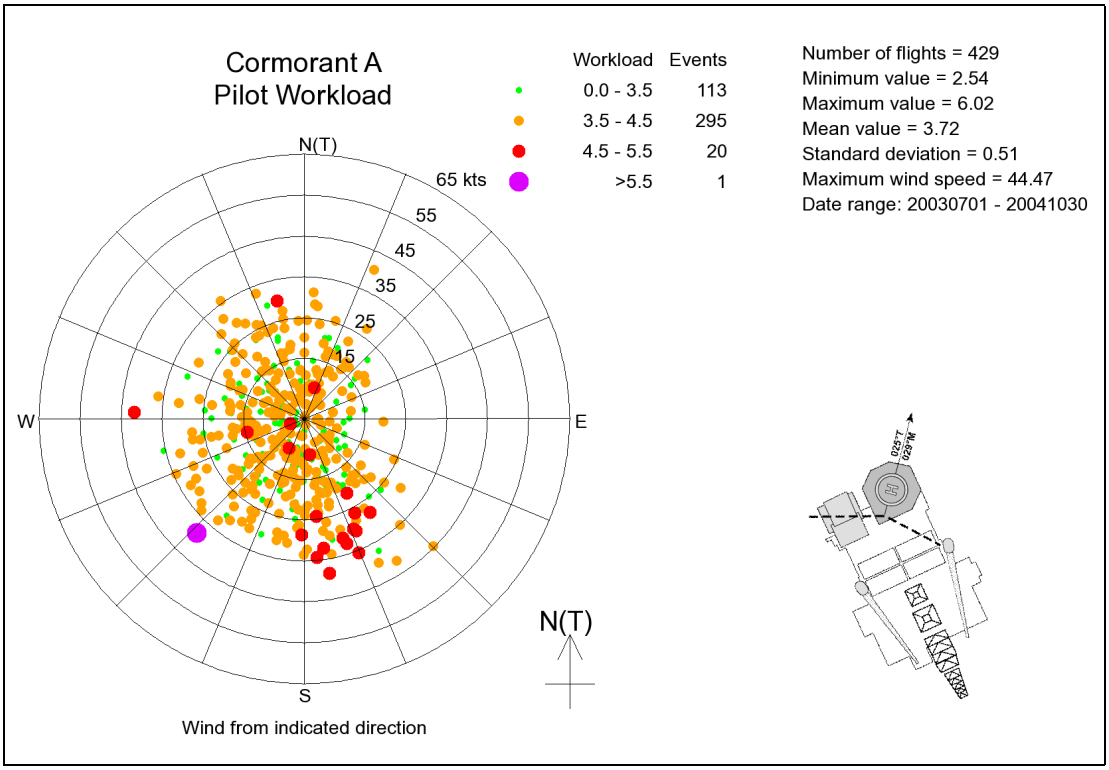

Figure 45 Cormorant A Platform pilot workload

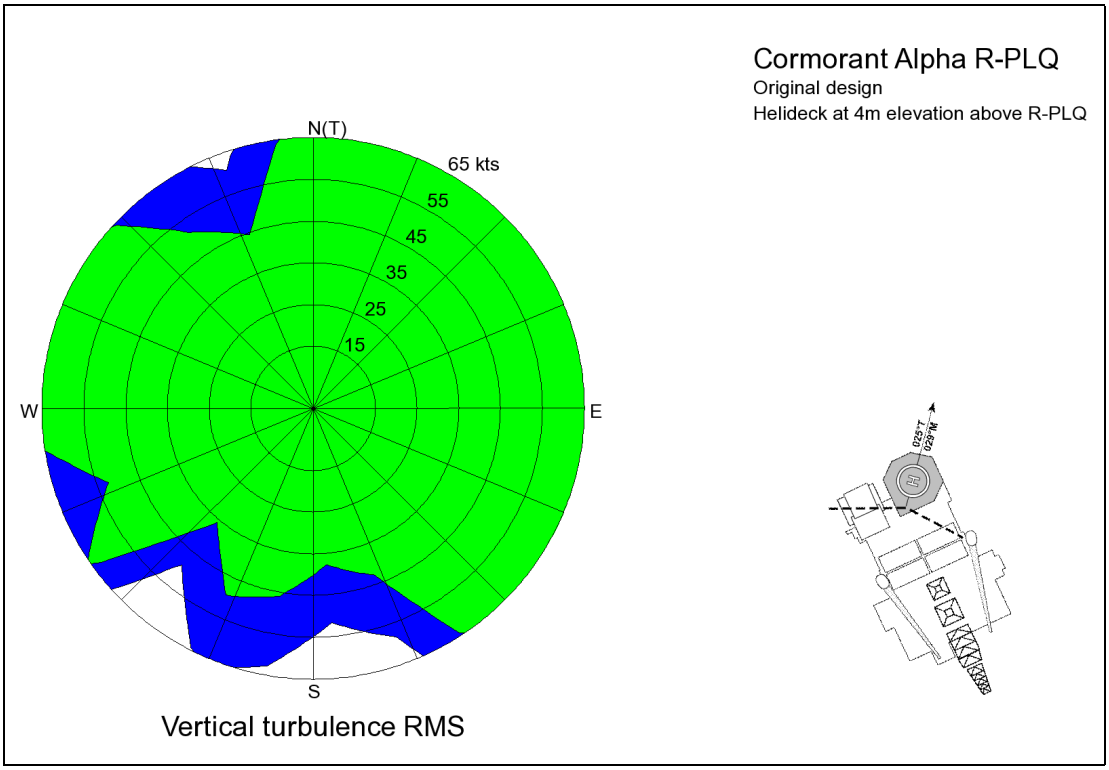

Figure 46 Cormorant A Platform vertical turbulance –
green boundary u_{rms}>1.75 m/s, blue boundary u_{rms} >2.4 m/s

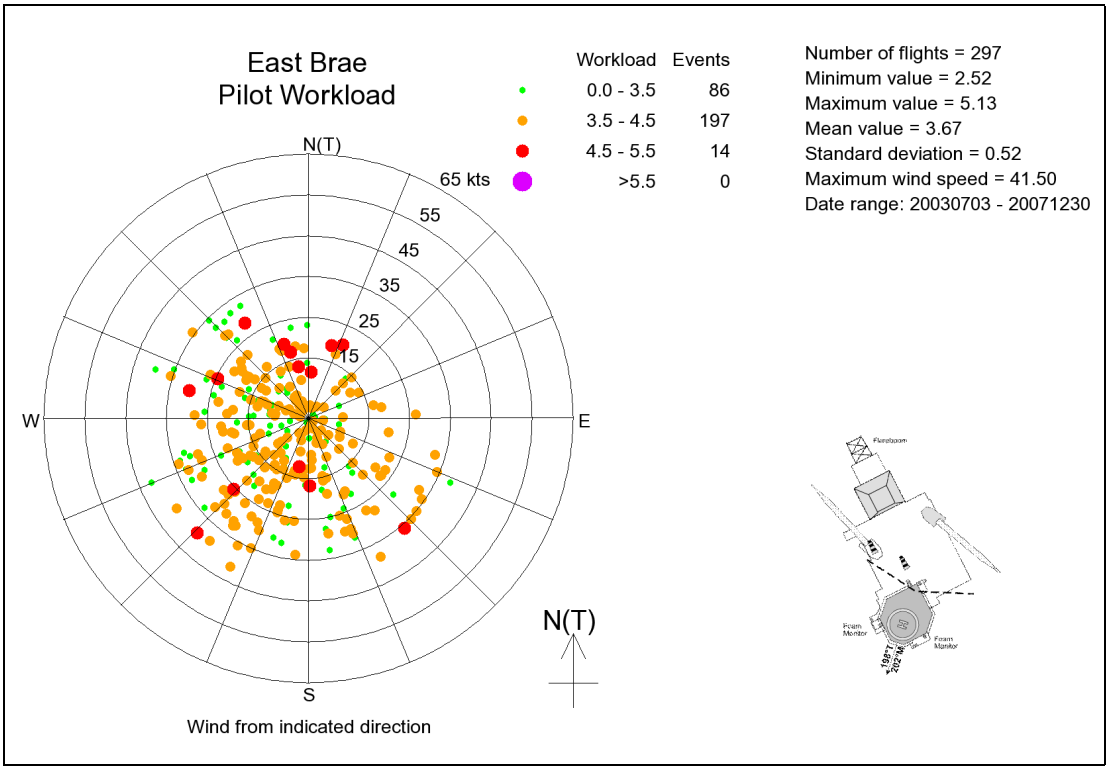

Figure 47 East Brae Platform pilot workload

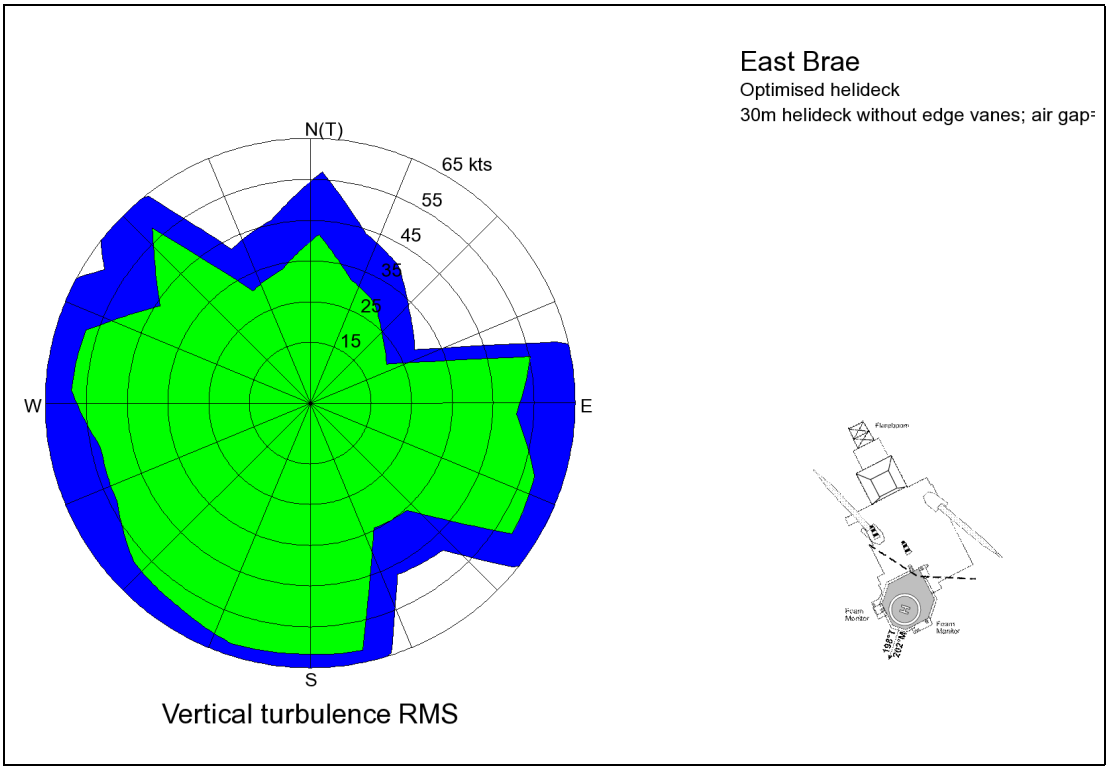

Figure 48 East Brae Platform vertical turbulance – green boundary u_{rms}>1.75 m/s, blue boundary u_{rms} >2.4 m/s

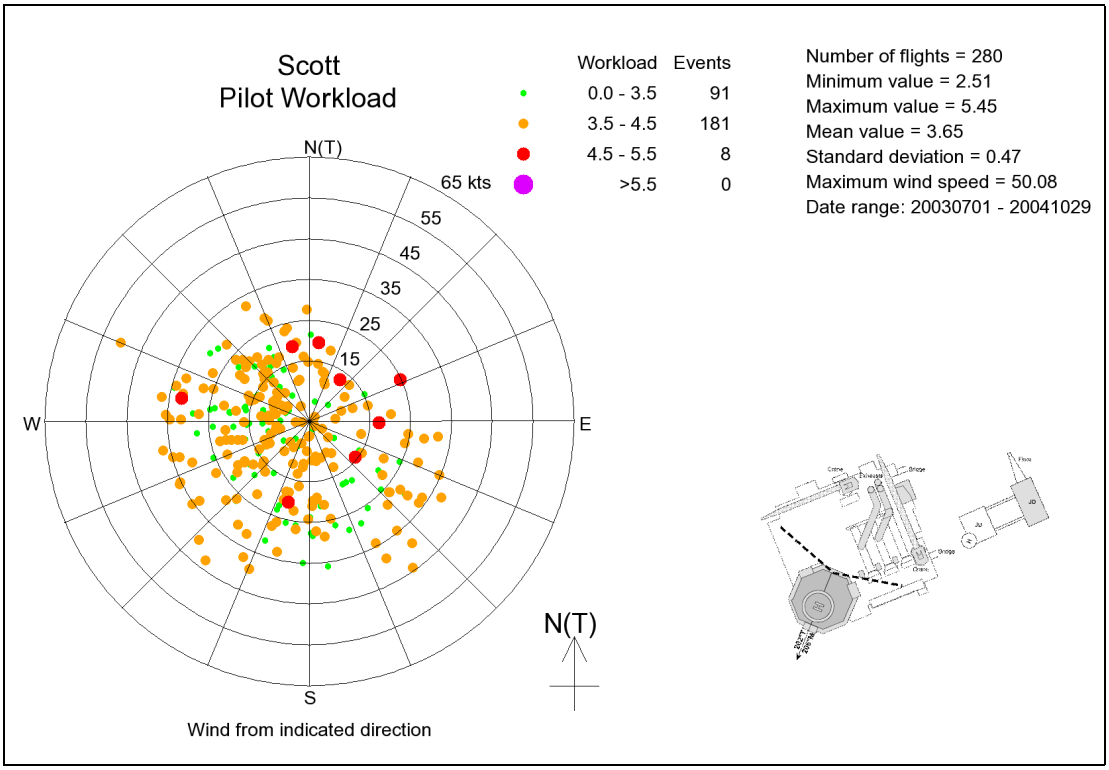

Figure 49 Scott Platform pilot workload

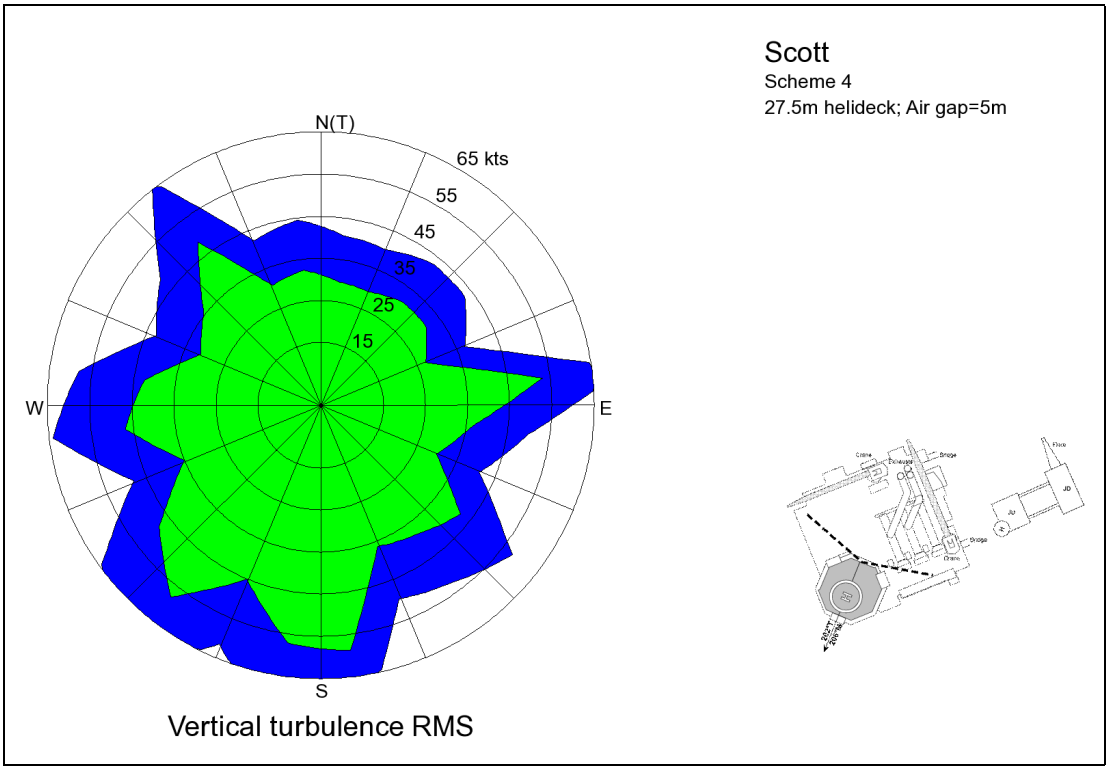

Figure 50 Scott Platform vertical turbulance – green boundary u_{rms}>1.75 m/s, blue boundary u_{rms} >2.4 m/s

12.5 Selected HOMP time series

Landings for 6 platforms were selected for detailed study on the basis of a clear trend of high workload with certain wind speed/direction combinations. The selected platforms were; Brent A, Brent B, Brent C, Britannia, Cormorant A and Ninian C. The top four pilot workload events recorded from each platform were then selected, checking that these events occurred within a clear pattern of wind speeds and directions (i.e. were not anomalous), giving a total of 24 selected landings. In only one case (Cormorant A) was it found that the 4th-ranked event was not part of the general wind speed direction pattern for high workload events, and so the 5th-ranked event was selected in its place. The selected landings are listed in Table 10.

Whilst examining the selected landings it was noted that they varied significantly in terms of the time taken to make the approach from 500m and the landing. Table 11 shows the time and the average speed from 500m out to touchdown. It also shows the time taken to fly the last 2m, and the time taken to fly the last 5m. It can be seen that the average speed over the ground from 500m varies between 3 m/s and 18 m/s, and the time in the hover (if we take it as the time taken to travel the final 5m to the touchdown point) varies from 3s to 17s. This would appear to indicate a wide range of landing techniques. However, when the speed over the ground for the 500m is corrected for wind speed into an approximate air speed (making the assumption that the approach is into wind) it can be seen that the airspeed range now varies between 19 m/s and 37 m/s with an average airspeed of 26.7 m/s (a little over 50 kt).

When a small number of relatively low workload landings were analysed in the same way, the range of speeds and hover times did not appear to be significantly different from the selected high workload landings.

These speeds and times have been plotted against the maximum workload in the following figures in order to seek any correlation. Figure 51 shows the time in the hover from 5m, and it is apparent that there is no correlation with the maximum workload. Similarly Figure 52 shows the same result for the time taken to cover the final 2m. Figure 53 shows the average speed over the ground from 500m to touchdown plotted against the maximum workload, and it is apparent that there is a very slight tendency for lower maximum workload in the faster approaches. This might indicate that more difficult approaches are taken slower, but the effect is very slight and perhaps not significant, and when the ground speed is corrected for wind speed into an estimated airspeed for the 500m of approach in Figure 54 the correlation is completely absent.

Table 10 High workload landings selected for detailed examination

Top 100 rank	LNDAP	Platform Name	Reg	DEPDATE	GMTTO	LAT_AT_TD	LONG_AT_TD	MX_W ORK_L DG	MX_W ORK_X DIST	MX_W ORK_Y DIST	COR_M X_WSP DLDG	COR_M X_WAN GLDG	MX_CO RWSPD LDG
20	BRITP	Britannia Platform	GBLRY	20041001	1219	58.05	1.13	5.76	-0.61	0.83	27.20	125.00	25.97
21	BRITP	Britannia Platform	GTIGT	20040429	1218	58.05	1.13	5.76	0.00	0.00	32.59	95.43	29.37
31	BRITP	Britannia Platform	GTIGT	20040421	638	58.05	1.13	5.63	0.00	0.00	32.60	145.62	28.48
34	BRITP	Britannia Platform	GBWWI	20040401	1209	58.05	1.13	5.60	0.00	0.00	44.00	132.60	37.92
6	BRNTA	Brent A	GTIGF	20040304	809	61.03	1.70	6.06	-2.29	1.99	38.00	169.80	33.63
14	BRNTA	Brent A	GBLPM	20040402	828	61.03	1.70	5.81	-0.21	0.14	36.19	140.61	31.97
27	BRNTA	Brent A	GTIGG	20031112	1440	61.03	1.70	5.66	-0.20	0.16	44.00	173.60	38.59
37	BRNTA	Brent A	GBWMG	20031126	1200	61.03	1.70	5.58	0.00	0.51	42.72	140.24	37.92
11	BRNTB	Brent B	GBWMG	20031127	1041	61.06	1.71	5.85	-0.38	0.35	45.78	157.77	41.58
18	BRNTB	Brent B	GTIGG	20040123	1538	61.06	1.71	5.79	0.47	3.78	29.60	165.00	26.96
29	BRNTB	Brent B	GTIGG	20040108	1423	61.06	1.71	5.64	-0.42	3.99	42.60	147.21	39.11
60	BRNTB	Brent B	GTIGR	20040916	1133	61.06	1.71	5.41	0.00	0.00	29.75	160.91	26.51
13	BRNTC	Brent C	GTIGL	20040110	944	61.10	1.72	5.82	0.00	0.00	47.79	161.18	42.75
38	BRNTC	Brent C	GTIGB	20040304	1514	61.10	1.72	5.58	-0.06	0.25	40.00	159.57	35.79
45	BRNTC	Brent C	GBWWI	20030911	1644	61.10	1.72	5.51	-0.04	0.51	25.00	179.20	21.93
47	BRNTC	Brent C	GTIGB	20040304	852	61.10	1.72	5.51	0.40	2.26	38.40	174.21	34.11
51	CORMA	Cormorant A	GTIGB	20040903	1333	61.10	1.07	5.47	-4.02	9.18	33.38	159.95	29.62
74	CORMA	Cormorant A	GTIGB	20040903	1222	61.10	1.07	5.32	0.00	0.00	29.80	155.83	26.20
84	CORMA	Cormorant A	GTIGL	20040203	1405	61.10	1.07	5.27	0.00	0.00	21.60	154.22	21.04
0	CORMA	Cormorant A	GTIGB	20040903	1408	61.10	1.07	5.12	-0.08	0.24	34.00	159.20	30.35
3	NIC	Ninian C	GTIGF	20040304	1136	60.86	1.47	6.24	-0.27	3.93	41.00	151.80	36.01
4	NIC	Ninian C	GTIGB	20040415	1448	60.86	1.47	6.14	-0.93	1.23	28.15	172.41	25.79
10	NIC	Ninian C	GTIGG	20031107	1620	60.86	1.47	5.89	-0.28	0.42	34.80	186.00	30.80
15	NIC	Ninian C	GTIGR	20041005	730	60.86	1.47	5.80	0.00	0.00	36.80	198.00	32.43

Table 11 High workload landings selected for detailed examination with speed and time

Top 100 rank	LNDAP	Platform Name	MX_WORK_LDG	Time from 500m (s)	Ave speed (m/s)	Ave air speed (m/s)	Time from 2m (s)	Time from 5m (s)
20	BRITP	Britannia Platform	5.8	45.0	11.1	24.5	3.5	6.0
21	BRITP	Britannia Platform	5.8	31.5	15.9	31.0	6.0	8.0
31	BRITP	Britannia Platform	5.6	27.0	18.5	33.2	5.5	6.5
34	BRITP	Britannia Platform	5.6	28.5	17.5	37.1	2.0	3.0
6	BRNTA	Brent A	6.1	60.0	8.3	25.6	5.5	9.5
14	BRNTA	Brent A	5.8	167.5	3.0	19.4	6.0	8.5
27	BRNTA	Brent A	5.7	64.0	7.8	27.7	6.5	11.5
37	BRNTA	Brent A	5.6	42.0	11.9	31.4	3.5	4.5
11	BRNTB	Brent B	5.9	59.0	8.5	29.9	9.0	12.0
18	BRNTB	Brent B	5.8	47.0	10.6	24.5	7.0	9.5
29	BRNTB	Brent B	5.6	79.0	6.3	26.5	5.0	17.0
60	BRNTB	Brent B	5.4	49.0	10.2	23.9	5.0	7.5
13	BRNTC	Brent C	5.8	62.0	8.1	30.1	9.0	12.0
38	BRNTC	Brent C	5.6	43.5	11.5	29.9	4.5	6.0
45	BRNTC	Brent C	5.5	46.5	10.8	22.0	6.5	8.0
47	BRNTC	Brent C	5.5	82.5	6.1	23.6	4.0	5.5
51	CORMA	Cormorant A	5.5	39.0	12.8	28.1	4.0	6.0
74	CORMA	Cormorant A	5.3	40.0	12.5	26.0	7.0	9.0
84	CORMA	Cormorant A	5.3	54.0	9.3	20.1	5.5	8.5
0	CORMA	Cormorant A	5.1	44.5	11.2	26.9	7.0	9.0
3	NIC	Ninian C	6.2	85.5	5.8	24.4	4.5	9.0
4	NIC	Ninian C	6.1	48.5	10.3	23.6	6.0	8.5
10	NIC	Ninian C	5.9	57.5	8.7	24.6	4.0	5.5
15	NIC	Ninian C	5.8	49.5	10.1	26.8	5.0	7.5
		Average		**56.4**	**10.3**	**26.7**	**5.5**	**8.3**
		Minimum		**27.0**	**3.0**	**19.4**	**2.0**	**3.0**
		Maximum		**167.5**	**18.5**	**37.1**	**9.0**	**17.0**
		Standard Deviation		**28.2**	**3.6**	**4.1**	**1.7**	**2.9**

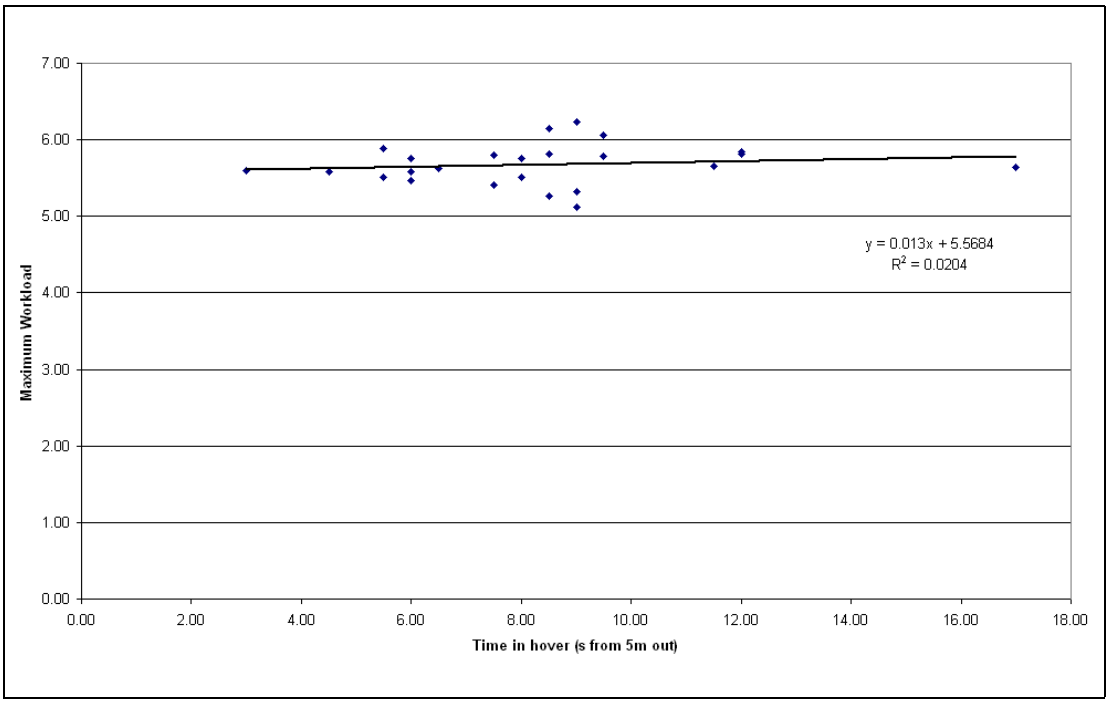

Figure 51 Showing lack of correlation between time in hover (time to cover last 5m to touchdown)

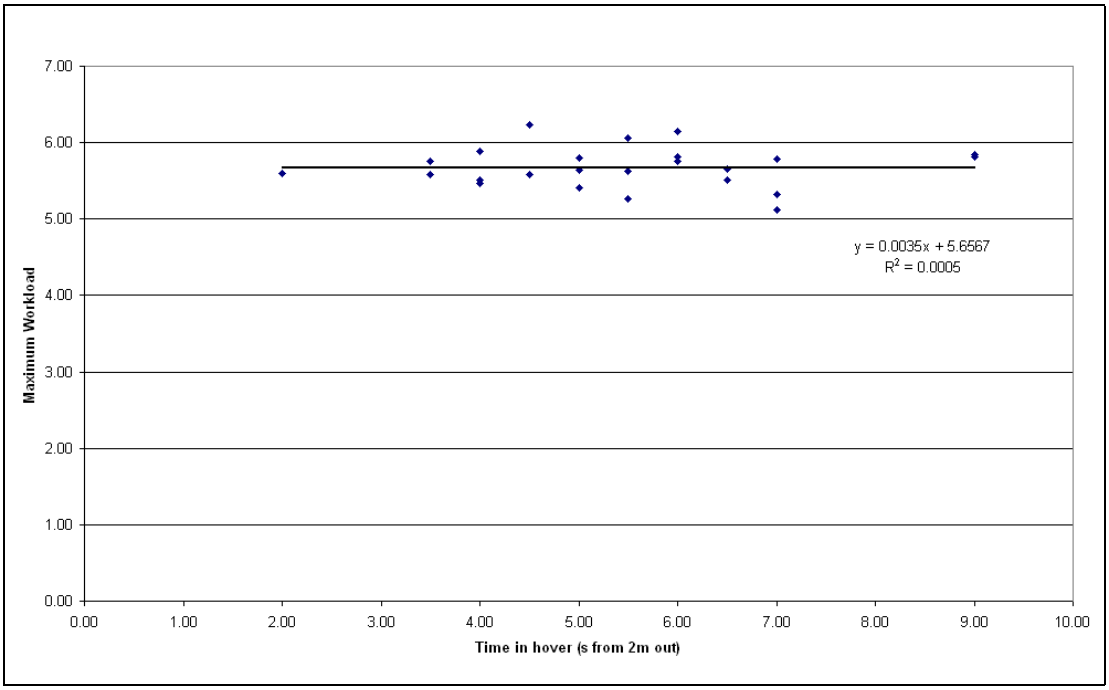

Figure 52 Showing lack of correlation between time in hover (time to cover last 2m to touchdown)

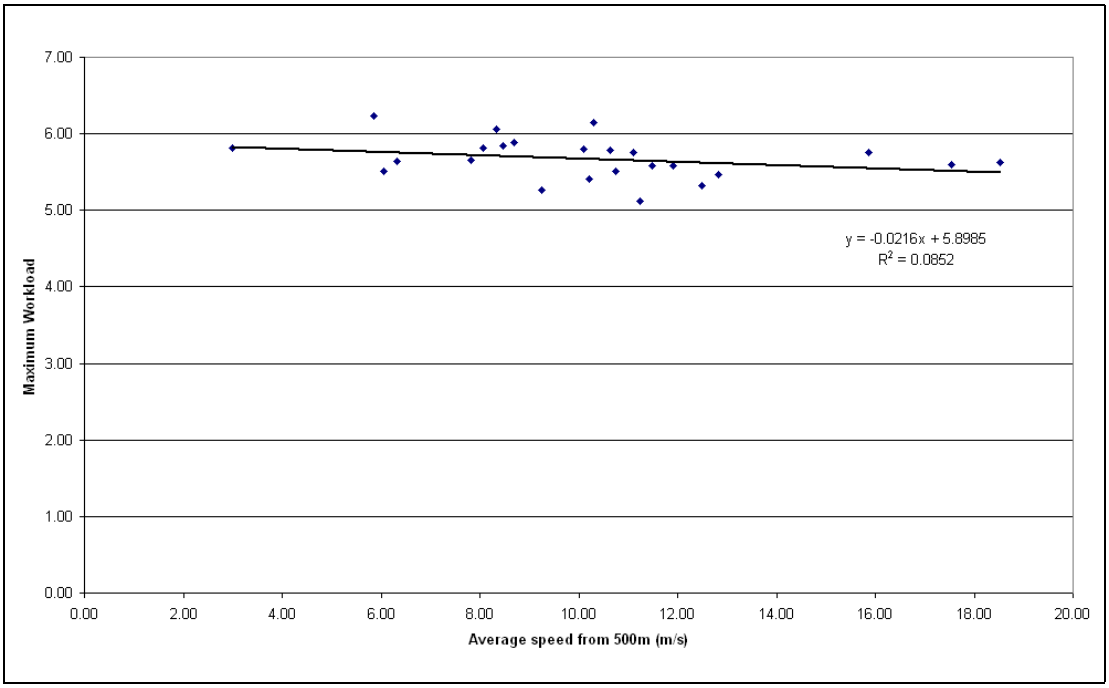

Figure 53 Showing lack of correlation between speed of approach and workload

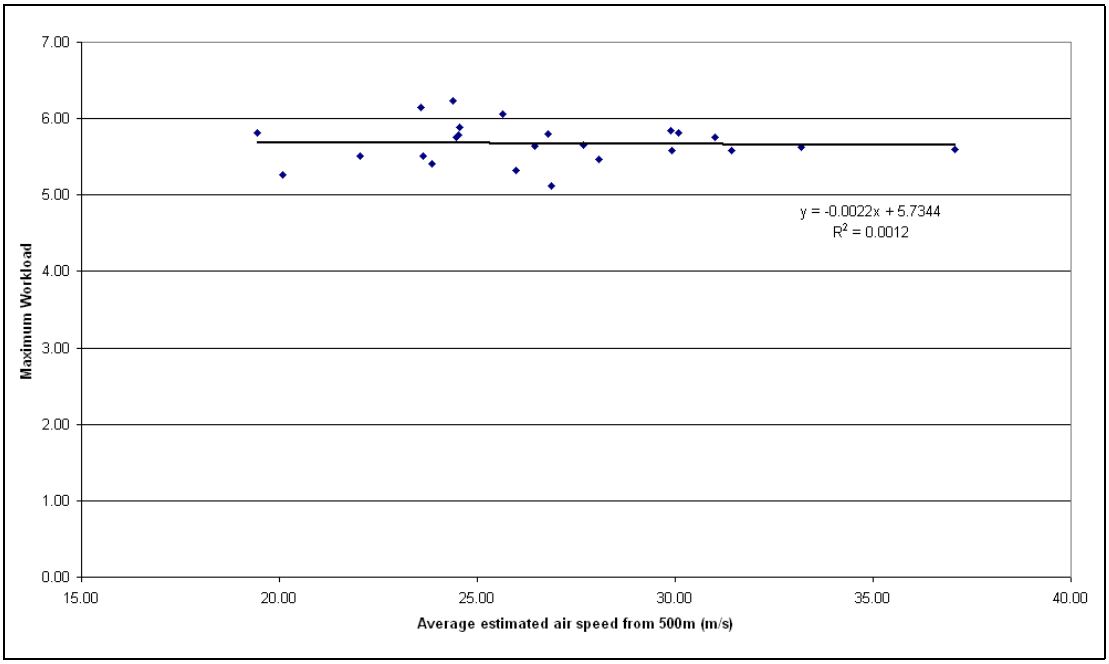

Figure 54 Showing lack of correlation between estimated airspeed of approach and workload

Appendix D shows the HOMP time series traces for the selected 24 high workload landings. In addition, 6 relatively low workload landings (all but one had a workload less than 3.0) are shown starting on Appendix D page 25. The traces show the last minute of the approach to touchdown.

The traces provide a graphic demonstration of how the workload algorithm works, and particularly the effect of the 17s 'window' over which the standard deviation of the control activity is evaluated. Figure 55 shows a detail from one of the landing traces presented in Appendix D.

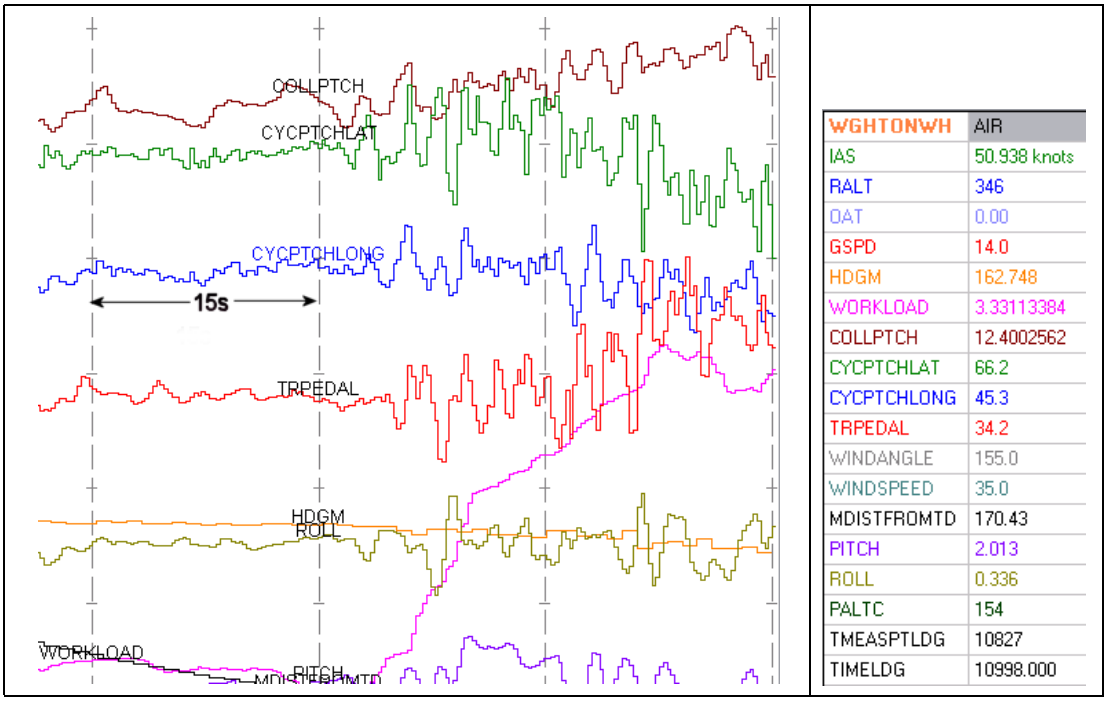

Figure 55 Detail of HOMP trace

It can be seen that the magenta workload trace starts at a low value at the bottom left of the figure, and remains at this low value for about 20 seconds (the vertical lines are 15s apart). It can be seen that during the first 20 seconds the collective pitch, and both axes of the cyclic pitch have relatively little activity. However, at about the 20s point there is considerable control activity in all axes starting with a burst of high activity and then reducing slightly. This is seen to produce an initial sharp rise in the workload followed by a lessening of the rate of increase. The workload continues to rise until about 17s after the start of the activity when it levels out although the control activity continues. This illustrates the effect of the 17s window. To register a high workload value control activity must be sustained for a number of seconds.

Plan views of the approach path were examined for each of the selected landings. In the vast majority of cases the approach from 500m out was relatively straight as shown in the example in Figure 56. However, in a very few cases the approach contained a sharp turn in relatively close proximity to the helideck, as shown in the example in Figure 57.

While generally interesting, the examination of the time series of the selected landings did not lead to any additional important insights into the nature of the high workload events.

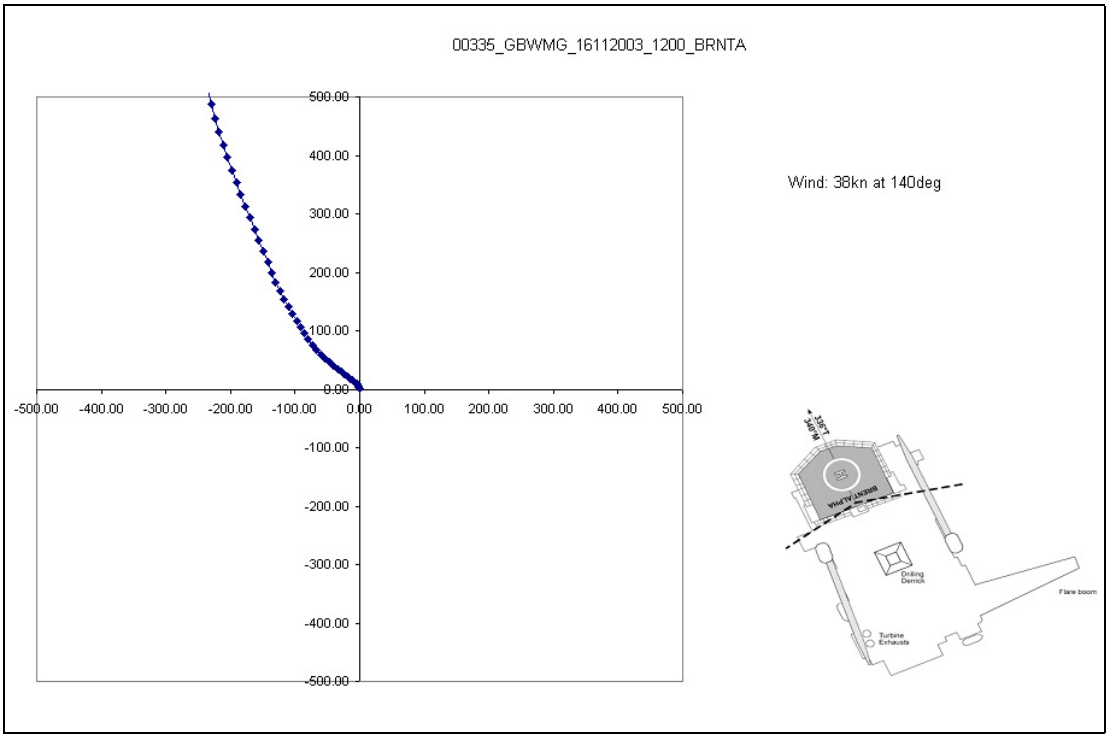

Figure 56 Example plan view of approach path

.

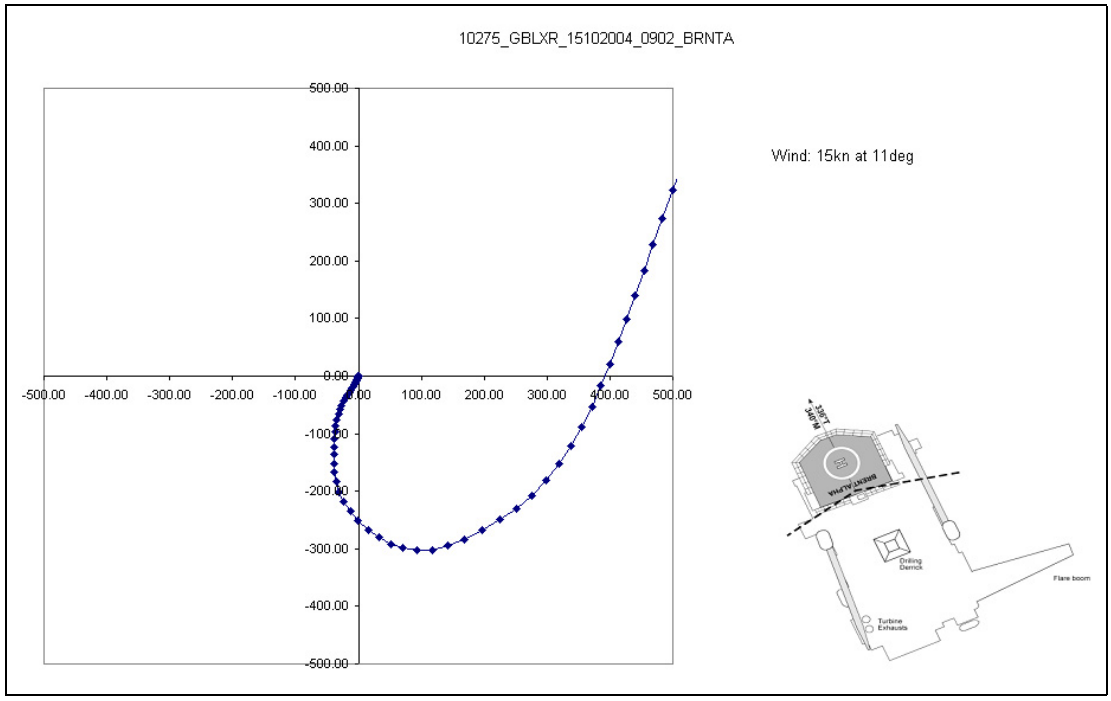

Figure 57 Example plan view of approach path

13 Discussion

The provisional turbulence criterion specified in the guidance [3] was set at 2.4 m/s based on the pilot workload boundary between safe and unsafe flight of HQR=6.5 (Section 2 and [1]). At the time it was noted that this criterion had been based on the assessment of three experienced test pilots flying a simulator in ideal visual cueing conditions. The criterion made no allowance for flight in reduced visual cueing conditions due to darkness, precipitation (rain, snow, hail) or poor visibility (mist, fog, low cloud), or for the less able or less experienced pilot. A clear link between pilot workload and visual cueing conditions has been established in other research [13]. It was evident from the outset, therefore, that there might be strong arguments for a reduction of the provisional turbulence criterion to a lower level to provide some allowance for these factors.

In the analysis of pilot workload from the HOMP data presented in this report (Section 12), it has been seen that only one helideck landing in 12,978 generated a pilot workload that exceeded the HQR=6.5 value. Such a frequency, however, seems inconsistent with the findings of an earlier pilot questionnaire survey [14], in which the pilots identified the principal safety hazard and source of highest workload during offshore operations as turbulence around platforms. It also conflicts with anecdotal evidence collected from a small sample of offshore pilots during a presentation in Aberdeen in November 2006 which suggests that, on average, pilots consider around 1 in 50 helideck landings to be significantly affected by turbulence.

If turbulence reports had been submitted by pilots during the 16-month period covered by the HOMP data archive, then these could have been correlated with the HOMP pilot workload values to help establish a lower limit. Unfortunately, however, the turbulence reporting system appears to have fallen into disuse, and there were no turbulence reports submitted during the period in question.

In addition to the above, there are also a number of confusing factors inherent in the application of the workload algorithm developed in the simulator to the HOMP data:

- Firstly, there is the much lower sampling rate of the HOMP data compared with that in the simulator. The effect of the lower sampling rate is to reduce the estimate of the pilot workload (see Figure 10). It was decided that no correction would be made to the coefficients to compensate for this effect, thus the data from HOMP will be an ***under-estimate*** of the actual workload experienced by the pilot. From Figure 10 the amount of the under-estimate appears to be of order 1 HQR point.
- Secondly the workload algorithm was adapted with a window and a filter in order to operate on the non-stationery HOMP data. When this filtering and windowing algorithm was applied to the simulator approach data it was found that the algorithm resulted in an ***over-estimate*** of the workload compared with the test pilot assigned value (see Figure 16). From the Figure it appears that this over-estimate might be in the range 1 to 2 HQR points for estimated HQRs in the range 4 to 8. That is, estimated 4 to 8 should be 3 to 6.
- Finally, the control movements measured in HOMP include the contribution from the AFCS for the cyclic control. This will result in an ***over-estimate*** of the actual workload experienced by the pilot.

As explained in Section 9.2, the first two effects approximately cancel each other out and so, on balance, we should expect the HOMP data to over-estimate the actual pilot workload somewhat leading to a higher than expected number of exceedances. Despite this, however, there is only 1 flight in 12,978 registering a workload above the 6.5 threshold.

In addition, the presence of AFCS (stability augmentation) on the collective control of the flight simulator, but not on most offshore helicopters, will have meant that the turbulence criterion will be non-conservative (see Section 8.5), i.e. too high.

All this appears to argue strongly that the turbulence criterion, and the associated pilot HQR limit for safe flight, ought to be reduced. If the anecdotal rate of 1 in 50 landings is accepted as being representative, the reduction applied should be sufficient to result in around 260 exceedances for the period covered by the HOMP data archive analysed. This would lead to an HQR threshold of about 5 which, given the nature of the HQR scale, would mean setting the limit at the boundary between HQR=4 and HQR=5, i.e. at HQR=4.5. However, there is also the effect of the presence of AFCS operating on the collective control in the simulator, which implies a degree of under estimation of the workload (see Section 8.5). In view of this and the uncertainty of the 1 in 50 rate, it could be argued that reducing the limit by two HQR points to 4.5 would be unduly restrictive. If an HQR limit of 6.5 is too high and a limit of 4.5 is possibly too low, an obvious option would be to initially set the limit at HQR=5.5. For the HOMP data archive, this would result in 62 exceedances, i.e. a rate of 1 in 211.

Taking all of the above into account, it is recommended that the turbulence criterion should now be set at 1.75 m/s (equivalent to HQR=5.5). In addition, it is proposed that the criterion be refined further based on in-service experience and, in particular, from turbulence reports from pilots. The launch of turbulence encounter monitoring and turbulence mapping using routine HOMP pilot workload analysis could be used as the motivation and stimulus to revitalise the turbulence reporting system and provide the necessary feedback. It would also seem sensible for there to be an overarching request in the HLL for pilots to complete turbulence reports wherever and whenever they experience turbulence, rather than as at present where the HLL only requests turbulence reports for certain platforms and certain wind conditions. When pilot turbulence reports are received, it will be possible to correlate them with the workload data from HOMP to obtain evidence of the HQR level that gives pilots significant concern.

14 Conclusions

14.1 Implementation of the Workload Predictor in HOMP

The pilot workload predictor developed in [1] has been successfully adapted for use with operational flight data generated by the Helicopter Operations Monitoring Programme (HOMP). The workload algorithm has been successfully implemented in the HOMP data analysis system by Smiths Aerospace, and its performance checked against the original QinetiQ version using three example flight records (Section 10). With regard to the detailed performance of the modified workload algorithm in the new application, it is concluded that:

14.1.1 The HQR predictor coefficients based on 20 Hz data are suitable for use on approach data sampled at 4 Hz when filtering and windowing is applied. The increase in predicted HQR through filtering and windowing is balanced by the decrease in predicted HQR caused by the reduction in the sampling rate. (Section 9.2)

14.1.2 HQR predictions from HOMP data follow the trend indicated by the "Digicoll" value. This trend is not necessarily an indication of a robust workload algorithm as the "Digicoll" has not been the subject of a rigorous validation exercise. (Section 9.3)

14.1.3 On the Bristow Helicopters Super Puma aircraft, HOMP cyclic and collective control activity is measured at the swash plate and, in the case of the cyclic, this includes contributions from both the pilot and the AFCS. The workload algorithm has, however, been developed using pilot control activity only. This inconsistency is likely to increase workload estimates made from similarly derived HOMP data. (Section 8)

14.1.4 The turbulence criterion will be slightly non-conservative for helicopters without AFCS on the collective control due to its presence in the simulator used to establish the limiting turbulence criterion. (Section 8.5)

14.2 Validation of the Workload Predictor using HOMP Data

The analysis of data from 12,978 landings contained in a 16 month archive of flights performed by the Bristow North Sea helicopter fleet resulted in the following key conclusions:

14.2.1 The maximum pilot workload determined in the analysis was 6.88. The mean value was 3.69, the 95-percentile value was 4.52, and the peak of the probability distribution was at 3.9. (Section 12.2)

14.2.2 There are two peaks in the workload probability distributions indicating the probable presence of two separate processes. There was some evidence that the lower peak at around HQR=2.7 could be due to the action of the AFCS in stabilising the aircraft, but it was not possible to draw a firm conclusion. In any event, it is not considered a material issue in the context of the validation of the turbulence criterion which is concerned with pilot workloads at higher levels. (Section 12.2)

14.2.3 Only one landing in the archive recorded a maximum pilot workload over the HQR=6.5 threshold (proposed in [1] as the workload limit for safe flight operations and used to develop the turbulence criterion). On the presumption that the vast majority of flights are operated safely, this may be taken as some evidence that the preliminary turbulence criterion was not set at too low a level. (Section 12.2)

14.2.4 It proved more difficult to use the data to verify that the turbulence criterion was not set at too high a level, and recommendations have been made concerning the continued monitoring of the HOMP pilot workload values and their correlation with pilot turbulence reports. (Section 12.2 and 13)

14.2.5 There was a clear difference in the pilot workload distributions for wind directions from 'turbulent' sectors and 'open' sectors. The difference was even more marked for individual platforms known to particularly suffer from turbulence. This, coupled with the plots of workload versus wind speed and direction presented for selected platforms, shows that a strong link between turbulence and pilot workload is confirmed by the HOMP operational data. (Sections 12.1 and 12.2)

14.2.6 Comparison of the pilot workload plots for individual platforms with their entries listed in the HLL shows a good degree of consistency. In most cases higher workload events seen in the HOMP data coincide with the 'turbulent' sectors as defined in the HLL. In some cases there is the suggestion that the HLL turbulent sector might be extended in terms of wind heading range. (Section 12.2)

14.2.7 Comparisons between the HOMP pilot workload values and the vertical turbulence component measured in wind tunnel tests were possible for five platforms in the BMT wind tunnel data archive. This comparison indicated that there was reasonably close agreement between occurrences of HQR>5.5 and vertical turbulence standard deviation of >1.75 m/s, thus indicating agreement with the turbulence workload relationship developed in [1] and presented here in Figure 3. (Sections 2, and 12.4)

14.2.8 The provisional turbulence criterion specified in the guidance [3] was set at 2.4 m/s based on the pilot workload boundary between safe and unsafe flight of HQR=6.5 (Section 2 and [1]). The criterion made no allowance for flight in reduced visual cueing conditions due to darkness, precipitation (rain, snow, hail) or poor visibility (mist, fog, low cloud), or for the less able or less experienced pilot. It has been concluded that, in order to take account of this and other factors, the turbulence criterion should be reduced to 1.75 m/s, equivalent to HQR=5.5. (Section 13)

14.3 'Incidental' Conclusions

14.3.1 In the cases of Gannet and Heather A it is suggested that consideration be given to including a defined turbulent sector in the HLL. (Section 12.2)

14.3.2 In a few cases it was found that the sketches of helideck and platform layout which had been obtained from the 'Aerad plates' contained errors. HCA and European Aeronautical Group, the publishers of the plates, have been informed of these errors. (Section 12.1)

15 Recommendations

It is recommended that:

15.1 The turbulence criterion of standard deviation of the vertical component of airflow should be reduced to 1.75 m/s (equivalent to a pilot workload of HQR=5.5), and that the guidance material [3] should be amended accordingly.

15.2 The criterion should be refined further using in-service experience and, in particular, based on turbulence reports from pilots.

15.3 Flow studies of offshore installation designs should present wind speed/ direction boundaries for the exceedance of the criterion.

15.4 The pilot workload algorithm developed in this project and programmed into the HOMP data analysis system should be made available to all helicopter operators.

15.5 The operators should be encouraged to use the analysis to routinely monitor turbulence around offshore installations, and to correlate these with turbulence reports submitted by pilots. It is recommended that a pilot workload event threshold lower than HQR=5.5 should be set in order to capture a range of higher workload events.

15.6 The launch of turbulence encounter monitoring and turbulence mapping using routine HOMP pilot workload analysis should be used as the motivation and stimulus to revitalise the pilot turbulence reporting system and provide the necessary feedback.

15.7 The HLL should encourage pilots to complete turbulence reports wherever and whenever they experience turbulence, rather than as at present only for certain platforms and certain wind conditions.

15.8 In particular operators should look for turbulence reports from pilots that occur at low HOMP HQR values, because these might indicate that the turbulence criterion has been set too high.

15.9 The outcome of routine monitoring should be passed to the Helideck Certification Agency (HCA) so that the HLL can be regularly updated to reflect the best information on turbulence.

16 Abbreviations

AFCS	Automatic Flight Control System
AFS	Advanced Flight Simulator, QinetiQ, Bedford
BHA	British Helicopter Association (was BHAB)
BHAB	British Helicopter Advisory Board (now BHA)
BMT	BMT Fluid Mechanics Limited
CAA	Civil Aviation Authority
Digicoll	Bristow HOMP Turbulence Parameter
FDR	Flight Data Recorder
GCU	Glasgow Caledonian University
HCA	Helicopter Certification Agency (previously BHAB Helidecks)
HLL	Helideck Limitation List (was IVLL)
HOMP	Helicopter Operations Monitoring Programme
HQR	Handling Qualities Rating (Cooper-Harper Scale)
IVLL	Installation/Vessel Limitation List (now HLL)
rms	root mean square
S-76	Sikorsky type S-76 helicopter
S-76X	The approximate numerical model of the S-76 used in the simulations.
SyCoS	GCU developed helicopter pilot model (Synthesis through Constrained Simulation)
UKOOA	United Kingdom Offshore Operators Association (Oil & Gas UK from 2007)

17 References

[1] *Helicopter Turbulence Criteria for Operations to Offshore Platforms*, CAA Paper 2004/03, 2004.

[2] *Installation/Vessel Limitation Lists*, Issued by the British Helicopter Advisory Board, Helideck Sub Committee, Issue No. 10 August 1999. (More recent lists have now been published by the Helideck Certification Agency, and are referred to as Helideck Limitations List or HLL. The latest version is available from http://www.helidecks.org.)

[3] *Offshore Helicopter Landing Areas – Guidance on Standards*, CAA CAP437, Aug 2005.[9]

[4] *Research on Offshore Helideck Environmental Issues*, CAA Paper 99004, August 2000.

[5] Cooper G E, Harper R P, *The use of pilot rating in the evaluation handling qualities*. Report NASA-TN-D-5153, April 1969.

[6] MacDonald C. 'The Development of an Objective Methodology for the Prediction of Helicopter Pilot Workload', PhD Thesis, Department of Mathematics, Glasgow Caledonian University, 2001.

[7] G. Padfield, J. Jones, M. Charlton, S. Howell and R. Bradley, '*Where does the Workload go when Pilots Attack Maneouvres? An Analysis of Results from Handling Qualities Theory and Experiment*', 20th European Rotorcraft Forum, Amsterdam, October 1994.

[8] *Final Report on the Helicopter Operations Monitoring Programme (HOMP) trial*, CAA Paper 2002/02, 2002.

[9] *Helicopter Operations Monitoring Programme (HOMP) – A helicopter Flight Data Monitoring (FDM) program*, Proceedings of the 59th Annual Forum of the American Helicopter Society, Phoenix, May 2003

[10] *Final Report on the Follow-on Activities to the HOMP Trial*, CAA Paper 2004/12, October 2004

[11] *Offshore Helideck Environmental Issues – Visualisation of Offshore Gas Turbine Exhaust Plumes,* CAA Paper 2007/02, 2007

[12] *Review of 0.9 m/s Vertical Wind Component Criterion for Helicopters*, CAA Paper 2008/02, Part 2.

[13] Helicopter Flight in Degraded Visual Conditions – CAA Paper 2007/03

[14] A Questionnaire Survey of Workload and Safety Hazards Associated with North Sea and Irish Sea Helicopter Operations 0150 – CAA Paper 97009

9. Now at 6th edition, Jan 2009.

Appendix A Specification of the HOMP Workload Algorithm

The following specifies the algorithm for workload estimation from control activity developed by QinetiQ for BMT Fluid Mechanics Ltd under contract 43431/sc/01 for the purposes of deriving a prediction of workload rating using records of control activity from operational data.

The following steps should be followed:

1 Extract control time history records from HOMP data. Do not include regions where weight-on-wheels flag is true.

2 Normalise the control time histories by the quantity relating to full travel for each axis and adjust to the following convention:

- Collective: 0, fully down and +1, fully up
- Lateral Cyclic: -1, fully left and +1, fully right
- Longitudinal Cyclic: -1, fully forward and +1 fully aft

3 Filter longitudinal cyclic, lateral cyclic and collective using a high pass eighth-order Butterworth filter with a cut-off frequency of 0.1 Hz[1].

4 Calculate the control rate time histories from the filtered control positions.

5 Apply the following to a Boxcar window of duration 17 seconds that begins with the first 17 seconds and moves through the time history advancing one sample interval at a time.

i) Calculate standard deviations of control positions and rates

ii) Combine the standard deviations using the following weighted sum to give a workload rating for each window:

$$\text{Workload Rating} = c_1 + c_2\,\sigma(\xi) + c_3\,\sigma^*(\xi) + c_4\,\sigma(\eta) + c_5\,\sigma^*(\eta) + c_6\,\sigma(\theta_0) + c_7\,\sigma^*(\theta_0)$$

Where,

$c_1 - c_7$ = predictor coefficients

ξ = lateral cyclic position

η = longitudinal cyclic position

θ_0 = collective lever position

$\sigma(x)$ = function : standard deviation of x

$\sigma^*(x)$ = function : standard deviation of first derivative of x with time

The values of coefficients are as follows:

c_1	2.4069
c_2	1.0356
c_3	3.9514
c_4	0.7333
c_5	2.8197
c_6	1.3430
c_7	4.4501

6 Identify the maximum value of workload rating for all windows to give the overall workload rating for the data sample.

1. The 8th order Butterworth filter proved difficult to implement in HOMP due to arithmetic precision problems, and so 4 x 2nd order filters were used instead - see Appendix B.

INTENTIONALLY LEFT BLANK

Appendix B Practical Issues Associated with Implementing The Pilot Workload Algorithm in a HOMP Software Environment

The specified pilot workload algorithm contained two elements that required some research and development activity to enable a satisfactory implementation of the algorithm within the existing HOMP software environment.

The first was a requirement to perform standard deviation calculations on moving windows of longitudinal cyclic, lateral cyclic and collective control position and rate data, with the windows having a duration of 17 seconds and advancing one sample interval at a time. This calculation could not be performed using the existing set of mathematical functions for flight data analysis, therefore it was necessary to implement a new standard deviation function within the HOMP software.

A more significant issue was the requirement to filter longitudinal cyclic, lateral cyclic and collective data using a high pass eighth-order Butterworth filter with a cut-off frequency of 0.1 Hz. It was found that a filter implementation within the HOMP software gave slightly different outputs to a previous development implementation within Matlab. An investigation indicated that this was due to differences in the rounding precision of internal calculations within the HOMP system and Matlab filter implementations.

Infinite Impulse Response (IIR) filters involve recursion (i.e. feedback terms) and this gives them their high performance. It also makes high order filters very sensitive to errors, and even unstable under some conditions. The error caused by truncating the coefficients and internal calculations is approximately proportional to the exponential of the filter order. It is therefore recommended that IIR filters are never implemented as having a higher order than 2. High order filters should be factorised into several concatenated stages of 2nd order filters. (Generally, 1st order stages would give rise to complex coefficients, therefore 2nd order stages are chosen with 2 roots that are complex conjugates, and this ensures real coefficients.) Figure 58 below shows how an 8th order IIR filter can be implemented as 4 stages of 2nd order filter (each stage having different coefficients) together with a final gain multiplier.

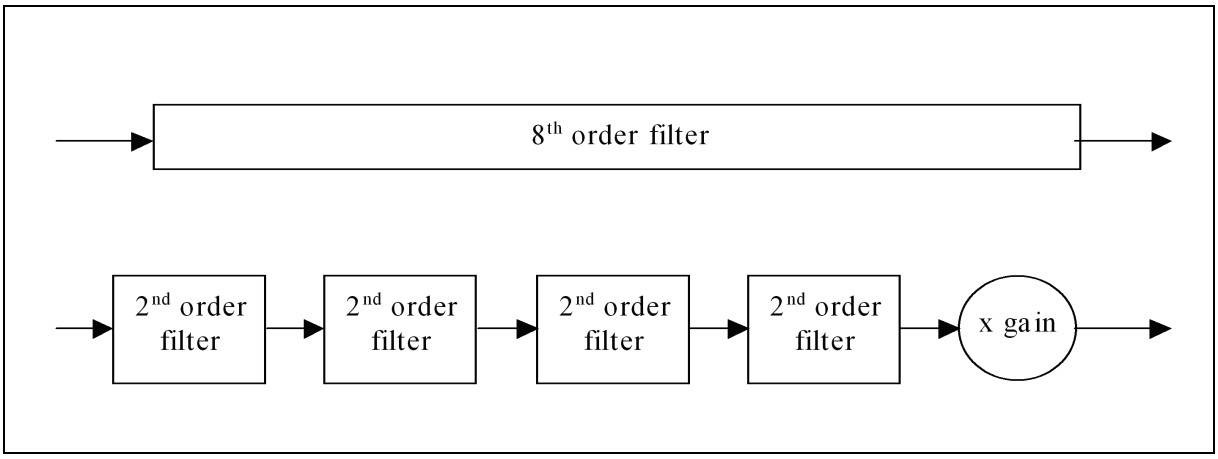

Figure 58 Structure of a second order section

Testing showed that this Second Order Section (SOS) implementation was extremely resilient to rounding errors. Compared with the original 8th order filter, the same performance could be obtained with far fewer decimal places in the precision of the coefficients, and the filter had better numerical stability.

INTENTIONALLY LEFT BLANK

Appendix C Comparison of HOMP Results with HLL Entries

NOTE: – Shaded HLL entries contain no reference to turbulence or hot gas hazards.

HOMP Data						HLL ENTRY						HOMP DATA PLOTS			
Rank	AIRPORT	CODE	DEPARTURES	LANDINGS	Weathervanes or heading unknown	D'			Wind(deg T)	Kts	Limitations/Comment	Comments on plots			
												Torque	Temp diff	pilot workload	General comment
34	AH001	AH001	222	225		22.2	B*	EP	0	0	• Max. weight shown as 8.6t ▪ Max. landing weight 8.6t (19,000 lbs) – due to dynamic load limit of deck ▪ Max take-off weight 9.3t (20,500 lbs) • Table 1(T) – all operations due to obstructions on all sides of the helideck	no significant features (NSF)	NSF	NSF	
14	Alba Northern	ALBA	499	501		22.8	A	PG	350-030 350-030	25-35 35 plus	• Table 2 (use 35-45 kts limitations) • No landings • Table 1(T) if overflight of South foam monitor platform unavoidable • Approved friction surface - No net	no landings at +35 apparent 350-30	NSF	Some high workload events (4.5-5.5) for winds 315-350 at 25-35kn. These are on the edge of the current HLL limitations and suggests that the turbulent sector in the HLL should be redefined.	Unobstructed sector markings wrongly aligned on platform sketch. KEVIN PAYNE WROTE: ... confirmS that there a 4° to 5° difference in helideck orientation (which, strangely, equates to the magnetic variation but the wrong way) HORG Plate 210°T. From Chevron as built drawing (1993) orientation measures 205°T. However, it should be noted that the OFS has been swung by 15° anticlockwise (as permitted under CAP 437, chpt 3, para 6.3 and Figure 1) to clear the plaform crane (west). The Aerad Plate is wrong in-so-much as it shows an un-swung sector passing through the jib of the western crane (the dominant obstacle!). The 150° LOS should be orientated 295°T to 85°T. [15° + 5° explains your 20°discrepancy!] Suggest that Aerad sketch should be corrected. Also suggest revision to HLL entry extending the turbulent sector to start at 315 deg.
28	Alba FSU	ALFSU	308	310	Y	22.2	B*	PG	0	0	• Table 1 (T) if overflight of tanker unavoidable	NSF	NSF	A few high workload events 4.5-5.6. Cannot interpret because weathervanes and we don't know heading.	
26	Anasuria	ANAS	328	328	Y	22.8	B*	A. Knight	340-360 rel to ships head	0	• Possible turbulence and high deck temperature due to turbines on port side of vessel. Check with log on initial contact. • Table 1(T) if overflight of aft foam monitor or shuttle tanker (when attached) is unavoidable.	NSF	a number of high temperature events 4 - 7.6 deg. FPSO and we don't know heading so cannot interpet wind direction data.	a number of high workload events (4.5 - 6.0). Do not appear to correlate closely with high temperature events, so turbulence probably also a factor.	
59	Armada	ARMAD	60	58		22.8	A	Alex Knight	0	0	• Maximum allowable mass 14t • Table 1(T) if overflight of crane boom and luffing wires at Northeast corner of helideck, is unavoidable. • Approved friction surface - no net.	NSF	NSF	NSF	

					22.2	A	P.Garia nd	All	0 to 15		NSF	NSF	5 high workload events (4.5 - 5.5) but little pattern.	
31	Auk A	AUKA	311	284						• Table 1(T) if overflight of accommodation module unavoidable. • Due to oversize perimeter net: AS332 - Hover with nose wheel near to deck edge S61 - T/Off weight -minus 300lbs S76 - Table 1(T) Other types TBA • Perimeter lights				
44	AWG-1	AWG1	126	127							NSF	NSF	NSF	
50	Balmoral	BALMO	104	97							NSF	NSF	NSF	
62	Berge Hugin	BHUG	56	49						• Nil	NSF	NSF	4 high workload events (4.5 - 5.5) this out of only 31 landings.	
6	Brae A	BRAEA	662	665	22.2	A	PG	305 - 067	0	• See 'Part E, Annex 1' for specific restrictions regarding turbulence Turbulence reports requested to assess above • Table 1(T) if overflight of Tropo dish on west side of platform is unavoidable • Parking area bounded by blue lights	pattern of high torque events when wind speed is low or from the turbulent (NE) sectors.	NSF	23 high workload events (>4.5), mainly when the wind is from the NW, but also some with wind from the (open) from S.	KEVIN PAYNE WROTE: ... confirms that there a 4° to 5° difference in helideck orientation (which, strangely, equates to the magnetic variation but the wrong way) HORG Plate 212°T. From Marathon Oil interim helideck marking drawing (Oct 1994) helideck orientation measures 208°T. On this occasion the bisector of the OFS is along the standard alignment and therefore the 150° LOS covers the arc 313°T to 103°T (compare 317°T to 107°T for Aerad HORG). This is interesting because based on the HLL entry for Brae A the westeren flare boom (at 305°T and well above helideck level) appears to be within the OFS but is not notified as an infringement. The HORG plate seems to place the west flare (not fully shown) in sector 1 and therefore within the LOS. The HLL orientates the OFS so that the western flare appears in the LOS - this is maybe correct since the western flare is not notified as a 210° OFS infringement in the HLL. Something is amiss!!
8	Brae B	BRAEB	642	644	22.8	A	AK	345-070	0	• See Annex A for specific restrictions regarding turbulence Turbulence reports requested to asses above • Table 1(T) if overflight of foam monitor platform on south corner of helideck is unavoidable • Aiming circle on deck centre	high torque events when wind speed less than 15kn.	NSF	high workload events (4.5 - 5.5) mainly when wind in NW to NE.	
12	Britannia Platform	BRITP	528	524	22.8	A	AK	70-129 70-129 130-140	30-40 40 plus	• Table 2 due to derrick, use 35-45 kts limitations Nil landings n.b. Sliding derrick - turbulent segment within sector will change depending on position of derrick (location of derrick available from BHL operations) • Table 2 due to phys	NSF	NSF	High pilot work load (4 in range 5.5 - 5.8) when wind in 90-140.	HLL turbulent sector should perhaps be extended to 140 deg.

16	Brent A	BRNTA	468	488		22.8	A	A.Knight	145-205	All	• Turbulence due to derrick S61 - Table 2 Other types - Exercise caution Turbulence reports requested • Table 1(T) if over flight of east side of helideck is unavoidable. • Caution. The perimeter line and lights along	NSF	NSF	A number of high workload events (22 in the range 4.5 - 6.0) when the wind is 135-180 at around 35-40kn. Looks like the turbulent sector in the HLL might be expanded to 135	HLL turbulent sector should perhaps be extended back to 135 deg.
5	Brent B	BRNTB	674	671		22.8	A	A.Knight	170-200	0-20	• Turbulence due to turbine exhausts S61 - Table 2 Other types - Exercise caution Turbulence reports requested • Approved friction surface - no net	NSF	a number of higher temperature events when wind is from 135-190, but none is over 4 deg.	33 high workload events (4.5 - 5.9) when wind is from 135 - 205, at higher wind speeds. Three >5.5 events from 150 deg at 35-45kn.	HLL turbulent sector should perhaps be extended back to 135 deg.
4	Brent C	BRNTC	674	674		22.8	A	AK	155-215	0	• Turbulence S61 - Table 2 Other types - Exercise caution Turbulence reports requested • Table 1(T) when overflight of east or west sides of helideck is unavoidable. • Approved friction surface - no net	a number of higher torque events when the wind is from turbulent directions 160-220.	2 temperature events in range 4 - 6.5 deg when wind is from 180.	4 high workload events (>5.5) when wind 160-180 at 25-45kn.	
9	Brent D	BRNTD	633	638		22.8	A	Alex Knight	135-195	0	• Turbulence S61 - Table 2 Other types - Exercise caution Turbulence reports requested • Approved friction surface - no net	generally higher torque values when wind is from sector 160-270.	Some higher temperature events when wind is from 140-200 but none greater than 4 deg.	Most high values (22 above 4.5, 2 above 5.5) when wind is from 155-250 at 25-55kn. Suggests that HLL turbulent sector should be expanded.	HLL turbulent sector should perhaps be extended to 250deg.
29	Captain FPSO	CAFPS	290	287	Y	22.8	B	0	0	0	• Nil	NSF	NSF	NSF	
25	Captain	CAPT	331	331		22.8	A	AK	097-189	0	• Table 2 due to moving clad derrick, restricted overshoot and turbine exhausts. (n.b turbulent segment will change within the sector depending on the position of the derrick. Location of derrick available from BHL/ChevronTexaco prior to depa	NSF	NSF	6 events in the range 4.5 - 5.5, two with wind from the open NW sector at 35-45kn.	Do open sector high workloads indicate a problem with control in the presence of a downdraft/updraft?
46	Clair	CLAIR	112	113		22.8	A	A. Knight	0	0	• Table 1(T) if overflight of foam monitor platforms is unavoidable.	Tendency for higher torques with wind in south, but none in the weight corrected and limited plots. Must be low weight cases?	NSF	5 high workload events (4.5 - 5.5) when wind is from the SE sector. (no sketch)	
10	Cormorant A	CORMA	618	626		22.8	A	AK	145-205	All	• All types - Turbulence reported S61 - Landing use restricted graph Turbulence reports requested to assess above. • Table 1(T) if overflight of 5:1 infringements is unavoidable. • Approved friction surface - no net	a number of higher torque event when the wind is low or from turbulent 135-200 sector.	NSF	21 high workload events above 4.5. Max 6.02. Most of the higher events are in the 135-200 sector, but the highest is at 220 deg and there are a couple with wind in N and W. 220 event which occurred right over the helideck, possible candidate for detailed examination?	
22	Dunlin	DUNLA	398	394		22.8	A	A.Knight	145-205 All	All 0-15	• Turbulence S61 - Table 2 Other types - Exercise caution • Due to oversize perimeter net AS332 - Hover with nose wheel near to deck edge - Nil Limitation S61 - WAT -300lbs S76 - Table 1 (T) Other types - TBA Voyage	Higher torque values generally with wind from turbulent sector.	NSF	19 landings with workload over 4.5. Higher values for higher winds in the sector140-250.	

.

13	East Brae	EBRAE	509	512		22.8	A	Alex Knight	335-035	30 plus	▪ Turbulence can be encountered when wind above 30kts Turbulence reports requested ▪ Table 1(T) if overflight of S&W foam monitor platforms unavoidable	NSF	NSF	14 events with workload above 4.5, but generally spread around the clock - both open and turbulent sectors.	
36	Eider	EIDER	199	203		22.8	A	A.Knight	0	0	▪ Table 1(T) if over flight of west side of platform is unavoidable. ▪ Approved friction surface - No net	NSF	NSF	NSF	
48	Erskine	ERSK	107	106		19.5	A	A.Knight	0	0	▪ NUI ▪ Maximum Allowable Mass 9.1t (20,000 lbs) due to deck stress ▪ Gullscat System installed - Beware loud irregular noises	NSF	NSF	NSF	
55	F3-FB-1	F3B	81	82								NSF	NSF	NSF	
18	Fulmar A	FUL	471	451		22.8	A	P. Garland	095 - 165	45 Plus	▪ Possible turbulence Turbulence reports requested ▪ Table 1(T) if overflight of crane rest unavoidable ▪ Perimeter lights and line not co-incidental - Red lights indicate unsafe sector ▪ Approved friction surface - no net	higher torques at low wind speeds and when 110deg.	2 high temperature events (highest 6.2 deg) with wind 90-100deg. Note that helicopter was 40m to the W when these occurred.	19 events over 4.5, mainly clustered for higher winds in the sector 90-160 deg. Don't seem to be associated with high temperature events because the high workload occurs over the deck.	
70	Galaxy 1	GAL1	20	20								NSF	NSF	NSF	
15	Gannet	GANET	459	490		22.8	A	A.Knight	0	0	▪ Possible turbulence due to proximity of turbine exhausts. Turbulence reports requested ▪ Table 1(T) if overflight of SE monitor platform is unavoidable. ▪ Perimeter lights in the NE corner of the deck do not reflect the Safe Landing area - Red l	high torque for low wind speeds and winds 180-340.	NSF	14 events over 4.5. Mainly for higher winds in the 250-360 sector. Highest event 5.5 at about 30kn 10deg.	Perhaps enhance HLL with info about the likely turbulent sector.
35	Goldeneye	GOLD	199	204		22.2	A	PG	0	0	▪ NUI ▪ Approved friction surface - no net	NSF	NSF	Higher workloads when wind above 25kn and in sector 110-280.	
49	GSF Rig 140	GR140	99	100		BVBD 22.8	B*	AK	160-200 rel to rig hdg	20-30 31-40 31-40 41 plus	▪ All types - Table 2, use 35-45 kts limitations AS332 - Max helipad weight Other types - Nil landings All types - Nil landings ▪ Table 1(T) if overflight of the fuel bund on the port side is unavoidable.	NSF	NSF	NSF	
23	Heather A	HETHA	396	391		22.2	A	PG	0	0	▪ Possible turbulence Turbulence reports requested ▪ Table 1 (T) if overflight of North access platform unavoidable ▪ Approved friction surface - no net	NSF	2 events over 4 deg with wind 65deg.	A number of high workload events, 16 above 4.5 and a maximum at nearly 7. Most high workload events are in the wind sector 115-180 with a few out at 250-270 (open).	Note - no turbulent sector given in the HLL. Perhaps enhance HLL with info about the likely turbulent sector. Wind direction for the 2 high temperature events seems odd - I.e. from the 'open' sector.
51	Judy	JUDY	94	95		22.2	A	A.Knight	0	0	▪ Table 1(T) if overflight of south Foam monitor platform is unavoidable. ▪ Approved friction surface - no net	NSF	NSF	NSF	
32	K14-FA-1	K14C	270	278								NSF	NSF	Seems to be a tendency for high workload when wind is from the 110-215 sector. Looks inconsistent with alignment pf sketch.	SEEMS TO BE A SEVERE ALIGNMENT PROBLEM WITH THE SKETCH OF THIS PLATFORM? APPEARS TO BE TWO HELIDECKS LISTED FOR THIS PLATFORM IN THE HOMP DATABASE. PRESUMABLY WE HAVE THE WRONG SKETCH?
38	K15-FA-1	K15A	159	158								NSF	NSF	NSF	SKETCH LOOKS INCONSISTENT WITH HELICOPTER LOCATIONS
39	K15-FB-1	K15B	153	152								NSF	NSF	One high value 5.6 with wind at 30kn from W (turbulent sector if sketch is correct).	

.

65	K15-FG-1	K15G	41	40								NSF	NSF	NSF	
42	K15-FS-1	K15S	136	134								NSF	NSF	One high value 5.5 with wind at 35kn from 235. No sketch but from helicopter locations looks like turbulent sector.	
47	K7-FA-1	K71	114	107								NSF	NSF	NSF	
37	K8-FA-1	K81	181	180								NSF	NSF	NSF	
60	K8-FA-2	K82	54	56								NSF	NSF	NSF	
57	K8-FA-3	K83	57	59								NSF	NSF	NSF	
53	Kittiwake	KITTI	82	84		22.2	A	P.Garland	0	0 - 15	• Overflight of the south foam monitor platform to be avoided • Approved friction surface - no net	NSF	NSF	NSF	
40	L13-FC-1	L13C	144	144								NSF	NSF	NSF	
68	L13-FD-1	L13D	26	26								NSF	NSF	NSF	
67	L13-FE-1	L13E	33	33								NSF	NSF	NSF	
54	L15-FA-1	L15A	84	84								NSF	NSF	NSF	
63	L2-FA-1	L2A	44	44								NSF	NSF	NSF	
58	L5-FA-1	L5A	59	58								NSF	NSF	NSF	
41	L9-FF-1	L9F	137	138								NSF	NSF	NSF	
61	MacCulloch	MACC	55	52		22.2	B*	0	0	0	• Turbulence and temperature rise can be expected due to funnel exhausts (directly forward of helideck) and turbine exhausts (starboard/forward). Turbulence reports requested	NSF	NSF	6 high workload events at wind speeds around 20-25kn. No heading information. Highest 5.0.	No evidence of the temperature problems though only 30 flights recorded.
21	Magnus	MAG	413	413		BVOD 22.8	A	AK	100-140 040-100	All 30 plus	• Table 2 due to turbine exhaust, derrick and flare • Possible turbulence due to turbines and flare stack Turbulence reports requested • Table 1(T) if overflight of foam/access platform (S) unavoidable • Approved friction surface - No net	tendency for higher torque events with wind from the turbulent sectors.	1 event over 4 deg with wind at 70deg.	22 events over 4.5 mainly with wind from the turbulent sector 45-270.	Note that the turbulent sector in the IVLL might be extended back to 45deg.
17	Maersk Endurer	MEND	487	467		22.2	C	AK	0	0-15	• Overflight of Foam Monitor Platforms to be avoided on take off • Stable deck conditions to apply for operations whilst under tow i.e. maximum 1° Pitch and Roll and 2m Heave.	NSF	NSF	NSF	
69	Miller	MILLR	22	23		22.8	A	PG	065-085 110-145	All	• Possible turbulence & temperature rise - Turbine exhausts • Table 2 due to turbulence from derrick (Moveable Derrick) Turbulence reports requested • Table 1 (T) if overflight of West Foam Monitor platform unavoidable • Approved friction surface	NSF	NSF	NSF	
27	Murchison	MURCH	328	327		22.2	A	PG	065-105	40 plus	• Severe turbulence close to and over the helideck • Table 1(T) if overflight of living quarters unavoidable • Approved friction surface - no net	NSF	NSF	16 events over 4.5. Max 5.9. High workload events mainly with wind from the turbulent 20-220 sectors. Highest events with wind from 160-180.	Is there some suggestion that the worst occurs at the endges of the HLL turbulent sector? Perhaps with wind deflected up the sides of a large platform? Or does it look like this because there a reduced numbers of flights in the main part of the sector due to the HLL advice?
56	Nordic Apollo	NAPOL	66	68								NSF	NSF	NSF	

7	North Cormorant	NCORM	654	650		22.8	A	A,Knight	305-005	All	• Turbulence due to flare and turbine S61 - Table 2 Other types - Exercise caution Turbulence reports requested • Table 1(T) if over flight of East or West sides of helideck is unavoidable. • The perimeter lights do not reflec	Higher torque values when wind is from 90-270 (open sector), but speeds generally less than 15kn.	3 events over 4deg, but no descernable pattern to them.	27 events over 4.5, but these are spread over a wide range of wind speeds and directions 135-340. Is the incomplete helideck sketch correctly aligned? Looks wrong.	Is the incomplete helideck sketch correctly aligned? Looks wrong.
20	Nelson	NELSO	401	416		22.8	A	PG	0	0-15	• Turbine exhausts East side of helideck. Possible temperature rise and turbulence • Overflight of SW Foam monitor platform to be avoided on take off	NSF	NSF	10 events over 4.5, but no strong pattern. Mostly at wind speeds 25-35kn.	no evidence of temperature problem.
1	Ninian C	NIC	835	839		22.2	A	PG	145-175 145-175 145-175 145-175	10-24 25-44 10-44 45 plus	• Due to turbulence (use 35-45kt limitations) - Day Flight through the exhaust plume should be avoided at all times. If this, approach or departure profile needs to be modified to achieve consideration must be given to re	Lots of high torque events mainly with wind in sector 90-200.	22 events over 4 deg Concentrated with wind in sector 90-180.	85 events over 4.5 Max value 6.2. High values are generally in the turbulent wind sector 90-210, with the very highest values 140-210 at 20-45kn.	Perhaps the HLL turbulent sectors should be extended to 210 deg? There are a lot of events occuring beyond 175 deg.
3	Ninian N	NIN	724	727		22.2	A	PG	0	0	• Table 1(T) if overflight of accomodation modules and access platforms on South West sides of deck, or the east crane when it is in the rest, is unavoidable. • Caution on approaches/departures from/to East due to proximity of crane luffing wire	NSF	NSF	8 events over 4.5. Highest with wind at 30kn from 325.	
2	Ninian S	NIS	769	778		22.2	A	PG	215-275 215-275 215-275 215-275	10-24 25-44 10-44 45 plus 0-15	• Due to turbulence - Day Flight through the exhaust plume should be avoided at all times. If this, approach or departure profile needs to be modified to achieve consideration must be given to reducing max weight to Tabl	Many high torque events mainly with wind in 200-270 sector.	15 events over 4 deg All for winds in sector 225-280.	44 events over 4.5. Highest is 5.8. High values are for wind speeds 25-40kn from 230-260.	

.

64	Northern Producer	NPROD	39	41		22.2	B*	A Knight	0	0	▪ Semi Sub with helideck on Port forward corner. ▪ Table 1(T) if overflight of Sig 5:1 infringements is unavoidable.	NSF	NSF	NSF	
33	North West Hutton	NWHUT	232	233		22.2	A	AK	040-150	25-45	▪ NUI ▪ Daylight ops only ▪ Table 2 due to twin clad derrick (use 35-45 kts limitations) Turbulence reports requested to assess above	NSF	NSF	10 events over 4.5 Higher values for higher winds in secvtor 135-250.	Note the high workloads at the southern edge of the turbulent sector. Perhaps the HLL sector should be extended, but it is not obvious why this should be.
45	Ramform Banff	RBANF	128	127	Y	22.8	B*	PG	0	0-15	▪ Overflight of the forward foam monitor platform to be avoided on take off ▪ Due to peculiar deck motion the night p/r/h limitations are reduced to half the day limits.	NSF	NSF	7 events over 4.5. Highest 5.8 (could be associated with wave motions).	
19	Scott	SCOTT	439	440		22.8	A	EP	0	0	▪ Table 1(T) if overflight of south access unavoidable ▪ Approved friction surface - no net	NSF	NSF	NSF	
11	Tern	TERN	529	532		22.8	A	AK	295-355	All	▪ Turbulence due to turbine exhaust S61 - Table 2 Other types - Exercise caution Turbulence reports requested ▪ Table 1(T) if over flight of west side of helideck is unavoidable. ▪ Approved friction surface - no net	NSF	1 event over 4 deg with wind speed low from 225.	13 events over 4.5. No strong pattern with wind direction. One high value with wind from the (open) 190 direction. Perhaps this is a candidate for detailed examination?	
24	Thistle	THISA	375	376		22.2	A	PG	355-045	0	▪ Possible turbulence from turbine Exhaust (E) approx 40ft ADL. Turbulence reports requested ▪ Table 1 (T) if overflight of Sig 5;1 infringements unavoidable ▪ Approved friction surface - No net	Higher values for low wind speeds from S (open).	NSF	7 events over 4.5. Not much of a pattern.	
52	Tiffany	TIFF	98	94		22.8	A	PG	0	0	▪ Table 1 (T) if overflight of Foam Monitors (S & W) unavoidable ▪ Possible turbulence from exhaust ▪ Inform helicopter companies when A/C parked in run off area as the 150° LOS will be infringed.	NSF	NSF	NSF	
30	Triton	TRIT	283	286		22.8	B*	PG	030-050 rel to ships hdg	0-15	▪ Possible turbulence due to turbine exhausts Turbulence reports requested ▪ Overflight of Port Foam Monitor Platform to be avoided on take off	NSF	NSF	14 events over 4.5, but no pattern (we don't know vessel heading).	
43	Uisge Gorm	UGORM	132	131		22.8	B*	PG	0	0	▪ Table 1(T) if overflight of shuttle tanker unavoidable	NSF	NSF	12 events over 4.5, but no pattern (we don't know vessel heading).	
66	West Navigator	WNAV	38	38		22.8	C*	PG	0	0-15	▪ Special p/r/h limitations apply when using DP - See Part E Annex 4 ▪ Overflight of Forward Foam Monitor platform to be avoided on take-off	NSF	NSF	NSF	

INTENTIONALLY LEFT BLANK

Appendix D Example Time Series – HOMP Trace Plots

1 High Workload Landings Example Homp Traces

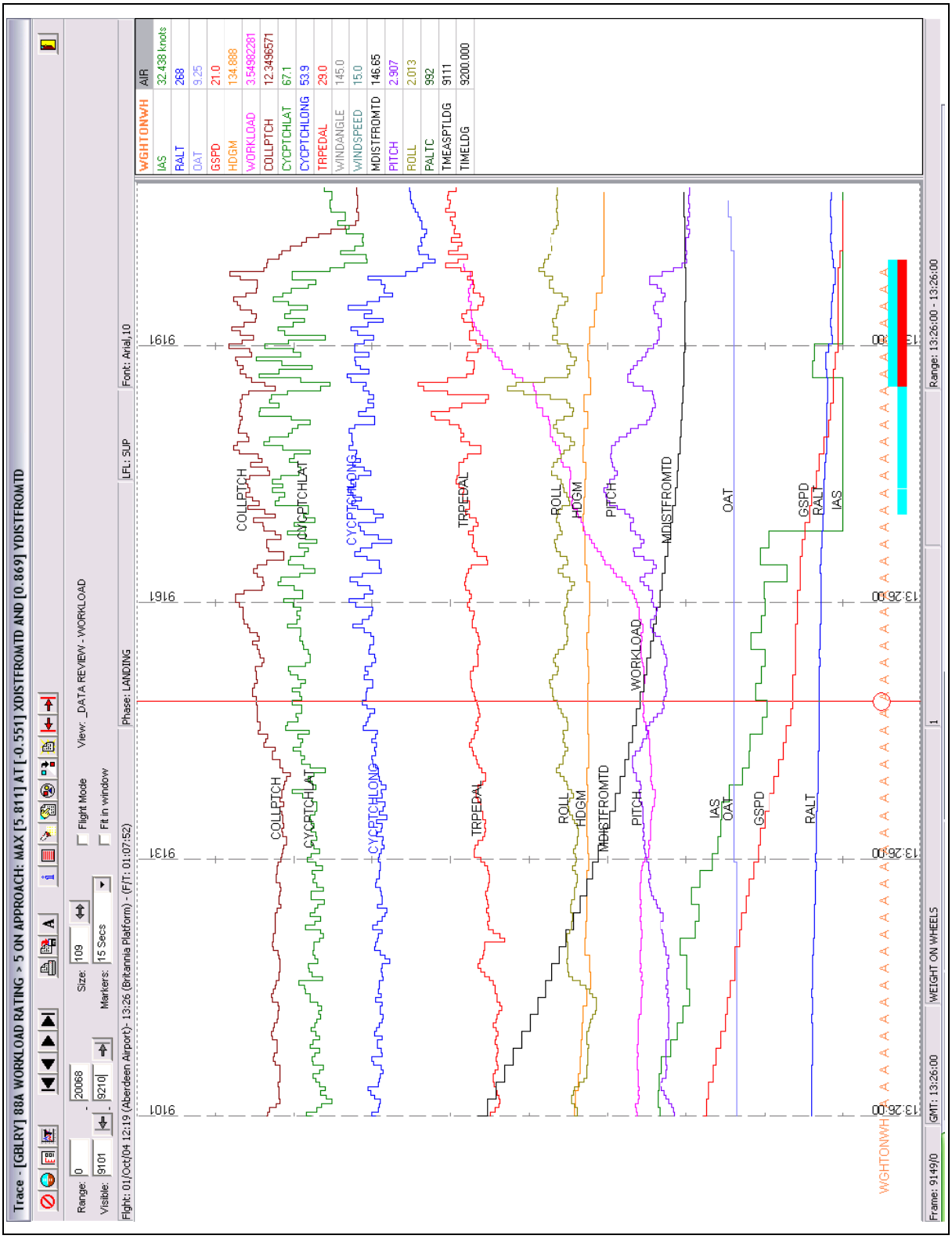

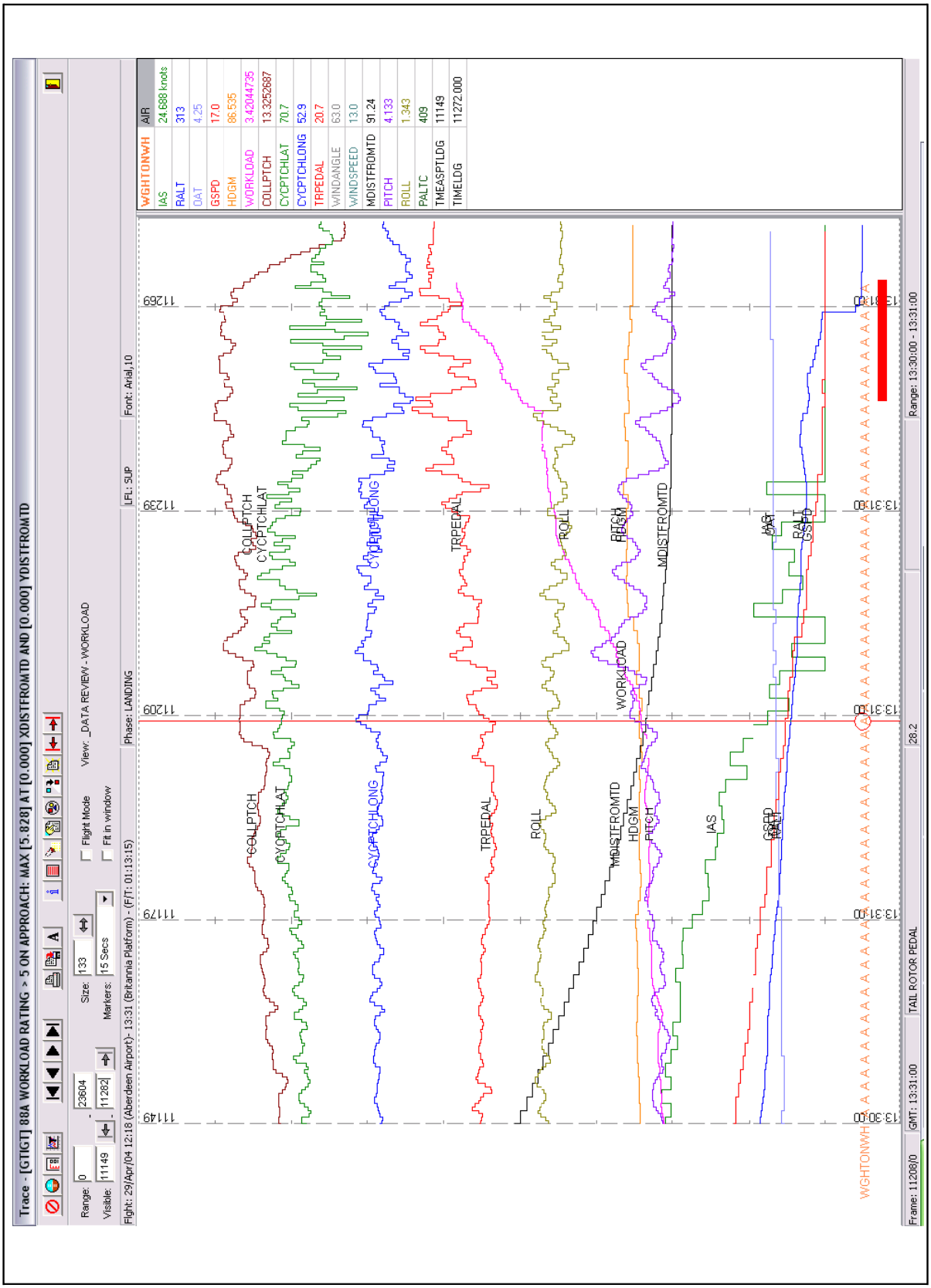
Trace - [GTIGT] 88A WORKLOAD RATING > 5 ON APPROACH: MAX [5.828] AT [0.000] XDISTFROMTD AND [0.000] YDISTFROMTD
Range: 0 23604
Visible: 11149 11282
Size: 133
Markers: 15 Secs
Flight Mode
Fit in window
View: _DATA REVIEW - WORKLOAD
Flight: 29/Apr/04 12:18 (Aberdeen Airport) - 13:31 (Britannia Platform) - (F/T: 01:13:15)
Phase: LANDING
LFL: SUP
Font: Arial,10
WGHTONWH AIR
IAS 24.688 knots
RALT 313
OAT 4.25
GSPD 17.0
HDGM 86.535
WORKLOAD 3.42044735
COLLPTCH 13.3252687
CYCPTCHLAT 70.7
CYCPTCHLONG 52.9
TRPEDAL 20.7
WINDANGLE 63.0
WINDSPEED 13.0
MDISTFROMTD 91.24
PITCH 4.133
ROLL 1.343
PALTC 409
TMEASPTLDG 11149
TIMELDG 11272.000
11269
11239
11209
11179
11149
13:30:00
13:31:00
13:31:30
GMT: 13:31:00
TAIL ROTOR PEDAL
Range: 13:30:00 - 13:31:00
Frame: 11208/0
28.2

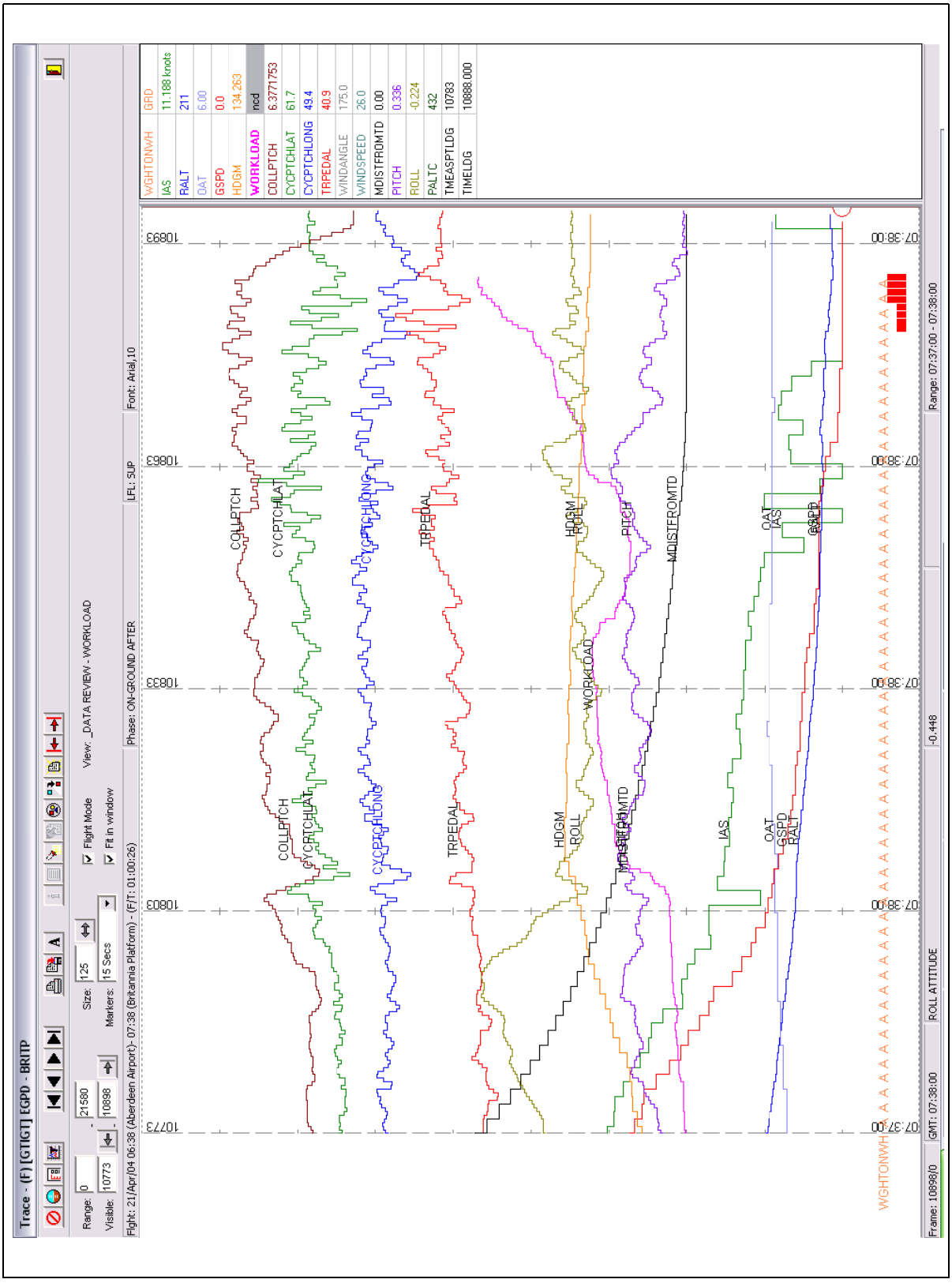
Trace - (F) [GTIGT] EGPD - BRITP
Range: 0 21580
Visible: 10773 10898
Size: 125
Markers: 15 Secs
Flight Mode
Fit in window
View: _DATA REVIEW - WORKLOAD
Font: Arial,10
Flight: 21/Apr/04 06:38 (Aberdeen Airport)- 07:38 (Britannia Platform) - (F/T: 01:00:26)
Phase: ON-GROUND AFTER
LFL: SUP
WGHTONWH GRD
IAS 11.188 knots
RALT 211
OAT 6.00
GSPD 0.0
HDGM 134.263
WORKLOAD ncd
COLLPTCH 6.3771753
CYCPTCHLAT 61.7
CYCPTCHLONG 49.4
TRPEDAL 40.9
WINDANGLE 175.0
WINDSPEED 26.0
MDISTFROMTD 0.00
PITCH 0.336
ROLL -0.224
PALTC 432
TMEASPTLDG 10783
TIMELDG 10888.000
10773
10803
10833
10863
10893
07:37:00
07:38:00
Range: 07:37:00 - 07:38:00
Frame: 10898/0
GMT: 07:38:00
ROLL ATTITUDE
-0.448
WGHTONWH

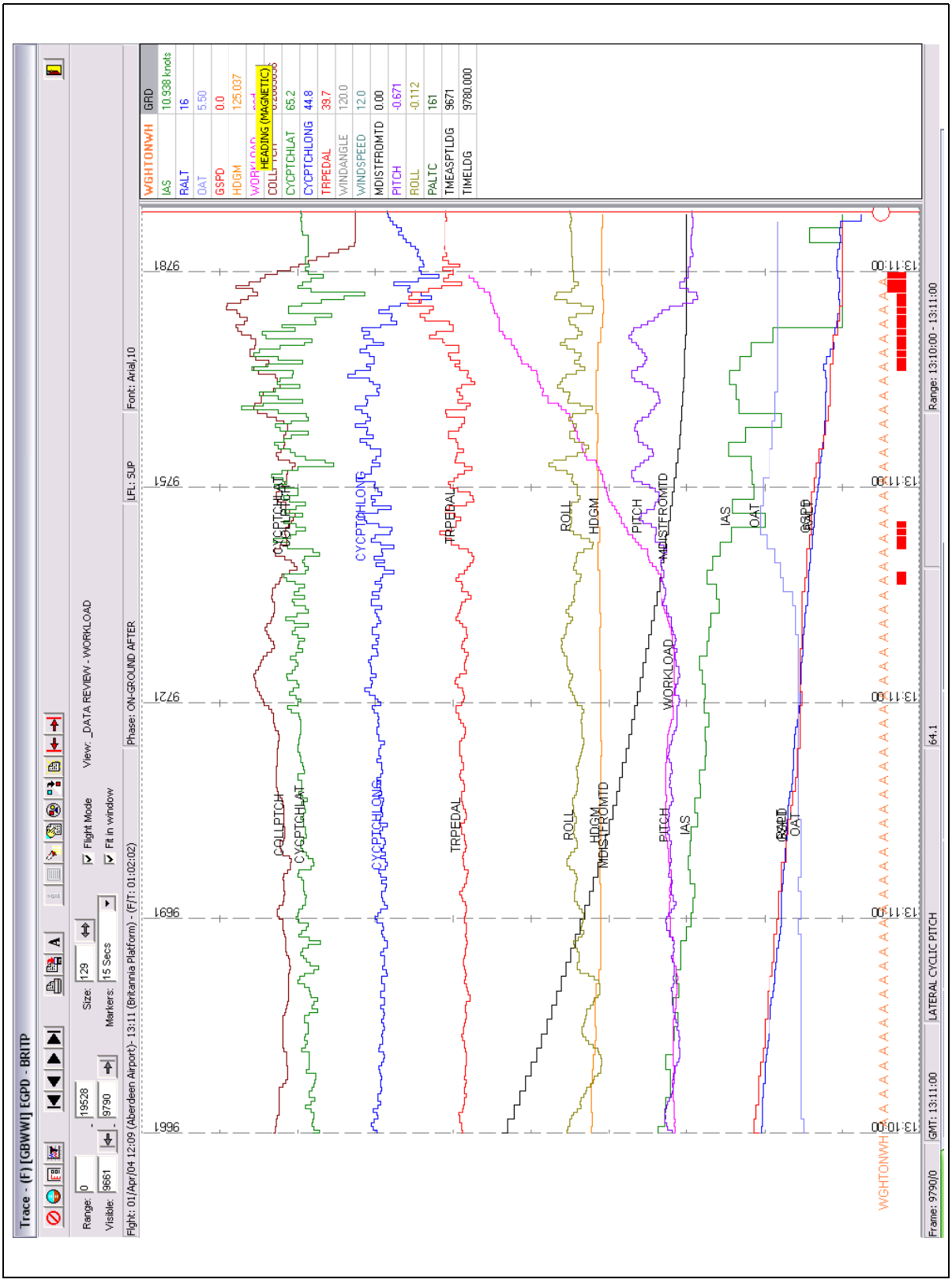
Trace - (F) [GBWWJ] EGPD - BRITP
Flight: 01/Apr/04 12:09 (Aberdeen Airport)- 13:11 (Britannia Platform) - (F/T: 01:02:02)
Phase: ON-GROUND AFTER
LFL: SUP
Font: Arial,10
View: _DATA REVIEW - WORKLOAD
Flight Mode
Fit in window
Range: 0 - 19528
Visible: 9661 - 9790
Size: 129
Markers: 15 Secs
WGHTONWH GRD
IAS 10.938 knots
RALT 16
OAT 5.50
GSPD 0.0
HDGM 125.037
WORKLOAD
COLLPITCH 0.2863636
CYCPTCHLAT 65.2
CYCPTCHLONG 44.8
TRPEDAL 39.7
WINDANGLE 120.0
WINDSPEED 12.0
MDISTFROMTD 0.00
PITCH -0.671
ROLL -0.112
PALTC 161
TMEASPTLDG 9671
TIMELDG 9780.000
HEADING (MAGNETIC)
9781
9751
9721
9691
9661
13:10:00
13:11:00
Range: 13:10:00 - 13:11:00
Frame: 9790/0
GMT: 13:11:00
LATERAL CYCLIC PITCH
64.1

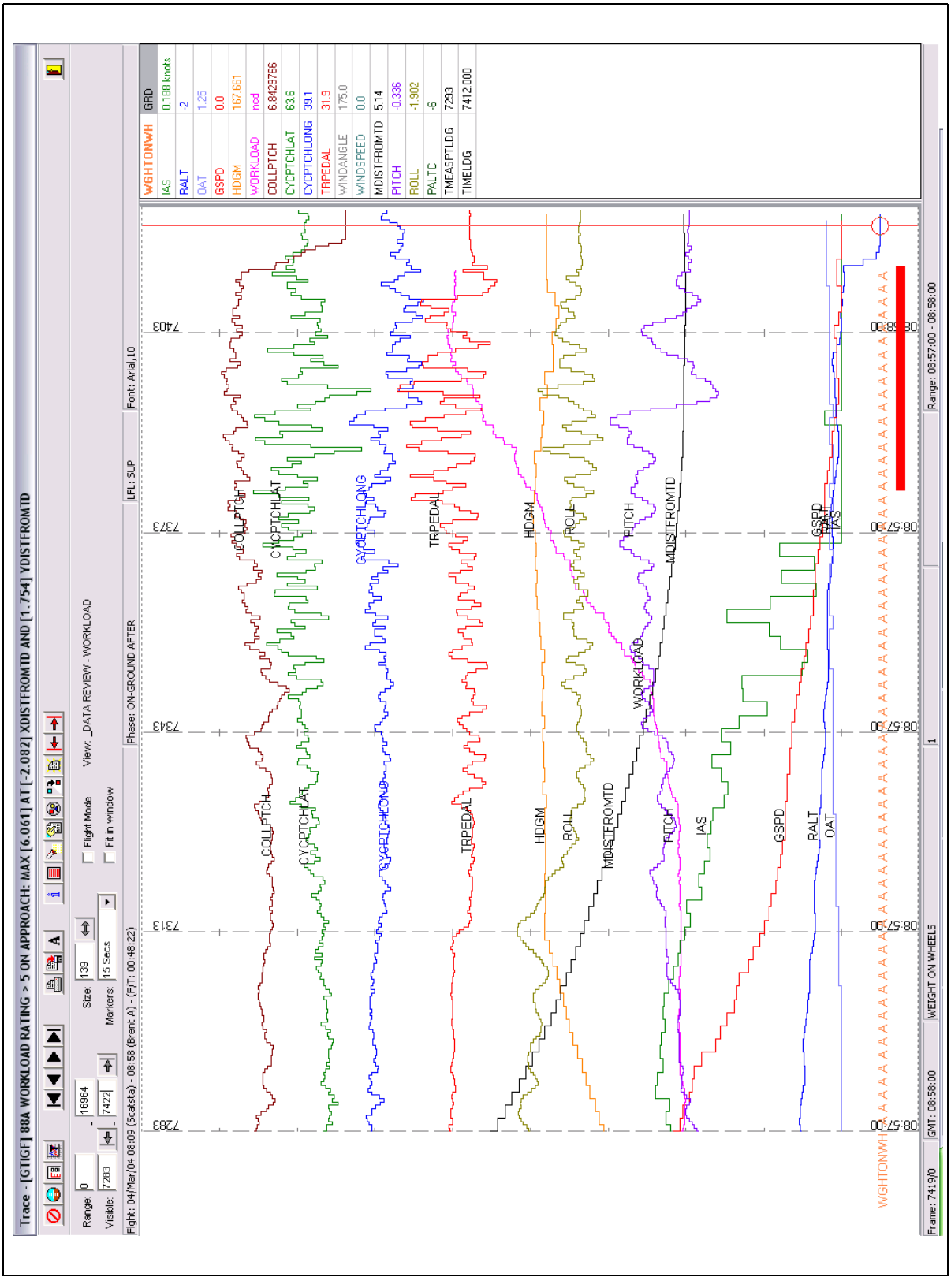
Trace - [GTIGF] 88A WORKLOAD RATING > 5 ON APPROACH: MAX [6.061] AT [-2.082] XDISTFROMTD AND [1.754] YDISTFROMTD
Range: 0 16964
Visible: 7283 7422
Size: 139
Markers: 15 Secs
Flight Mode
Fit in window
View: _DATA REVIEW - WORKLOAD
Flight: 04/Mar/04 08:09 (Scatsta) - 08:58 (Brent A) - (F/T: 00:48:22)
Phase: ON-GROUND AFTER
LFL: SUP
Font: Arial,10
WGHTONWH GRD
IAS 0.188 knots
RALT -2
OAT 1.25
GSPD 0.0
HDGM 167.661
WORKLOAD ncd
COLLPTCH 6.8423766
CYCPTCHLAT 63.6
CYCPTCHLONG 39.1
TRPEDAL 31.9
WINDANGLE 175.0
WINDSPEED 0.0
MDISTFROMTD 5.14
PITCH -0.336
ROLL -1.902
PALTC -6
TMEASPTLDG 7293
TIMELDG 7412.000
7403
7373
7343
7313
7283
08:57:00
08:58:00
Frame: 7419/0
GMT: 08:58:00
WEIGHT ON WHEELS
Range: 08:57:00 - 08:58:00

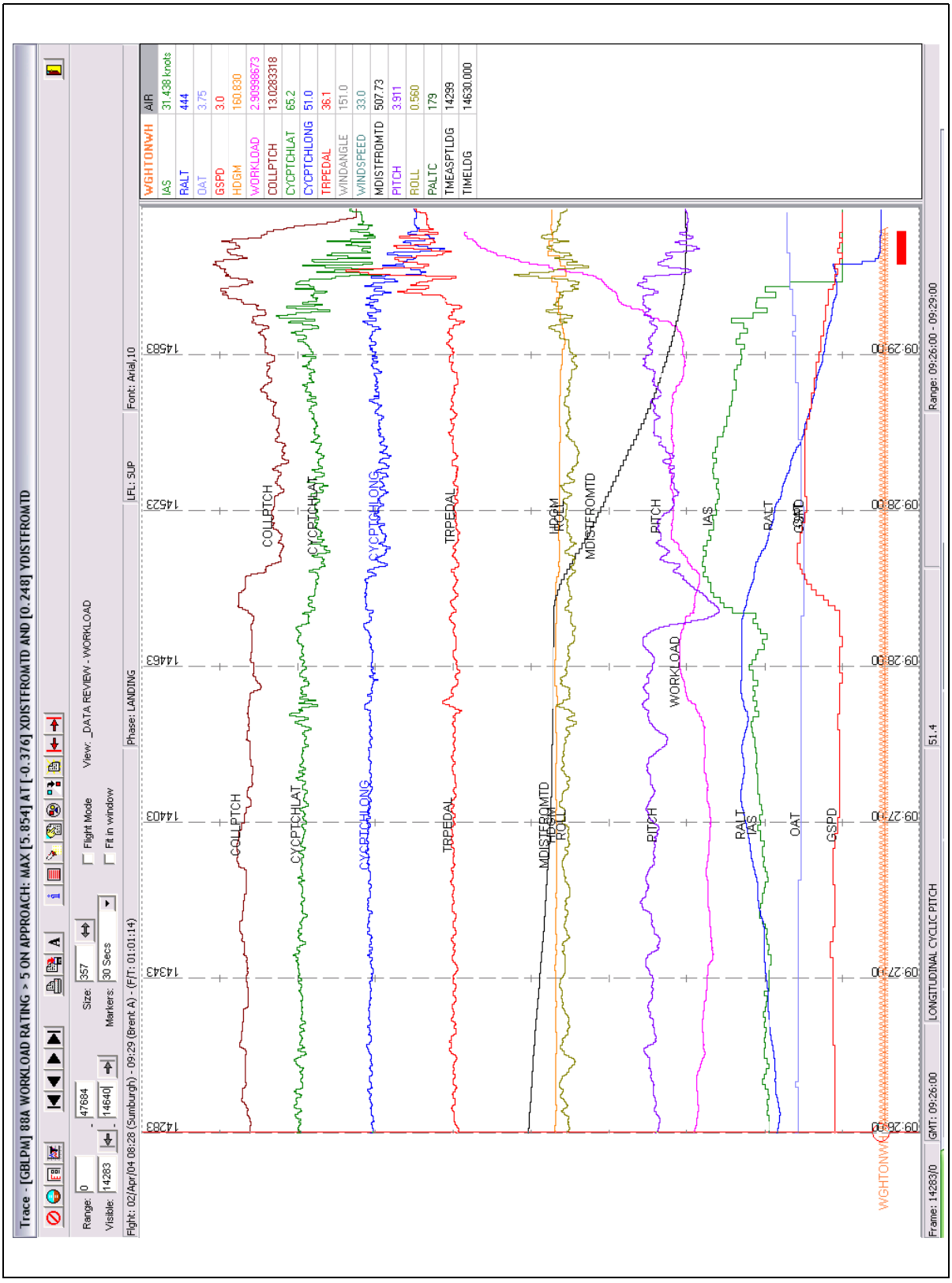
Trace - [GBLPM] 88A WORKLOAD RATING > 5 ON APPROACH: MAX [5.854] AT [-0.376] XDISTFROMTD AND [0.248] YDISTFROMTD
Flight: 02/Apr/04 08:28 (Sumburgh) - 09:29 (Brent A) - (F/T: 01:01:14)
Phase: LANDING
LFL: SUP
Font: Arial,10
Range: 0 - 47684
Visible: 14283 - 14640
Size: 357
Markers: 30 Secs
Flight Mode
Fit in window
View: _DATA REVIEW - WORKLOAD
WGHTONWH AIR
IAS 31.438 knots
RALT 444
OAT 3.75
GSPD 3.0
HDGM 160.830
WORKLOAD 2.90986673
COLLPTCH 13.0283318
CYCPTCHLAT 65.2
CYCPTCHLONG 51.0
TRPEDAL 36.1
WINDANGLE 151.0
WINDSPEED 33.0
MDISTFROMTD 507.73
PITCH 3.911
ROLL 0.560
PALTC 179
TMEASPTLDG 14299
TIMELDG 14630.000
14283
14343
14403
14463
14523
14583
09:26:00
09:27:00
09:28:00
09:29:00
Range: 09:26:00 - 09:29:00
Frame: 14283/0
GMT: 09:26:00
LONGITUDINAL CYCLIC PITCH
51.4
WGHTONWH
COLLPTCH
CYCPTCHLAT
CYCPTCHLONG
TRPEDAL
MDISTFROMTD
HDGM
ROLL
PITCH
WORKLOAD
IAS
RALT
OAT
GSPD

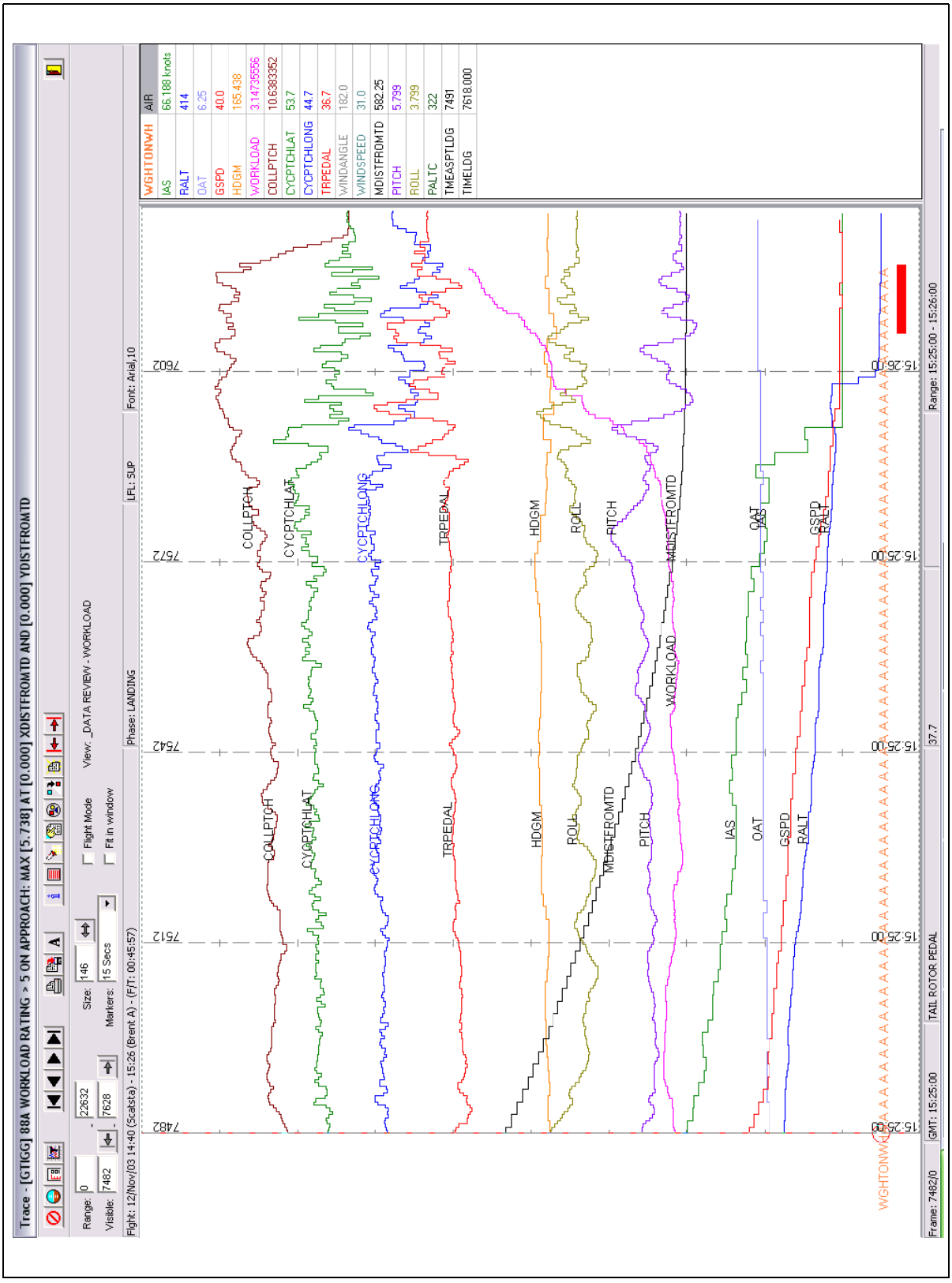
Trace - [GTIGG] 88A WORKLOAD RATING > 5 ON APPROACH: MAX [5.738] AT [0.000] XDISTFROMTD AND [0.000] YDISTFROMTD
Flight: 12/Nov/03 14:40 (Scatsta) - 15:26 (Brent A) - (F/T: 00:45:57)
Phase: LANDING
LFL: SUP
Font: Arial,10
WGHTONWH AIR
IAS 66.188 knots
RALT 414
OAT 6.25
GSPD 40.0
HDGM 165.438
WORKLOAD 3.14735556
COLLPTCH 10.6383352
CYCPTCHLAT 53.7
CYCPTCHLONG 44.7
TRPEDAL 36.7
WINDANGLE 182.0
WINDSPEED 31.0
MDISTFROMTD 582.25
PITCH 5.799
ROLL 3.799
PALTC 322
TMEASPTLDG 7491
TIMELDG 7618.000
COLLPTCH
CYCPTCHLAT
CYCPTCHLONG
TRPEDAL
HDGM
ROLL
PITCH
MDISTFROMTD
WORKLOAD
IAS
OAT
GSPD
RALT
WGHTONWH
7482
7512
7542
7572
7602
15:25:00
15:25:30
15:26:00
Frame: 7482/0
GMT: 15:25:00
TAIL ROTOR PEDAL
37.7
Range: 15:25:00 - 15:26:00

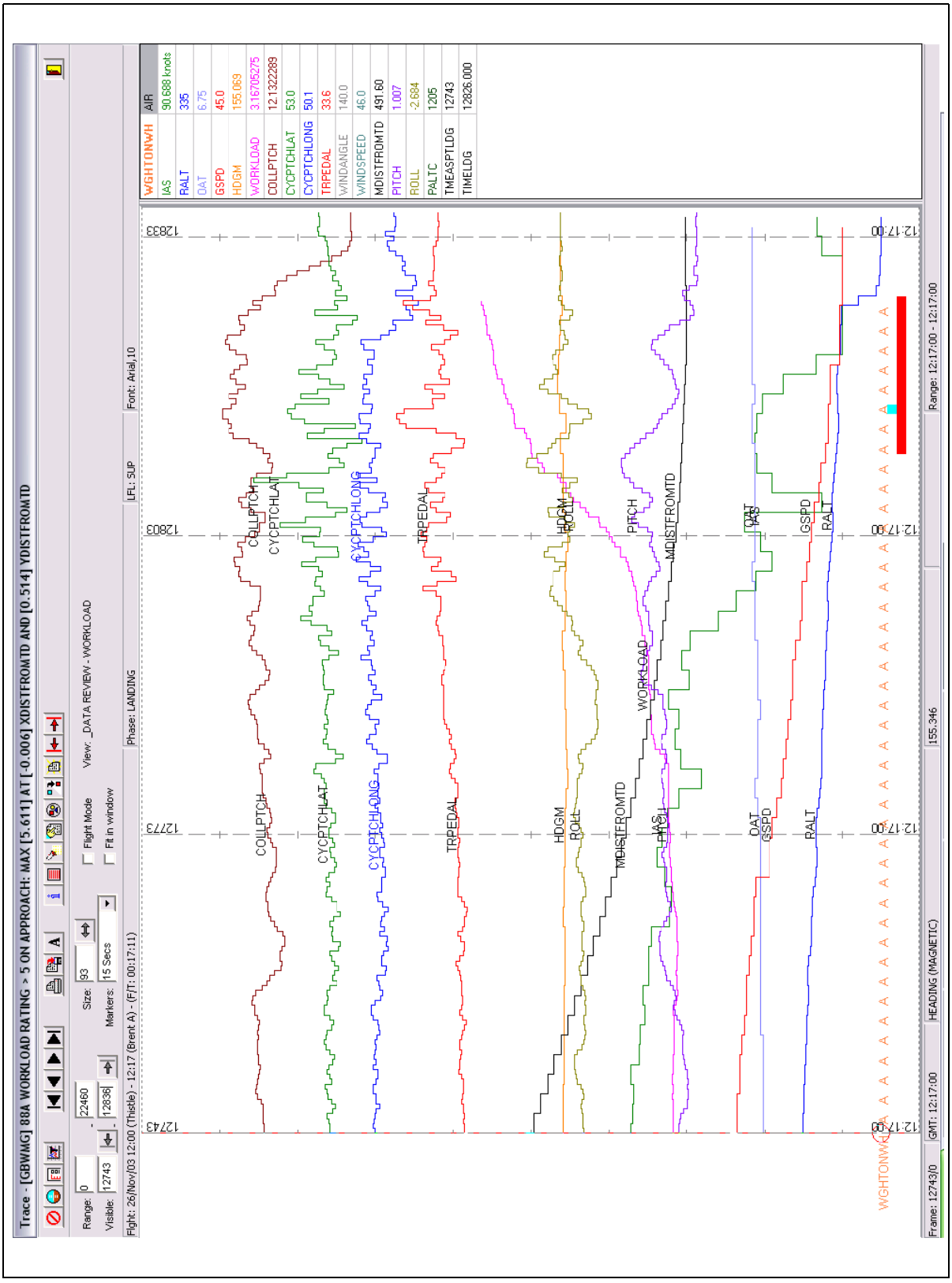
Trace - [GBWMG] 88A WORKLOAD RATING > 5 ON APPROACH: MAX [5.611] AT [-0.006] XDISTFROMTD AND [0.514] YDISTFROMTD
Range: 0 - 22460
Visible: 12743 - 12836
Size: 93
Markers: 15 Secs
Flight Mode
Fit in window
View: _DATA REVIEW - WORKLOAD
Font: Arial,10
Flight: 26/Nov/03 12:00 (Thistle) - 12:17 (Brent A) - (F/T: 00:17:11)
Phase: LANDING
LFL: SUP
WGHTONWH AIR
IAS 90.688 knots
RALT 335
OAT 6.75
GSPD 45.0
HDGM 155.069
WORKLOAD 3.167705275
COLLPTCH 12.1322289
CYCPTCHLAT 53.0
CYCPTCHLONG 50.1
TRPEDAL 33.6
WINDANGLE 140.0
WINDSPEED 46.0
MDISTFROMTD 491.60
PITCH 1.007
ROLL -2.684
PALTC 1205
TMEASPTLDG 12743
TIMELDG 12826.000
12833
12803
12773
12743
12:17:00
Frame: 12743/0
GMT: 12:17:00
HEADING (MAGNETIC)
155.346
Range: 12:17:00 - 12:17:00
WGHTONWH
COLLPTCH
CYCPTCHLAT
CYCPTCHLONG
TRPEDAL
HDGM
ROLL
MDISTFROMTD
IAS
PITCH
WORKLOAD
OAT
GSPD
RALT

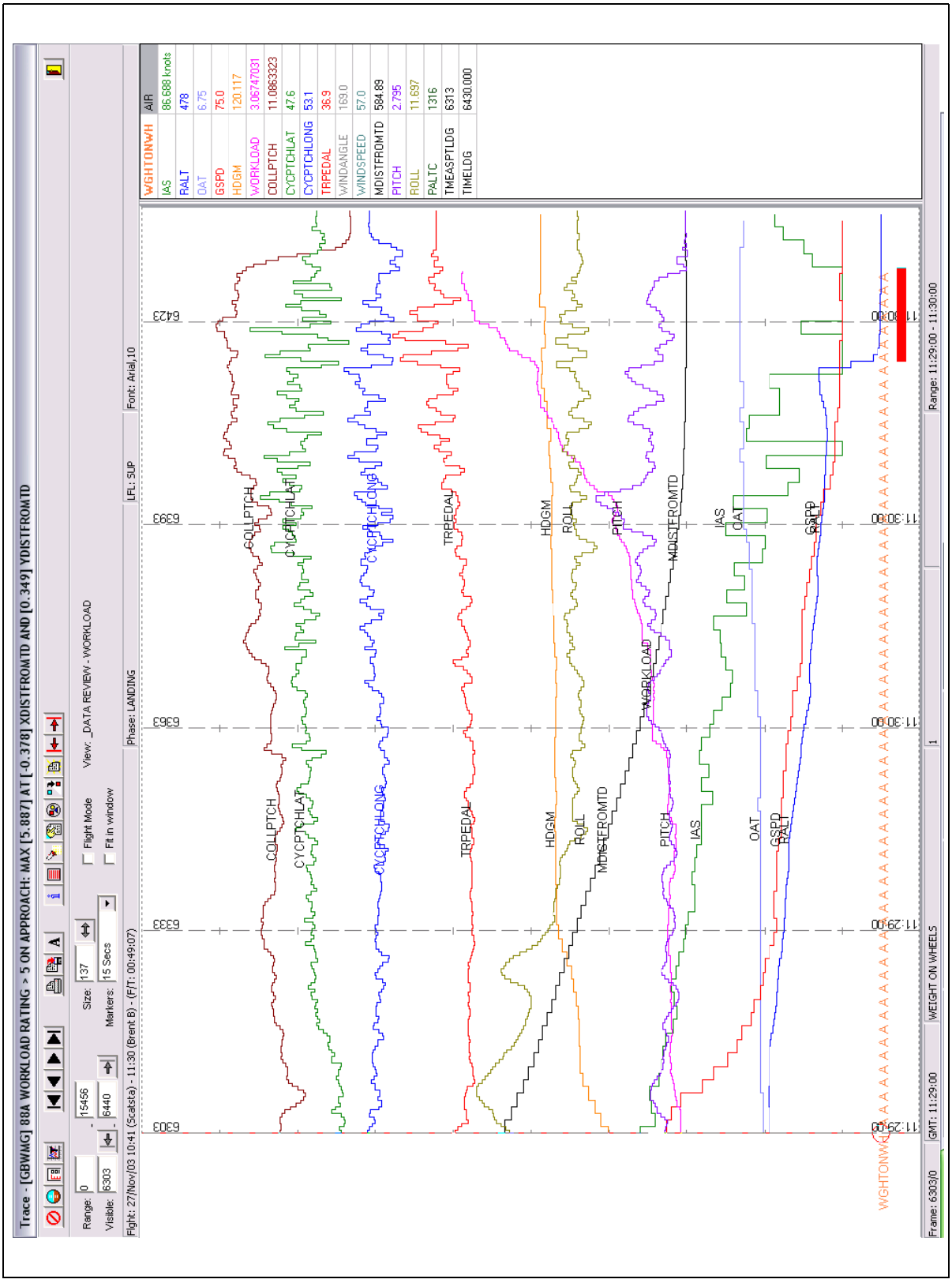
Trace - [GBWMG] 88A WORKLOAD RATING > 5 ON APPROACH: MAX [5.887] AT [-0.378] XDISTFROMTD AND [0.349] YDISTFROMTD
Range: 0 15456
Visible: 6303 6440
Size: 137
Markers: 15 Secs
Flight Mode
Fit in window
View: _DATA REVIEW - WORKLOAD
Font: Arial,10
Flight: 27/Nov/03 10:41 (Scatsta) - 11:30 (Brent B) - (F/T: 00:49:07)
Phase: LANDING
LFL: SUP
WGHTONWH AIR
IAS 86.688 knots
RALT 478
OAT 6.75
GSPD 75.0
HDGM 120.117
WORKLOAD 3.06747031
COLLPTCH 11.0863323
CYCPTCHLAT 47.6
CYCPTCHLONG 53.1
TRPEDAL 36.9
WINDANGLE 163.0
WINDSPEED 57.0
MDISTFROMTD 584.89
PITCH 2.795
ROLL 11.697
PALTC 1316
TMEASPTLDG 6313
TIMELDG 6430.000
6423
6393
6363
6333
6303
11:29:00
11:30:00
Range: 11:29:00 - 11:30:00
Frame: 6303/0
GMT: 11:29:00
WEIGHT ON WHEELS
WGHTONWH

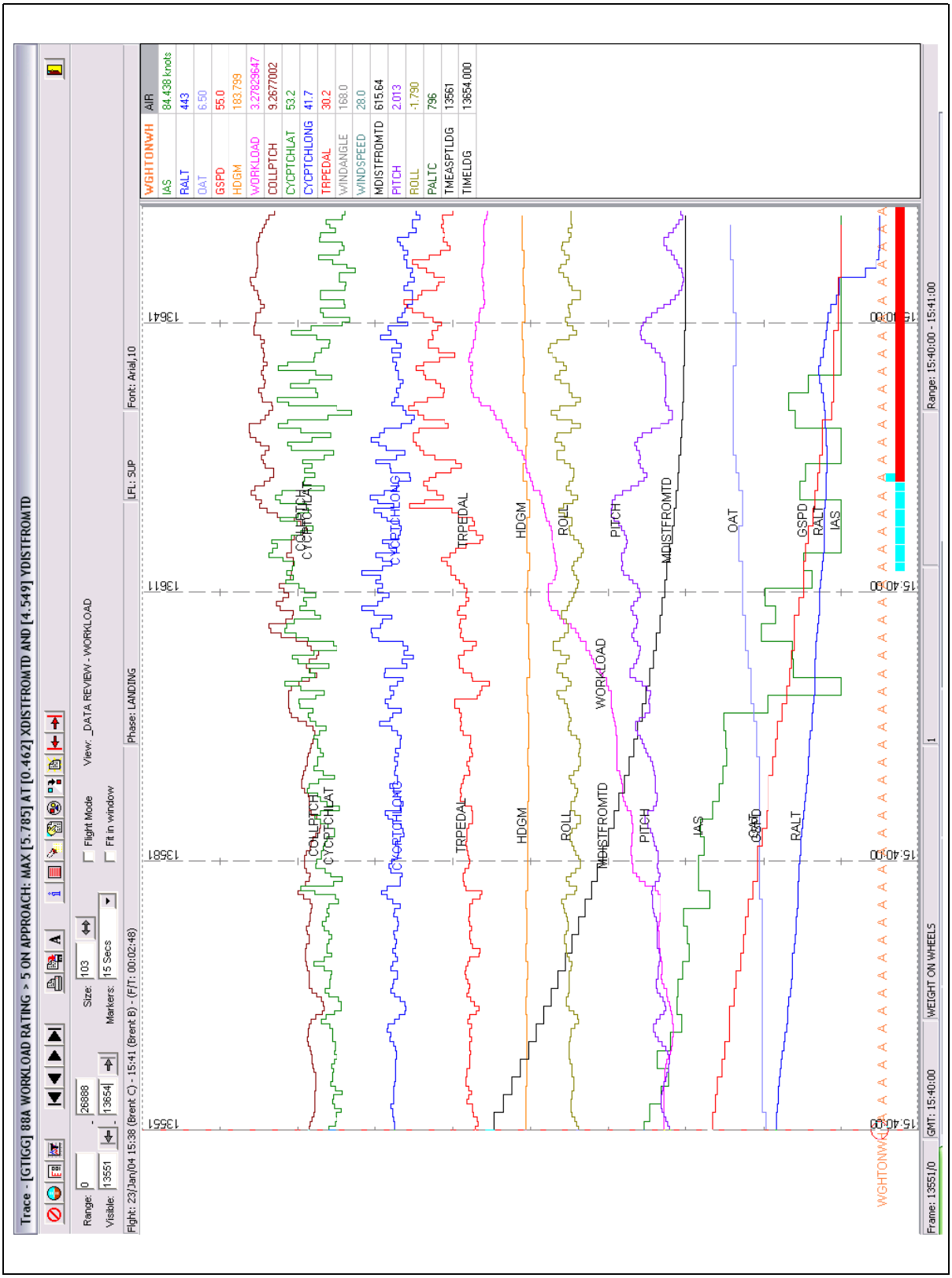
Trace - [GTIGG] 88A WORKLOAD RATING > 5 ON APPROACH: MAX [5.785] AT [0.462] XDISTFROMTD AND [4.549] YDISTFROMTD
Flight: 23/Jan/04 15:38 (Brent C) - 15:41 (Brent B) - (F/T: 00:02:48)
Phase: LANDING
Font: Arial,10
Range: 0 - 26888
Visible: 13551 - 13654
Size: 103
Markers: 15 Secs
Flight Mode
Fit in window
View: _DATA REVIEW - WORKLOAD
WGHTONWH AIR
IAS 84.438 knots
RALT 443
OAT 6.50
GSPD 55.0
HDGM 183.799
WORKLOAD 3.27829647
COLLPTCH 9.2677002
CYCPTCHLAT 53.2
CYCPTCHLONG 41.7
TRPEDAL 30.2
WINDANGLE 168.0
WINDSPEED 28.0
MDISTFROMTD 615.64
PITCH 2.013
ROLL -1.790
PALTC 796
TMEASPTLDG 13561
TIMELDG 13654.000
13551
13581
13611
13641
15:40:00
15:40:00
15:40:00
15:40:00
Frame: 13551/0
GMT: 15:40:00
WEIGHT ON WHEELS
Range: 15:40:00 - 15:41:00

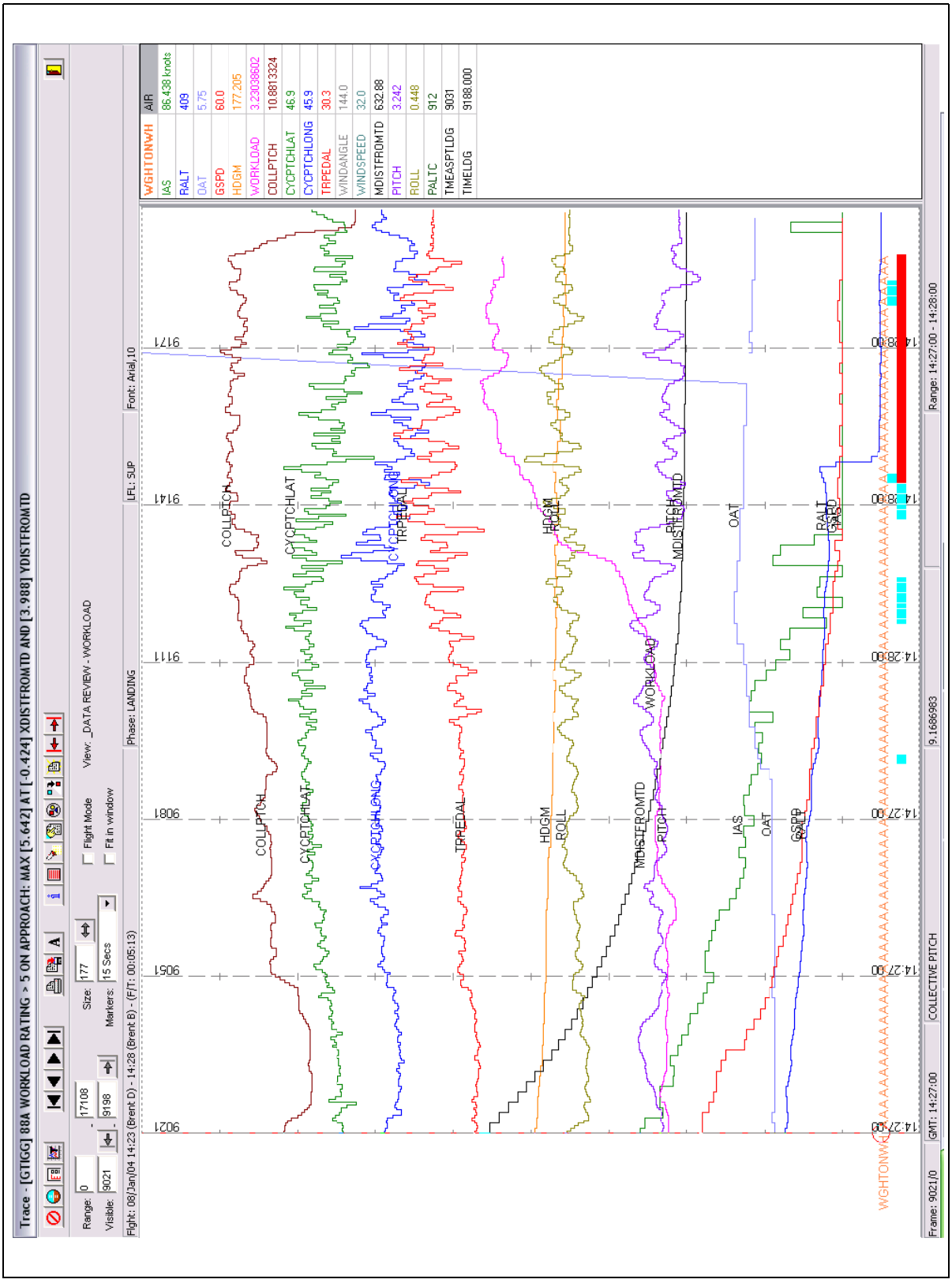
Trace - [GTIGG] 88A WORKLOAD RATING > 5 ON APPROACH: MAX [5.642] AT [-0.424] XDISTFROMTD AND [3.988] YDISTFROMTD
Range: 0 17108
Visible: 9021 9198
Size: 177
Markers: 15 Secs
Flight Mode
Fit in window
View: _DATA REVIEW - WORKLOAD
Font: Arial,10
LFL: SUP
Phase: LANDING
Flight: 08/Jan/04 14:23 (Brent D) - 14:28 (Brent B) - (F/T: 00:05:13)
WGHTONWH AIR
IAS 86.438 knots
RALT 409
OAT 5.75
GSPD 60.0
HDGM 177.205
WORKLOAD 3.23038602
COLLPTCH 10.8813324
CYCPTCHLAT 46.9
CYCPTCHLONG 45.9
TRPEDAL 30.3
WINDANGLE 144.0
WINDSPEED 32.0
MDISTFROMTD 632.88
PITCH 3.242
ROLL 0.448
PALTC 912
TMEASPTLDG 9031
TIMELDG 9188.000
9171
9141
9111
9081
9051
9021
14:28:00
14:27:00
Range: 14:27:00 - 14:28:00
Frame: 9021,0
GMT: 14:27:00
COLLECTIVE PITCH
9.1686983

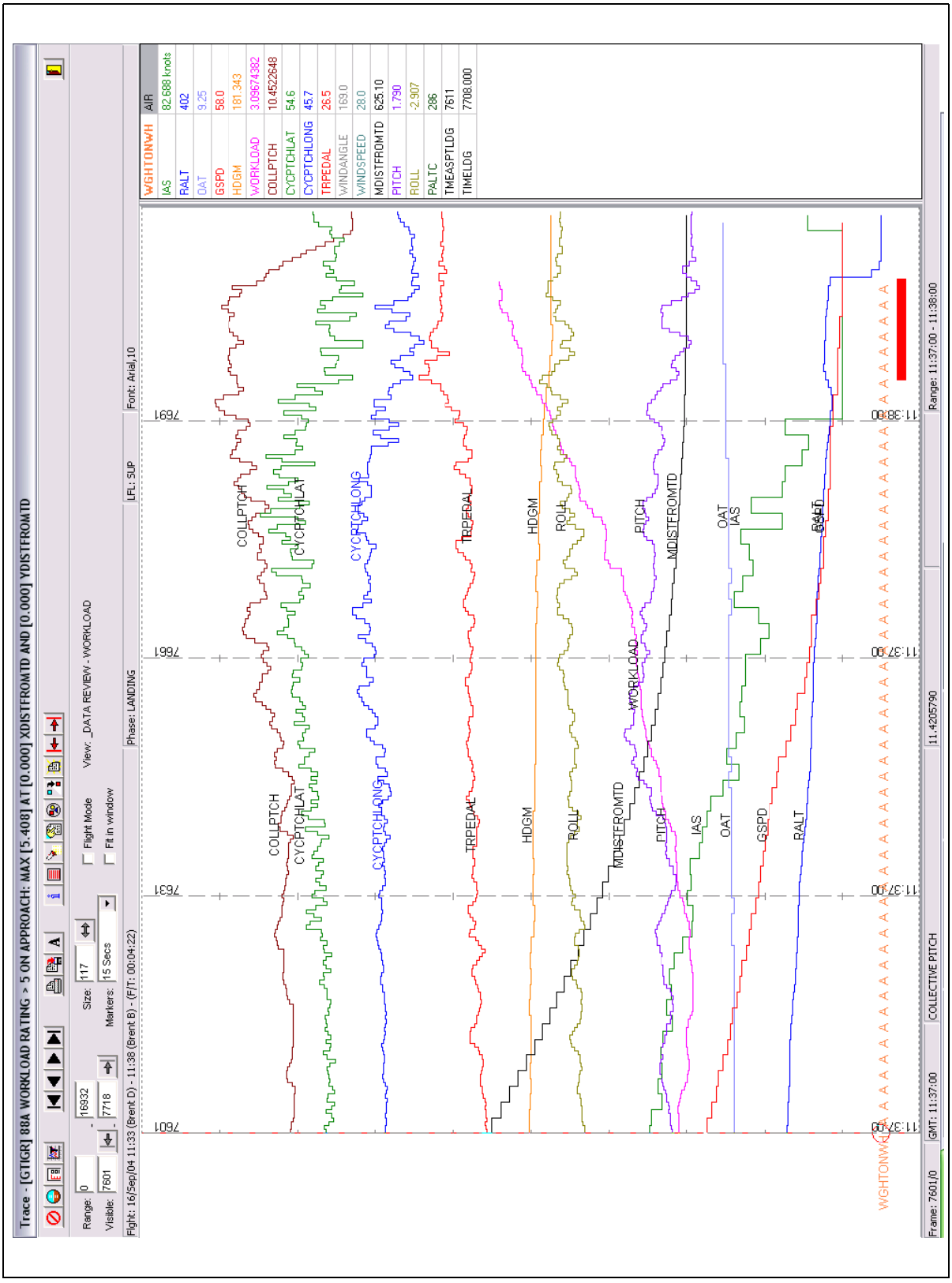
Trace - [GTIGR] 88A WORKLOAD RATING > 5 ON APPROACH: MAX [5.408] AT [0.000] XDISTFROMTD AND [0.000] YDISTFROMTD
Range: 0 16932
Visible: 7601 7718
Size: 117
Markers: 15 Secs
Flight Mode
Fit in window
View: _DATA REVIEW - WORKLOAD
Font: Arial,10
Flight: 16/Sep/04 11:33 (Brent D) - 11:38 (Brent B) - (F/T: 00:04:22)
Phase: LANDING
LFL: SUP
WGHTONWH AIR
IAS 82.688 knots
RALT 402
OAT 9.25
GSPD 58.0
HDGM 181.343
WORKLOAD 3.09674382
COLLPTCH 10.4522648
CYCPTCHLAT 54.6
CYCPTCHLONG 45.7
TRPEDAL 26.5
WINDANGLE 163.0
WINDSPEED 28.0
MDISTFROMTD 625.10
PITCH 1.790
ROLL -2.907
PALTC 286
TMEASPTLDG 7611
TIMELDG 7708.000
7691
7661
7631
7601
11:38:00
11:37:00
11:37:00
11:37:00
COLLPTCH
CYCPTCHLAT
CYCPTCHLONG
TRPEDAL
HDGM
ROLL
MDISTFROMTD
WORKLOAD
PITCH
IAS
OAT
GSPD
RALT
WGHTONWH
Frame: 7601/0
GMT: 11:37:00
COLLECTIVE PITCH
11.4205790
Range: 11:37:00 - 11:38:00

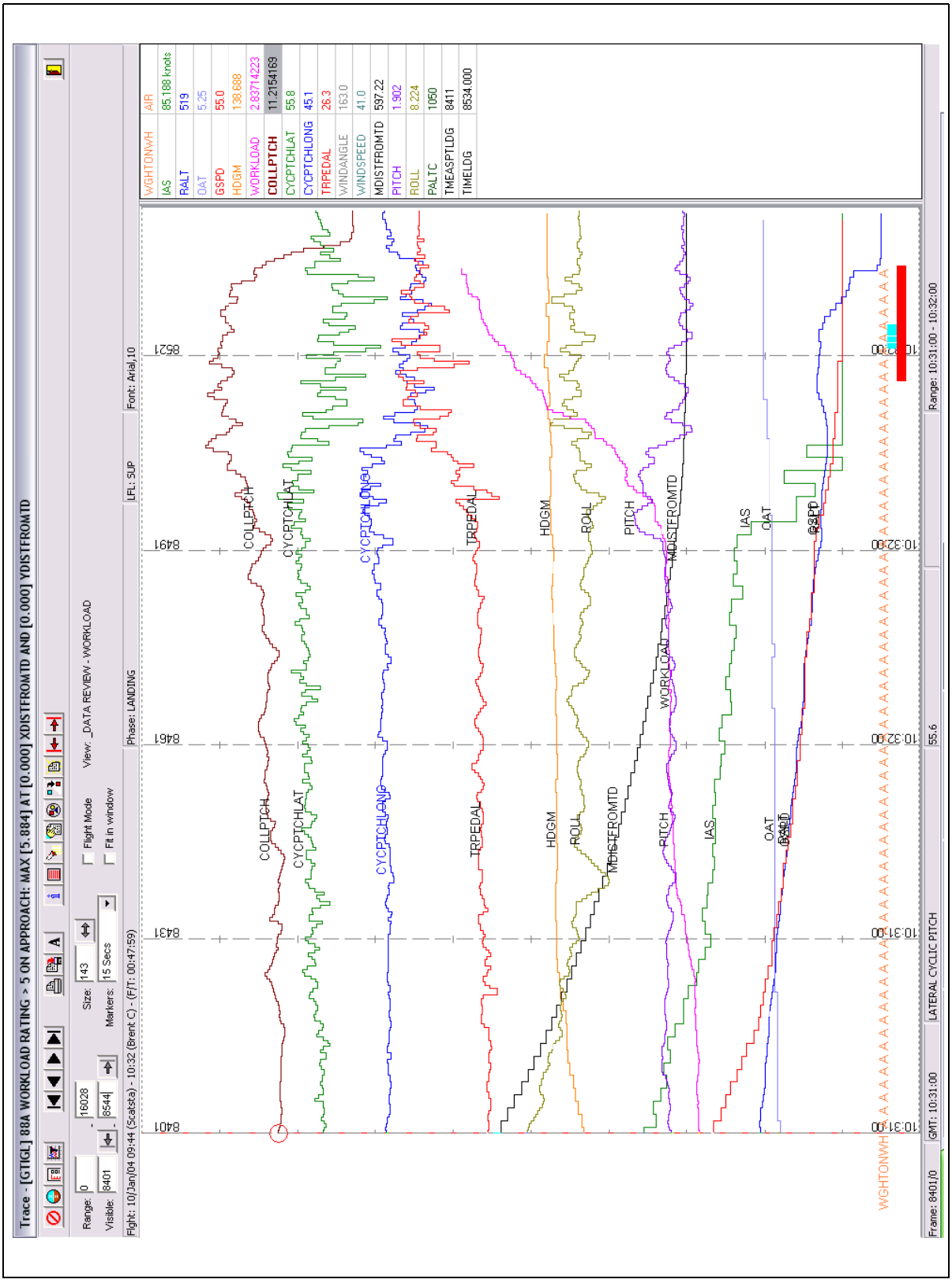
Trace - [GTIGL] 88A WORKLOAD RATING > 5 ON APPROACH: MAX [5.884] AT [0.000] XDISTFROMTD AND [0.000] YDISTFROMTD
Flight: 10/Jan/04 09:44 (Scatsta) - 10:32 (Brent C) - (F/T: 00:47:59)
Phase: LANDING
LFL: SUP
Font: Arial,10
Range: 0 16028
Visible: 8401 8544
Size: 143
Markers: 15 Secs
Flight Mode
Fit in window
View: _DATA REVIEW - WORKLOAD
WGHTONWH AIR
IAS 85.188 knots
RALT 519
OAT 5.25
GSPD 55.0
HDGM 138.688
WORKLOAD 2.83714223
COLLPTCH 11.2154169
CYCPTCHLAT 55.8
CYCPTCHLONG 45.1
TRPEDAL 26.3
WINDANGLE 163.0
WINDSPEED 41.0
MDISTFROMTD 597.22
PITCH 1.902
ROLL 8.224
PALTC 1050
TMEASPTLDG 8411
TIMELDG 8534.000
8521
8491
8461
8431
8401
10:31:00
10:32:00
Frame: 8401/0
GMT: 10:31:00
LATERAL CYCLIC PITCH
55.6
Range: 10:31:00 - 10:32:00
WGHTONWH
COLLPTCH
CYCPTCHLAT
CYCPTCHLONG
TRPEDAL
HDGM
ROLL
MDISTFROMTD
PITCH
WORKLOAD
IAS
OAT
GSPD
PALTC

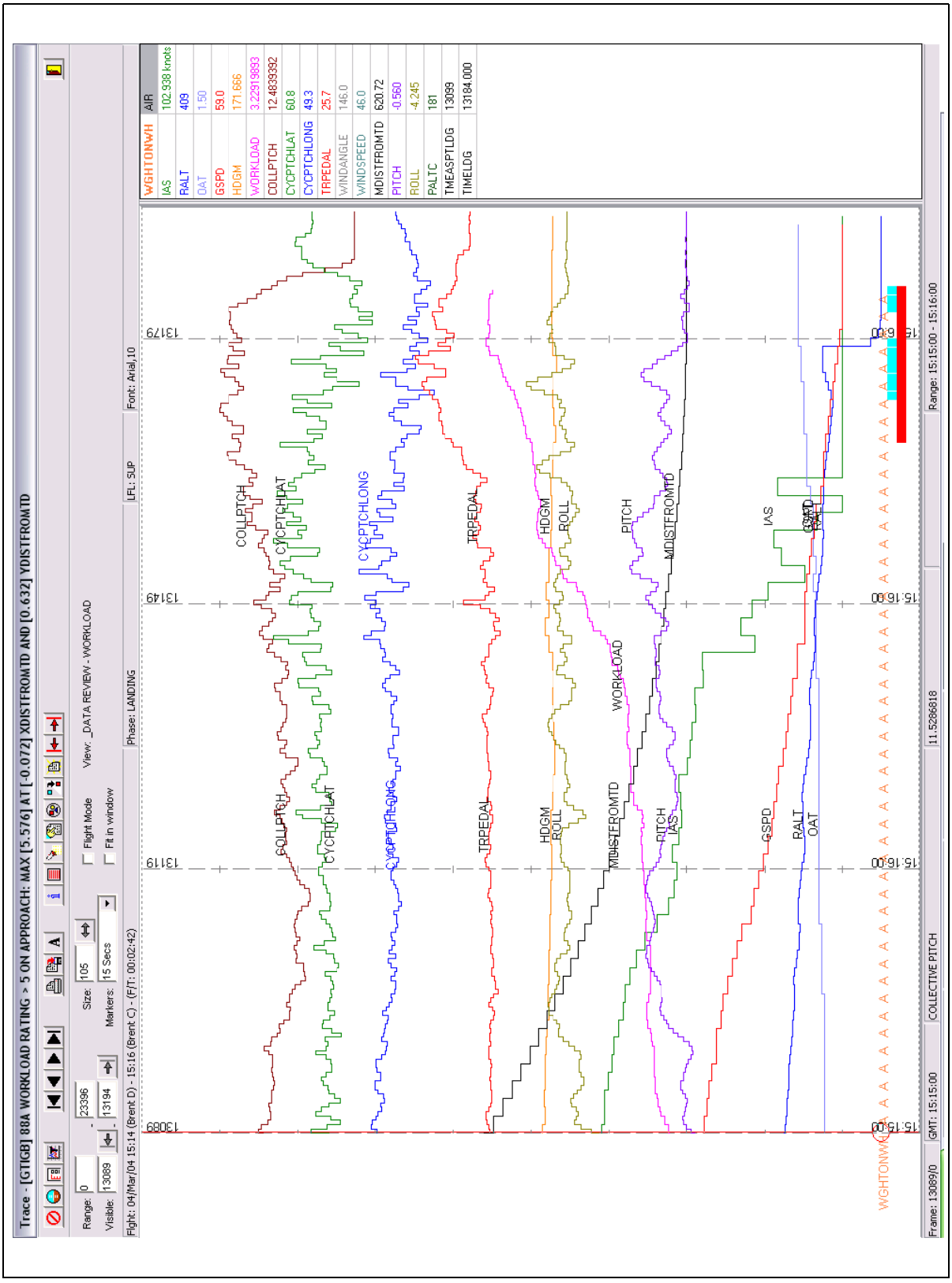
Trace - [GTIGB] 88A WORKLOAD RATING > 5 ON APPROACH: MAX [5.576] AT [-0.072] XDISTFROMTD AND [0.632] YDISTFROMTD
Flight: 04/Mar/04 15:14 (Brent D) - 15:16 (Brent C) - (F/T: 00:02:42)
Phase: LANDING
LFL: SUP
Font: Arial,10
View: _DATA REVIEW - WORKLOAD
Flight Mode
Fit in window
Range: 0 - 23396
Visible: 13089 - 13194
Size: 105
Markers: 15 Secs
WGHTONWH AIR
IAS 102.938 knots
RALT 409
OAT 1.50
GSPD 59.0
HDGM 171.666
WORKLOAD 3.22919893
COLLPTCH 12.4839392
CYCPTCHLAT 60.8
CYCPTCHLONG 49.3
TRPEDAL 25.7
WINDANGLE 146.0
WINDSPEED 46.0
MDISTFROMTD 620.72
PITCH -0.560
ROLL -4.245
PALTC 181
TMEASPTLDG 13099
TIMELDG 13184.000
13089
13119
13149
13179
15:15:00
15:16:00
COLLPTCH
CYCPTCHLAT
CYCPTCHLONG
TRPEDAL
HDGM
ROLL
MDISTFROMTD
WORKLOAD
PITCH
IAS
GSPD
RALT
OAT
WGHTONWH
Frame: 13089/0
GMT: 15:15:00
COLLECTIVE PITCH
11.5286818
Range: 15:15:00 - 15:16:00

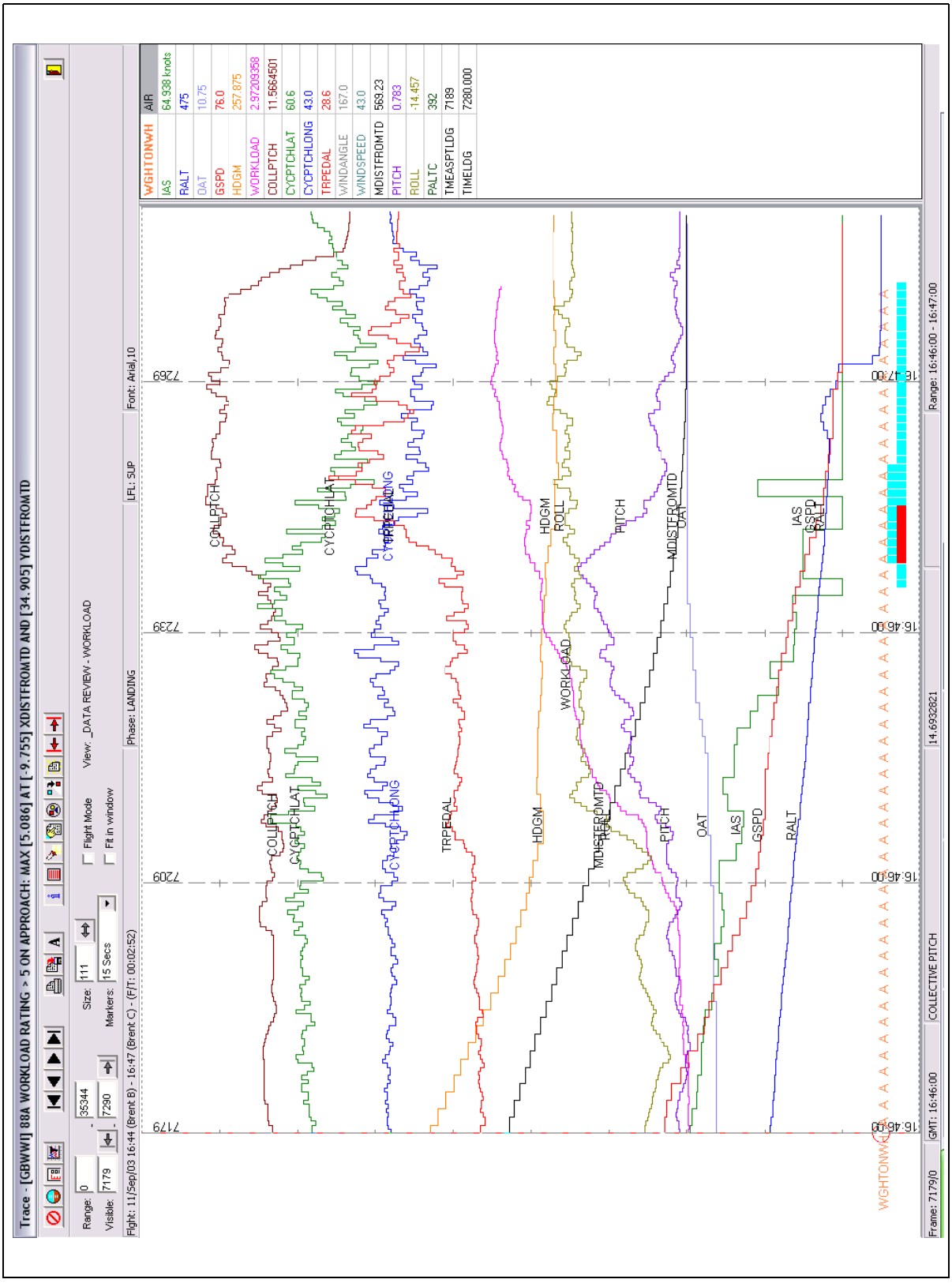
Trace - [GBWWJ] 88A WORKLOAD RATING > 5 ON APPROACH: MAX [5.086] AT [-9.755] XDISTFROMTD AND [34.905] YDISTFROMTD
Flight: 11/Sep/03 16:44 (Brent B) - 16:47 (Brent C) - (F/T: 00:02:52)
Phase: LANDING
LFL: SUP
Font: Arial,10
Range: 0 - 35344
Visible: 7179 - 7290
Size: 111
Markers: 15 Secs
Flight Mode
Fit in window
View: _DATA REVIEW - WORKLOAD
WGHTONWH AIR
IAS 64.938 knots
RALT 475
OAT 10.75
GSPD 76.0
HDGM 257.875
WORKLOAD 2.97209358
COLLPTCH 11.5664501
CYCPTCHLAT 60.6
CYCPTCHLONG 43.0
TRPEDAL 28.6
WINDANGLE 167.0
WINDSPEED 43.0
MDISTFROMTD 569.23
PITCH 0.783
ROLL -14.457
PALTC 392
TMEASPTLDG 7189
TIMELDG 7280.000
7269
7239
7209
7179
16:47:00
16:46:00
16:46:00
16:46:00
Frame: 7179/0
GMT: 16:46:00
COLLECTIVE PITCH
14.6932821
Range: 16:46:00 - 16:47:00
WGHTONWH
COLLPTCH
CYCPTCHLAT
CYCPTCHLONG
TRPEDAL
HDGM
ROLL
WORKLOAD
MDISTFROMTD
PITCH
OAT
IAS
GSPD
RALT

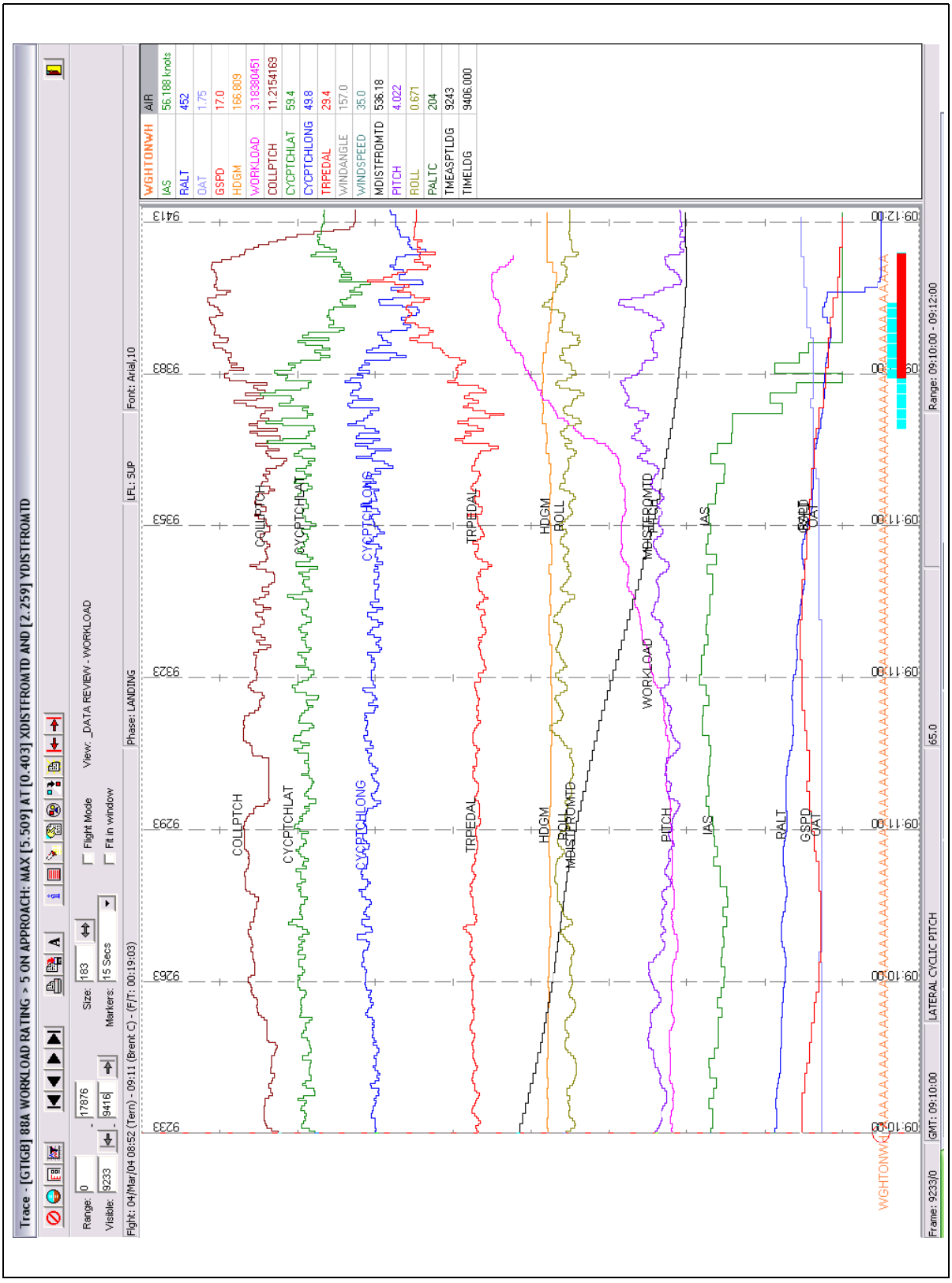
Trace - [GTIGB] 88A WORKLOAD RATING > 5 ON APPROACH: MAX [5.509] AT [0.403] XDISTFROMTD AND [2.259] YDISTFROMTD
Flight: 04/Mar/04 08:52 (Tern) - 09:11 (Brent C) - (F/T: 00:19:03)
Phase: LANDING
LFL: SUP
Font: Arial,10
Range: 0
Visible: 9233
17876
9416
Size: 183
Markers: 15 Secs
Flight Mode
Fit in window
View: _DATA REVIEW - WORKLOAD
WGHTONWH AIR
IAS 56.188 knots
RALT 452
OAT 1.75
GSPD 17.0
HDGM 166.809
WORKLOAD 3.18380451
COLLPTCH 11.2154169
CYCPTCHLAT 59.4
CYCPTCHLONG 49.8
TRPEDAL 29.4
WINDANGLE 157.0
WINDSPEED 35.0
MDISTFROMTD 536.18
PITCH 4.022
ROLL 0.671
PALTC 204
TMEASPTLDG 9243
TIMELDG 9406.000
9413
9383
9353
9323
9293
9263
9233
09:12:00
09:11:00
09:10:00
Frame: 9233/0
GMT: 09:10:00
LATERAL CYCLIC PITCH
65.0
Range: 09:10:00 - 09:12:00

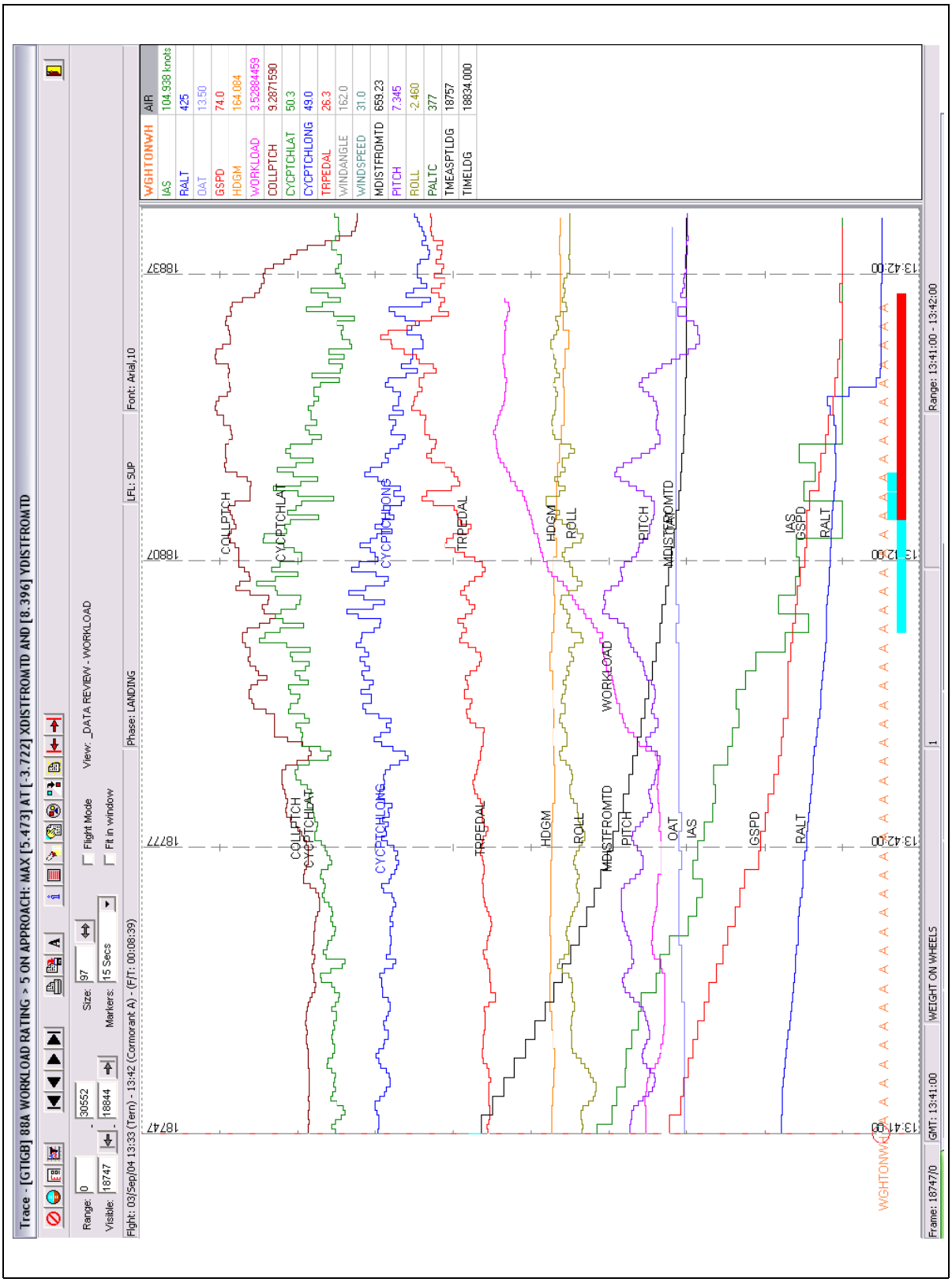
Trace - [GTIGB] 88A WORKLOAD RATING > 5 ON APPROACH: MAX [5.473] AT [-3.722] XDISTFROMTD AND [8.396] YDISTFROMTD
Flight: 03/Sep/04 13:33 (Tern) - 13:42 (Cormorant A) - (F/T: 00:08:39)
Phase: LANDING
LFL: SUP
Font: Arial,10
Range: 0
Visible: 18747
Size: 97
Markers: 15 Secs
Flight Mode
Fit in window
View: _DATA REVIEW - WORKLOAD
WGHTONWH AIR
IAS 104.938 knots
RALT 425
OAT 13.50
GSPD 74.0
HDGM 164.084
WORKLOAD 3.52884459
COLLPTCH 9.2871590
CYCPTCHLAT 50.3
CYCPTCHLONG 49.0
TRPEDAL 26.3
WINDANGLE 162.0
WINDSPEED 31.0
MDISTFROMTD 659.23
PITCH 7.345
ROLL -2.460
PALTC 377
TMEASPTLDG 18757
TIMELDG 18834.000
18747
18777
18807
18837
13:41:00
13:42:00
Range: 13:41:00 - 13:42:00
Frame: 18747/0
GMT: 13:41:00
WEIGHT ON WHEELS

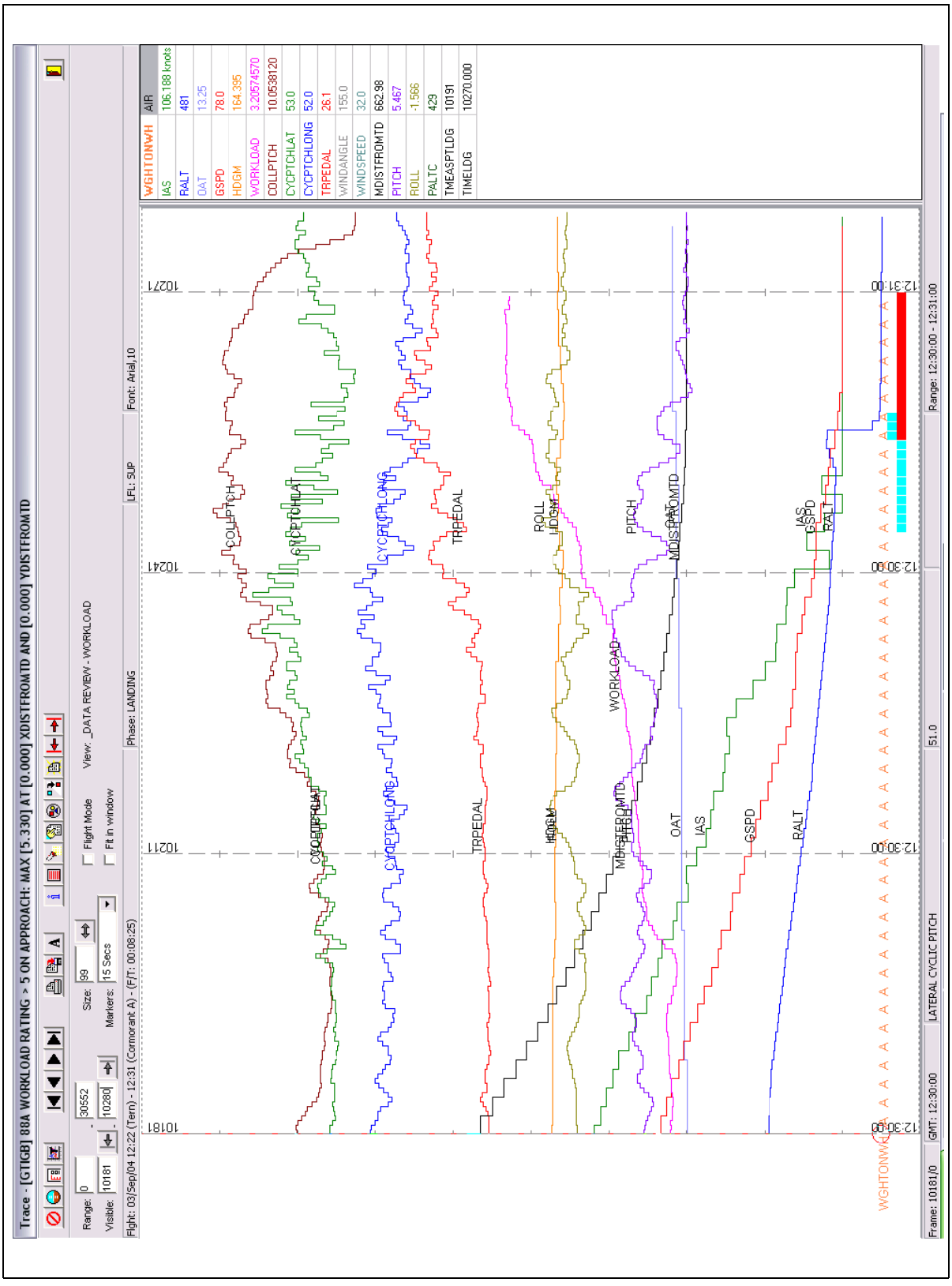
Trace - [GTIGB] 88A WORKLOAD RATING > 5 ON APPROACH: MAX [5.330] AT [0.000] XDISTFROMTD AND [0.000] YDISTFROMTD
Flight: 03/Sep/04 12:22 (Tern) - 12:31 (Cormorant A) - (F/T: 00:08:25)
Phase: LANDING
LFL: SUP
Font: Arial,10
Range: 0
Visible: 10181
30552
10280
Size: 99
Markers: 15 Secs
Flight Mode
Fit in window
View: _DATA REVIEW - WORKLOAD
WGHTONWH
IAS 106.188 knots
RALT 481
OAT 13.25
GSPD 78.0
HDGM 164.395
WORKLOAD 3.20574570
COLLPTCH 10.0538120
CYCPTCHLAT 53.0
CYCPTCHLONG 52.0
TRPEDAL 26.1
WINDANGLE 155.0
WINDSPEED 32.0
MDISTFROMTD 662.98
PITCH 5.467
ROLL -1.566
PALTC 429
TMEASPTLDG 10191
TIMELDG 10270.000
AIR
10271
10241
10211
10181
12:31:00
12:30:00
12:30:00
12:30:00
Frame: 10181/0
GMT: 12:30:00
LATERAL CYCLIC PITCH
51.0
Range: 12:30:00 - 12:31:00

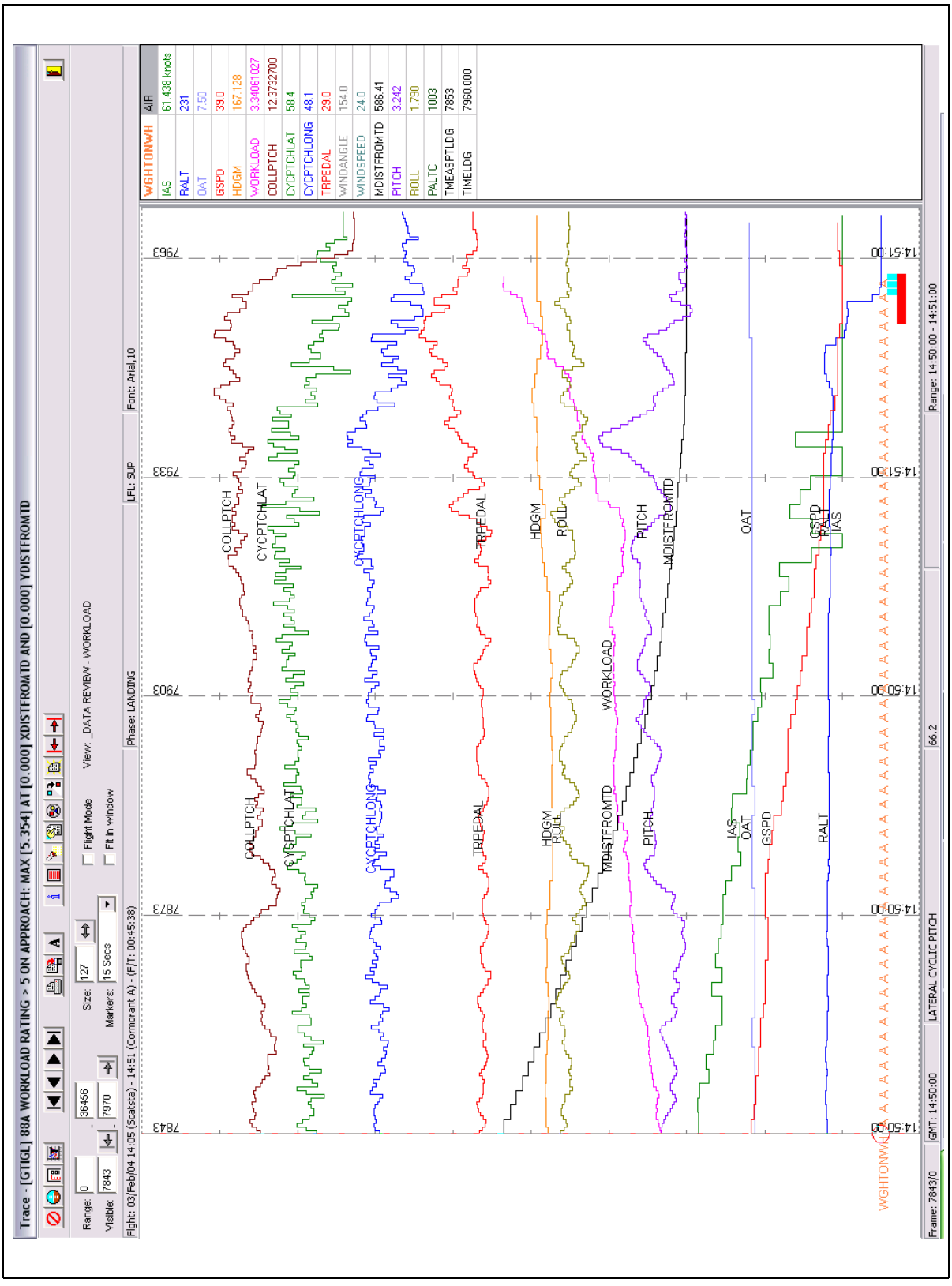
Trace - [GTIGL] 88A WORKLOAD RATING > 5 ON APPROACH: MAX [5.354] AT [0.000] XDISTFROMTD AND [0.000] YDISTFROMTD
Flight: 03/Feb/04 14:05 (Scatsta) - 14:51 (Cormorant A) - (F/T: 00:45:38)
Phase: LANDING
LFL: SUP
Font: Arial,10
Range: 0
Visible: 7843
36456
7970
Size: 127
Markers: 15 Secs
Flight Mode
Fit in window
View: _DATA REVIEW - WORKLOAD
WGHTONWH AIR
IAS 61.438 Knots
RALT 231
OAT 7.50
GSPD 39.0
HDGM 167.128
WORKLOAD 3.34061027
COLLPTCH 12.3732700
CYCPTCHLAT 58.4
CYCPTCHLONG 48.1
TRPEDAL 29.0
WINDANGLE 154.0
WINDSPEED 24.0
MDISTFROMTD 588.41
PITCH 3.242
ROLL 1.790
PALTC 1003
TMEASPTLDG 7853
TIMELDG 7960.000
7963
7933
7903
7873
7843
14:51:00
14:50:00
Frame: 7843/0
GMT: 14:50:00
LATERAL CYCLIC PITCH
66.2
Range: 14:50:00 - 14:51:00

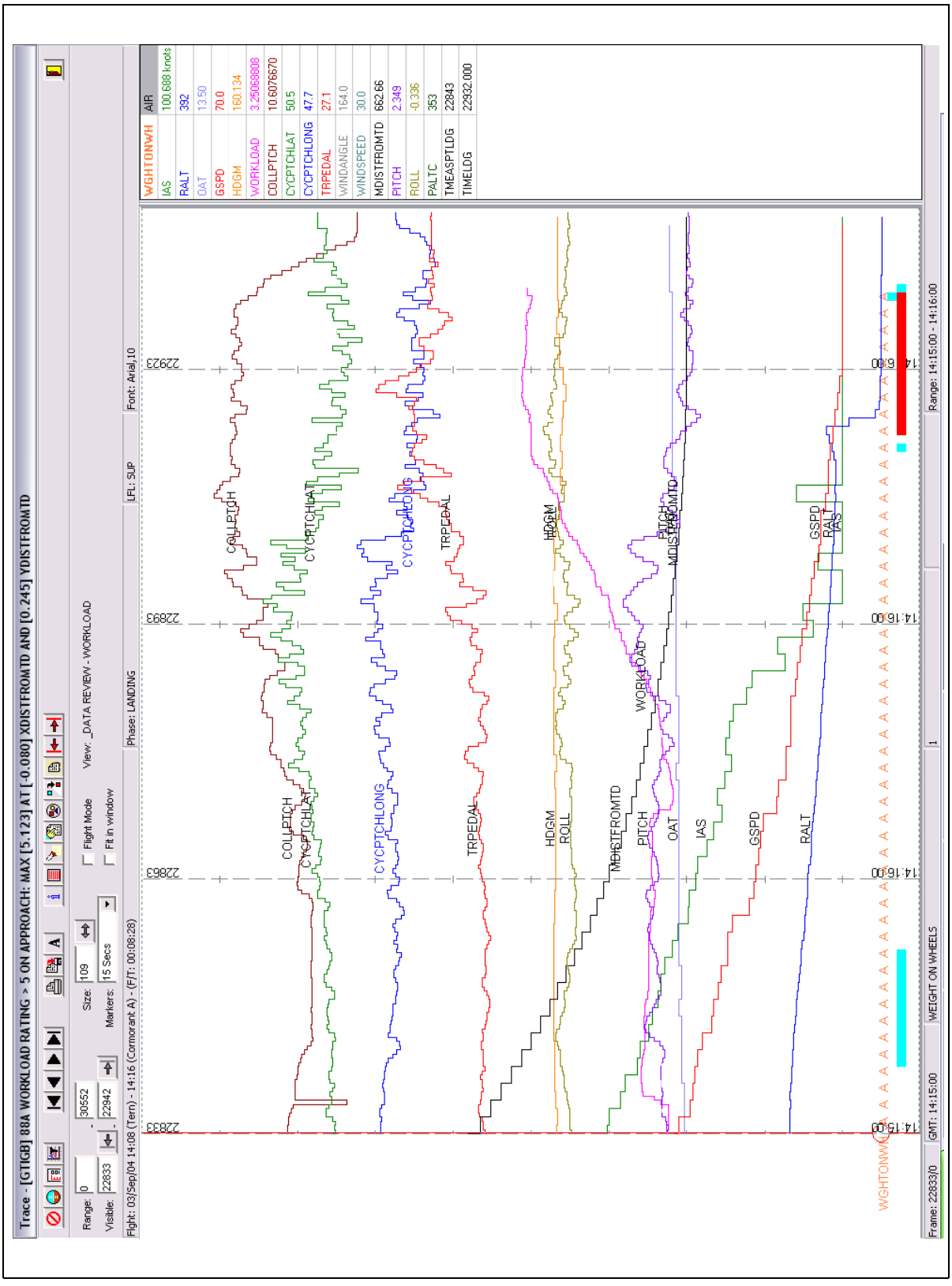
Trace - [GTIGB] 88A WORKLOAD RATING > 5 ON APPROACH: MAX [5.123] AT [-0.080] XDISTFROMTD AND [0.245] YDISTFROMTD
Range: 0 - 30552
Visible: 22833 - 22942
Size: 109
Markers: 15 Secs
Flight Mode
Fit in window
View: _DATA REVIEW - WORKLOAD
Flight: 03/Sep/04 14:06 (Tern) - 14:16 (Cormorant A) - (F/T: 00:08:28)
Phase: LANDING
LFL: SUP
Font: Arial,10
WGHTONWH AIR
IAS 100.688 knots
RALT 392
OAT 13.50
GSPD 70.0
HDGM 160.134
WORKLOAD 3.25068808
COLLPTCH 10.6076670
CYCPTCHLAT 50.5
CYCPTCHLONG 47.7
TRPEDAL 27.1
WINDANGLE 164.0
WINDSPEED 30.0
MDISTFROMTD 662.66
PITCH 2.349
ROLL -0.336
PALTC 353
TMEASPTLDG 22843
TIMELDG 22932.000
22923
22893
22863
22833
14:15:00
14:16:00
14:16:00
14:16:00
Range: 14:15:00 - 14:16:00
Frame: 22833/0
GMT: 14:15:00
WEIGHT ON WHEELS
WGHTONWH
COLLPTCH
CYCPTCHLAT
CYCPTCHLONG
TRPEDAL
HDGM
ROLL
MDISTFROMTD
PITCH
WORKLOAD
OAT
IAS
GSPD
RALT

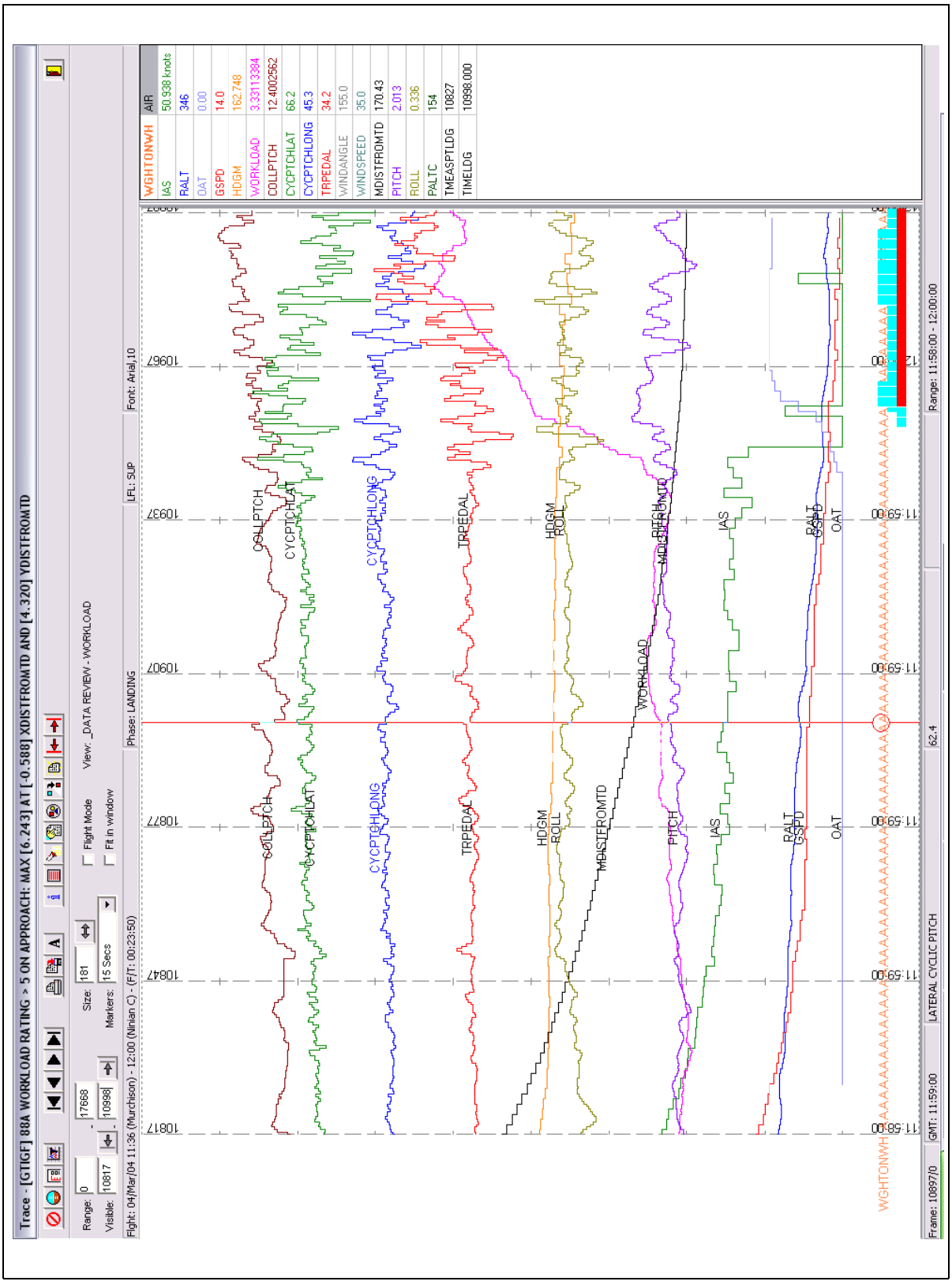
Trace - [GTIGF] 88A WORKLOAD RATING > 5 ON APPROACH: MAX [6.243] AT [-0.588] XDISTFROMTD AND [4.320] YDISTFROMTD
Flight: 04/Mar/04 11:36 (Murchison) - 12:00 (Ninian C) - (F/T: 00:23:50)
Phase: LANDING
LFL: SUP
Font: Arial,10
View: _DATA REVIEW - WORKLOAD
Flight Mode
Fit in window
Size: 181
Markers: 15 Secs
Range: 0 - 17668
Visible: 10817 - 10998
WGHTONWH AIR
IAS 50.938 Knots
RALT 346
OAT 0.00
GSPD 14.0
HDGM 162.748
WORKLOAD 3.33113384
COLLPTCH 12.4002562
CYCPTCHLAT 66.2
CYCPTCHLONG 45.3
TRPEDAL 34.2
WINDANGLE 155.0
WINDSPEED 35.0
MDISTFROMTD 170.43
PITCH 2.013
ROLL 0.336
PALTC 154
TMEASPTLDG 10827
TIMELDG 10998.000
10967
10937
10907
10877
10847
10817
11:59:00
11:58:00
Range: 11:58:00 - 12:00:00
Frame: 10897/0
GMT: 11:59:00
LATERAL CYCLIC PITCH
62.4

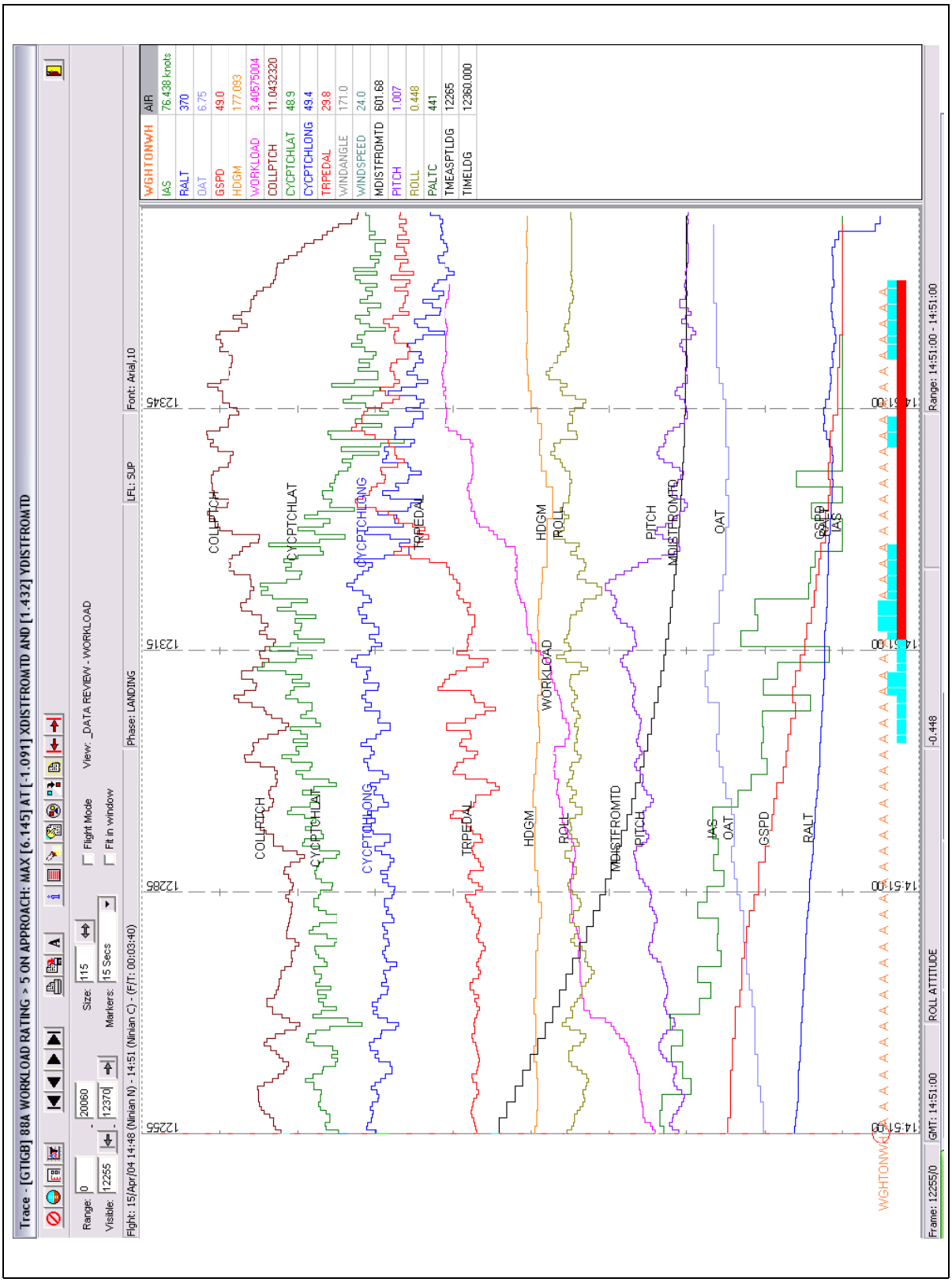
Trace - [GTIGB] 88A WORKLOAD RATING > 5 ON APPROACH: MAX [6.145] AT [-1.091] XDISTFROMTD AND [1.432] YDISTFROMTD
Flight: 15/Apr/04 14:46 (Ninian N) - 14:51 (Ninian C) - (F/T: 00:03:40)
Phase: LANDING
LFL: SUP
Font: Arial,10
WGHTONWH AIR
IAS 76.438 knots
RALT 370
OAT 6.75
GSPD 49.0
HDGM 177.093
WORKLOAD 3.40575004
COLLPTCH 11.0432320
CYCPTCHLAT 48.9
CYCPTCHLONG 49.4
TRPEDAL 29.8
WINDANGLE 171.0
WINDSPEED 24.0
MDISTFROMTD 601.68
PITCH 1.007
ROLL 0.448
PALTC 441
TMEASPTLDG 12265
TIMELDG 12360.000
Range: 0 20060
Visible: 12255 12370
Size: 115
Markers: 15 Secs
Flight Mode
Fit in window
View: _DATA REVIEW - WORKLOAD
12345
12315
12285
12255
14:51:00
Range: 14:51:00 - 14:51:00
-0.448
Frame: 12255/0
GMT: 14:51:00
ROLL ATTITUDE
COLLPTCH
CYCPTCHLAT
CYCPTCHLONG
TRPEDAL
HDGM
ROLL
WORKLOAD
MDISTFROMTD
PITCH
IAS
OAT
GSPD
RALT

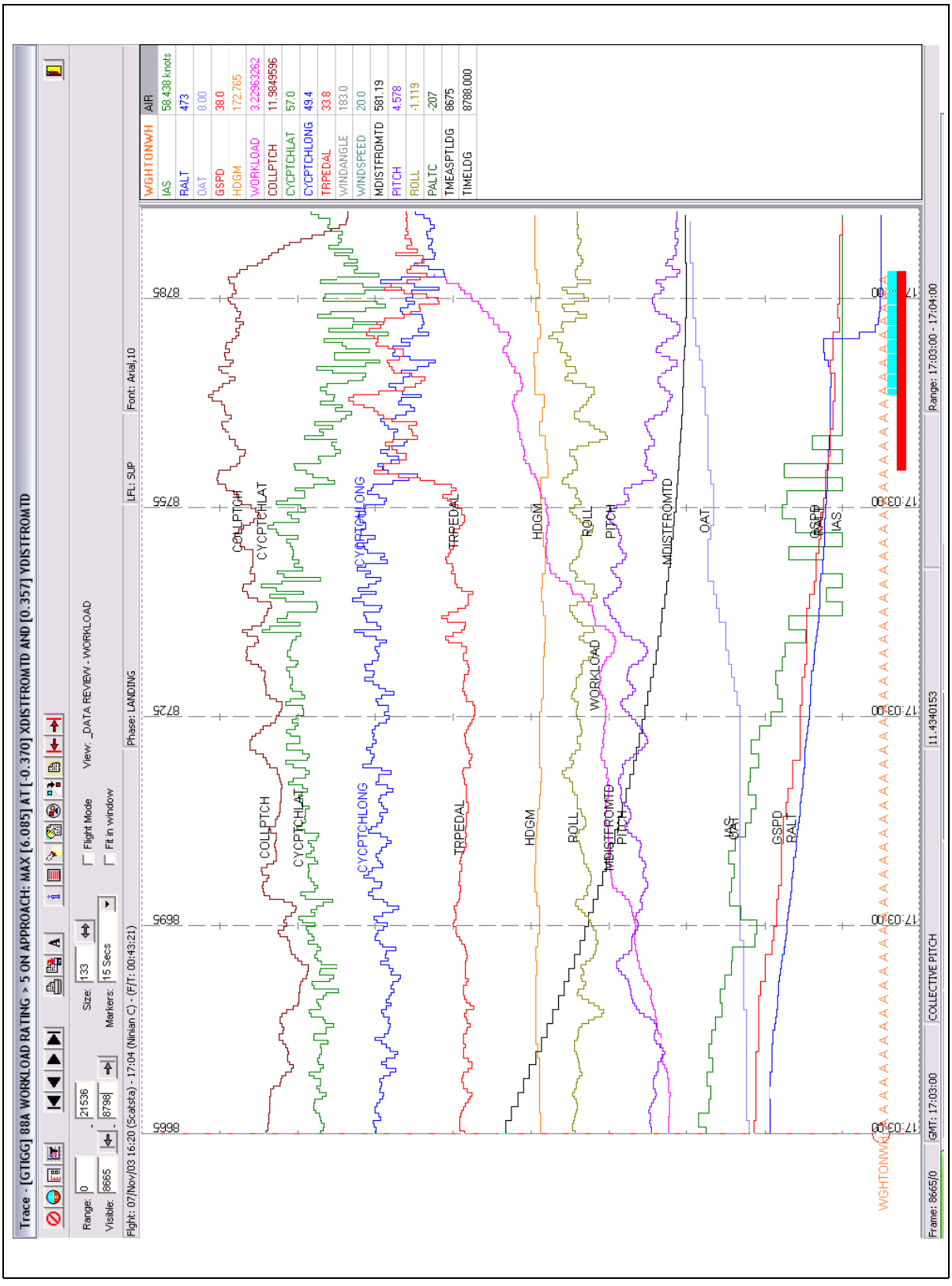
Trace - [GTIGG] 88A WORKLOAD RATING > 5 ON APPROACH: MAX [6.085] AT [-0.370] XDISTFROMTD AND [0.357] YDISTFROMTD
Flight: 07/Nov/03 16:20 (Scatsta) - 17:04 (Ninian C) - (F/T: 00:43:21)
Phase: LANDING
LFL: SUP
Font: Arial,10
Range: 0
Visible: 8665
21536
8798
Size: 133
Markers: 15 Secs
Flight Mode
Fit in window
View: _DATA REVIEW - WORKLOAD
WGHTONWH AIR
IAS 58.438 Knots
RALT 473
OAT 8.00
GSPD 38.0
HDGM 172.765
WORKLOAD 3.22963262
COLLPTCH 11.3849596
CYCPTCHLAT 57.0
CYCPTCHLONG 49.4
TRPEDAL 33.8
WINDANGLE 183.0
WINDSPEED 20.0
MDISTFROMTD 581.19
PITCH 4.578
ROLL -1.119
PALTC -207
TMEASPTLDG 8675
TIMELDG 8788.000
8785
8755
8725
8695
8665
17:03:00
17:04:00
Range: 17:03:00 - 17:04:00
Frame: 8665/0
GMT: 17:03:00
COLLECTIVE PITCH
11.4340153
WGHTONWH
COLLPTCH
CYCPTCHLAT
CYCPTCHLONG
TRPEDAL
HDGM
ROLL
WORKLOAD
PITCH
MDISTFROMTD
OAT
IAS
GSPD
RALT

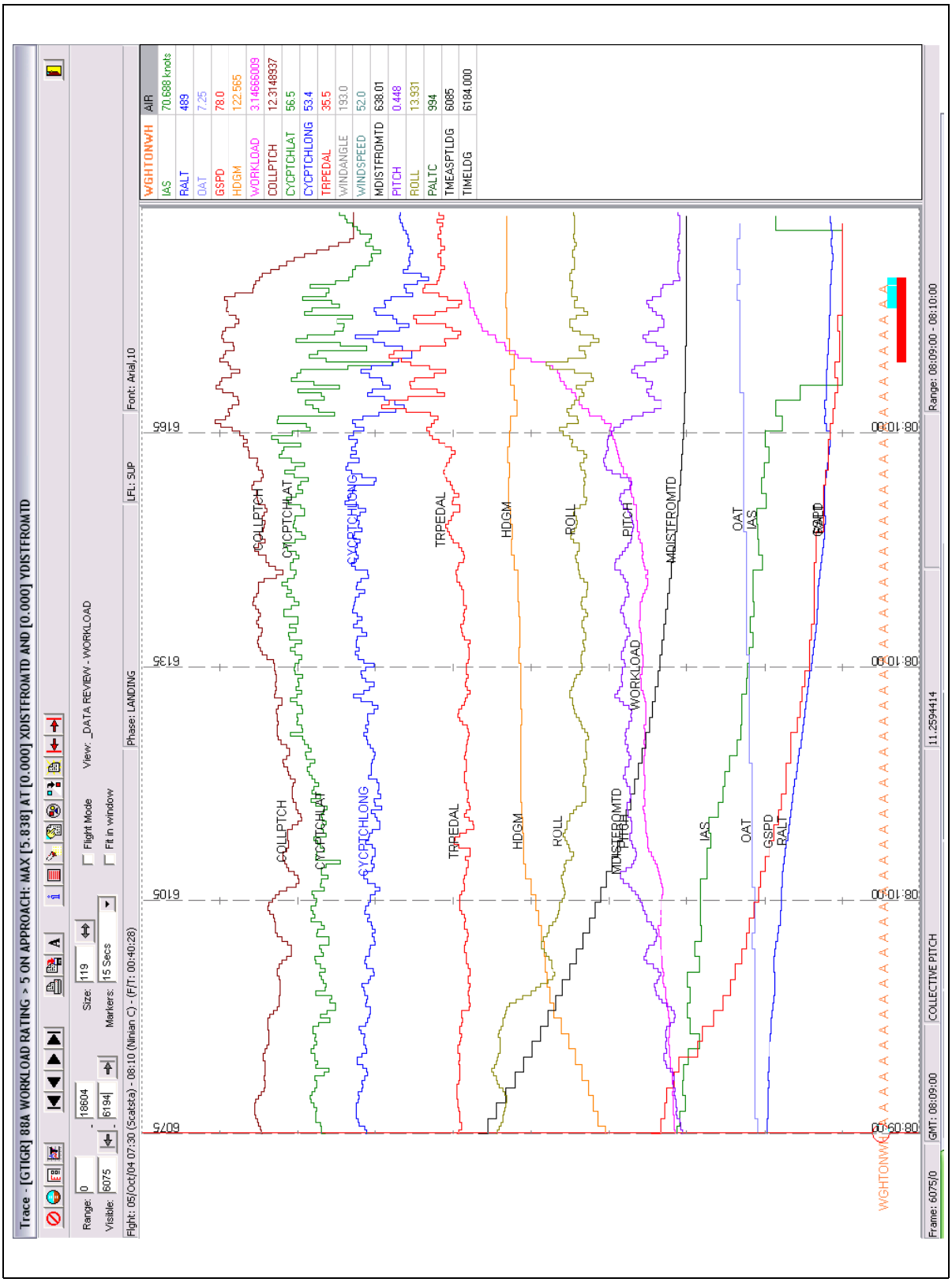
Trace - [GTIGR] 88A WORKLOAD RATING > 5 ON APPROACH: MAX [5.838] AT [0.000] XDISTFROMTD AND [0.000] YDISTFROMTD
Flight: 05/Oct/04 07:30 (Scaksta) - 08:10 (Ninian C) - (F/T: 00:40:28)
Phase: LANDING
LFL: SUP
Font: Arial,10
WGHTONWH AIR
IAS 70.688 knots
RALT 489
OAT 7.25
GSPD 78.0
HDGM 122.565
WORKLOAD 3.14666009
COLLPTCH 12.3148937
CYCPTCHLAT 56.5
CYCPTCHLONG 53.4
TRPEDAL 35.5
WINDANGLE 193.0
WINDSPEED 52.0
MDISTFROMTD 638.01
PITCH 0.448
ROLL 13.931
PALTC 994
TMEASPTLDG 6085
TIMELDG 6184.000
COLLPTCH
CYCPTCHLAT
CYCPTCHLONG
TRPEDAL
HDGM
ROLL
PITCH
WORKLOAD
MDISTFROMTD
IAS
OAT
GSPD
RALT
WGHTONWH
6075
6105
6135
6165
08:10:00
Range: 08:09:00 - 08:10:00
Frame: 6075/0
GMT: 08:09:00
COLLECTIVE PITCH
11.2594414

2 Low Workload Landing Example HOMP Traces

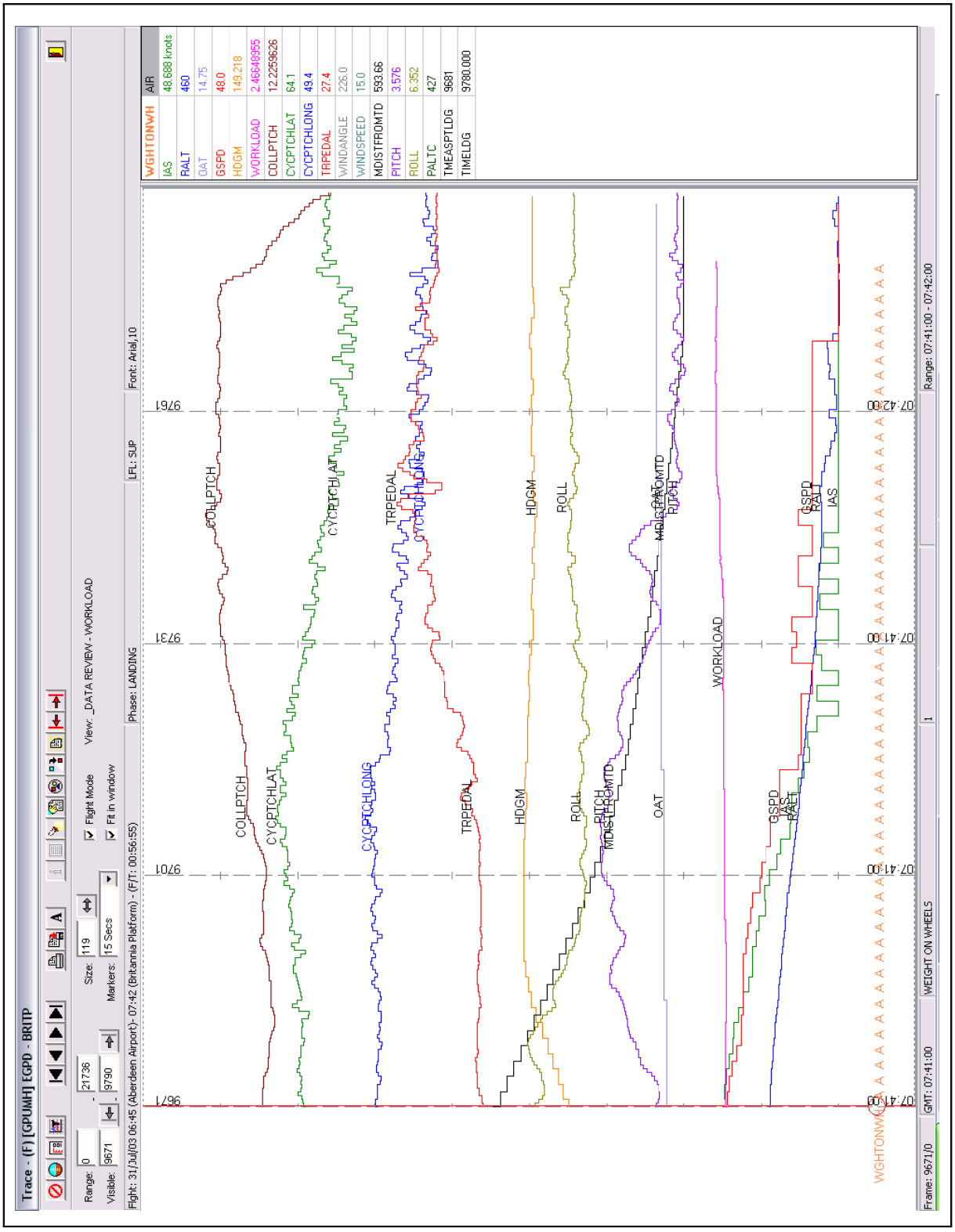

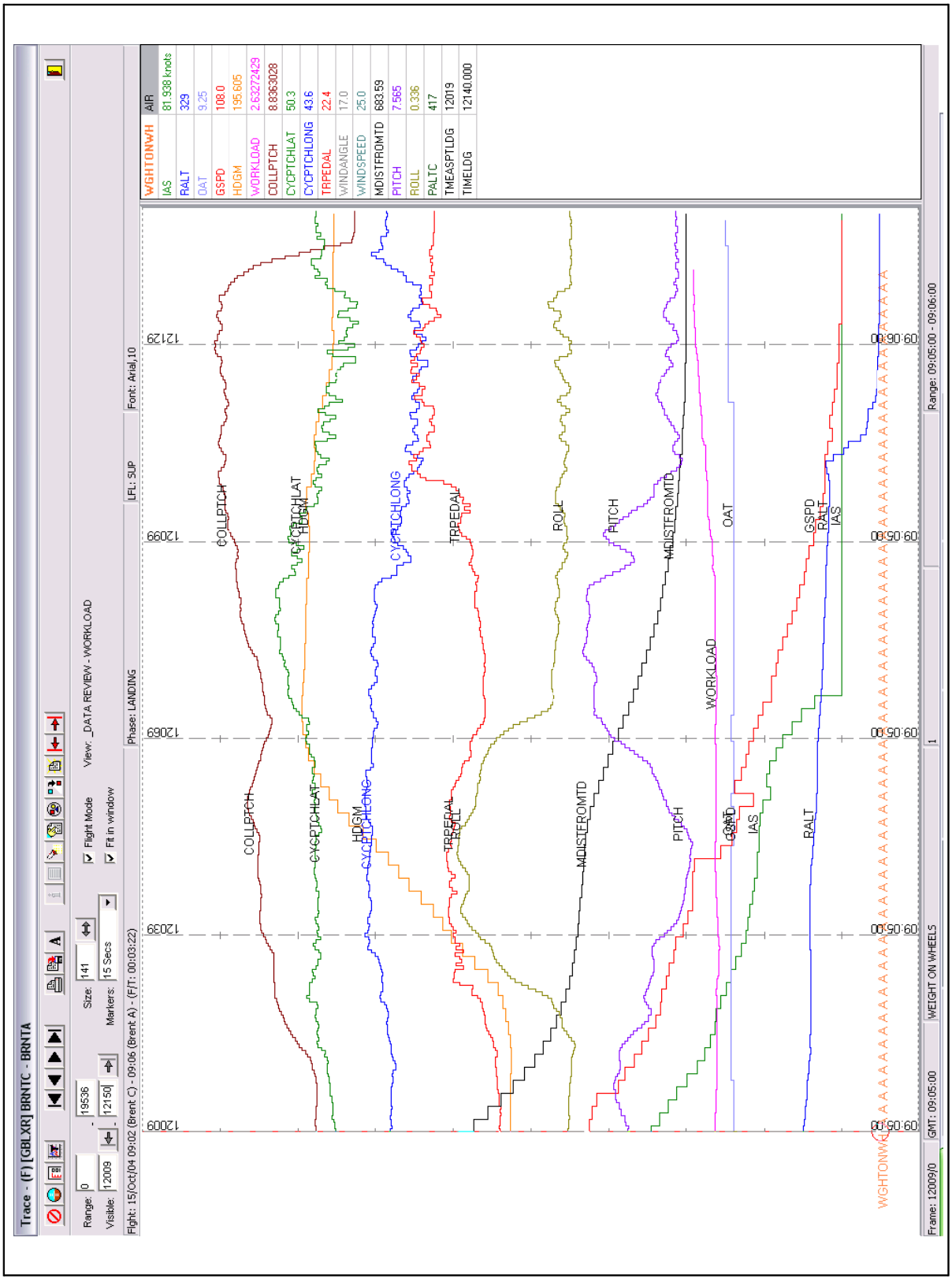
Trace - (F) [GBLXR] BRNTC - BRNTA
Flight: 15/Oct/04 09:02 (Brent C) - 09:06 (Brent A) - (F/T: 00:03:22)
Phase: LANDING
LFL: SUP
Font: Arial,10
View: _DATA REVIEW - WORKLOAD
Flight Mode
Fit in window
Size: 141
Markers: 15 Secs
Range: 0
Visible: 12009
19536
12150
WGHTONWH
IAS 81.938 Knots
RALT 329
OAT 9.25
GSPD 108.0
HDGM 195.605
WORKLOAD 2.63272429
COLLPTCH 8.8363028
CYCPTCHLAT 50.3
CYCPTCHLONG 43.6
TRPEDAL 22.4
WINDANGLE 17.0
WINDSPEED 25.0
MDISTFROMTD 683.59
PITCH 7.565
ROLL 0.336
PALTC 417
TMEASPTLDG 12019
TIMELDG 12140.000
AIR
12009
12039
12069
12099
12129
00:50:60
00:90:60
Frame: 12009/0
GMT: 09:05:00
WEIGHT ON WHEELS
Range: 09:05:00 - 09:06:00

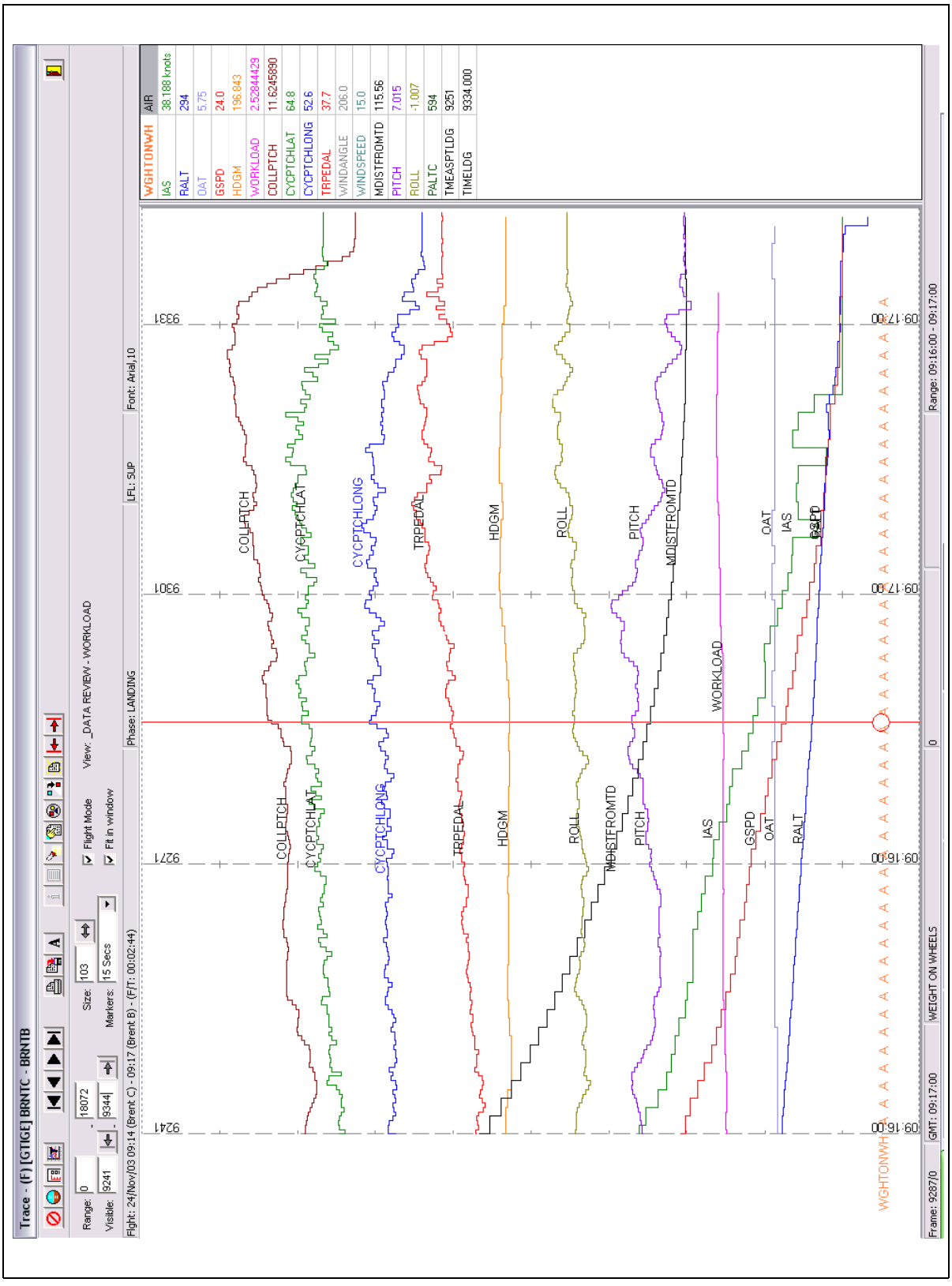
Trace - (F) [GTIGE] BRNTC - BRNTB
WGHTONWH AIR
IAS 38.188 knots
RALT 294
OAT 5.75
GSPD 24.0
HDGM 196.843
WORKLOAD 2.52844429
COLLPTCH 11.6245890
CYCPTCHLAT 64.8
CYCPTCHLONG 52.6
TRPEDAL 37.7
WINDANGLE 206.0
WINDSPEED 15.0
MDISTFROMTD 115.56
PITCH 7.015
ROLL -1.007
PALTC 594
TMEASPTLDG 9251
TIMELDG 9334.000
Flight: 24/Nov/03 09:14 (Brent C) - 09:17 (Brent B) - (F/T: 00:02:44)
Phase: LANDING
LFL: SUP
Font: Arial,10
Range: 09:16:00 - 09:17:00
Frame: 9287/0
GMT: 09:17:00
WEIGHT ON WHEELS
9331
9301
9271
9241
09:16:00
09:17:00
COLLPTCH
CYCPTCHLAT
CYCPTCHLONG
TRPEDAL
HDGM
ROLL
PITCH
MDISTFROMTD
WORKLOAD
IAS
GSPD
OAT
RALT
WGHTONWH

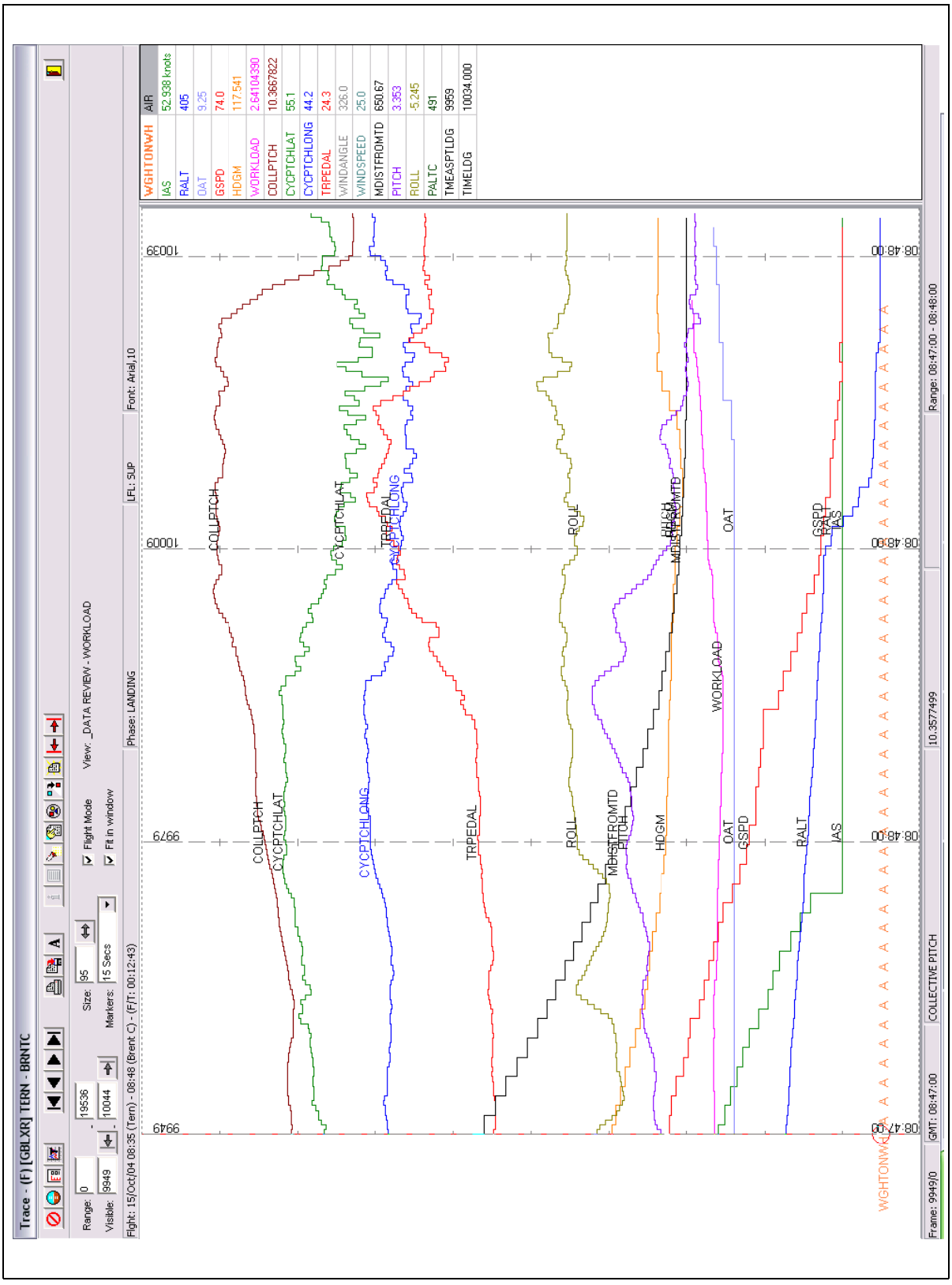
Trace - (F) [GBLXR] TERN - BRNTC
Flight: 15/Oct/04 08:35 (Tern) - 08:48 (Brent C) - (F/T: 00:12:43)
Phase: LANDING
LFL: SUP
Font: Arial,10
WGHTONWH AIR
IAS 52.938 knots
RALT 405
OAT 9.25
GSPD 74.0
HDGM 117.541
WORKLOAD 2.64104390
COLLPTCH 10.3667822
CYCPTCHLAT 55.1
CYCPTCHLONG 44.2
TRPEDAL 24.3
WINDANGLE 326.0
WINDSPEED 25.0
MDISTFROMTD 650.67
PITCH 3.353
ROLL -5.245
PALTC 491
TMEASPTLDG 9959
TIMELDG 10034.000
10039
10009
9979
9949
08:48:00
08:47:00
COLLPTCH
CYCPTCHLAT
CYCPTCHLONG
TRPEDAL
ROLL
MDISTFROMTD
PITCH
HDGM
OAT
WORKLOAD
GSPD
RALT
IAS
WGHTONWH
Frame: 9949/0
GMT: 08:47:00
COLLECTIVE PITCH
10.3577499
Range: 08:47:00 - 08:48:00

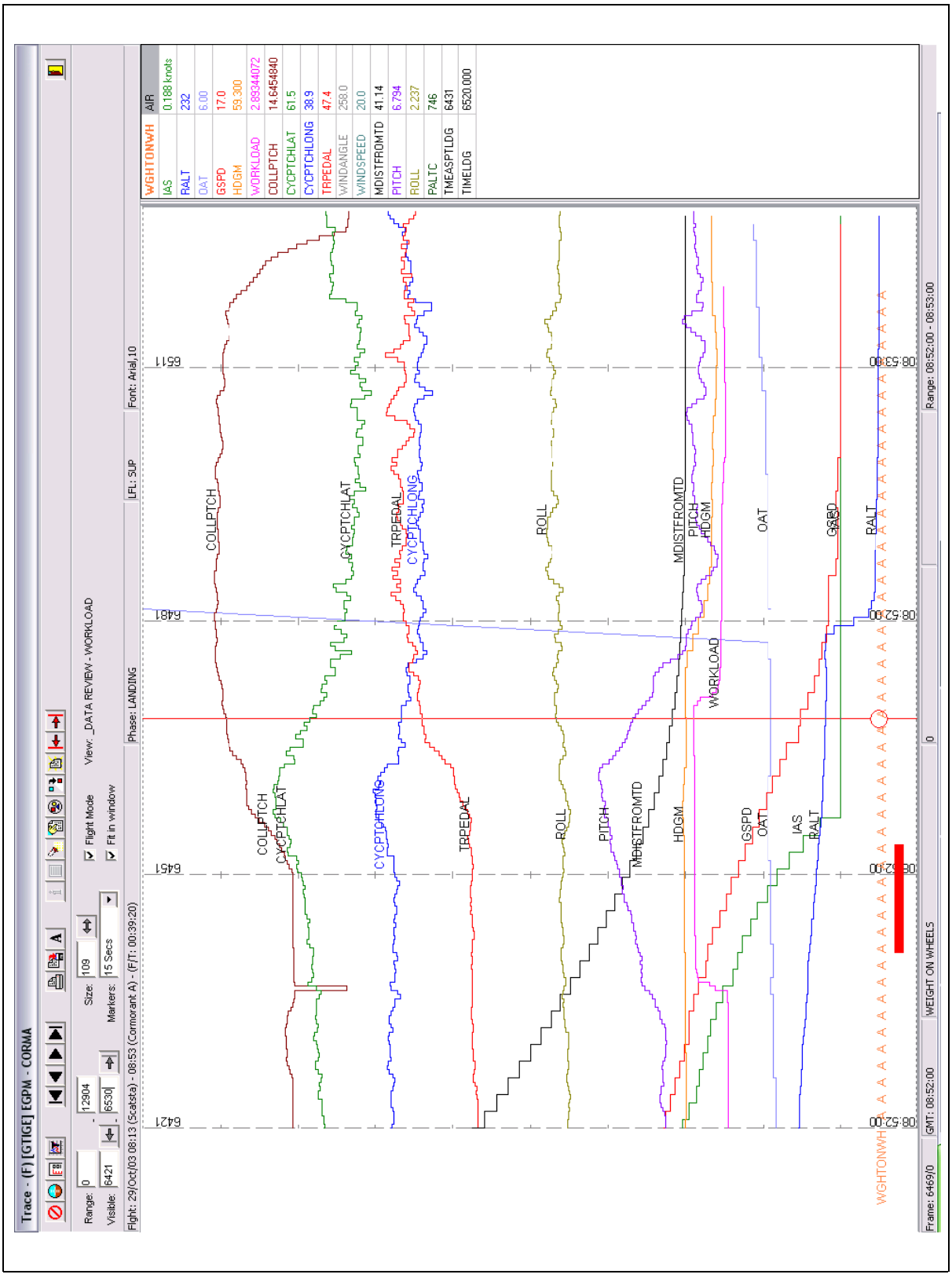
Trace - (F) [GTIGE] EGPM - CORMA
Flight: 29/Oct/03 08:13 (Scatsta) - 08:53 (Cormorant A) - (F/T: 00:39:20)
Phase: LANDING
LFL: SUP
Font: Arial,10
View: _DATA REVIEW - WORKLOAD
Flight Mode
Fit in window
Range: 0 - 12904
Visible: 6421 - 6530
Size: 109
Markers: 15 Secs
WGHTONWH AIR
IAS 0.188 knots
RALT 232
OAT 6.00
GSPD 17.0
HDGM 59.300
WORKLOAD 2.89344072
COLLPTCH 14.6454840
CYCPTCHLAT 61.5
CYCPTCHLONG 38.9
TRPEDAL 47.4
WINDANGLE 258.0
WINDSPEED 20.0
MDISTFROMTD 41.14
PITCH 6.794
ROLL 2.237
PALTC 746
TMEASPTLDG 6431
TIMELDG 6520.000
6511
6481
6451
6421
08:52:00
08:53:00
COLLPTCH
CYCPTCHLAT
CYCPTCHLONG
TRPEDAL
ROLL
PITCH
MDISTFROMTD
HDGM
WORKLOAD
GSPD
OAT
IAS
RALT
Frame: 6469/0
GMT: 08:52:00
WEIGHT ON WHEELS
Range: 08:52:00 - 08:53:00

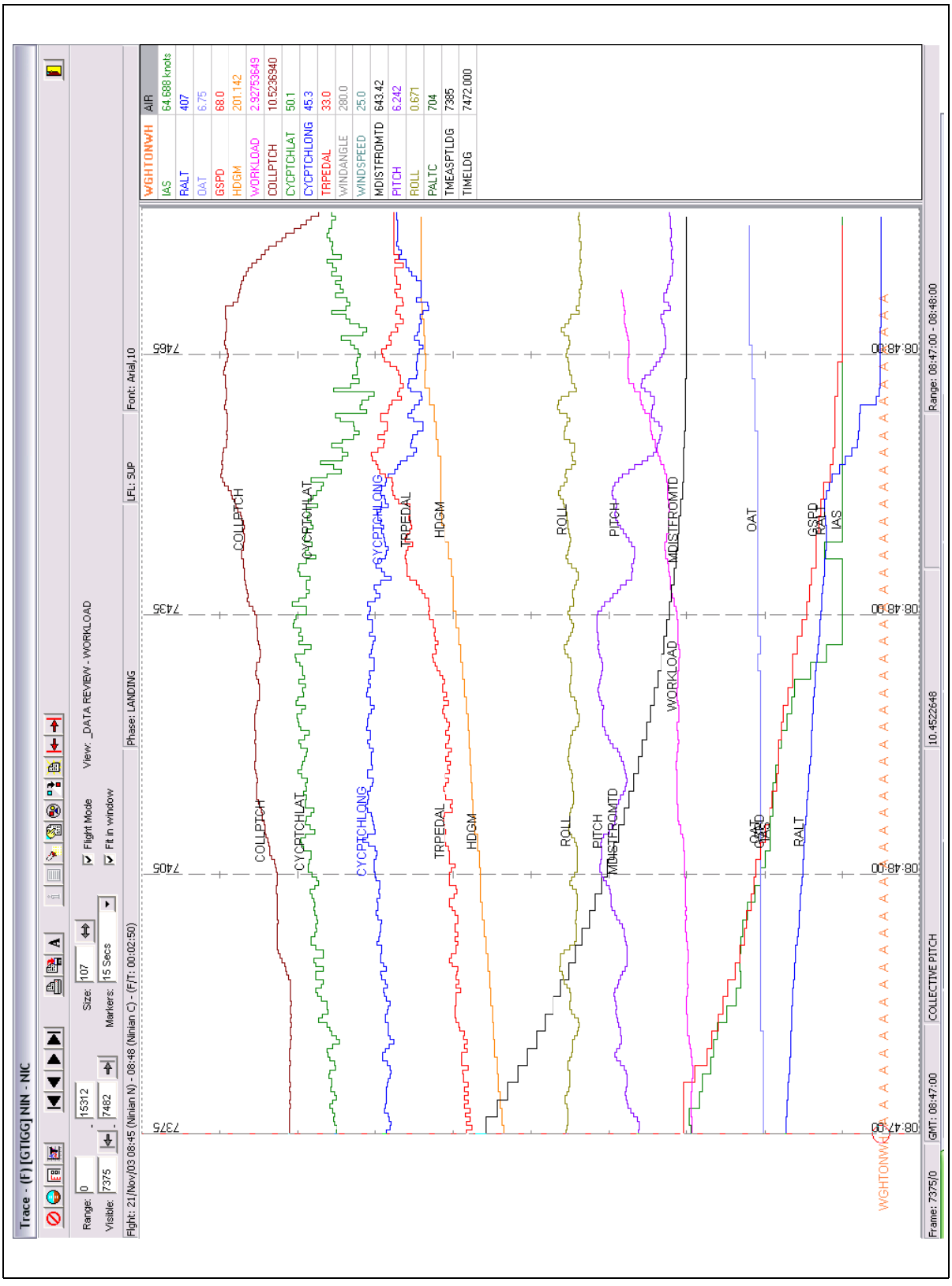
Trace - (F) [GTIGG] NIN - NIC
Range: 0 - 15312
Visible: 7375 - 7482
Size: 107
Markers: 15 Secs
Flight Mode
Fit in window
View: _DATA REVIEW - WORKLOAD
Flight: 21/Nov/03 08:45 (Ninian N) - 08:48 (Ninian C) - (F/T: 00:02:50)
Phase: LANDING
LFL: SUP
Font: Arial,10
WGHTONWH AIR
IAS 64.688 Knots
RALT 407
OAT 6.75
GSPD 68.0
HDGM 201.142
WORKLOAD 2.92753649
COLLPTCH 10.5236940
CYCPTCHLAT 50.1
CYCPTCHLONG 45.3
TRPEDAL 33.0
WINDANGLE 280.0
WINDSPEED 25.0
MDISTFROMTD 643.42
PITCH 6.242
ROLL 0.671
PALTC 704
TMEASPTLDG 7385
TIMELDG 7472.000
7465
7435
7405
7375
08:48:00
08:47:00
COLLPTCH
CYCPTCHLAT
CYCPTCHLONG
TRPEDAL
HDGM
ROLL
PITCH
MDISTFROMTD
WORKLOAD
OAT
GSPD
RALT
IAS
WGHTONWH
Frame: 7375/0
GMT: 08:47:00
COLLECTIVE PITCH
10.4522648
Range: 08:47:00 - 08:48:00

Safety Regulation Group

CAA PAPER 2008/02

Offshore Helideck Environmental Research

Part 2 – Review of 0.9 m/s Vertical Wind Component Criterion for Helicopters Operating to Offshore Platforms

May 2009

INTENTIONALLY LEFT BLANK

Part 2 – Review of 0.9 m/s Vertical Wind Component Criterion for Helicopters Operating to Offshore Platforms

Executive Summary

Following the establishment of a new turbulence criterion for helicopters operating to offshore installations, the need for retention of the longstanding CAP 437 criterion relating to a vertical wind component of 0.9 m/s has been reviewed. This report presents the results of a four-phase study to evaluate the effectiveness of the criterion.

The overall objective for the project was to determine whether the existing 0.9 m/s vertical flow criterion was protecting offshore helicopters against an identifiable hazard other than turbulence and, if so, establish whether the form of the present criterion was the most appropriate, or whether a new criterion was required to form a rational link with helicopter performance or handling. Alternatively, it might be established that a vertical flow criterion was not necessary.

Overall it is concluded that violation of the 0.9 m/s vertical mean flow criterion cannot be linked to any helicopter performance (i.e. torque-related), or handling (i.e. pilot workload-related) hazard. The highest vertical components of flow almost always occur when the wind is from an 'open' or unobstructed direction. These are conditions when the horizontal component of flow is likely to be high ensuring that the helicopter has a high margin of lift, and when turbulence levels are likely to be low, resulting in relatively low torque and pilot workload values.

As it has not proven possible to link the criterion to a helicopter performance or handling hazard, consideration should be given to removing the 0.9 m/s criterion from the guidance material. The first step should be consultation with the helicopter operators in order to seek their views on the validity or otherwise of the criterion from an operational perspective, and to check whether there may be safety benefits implicit in the criterion that have not been evident during the study.

Concerns that removal of the 0.9 m/s criterion might reduce the pressure on the platform design process to include a generous air gap between the helideck and the accommodation block, have been allayed to some extent. Wind tunnel tests on an example of a large North Sea platform demonstrated that the application of the new turbulence criterion was also likely to result in the inclusion of a significant air gap.

INTENTIONALLY LEFT BLANK

Part 2 – Review of 0.9 m/s Vertical Wind Component Criterion for Helicopters Operating to Offshore Platforms

1 Introduction

Following the establishment of a new turbulence criterion for helicopter operations to offshore installations, the need for the longstanding CAP 437 criterion relating to a vertical wind component of 0.9 m/s has been reviewed. This report presents the results of a four-phase study to evaluate the effectiveness of the criterion.

Currently CAP 437 [1] uses the following wording:

2.3.2 As a general rule, the vertical mean wind speed above the helideck should not exceed ± 0.9 m/s (1.75 kt) for a windspeed of up to 25 m/s (48.6 kt). This equates to a wind vector slope of 2°.

The Research on Offshore Helideck Environmental Issues report [2] linked the 0.9 m/s with a hover-thrust margin of 3%. The report says:

Simple theory suggests that, in the absence of ground effect, a thrust margin of at least 3% would be required to overcome the effects of this magnitude of gust and maintain a hover over the deck in zero wind. However, it should be noted that it is unlikely that with current helideck designs a helicopter could ever experience a 0.9 m/s downdraught in the absence of the beneficial effect on thrust margin of a significant horizontal wind component.

No detailed evaluation had been performed prior to this study, but experience of wind tunnel testing many platforms at BMT Fluid Mechanics (BMT) had suggested that the 0.9 m/s (mean) vertical wind component is usually only exceeded in wind directions that are clear of upstream obstructions ('open' sectors). One of the objectives of the current study was to verify this perception. In such cases the 0.9 m/s criterion is exceeded because of the general curvature of the flow around the bulk of the platform, and the vertical component is therefore accompanied by a horizontal component of similar magnitude to the 25 m/s free wind speed. Clearly this horizontal component gives the helicopter a major lift performance benefit, and the 3% still air hover thrust margin does not appear to be particularly relevant.

Furthermore, the consideration in [2] which resulted in the 3% hover thrust margin conclusion was based on an analysis of pilot/helicopter response to a sudden 'vertical gust'. It was therefore very much an analysis of a transient situation in a temporal sense. It seems probable that any hazard that is being protected against is also primarily a transient hazard but caused by flying from one flow field into another, and so it is possible that a better criterion might explicitly recognise the spatial change of this vertical component.

Questions raised by the above are therefore:

1 Does violation of the existing 0.9 m/s vertical component in the presence of a high horizontal wind speed pose any real hazard to the helicopter? If it does, then what is the precise nature of the hazard, and does the existing criterion adequately protect against it?

2 If the application of the existing 0.9 m/s vertical component criterion is not currently protecting against an identifiable hazard, then what is the nature of the real hazard (if any), and how should a new criterion be framed? Should the criterion be framed more in terms of a transient phenomenon (e.g. the spatial

variation in mean vertical velocity).[1] Alternatively, if there is no real hazard then consideration should be given to removing any flight restrictions on platforms in these 'high horizontal flow' cases.

With the above questions in mind, BMT produced two proposals [3, 4]. These suggested that a useful initial step would be to analyse the Bristow Helicopters Helicopter Operations Monitoring Programme (HOMP) data archive (which was already being analysed in support of the turbulence criterion validation [5]) to look for any evidence of high torque events that might indicate a performance-related hazard for the helicopter.

Following on from this, the BMT archive of wind tunnel data was analysed to evaluate the occurrence of violations of the 0.9 m/s criterion and confirm, or otherwise, the perception that this criterion was mostly exceeded in the 'open' wind directions, clear of upstream obstructions.

The wind tunnel data were correlated with torque and pilot workload data gathered in the initial phase to seek any correlations between the HOMP measured parameters and the vertical wind components in these open wind directions.

Finally, a programme of wind tunnel testing was performed on a model of the Brae-A platform in order to investigate the likely effect of removing the 0.9 m/s criterion on the selection of a helideck height / clearance (air gap) from the accommodation block.

2 Objectives

The overall objectives for the project were defined as follows:

2.1 To determine whether the existing 0.9 m/s vertical flow criterion is protecting offshore helicopters against an identifiable hazard. If so, refine the magnitude of the criterion so that there is a rational link with helicopter performance and/or handling.

2.2 If the existing 0.9 m/s criterion cannot be linked to an identifiable hazard, then establish the nature of any associated vertical flow hazard and develop a new flow criterion that satisfactorily protects against the hazard. Alternatively, determine whether the existing 0.9 m/s vertical flow criterion can be removed.

3 Phase 1 – HOMP Torque Analysis

3.1 Introduction

The helideck turbulence criterion project Phase 2 (Helicopter Operational Monitoring Programme (HOMP) validation [5]), offered the possibility to examine the HOMP data archive [6, 7] for evidence of performance-related hazards during the approach which might be linked to a vertical wind component. It was proposed that the maximum torque, and the maximum increase in torque (over a 2 second period), should be studied. These would then be plotted against wind speed and direction (much as it is intended to plot pilot workload and ambient temperature), and overlaid on sketches of the platform plans[2].

1. BMT currently uses some empirically derived pilot workload criteria for warship flight decks that are based on spatial gradients of longitudinal mean, longitudinal rms, lateral mean and vertical mean wind speed. They were derived by correlating Ship Helicopter Operating Limitation (SHOL) data against wind tunnel measurements down the flight path. Unfortunately the same method is not directly applicable to an offshore helideck because there isn't a well-defined approach flight path.
2. Appropriate sketches of most platforms were obtained from the 'Aerad Plates' published by European Aeronautical Group (now part of Navtech Inc).

In BMT's experience, the 0.9 m/s criterion is routinely **not** met at high wind speeds in 'open' sectors. The plots generated would therefore be examined for evidence that high torque values, or sudden large increases in torque, occurred in high wind speeds and 'open' wind directions.[3] The rationale was that any such occurrences might lend support to the notion that the current 0.9 m/s criterion was performing a useful function, the assumption being that the data would likely contain instances of helicopters being exposed to vertical flows in excess of 0.9 m/s. On the other hand, an absence of such occurrences *might* be interpreted to suggest that the current criterion is inappropriate or redundant

However, vertical flows in excess of 0.9 m/s are unlikely to present a hazard to helicopters in the presence of high horizontal flows, but rapid changes in the airflow could [2]. The hazard of temporal variation of the airflow (turbulence) is now accounted for by the recently developed turbulence criterion [5, 8]. However, disturbances to the airflow in 'open' sectors resulting in high torque values, or sudden large increases in torque, could be the result of spatial variation, i.e. shear, which arguably is not adequately covered. The presence of any such occurrences might therefore indicate a need for a new criterion to address spatial variation that would replace the present 0.9 m/s criterion.

It was accepted that the HOMP maximum torque values might be difficult to use in this context for a number of reasons, including the effects of helicopter weight and ground effect. However, if there was a genuine lift performance hazard associated with vertical wind component in the presence of high horizontal flow speeds, then some evidence of high torque values in high wind speeds and 'open' wind directions ought to be apparent in the HOMP data. The inclusion of the maximum increase in torque in the analysis was expected to make interpretation of the torque somewhat easier.

The task therefore included the following main activities:

3.1.1 Gather and present HOMP maximum torque and maximum positive increase in torque data.

3.1.2 Gather sketches of platform helidecks in order to identify the 'open' wind directions.

3.1.3 Evaluate the data to identify any evidence of high torque / torque increase performance challenges in the 'open' wind sectors.

3. Helidecks for floating systems / FPSOs were omitted from this analysis because vessel heading information was not readily available.

3.2 Measured Parameters

The HOMP parameters used in this analysis were as follows:

Table 1 HOMP Parameters used in the torque analysis

Variable name	Description
MX_LDGWGHT	Landing weight (lb)
MX_WSPEEDLDG	Average wind speed at measurement point (1500 m from Landing) (m/s)
MX_WANGLELDG	Average wind direction at measurement point (1500 m from Landing) (degrees magnetic)
FlightType	Flight type (from imported ops data, 1,2,6 = revenue, 4 = training, 5 = air test)
MXTORQ	Maximum Total Torque from 500 m to landing (%)
MXTORQTIMLDG	Number of Frames from Landing point to recorded MXTORQ (2 frames = 1 sec)
MX_TORQ_XDIST	Lateral distance between MXTORQ and Landing Point (m)
MX_TORQ_YDIST	Longitudinal distance between MXTORQ and Landing Point (m)
MXINCRTORQ	Maximum Increase in Torque from 500 m to Landing Point (%)
MXINCTRQTIMLDG	Number of Frames from Landing point to recorded MXINCRTORQ (2 frames = 1 sec)
MX_INCRTQ_XDIST	Lateral distance between maximum MXINCTORQ and Landing Point (m)
MX_INCRTQ_YDIST	Longitudinal distance between maximum MXINCTORQ and Landing Point (m)
MX_INCRTQ_TORQ	Total Torque at finish point of MXINCTORQ (%)
COR_MX_WSPDLDG	Wind speed in the Landing Phase at Measurement Point (1500 m from Landing) (m/s)
COR_MX_WANGLDG	Wind angle in the Landing Phase at Measurement Point (1500 m from Landing) (m/s)
MX_CORWSPDLDG	COR_MX_WSPDLDG corrected to helideck height (m/s)

3.3 Derived Parameters

3.3.1 Maximum torque corrected for helicopter landing weight

It was recognised that the maximum torque values recorded during a landing would be very much dependent on the landing weight of the helicopter. This is borne out by Figure 1, which shows all valid maximum torque values plotted against helicopter landing weight. It can be seen that there is a clear and unsurprising trend of increasing maximum torque with landing weight.

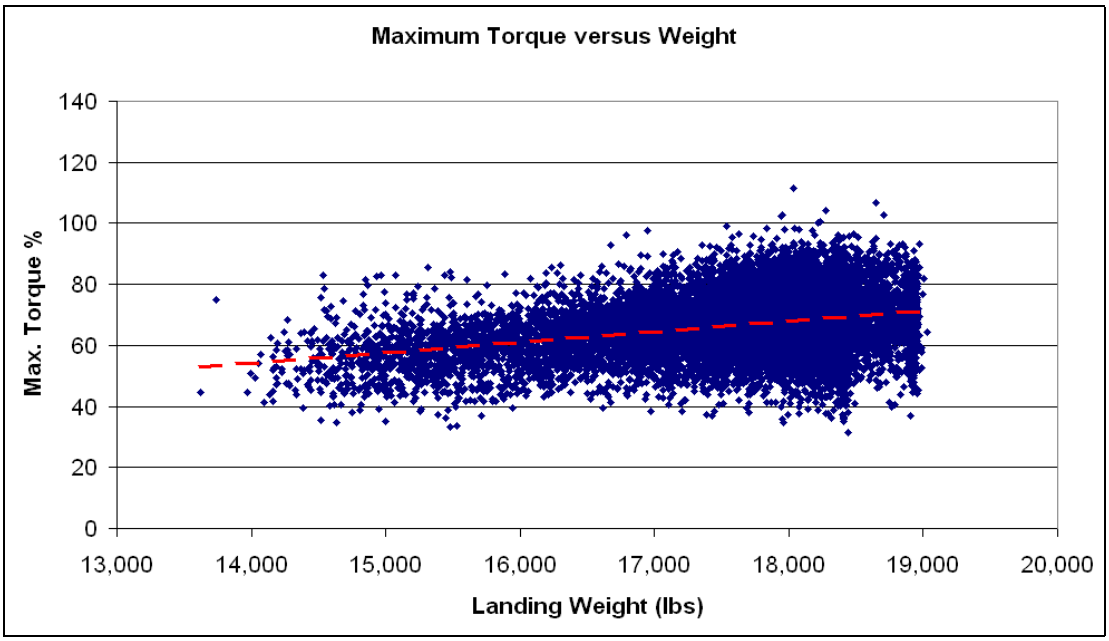

Figure 1 Maximum torque versus landing weight

It was proposed [9] that the maximum torque might be corrected for the effect of weight, and it was hoped that the maximum torque values corrected in this way would prove to be a better indicator of the presence of a performance or lift hazard. A correction of the following form was proposed:

$$Tq_2 = Tq_1(W_2/W_1)^{3/2}$$

where:

Tq_2 = max torque value to be plotted

Tq_1 = max torque value from the HOMP data (MXTORQ)

W_2 = max landing weight (18,960 lb)

W_1 = actual landing weight from the HOMP data (MX_LDGWGHT).

However, when maximum torque data corrected in this way were examined it was clear that there were now many high 'corrected torque' events, and that they were associated with lower landing weights. Figure 2 shows this trend of higher corrected maximum torques at lower landing weights.

It was suspected that the reason for this preponderance of high corrected torque values at lower weights was due to pilot behaviour. A pilot flying at close to maximum weight and/or in light winds will be very aware of a real torque limit, and will be using the collective lever judiciously to avoid an over-torque. In contrast, a pilot flying a light helicopter or flying in a strong wind will know that he has plenty of torque in hand, and may therefore use the collective lever more freely to maintain his desired flight path. Such free use of the collective lever will tend to appear as high corrected torque values at low landing weights.

In order to reduce this effect in the results it was decided to plot the corrected maximum torque over a restricted range of landing weights. It was found that about 60% of landings were at a landing weight in the range 17,000lb – 18,500lb, and so corrected maximum torque plots were plotted for this range of landing weights only.

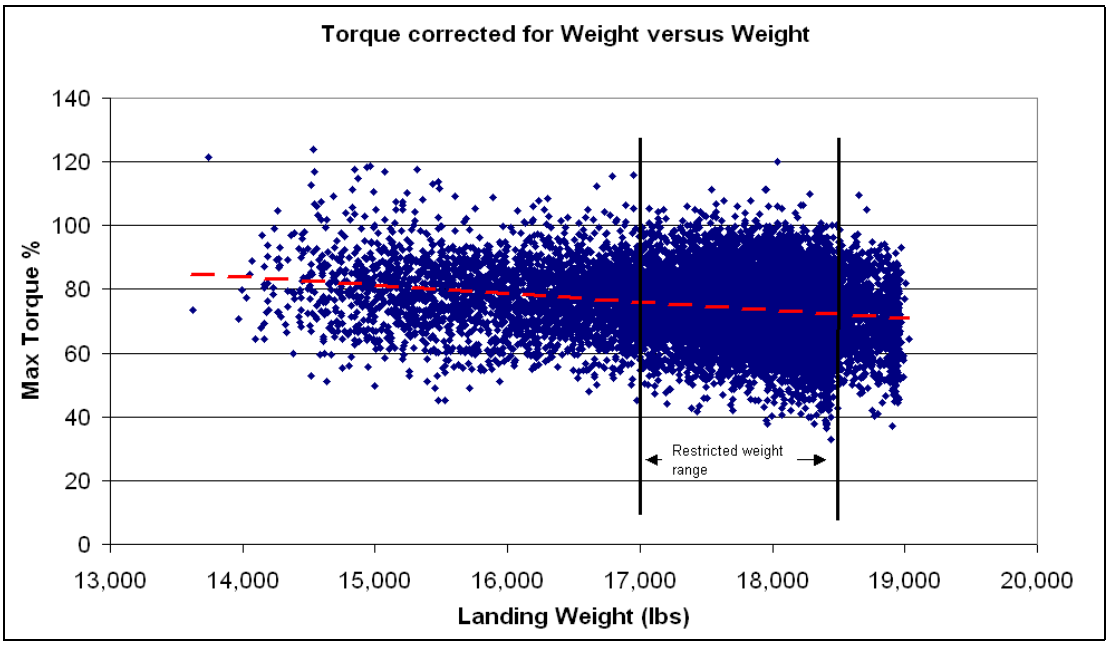

Figure 2 Maximum torque corrected for weight versus landing weight

3.3.2 Maximum torque increase expressed as a percentage of instantaneous torque margin

There was a similar issue in relation to the interpretation of the maximum torque increase experienced in 2 seconds. At low weights and/or in high wind speeds less collective and less torque is required to effect a given flight path correction, and a pilot who knows that he has plenty of torque margin in hand will be less averse to applying a large torque increase in order to maintain his desired flight path, and will thus register a high torque increase value in the HOMP database. A pilot flying close to the torque limit will be very much more careful with the collective lever.

In order to take some account of this in the interpretation of the results it was decided to derive a parameter for the torque increase as a percentage of remaining torque margin. The expression for this in terms of the HOMP measurements is as follows:

$$T_{incrm} = 100\ T_{incr} / (100 - (T_{Ti} - T_{incr}))$$

Where:

T_{incrm} = max torque increase as percentage of the instantaneous torque margin

T_{incr} = max torque increase from HOMP data (MXINCRTORQ)

T_{Ti} = Torque value at the end of the 2 second max increase in torque (MX_INCRTQ_TORQ)

Thus a pilot applying a 25% increase in torque over 2 seconds from an initial torque of 50% will register a 50% of torque margin value. Similarly a pilot applying a 5% increase in torque from a 90% value will also register a 50% torque margin value.

3.4 Results

A complete set of results for all the torque parameters, and all the platform landings in the HOMP archive (with 20+ landings) can be found in [10]. Some selected examples of these plots are presented in the following in order to illustrate the main features of the torque data.

3.4.1 Torque Plot Examples

A complete set of the five different torque plotting options is presented for one platform (Brae-A) in order to emphasise the importance of the derived parameters outlined in Sections 3.3.1 and 3.3.2.

Figure 3 and Figure 4 show the 'raw' maximum torque increase data for the 445 landings in the database for the Brae-A platform. The upper plot Figure 3 shows the torque increase values with points colour coded according to the maximum torque value, and with the position of the point showing the wind speed and direction at the time of the landing. The lower plot Figure 4 shows the same data, but in this case the position of the coloured point on the plot shows the position of the helicopter relative to the helideck touchdown point at the time the maximum torque occurred, and the vector arrows associated with each point indicate the speed and direction of the wind. Each plot includes a small sketch of the platform layout correctly orientated with respect to true North, so that the relationship between wind directions and platform obstructions that might cause turbulence can be assessed.

It should be noted that, although the theoretical accuracy of the helicopter position relative to the actual touchdown point is reasonably high (≈1 m), the plots showing the position of the helicopter at the time of the maximum torque are subject to a number of sources of error. In particular the plots assume that all landings touchdown at the centre of the helideck, and the helicopter locations are worked back from this origin. In reality, although the pilot is permitted to land anywhere within the safe landing area (typically 22 m 'diameter'), the pilot will normally touchdown by reference to the aiming circle (typically having an 11 m inner diameter). Furthermore, the fact that the GPS antenna is located partway down the helicopter tail boom introduces a further helicopter heading-related error into the plots. In view of these inaccuracies it is considered that the positions shown on the plots are probably only reliable to about ±5 m.

It can be seen from Figure 3 that the highest value in the 445 landings is an increase of 34.7%, and the four highest values in the range 30%-40% all occur either in still conditions, or in winds of about 15-20 kt from the N-E sector. Wind from these directions will contain turbulence caused by the upstream bulk of the platform.

Figure 4 shows that these higher torque increase events occurred when the helicopter was either directly over the helideck or about 20 m to the SW of the touchdown point.

In Figure 5 and Figure 6 the same torque data has been expressed as a percentage of the torque margin (as per the formula given above in Section 3.3.2). The pattern looks a little different because of the different numeric ranges and colour coding, but it can be seen that, once again, the 3 landings that utilised 80% or more of the torque margin all occurred in still or NE wind conditions, and with the helicopter either over the landing spot or to the SW of it.

None of the plots in Figures 3 to 6 would appear to provide any evidence of high torque events occurring in high winds from the 'open' sector.

The maximum torque data is presented in Figure 7 and Figure 8. Figure 7 shows a pattern not dissimilar to the torque increase data of Figure 3. The high values are generally experienced in lower wind speeds and in winds from the turbulent N-E sector.

When the landing weight correction is applied to the maximum torque for the full range of landing weights in Figure 9 and Figure 10 there is a much larger number of high torque events, and the winds in which they occur are spread more evenly around the compass. However, none of the >100% events occur in wind speeds over 20 kt.

When the correction is applied and presented for only a limited range of landing weights (17,000lb – 18,500lb) in Figure 11 and Figure 12, the number of landings is reduced by about half to 220, but the overall pattern of the high torque values does not appear to change significantly.

None of the plots in Figures 7 to 12 show any evidence that high torque events occur in winds from the 'open' sectors.

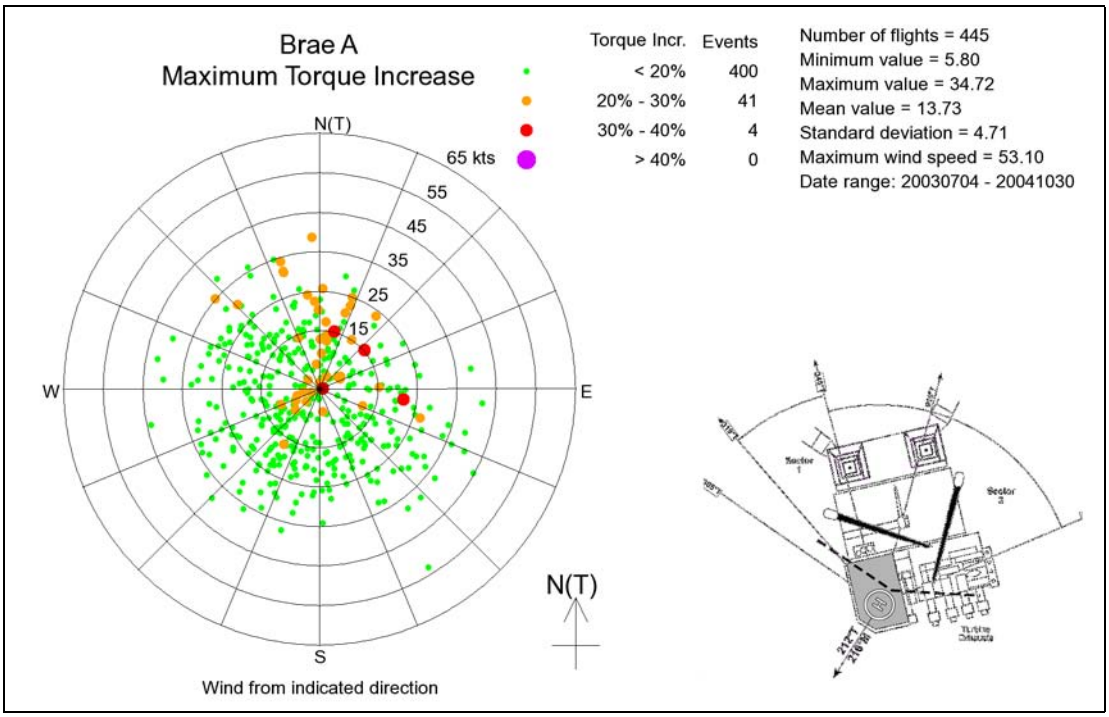

Figure 3 Brae-A 'raw' maximum torque increase data – wind rose plot

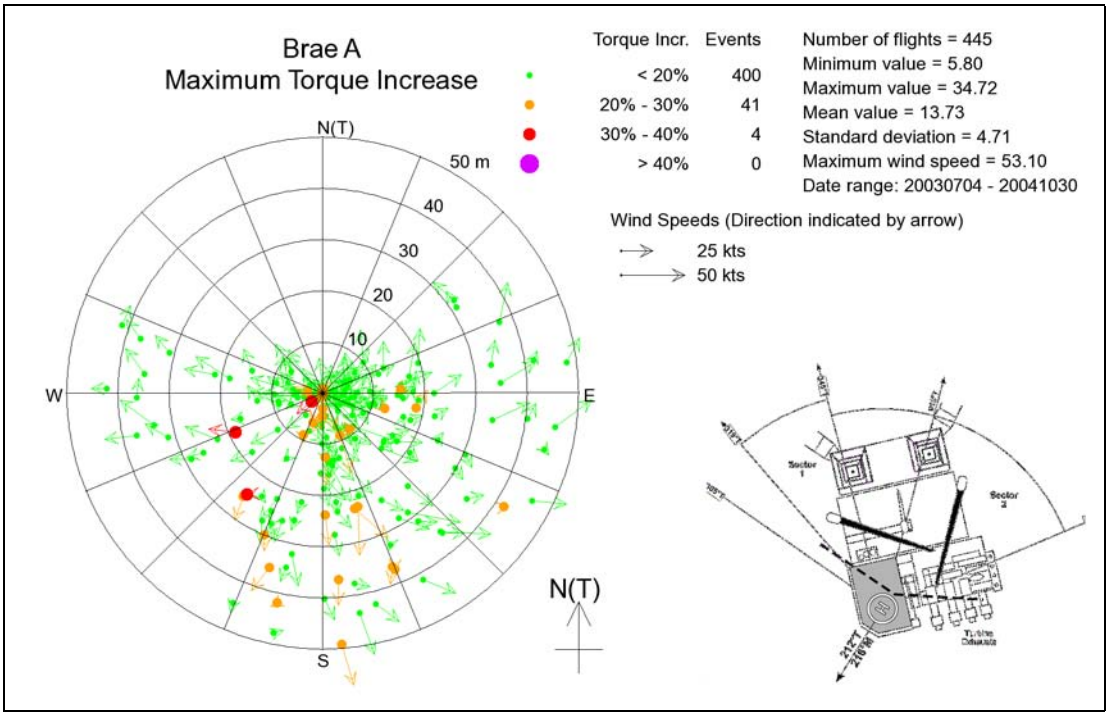

Figure 4 Brae-A 'raw' maximum torque increase data – helicopter location plot

.

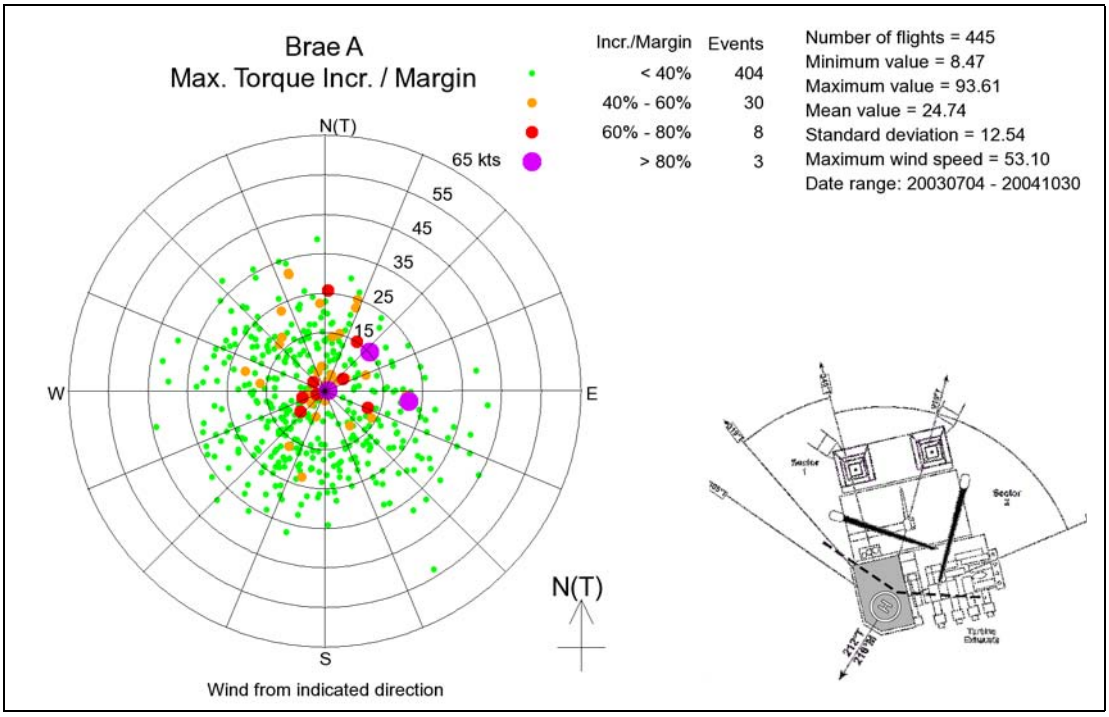

Figure 5 Brae-A percentage of torque margin data – wind rose plot

.

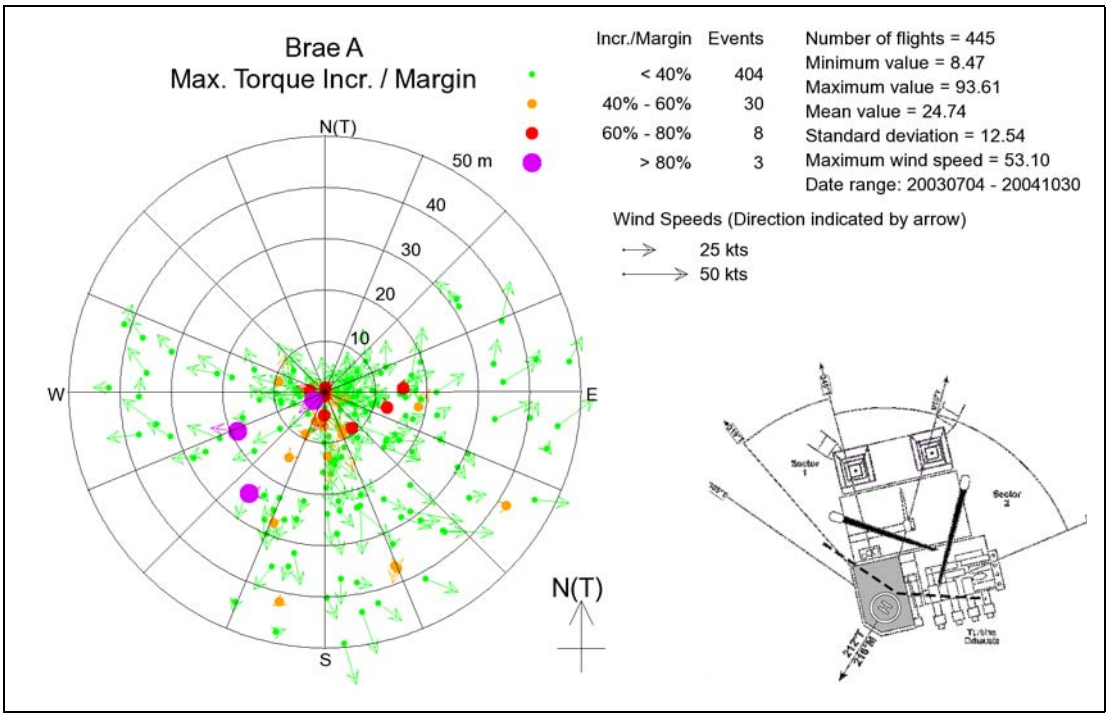

Figure 6 Brae-A percentage of torque margin data – helicopter location plot

.

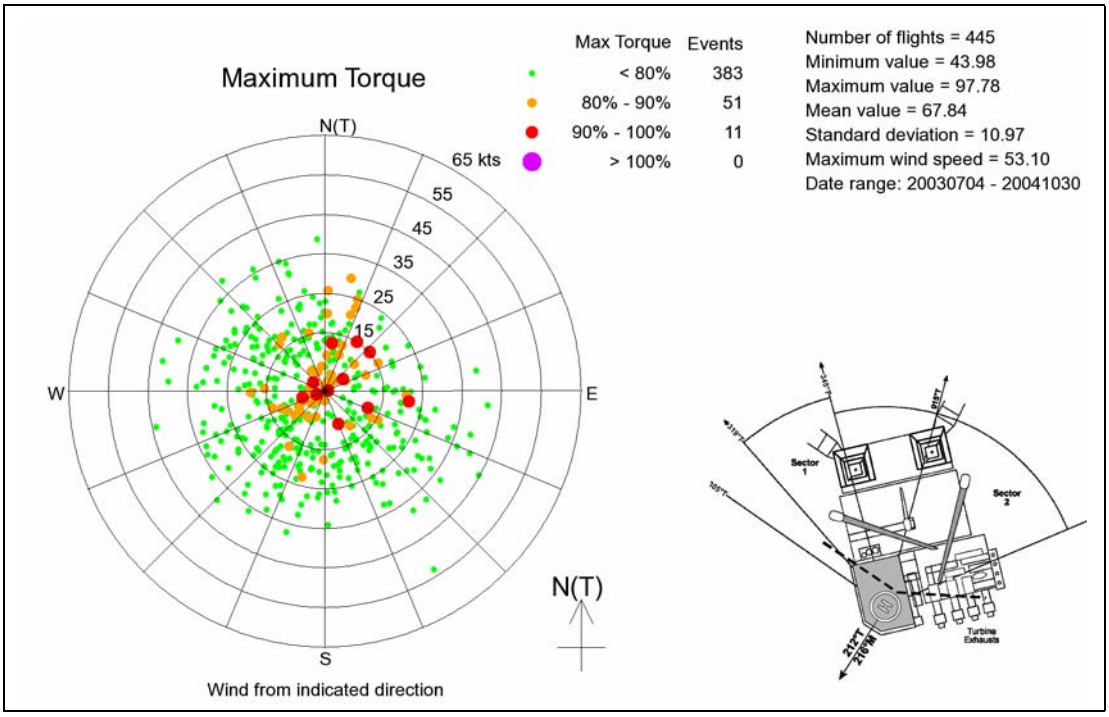

Figure 7 Brae-A 'raw' maximum torque data – wind rose plot

.

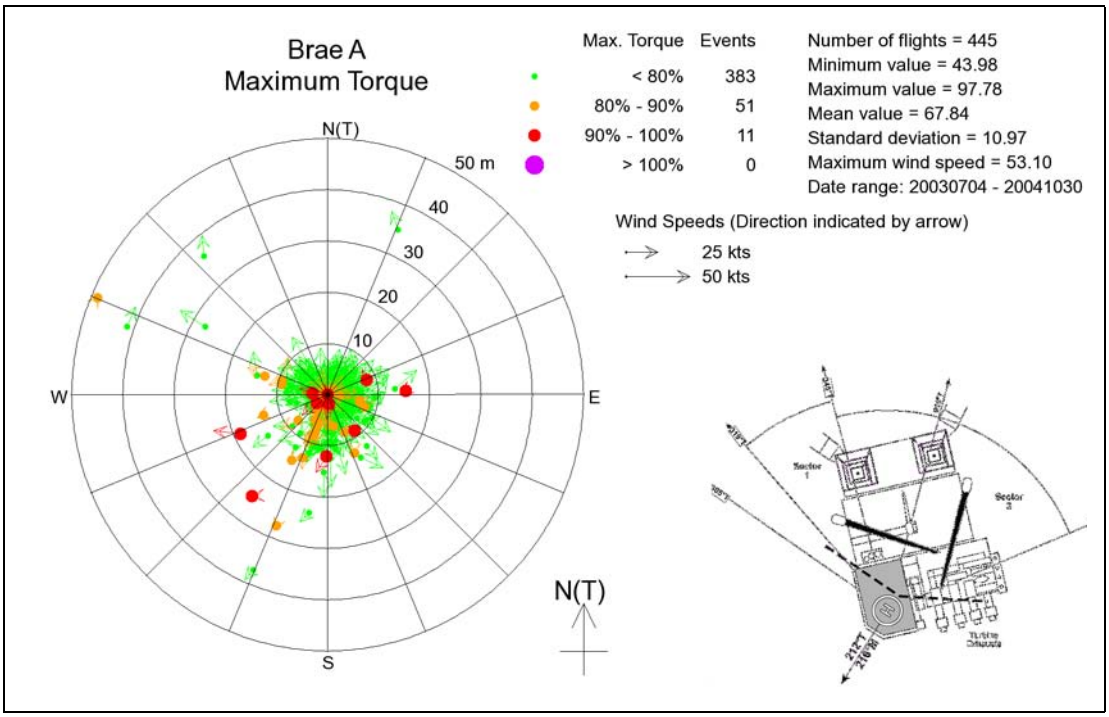

Figure 8 Brae-A 'raw' maximum torque data – helicopter location plot

.

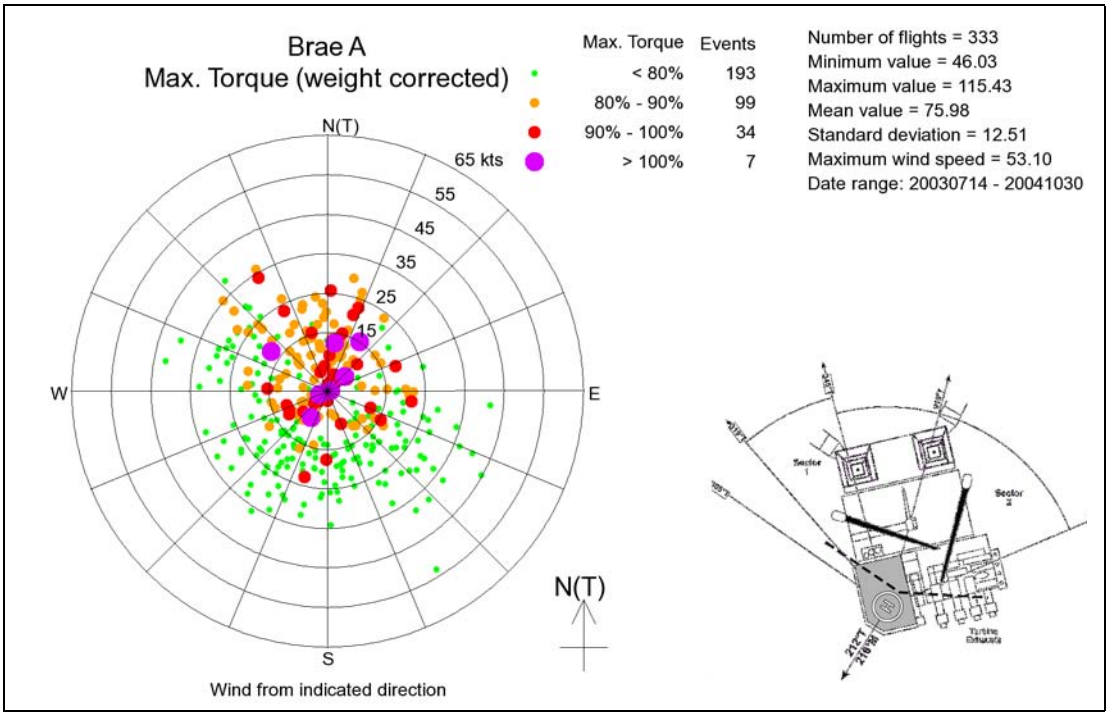

Figure 9 Brae-A 'weight corrected' maximum torque data – wind rose plot

.

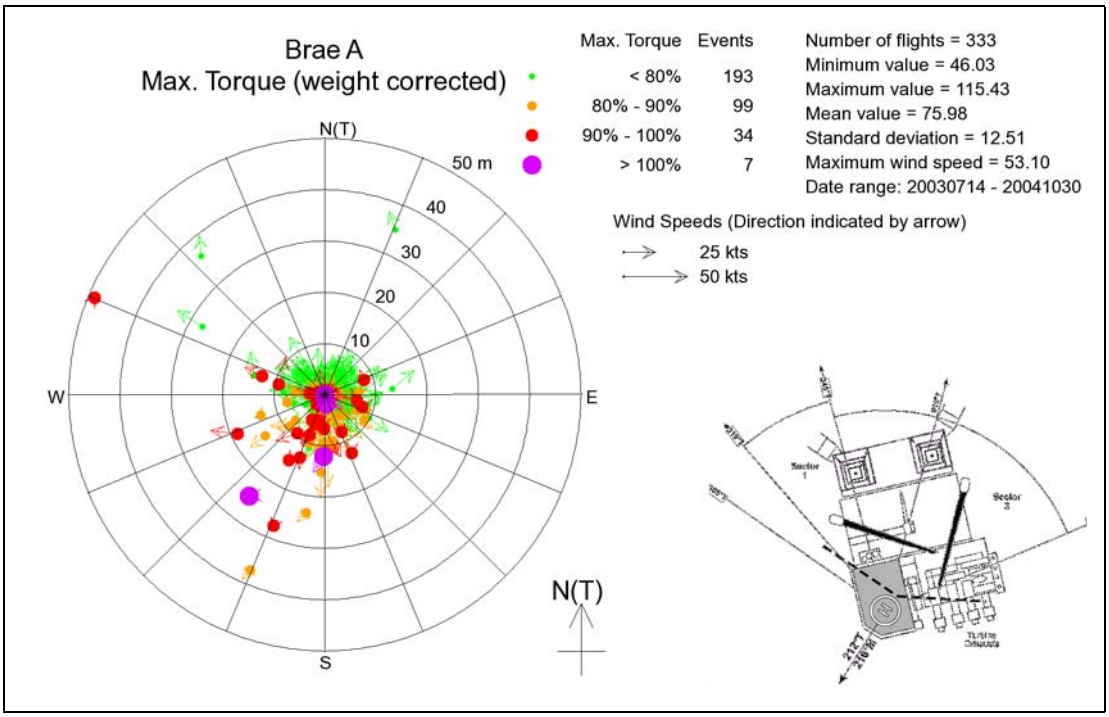

Figure 10 Brae-A 'weight corrected' maximum torque data – helicopter location plot

.

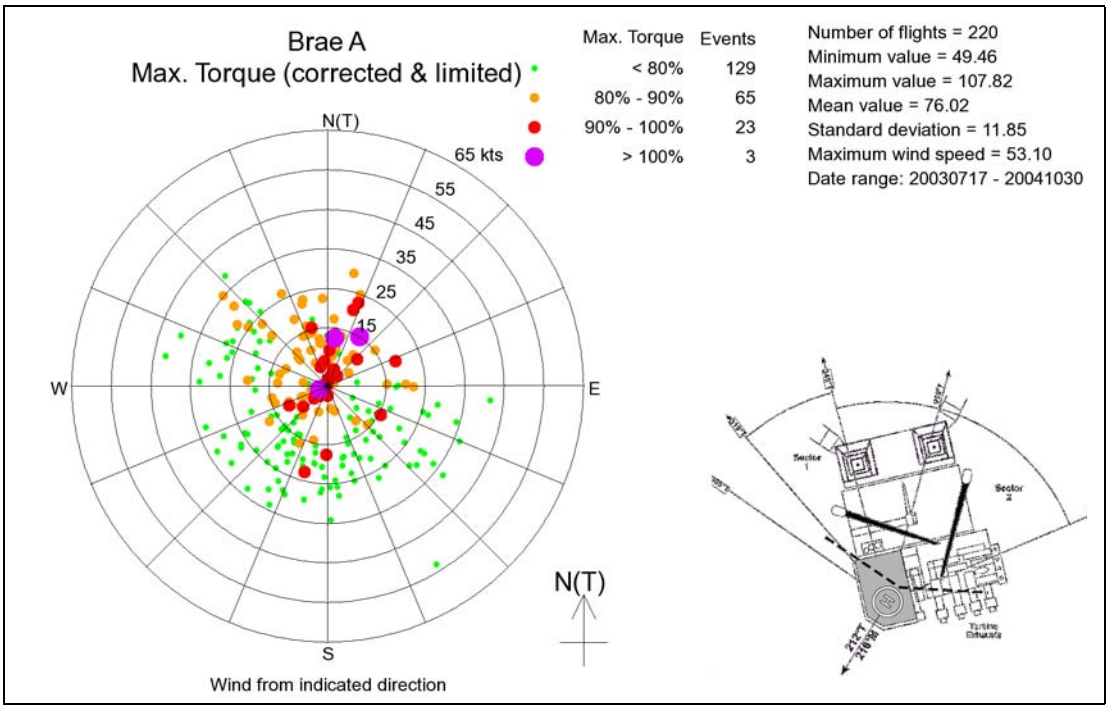

Figure 11 Brae-A 'weight corrected' maximum torque data for limited weight range – wind rose plot

.

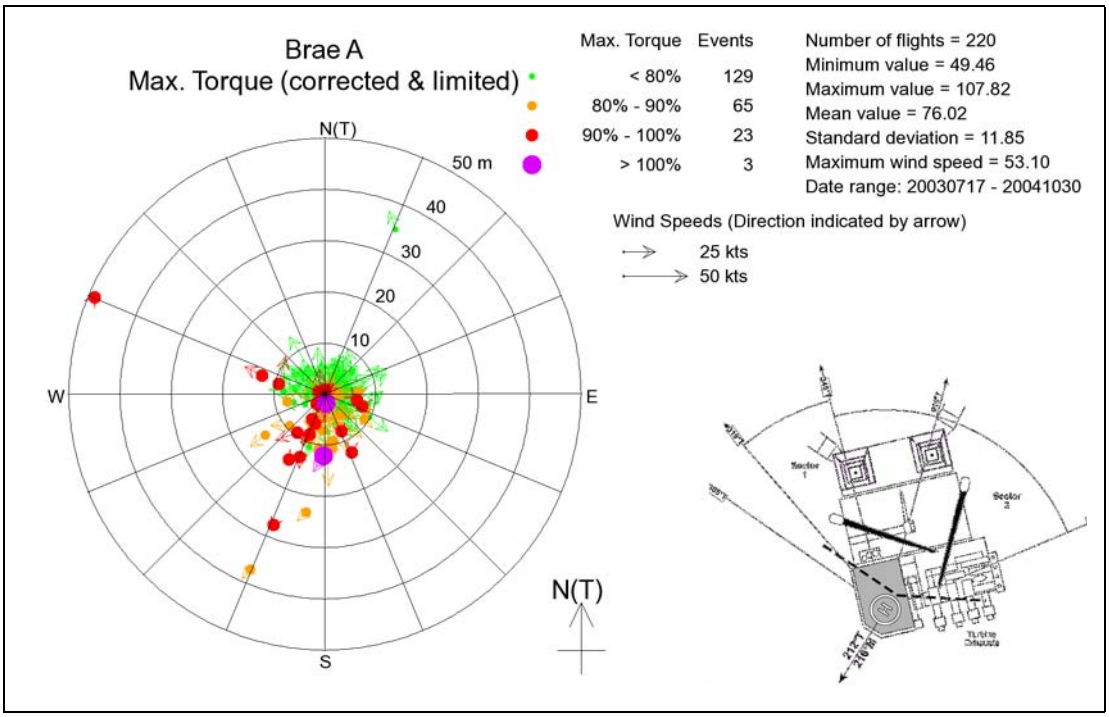

Figure 12 Brae-A 'weight corrected' maximum torque data for limited weight range – helicopter location plot

3.4.2 **Torque values from typical Platforms**

The figures presented in this section provide examples of the torque increase/margin, and the weight-corrected maximum torque for a limited weight range, for two platforms considered to be generally typical of the range of values found in the entire HOMP archive [10].

Alba Northern is regarded as a relatively benign platform, and torque increase/margin values for the 238 landings in the archive are presented in Figure 13 and Figure 14. It can be seen that the highest values all occur at low wind speeds. The corrected and limited weight range maximum torque data is shown in Figure 15 and Figure 16, and presents a similar picture.

Figure 17 and Figure 18 show torque increase/margin data for the much more challenging Ninian Central platform. This platform has more landings in the archive (550) and there are a larger percentage of high values. However, it is clear that the vast majority of the high values are for low wind speeds, or for wind directions from the 'turbulent' E-S wind sector.

The pattern exhibited by the corrected maximum torque data in Figure 19 and Figure 20 is very similar. The highest values are associated with either low wind speeds or wind directions from the E-S sector.

Once again there is no evidence of any higher torque events in winds from the open sector.

.

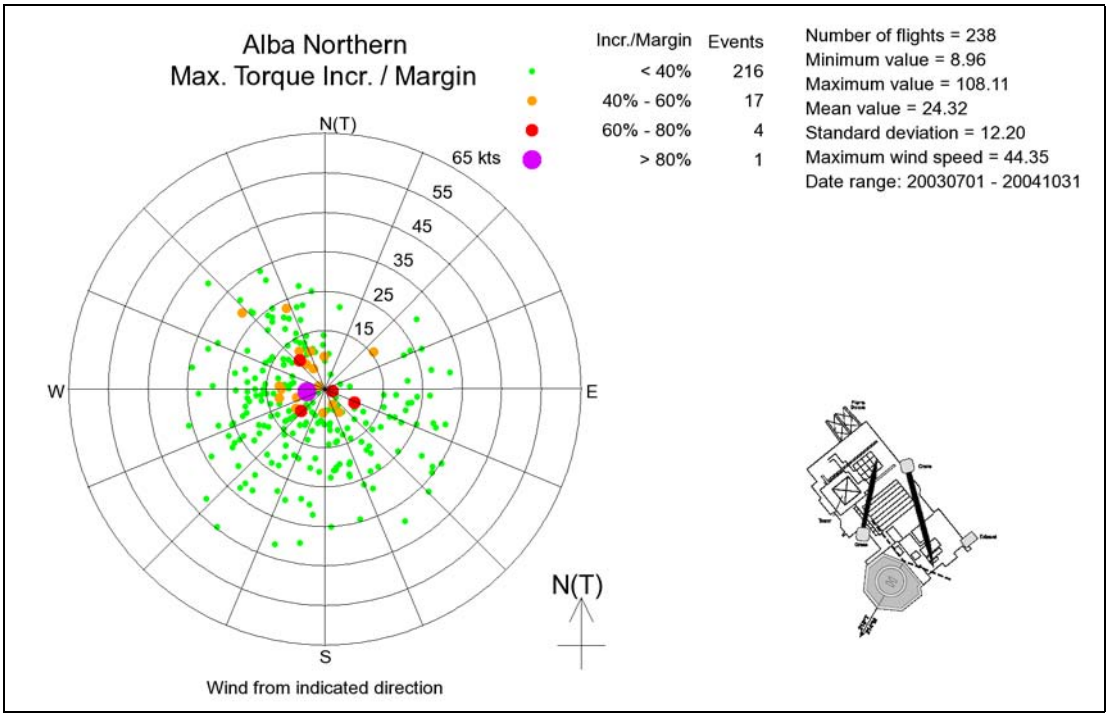

Figure 13 Alba Northern percentage of torque margin data – wind rose plot

.

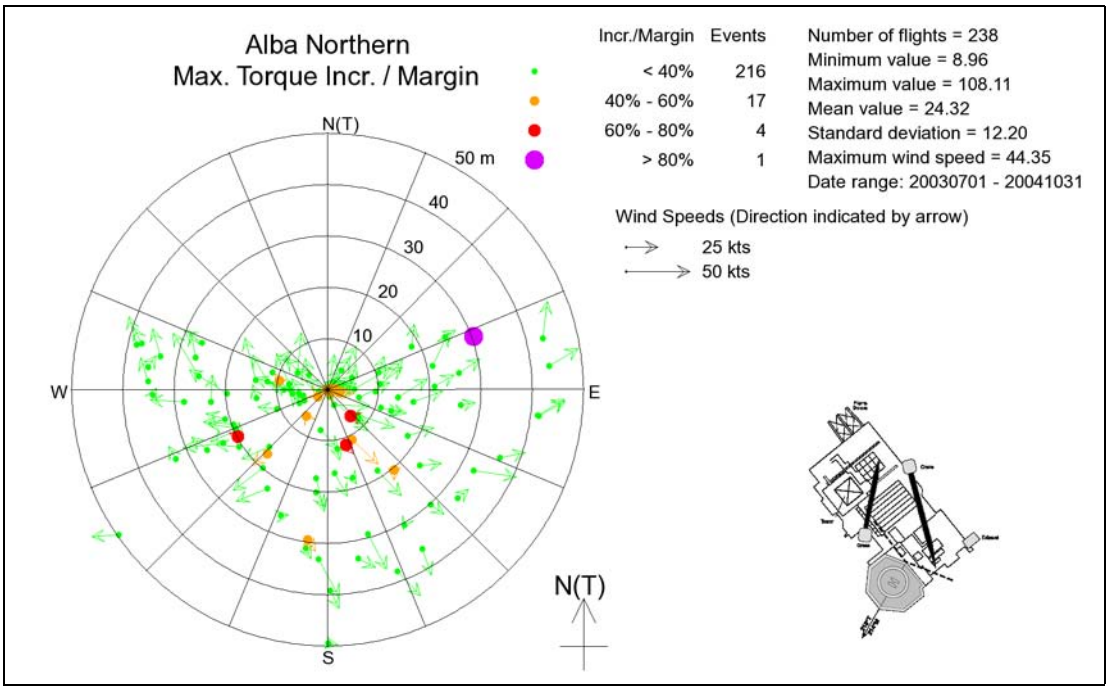

Figure 14 Alba Northern percentage of torque margin data – helicopter location plot

.

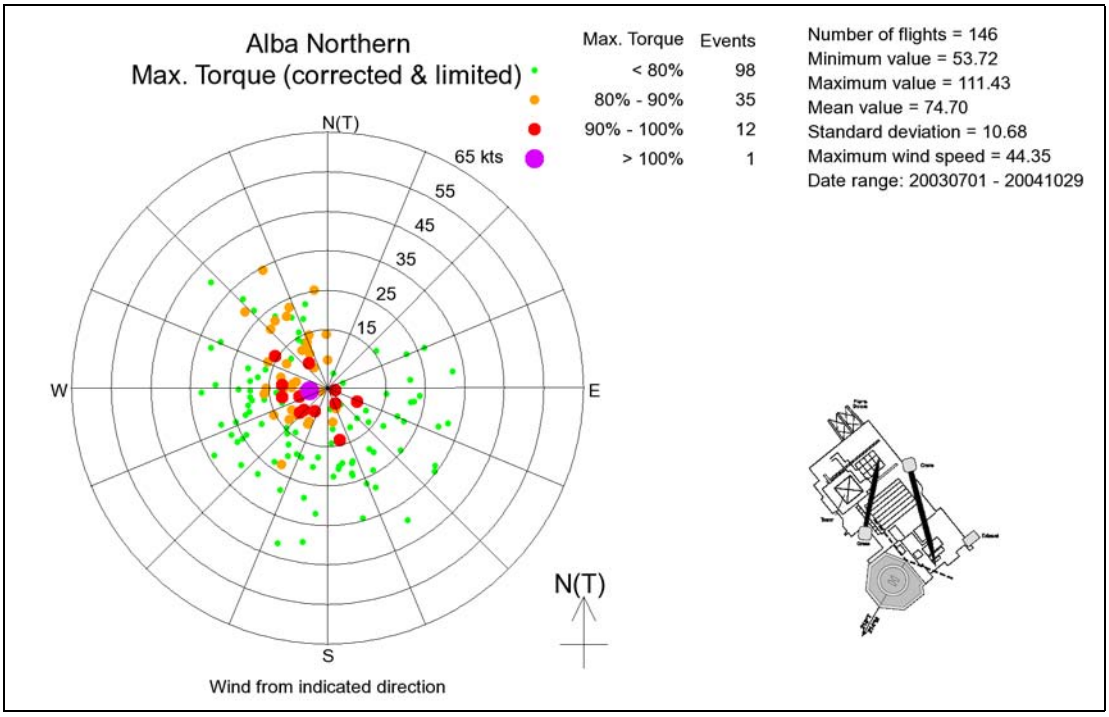

Figure 15 Alba Northern 'weight corrected' maximum torque data for limited weight range – wind rose plot

.

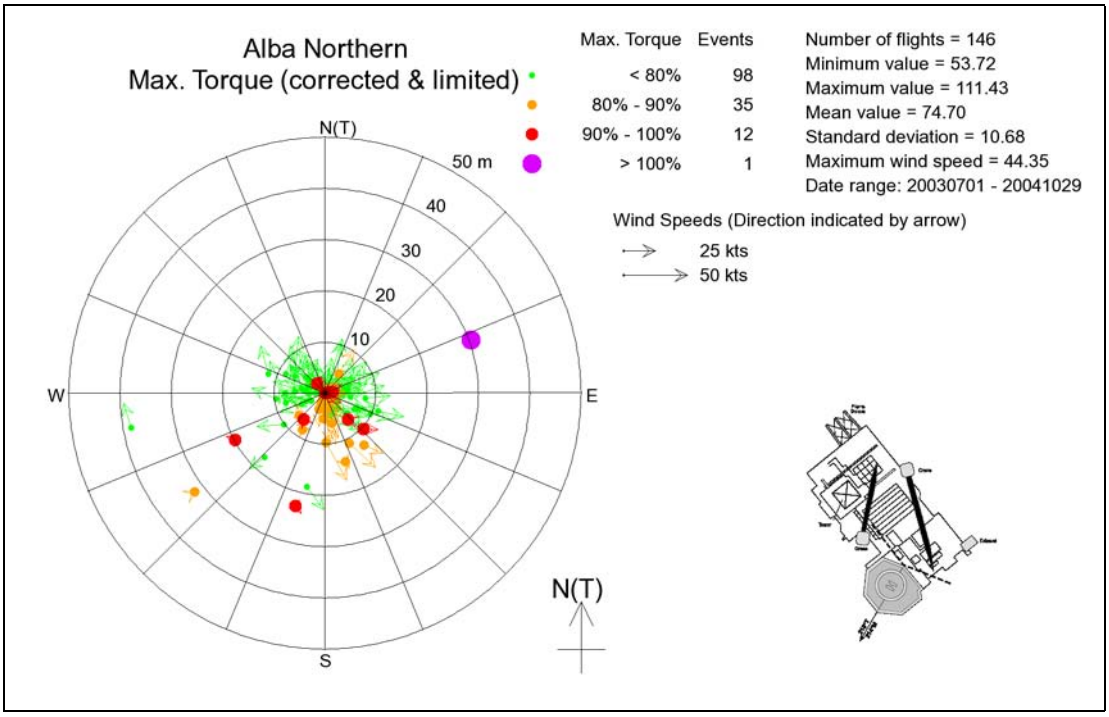

Figure 16 Alba Northern 'weight corrected' maximum torque data for limited weight range – helicopter location plot

.

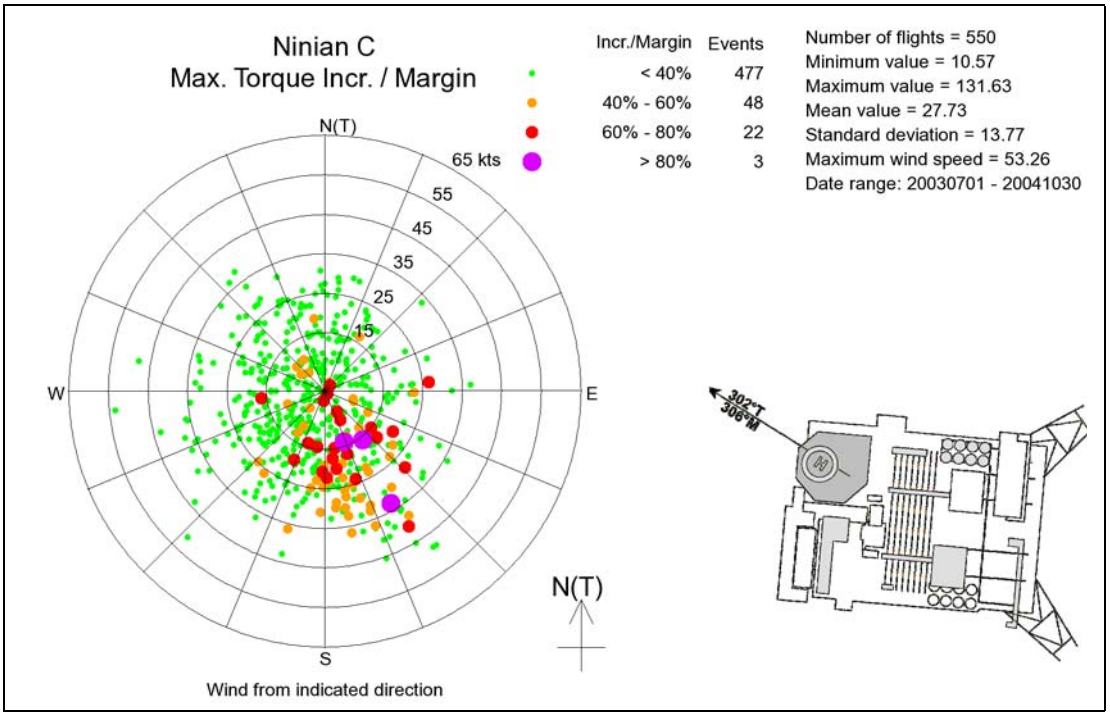

Figure 17 Ninian C percentage of torque margin data – wind rose plot

.

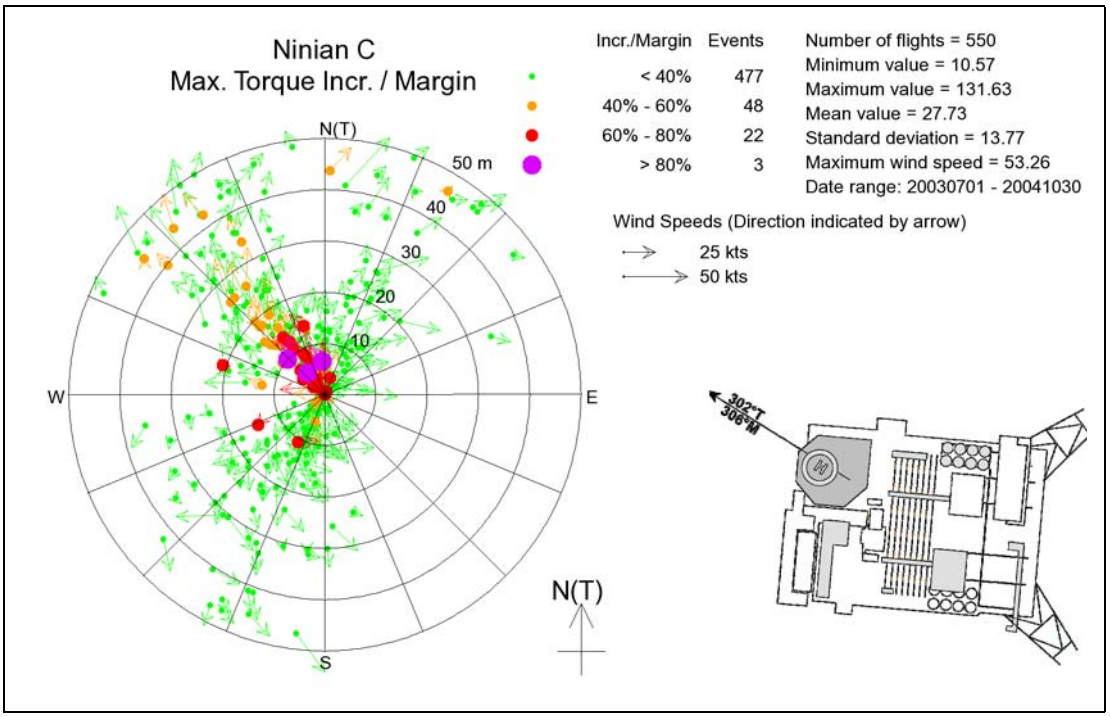

Figure 18 Ninian C percentage of torque margin data – helicopter location plot

.

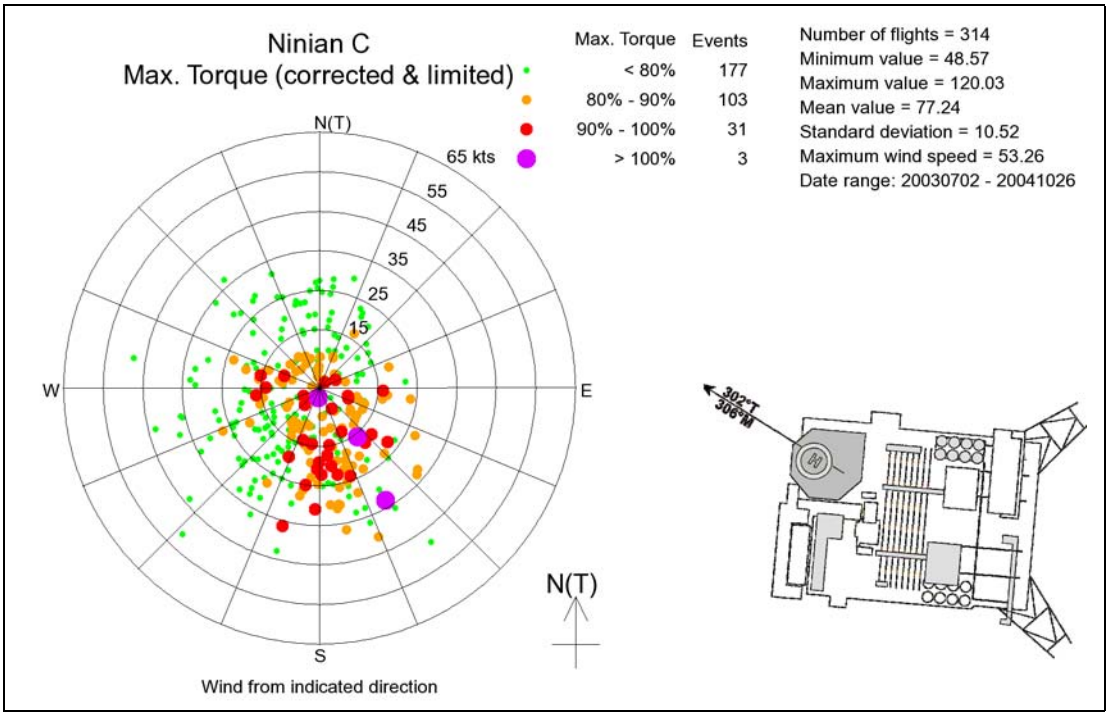

Figure 19 Ninian C 'weight corrected' maximum torque data for limited weight range – wind rose plot

.

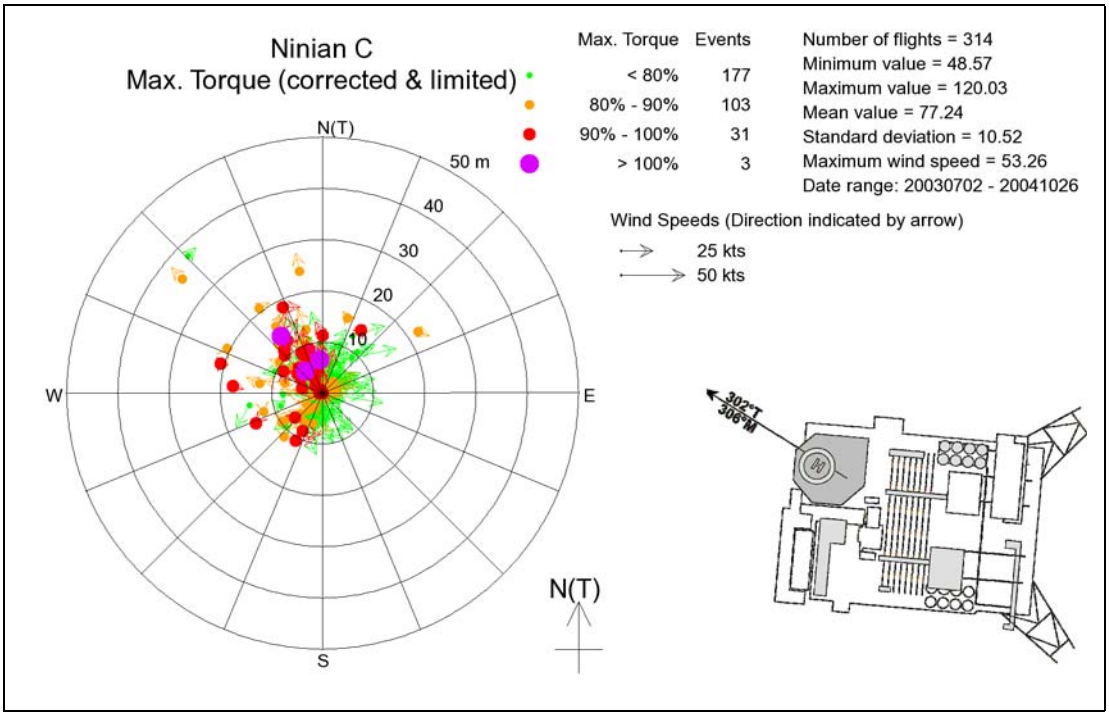

Figure 20 Ninian C 'weight corrected' maximum torque data for limited weight range – helicopter location plot

3.4.3 Ensemble Data

Examination of the plots for all the platforms [10] generally shows the same pattern of high values as demonstrated in the previous section. However, for the 44 platforms for which sketches were available, it is possible to segregate all the torque data into wind directions from inside the obstructed or 'turbulent' sectors, and the remaining 'open' sectors. In the following figures data for maximum torque and maximum torque increase are presented against wind speed.

Figure 21 shows the maximum torque corrected for weight, but plotted for only a limited landing weight range (17,000 lb – 18,500 lb) in order to minimise any bias in the correction caused by pilot behaviour. The figure shows data for the obstructed wind directional sectors, whilst similar data is presented for the open sectors in Figure 22.

It can be seen that there is the expected trend of reducing maximum torque with wind speed, but this trend is stronger in the open sector data of Figure 22. This means that there is also a tendency for the corrected torque in wind from the obstructed sector to be higher than that from the open sector at higher wind speeds. . .

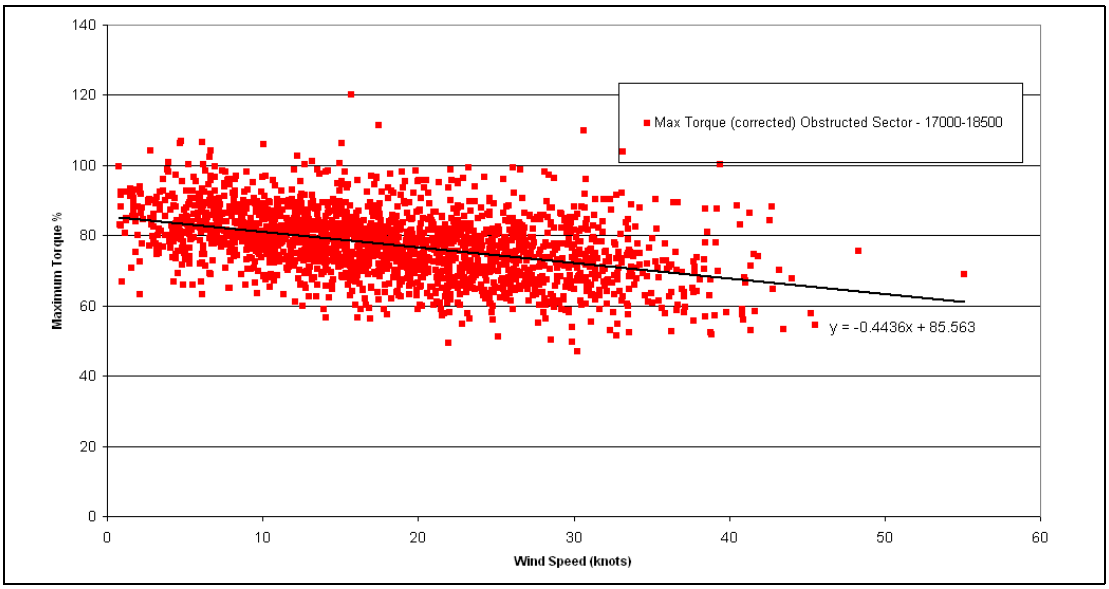

Figure 21 Maximum Torque, corrected for weight (17,000lb - 18,500lb) – Obstructed Sector

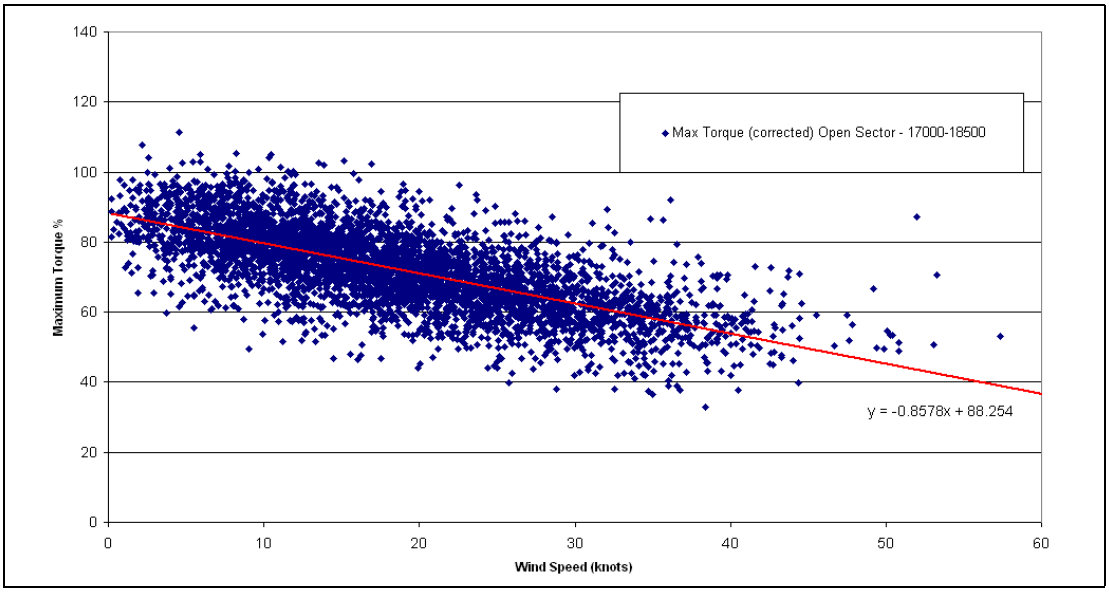

Figure 22 Maximum Torque, corrected for weight (17,000lb - 18,500lb) – Open Sector

Similarly, Figures 23 and 24 show torque increase data expressed as a percentage of the instantaneous torque margin presented in the same way for all the valid data landings to the 44 platforms. It can be seen that there is a noticeable reduction in the torque increase/margin with wind speed when the wind is from open sectors, but this trend is absent for winds from the obstructed or turbulent sectors. Torque increase/margin is higher in high winds from the obstructed sectors. Put another way, high values of torque increase/margin at higher wind speeds are invariably associated with turbulent conditions.

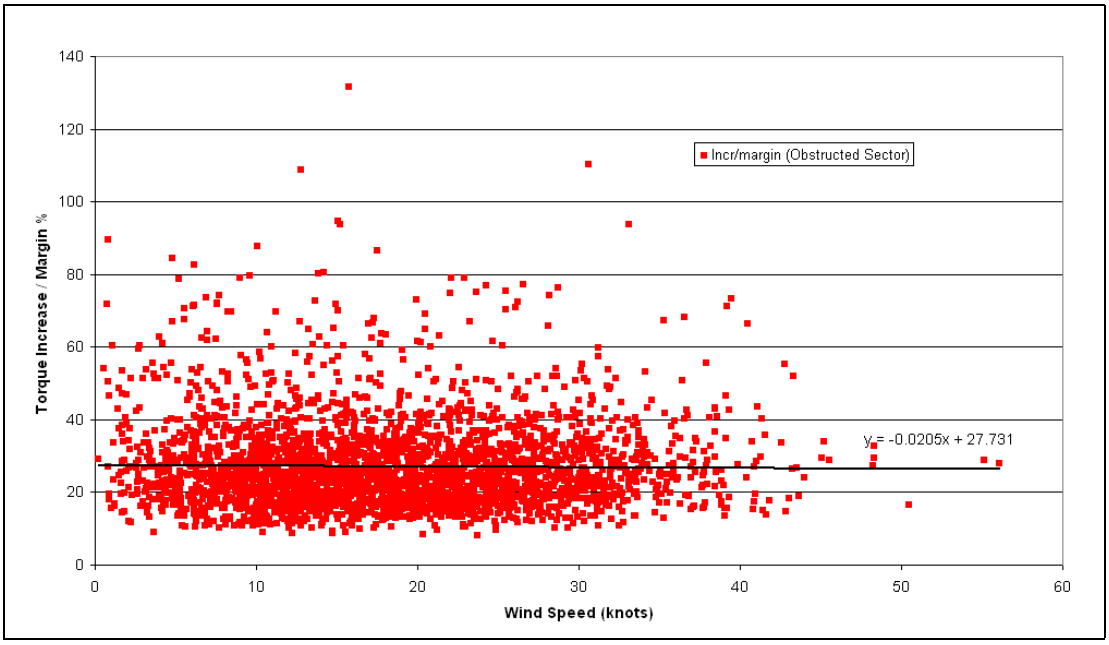

Figure 23 Torque increase as percentage of margin – Obstructed Sector

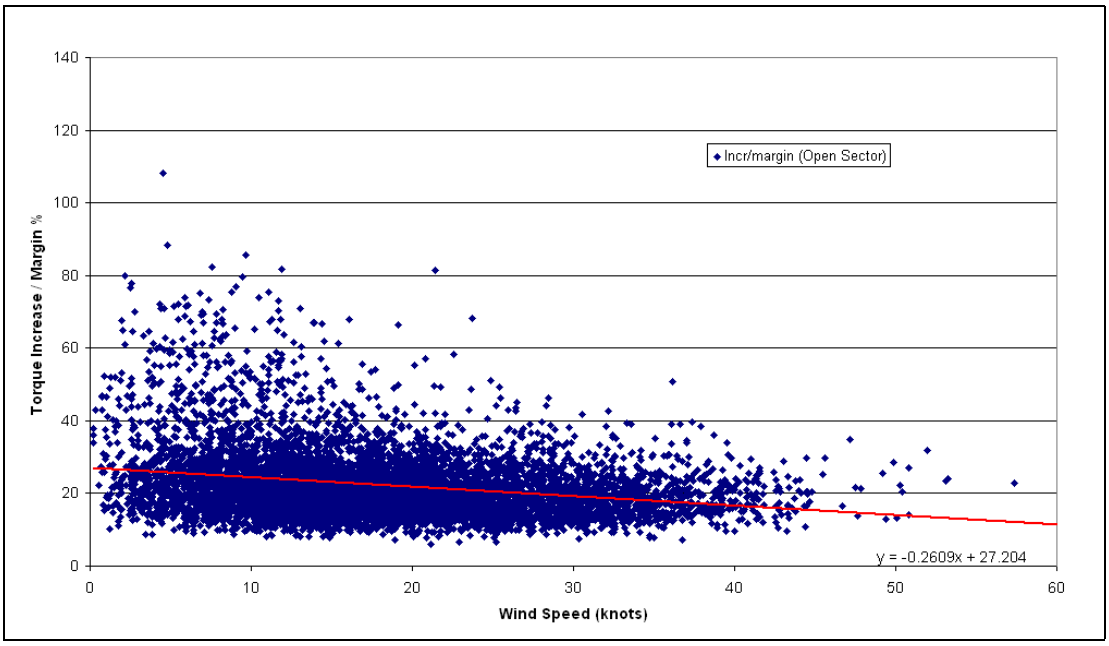

Figure 24 Torque increase as percentage of margin – Open Sector

4 Phase 2 – Evaluate 0.9 m/s Criterion Violations in BMT Archive

4.1 Introduction

In the original study (see Appendix A of [8]), wind tunnel data from sixteen platforms were reviewed. The objective at that time was to assess wind tunnel turbulence data held by BMT and compare these with the Helideck Limitations List (HLL) [11]. The study concentrated on the worst case horizontal and vertical turbulence standard deviation recorded above the helideck during wind tunnel tests on each platform.

The objective in Phase-2 of the current study was primarily to map the occurrence of 0.9 m/s violations in order to understand their physical relationship with the geometric properties of the platform and thus assist with objective 2.1 stated in Section 2. However, while entering the data archive it was also considered worth retrieving the turbulence data so that violations of the turbulence criterion could also be mapped onto the platform sketches

Consequently, the full data matrices of mean wind speed and turbulence standard deviation across all wind directions were included in the analysis. After the work of [8] had been performed, BMT had added a number of platforms to its database and so the analysis was performed for 19 platforms. Several of these platforms had been tested in a number of different design configurations with the result that a total of 68 cases were available in the database.

All the recorded wind data were retrieved and loaded into common format spreadsheets. The data comprised the longitudinal and vertical components of mean wind velocity and turbulence standard deviation recorded at a number of heights above the centre of the helideck.

Standardised polar plots of the wind tunnel measurements versus wind speed and direction were prepared. The data comprised the following parameters recorded above the helideck:

- Longitudinal mean wind speed
- Vertical mean wind speed
- Longitudinal turbulence standard deviation
- Vertical turbulence standard deviation

The plots were presented alongside plan sketches of the platforms to illustrate the relationship between the wind direction and likely causes of turbulence and wind shear. These were used to highlight the wind sectors where the existing vertical wind criterion and the new turbulence criterion were exceeded.

The plots were also used to help determine if exceedance of the criteria was associated with particular platform features. In particular, whether the maximum vertical mean wind speeds always occurred for the ‘open’ wind directions.

The criteria applied to the data were as shown in Table 2.

Table 2 Wind Flow Criteria

Flow property	Criterion	Source
Longitudinal mean wind speed (at 25 m/s wind speed)	±5.0 m/s	A BMT-derived criterion, developed from experience of interpreting results of wind tunnel tests.
Vertical mean wind speed (at 25 m/s wind speed)	±0.9 m/s	[1]
Longitudinal turbulence standard deviation	5.0 m/s	A BMT-derived criterion, developed from experience of interpreting results of wind tunnel tests.
Vertical turbulence standard deviation	1.75 m/s	[5]

Each chart presents four plots as follows:

1. Vertical turbulence rms: the undisturbed mean wind speed at helideck height at which the vertical turbulence criterion of standard deviation = 1.75 m/s is violated. The green-shaded area indicates where the turbulence criterion is *not* violated.
2. Longitudinal turbulence rms: the undisturbed mean wind speed at helideck height at which a nominal longitudinal turbulence criterion of standard deviation = 5.0 m/s is violated. The green-shaded area indicates where the criterion is *not* violated.
3. Vertical mean wind speed: the undisturbed mean wind speed at helideck height at which the vertical mean wind speed criterion of = ±0.9 m/s is violated. The green-shaded area indicates where the criterion is *not* violated. The violation zone, shown in red, extends to a wind speed of 25 m/s to reflect the fact that the criterion value is defined for wind speeds up to this value.
4. Longitudinal mean wind speed: the undisturbed mean wind speed at helideck height at which the nominal longitudinal mean wind speed criterion of 25 ± 5 m/s is violated. The violation zone is shown in red.

A summary of the key information for each of the 68 cases is provided in Table 3.

Note that the platforms have been de-identified, as the BMT wind tunnel data is owned by the companies who commissioned the original studies, and it was impractical to seek permission to publish.

In view of the similarity of the results from most of the alternate configurations available for a particular platform it was decided to present a single case for each platform graphically in Figure 25 to Figure 43. The 'as-built' configuration was selected when it was known. If it was not known, then the first configuration tested as listed in Table 3 was used. The maximum vertical mean flow component results for each platform are summarised in Table 4 in Section 4.2.

Table 3 Table of the key information shown in the charts

Platform Name	Date of test	Direction of Platform North	Client Case Name	Case Description
A	Jan 07	345	Air Gap Trials	Air Gap = 0 m
A	Jan 07	345	Air Gap Trials	Air Gap = 1 m
A	Jan 07	345	Air Gap Trials	Air Gap = 2 m
A	Jan 07	345	Air Gap Trials	Air Gap = 3 m
A	Jan 07	345	Air Gap Trials	Air Gap = 4 m (Final)
A	Jan 07	345	Air Gap Trials	Air Gap = 5 m
A	Jan 07	345	Air Gap Trials	Air Gap = 6 m
B	Jan-94		Original Scheme	Air Gap = 4 m
B	Jan-94		Final Scheme	Air Gap = 6 m
C	Nov-01	337.5	Original design	Horizontal Exhausts
D	Feb-96	330	Original design	23 m h/d at elevation 65.5 m
D	Feb-96	330	Modified design: Final	27 m h/d at elevation 65.5 m
E	Aug-03	45	Configuration 1	Existing design
E	Aug-03	45	Configuration 2	Without the roof module comprising Rooms 401 to 404 and the toilet/shower block
E	Aug-03	45	Configuration 3	Replacement of the existing Stores and Workshop with new Accommodation and Gym modules
E	Aug-03	45	Configuration 4	Replacement of the existing Stores and Workshop with a new module (Accommodation or Gym)
E	Aug-03	45	Configuration 5	Helideck raised by 3 m
F	Feb-05	320	Configuration 0	Air gap = 3.5 m
F	Feb-05	320	Configuration 1	Air gap under helideck = 5 m
F	Feb-05	320	Configuration 2	Air gap under helideck = 3.5 m, Lobby removed
F	Feb-05	320	Configuration 3	Air gap under helideck = 5 m, Lobby removed
F	Feb-05	320	Configuration 4	Air gap under helideck = 3.5 m, Lobby removed: Move h/d 5.5 m North
F	Feb-05	320	Configuration 5	Air gap 5 m: Lobby removed: H/d moved 5.5 m North

Table 3 Table of the key information shown in the charts (Continued)

Platform Name	Date of test	Direction of Platform North	Client Case Name	Case Description
F	Feb-05	320	Configuration 6	Air gap 5 m: Lobby removed: H/d moved 5.5 m north and extended 2.1 m west
F	Feb-05	320	Configuration 7	Air gap 5 m: Lobby removed: H/d moved 5.5 m north and aiming circle moved 2.1 m east
F	Feb-05	320	Configuration 8	Air gap 5 m: Lobby removed: H/d at original NS position and aiming circle moved 2.1 m east
F	Feb-05	320	Configuration 9	Repeat of 8. Air gap 5 m: Lobby removed: H/d at original NS position and aiming circle moved 2.1 m east
F	Mar-05	321	Configuration 10	Air gap 5 m: Lobby removed: H/d moved 5.5 m north, 2.1 m west and aiming circle moved 2.1 m east
G	Nov-94	340	Original design	Helideck at 4 m elevation above R-PLQ
H	Jul-92	354	Detailed Engineering Phase	Air gap = 8.2 m, less 2.8 m, less 2.4 m; without Tender Support Vessel
I	Jul-90	333	Idealised helideck	30 m helideck with edge vanes; air gap = 3 m
I	Jul-90	333	Optimised helideck: Final	30 m helideck without edge vanes; air gap = 3 m
J	Apr-98	10	2/4H at Option 2A location	Hotel platform located north of 2/4J, Gallant installed
J	Apr-98	10	2/4H at Option 2A location	Hotel platform located north of 2/4J, Gallant removed
J	Apr-98	10	2/4H at Option 2B location	Hotel platform located south of 2/4J, Gallant installed
J	Apr-98	10	2/4H at Option 2B location	Hotel platform located south of 2/4J, Gallant removed
J	Apr-98	10	2/4H at Option 2C location	Hotel platform located south east of 2/4J, Gallant installed
J	Apr-98	10	2/4H at Option 2C location	Hotel platform located south east of 2/4J, Gallant removed
K	Nov-97	303	Original design	Helideck as designed
K	Nov-97	303	Recommended design	Helideck extended by 3 m all round. Parking bay widened by 4.5 m

Table 3 Table of the key information shown in the charts (Continued)

Platform Name	Date of test	Direction of Platform North	Client Case Name	Case Description
L	Apr-90		Original design	Air gap = 3 m; With obstructions under the h/d
M	Jul-00	340	Base Case	No Jack-up present. Wire-lining eqp. on Jade weather deck. Diesel tank and 1 fire pump on main deck.
M	Jul-00	340	Alternative Case	No Jack-up present. Wire-lining eqp. on Jade weather deck. Diesel tank on weather deck and 2 fire pumps on main deck
M	Jul-00	340	Workover Case	Jack-up alongside. Wire-lining eqp. removed from Jade weather deck. Diesel tank and 1 fire pump on main deck
N	Dec-97		Original design	0
O	May-96	n/a	Original design	Wind ahead +- 30 degrees
P	Aug-99	22.5	As designed	As designed
Q	Nov-91		Final design	Horizontal exhausts
Q	Aug-95		Alternative design	Vertical exhausts
R	Sep-95	330	As designed	Helideck width = 22.5 m; Air gap = 3 m
R	Sep-95	330	Revised designed	Helideck width = 22.5 m; Air gap = 4 m
R	Sep-95	330	Revised designed	Helideck width = 22.5 m; Air gap = 5 m
R	Sep-95	330	Revised designed	Helideck width = 22.5 m; Air gap = 6 m
R	Sep-95	330	Revised designed	Helideck width = 22.5 m; Air gap = 8 m
R	Sep-95	330	Enclosed stair tower removed	Helideck width = 22.5 m; Air gap = 4 m
R	Sep-95	330	Enclosed stair tower removed	Helideck width = 28 m; Air gap = 3 m
R	Sep-95	330	Enclosed stair tower removed	Helideck width = 25.5 m and shifted 0.45 m south; Air gap = 3 m;
S	May-04	330	Config 0	Existing
S	May-04	330	Config 1	With added blocks 1, 2, 3 and 4

Table 3 Table of the key information shown in the charts (Continued)

Platform Name	Date of test	Direction of Platform North	Client Case Name	Case Description
S	May-04	330	Config 2	With added blocks 2, 3 and 4
S	May-04	330	Config 3	With added blocks 1, 2 and 3
S	May-04	330	Config 4	With added blocks 2 and 3 i.e. blocks 1 and 4 removed
T	Aug-96	n/a	As designed	Without parking area extension to helideck
T	Aug-96	n/a	Optional design	With parking area extension to helideck
U	Mar-91	338	Scheme 1	22.5 m helideck; Air gap = 3 m
U	Mar-91	338	Scheme 2	22.5 m helideck; Air gap = 5 m
U	Mar-91	338	Scheme 3	22.5 m helideck; Air gap = 8 m
U	Mar-91	338	Final Design	27.5 m helideck; Air gap = 5 m

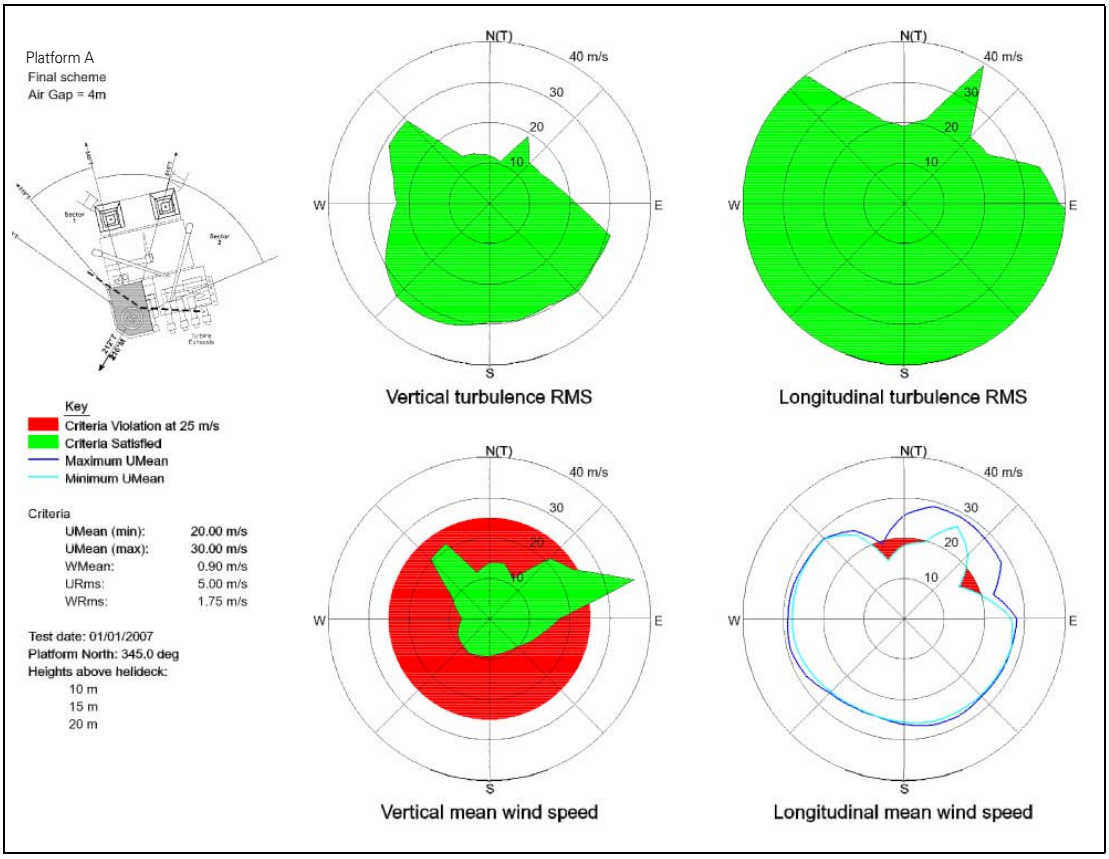

Figure 25 Platform A wind tunnel data

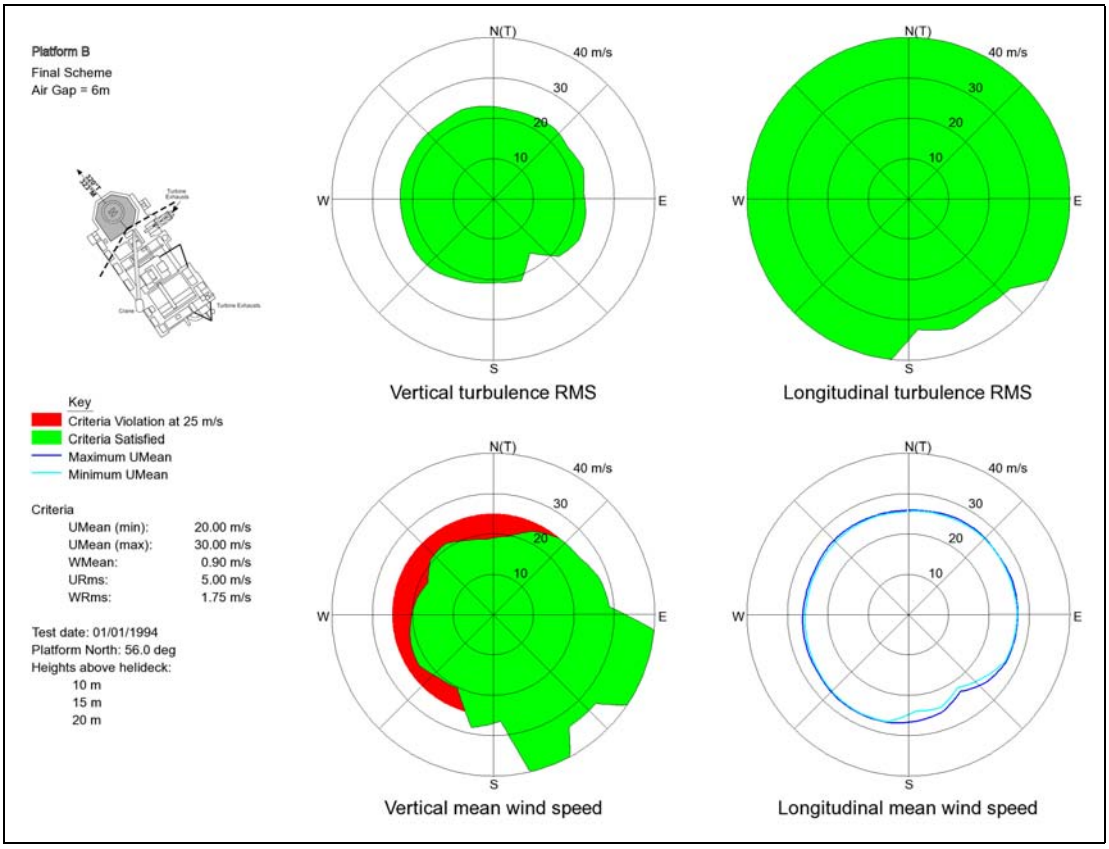

Figure 26 Platform B wind tunnel data

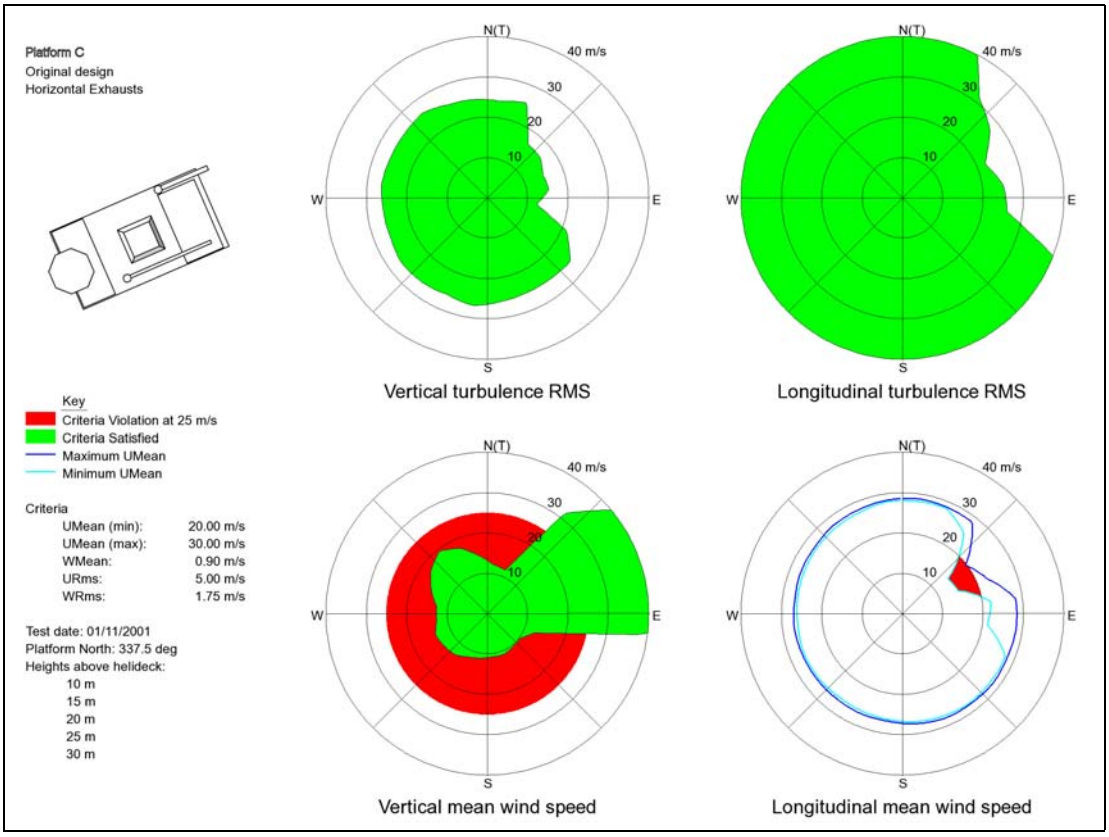

Figure 27 Platform C wind tunnel data

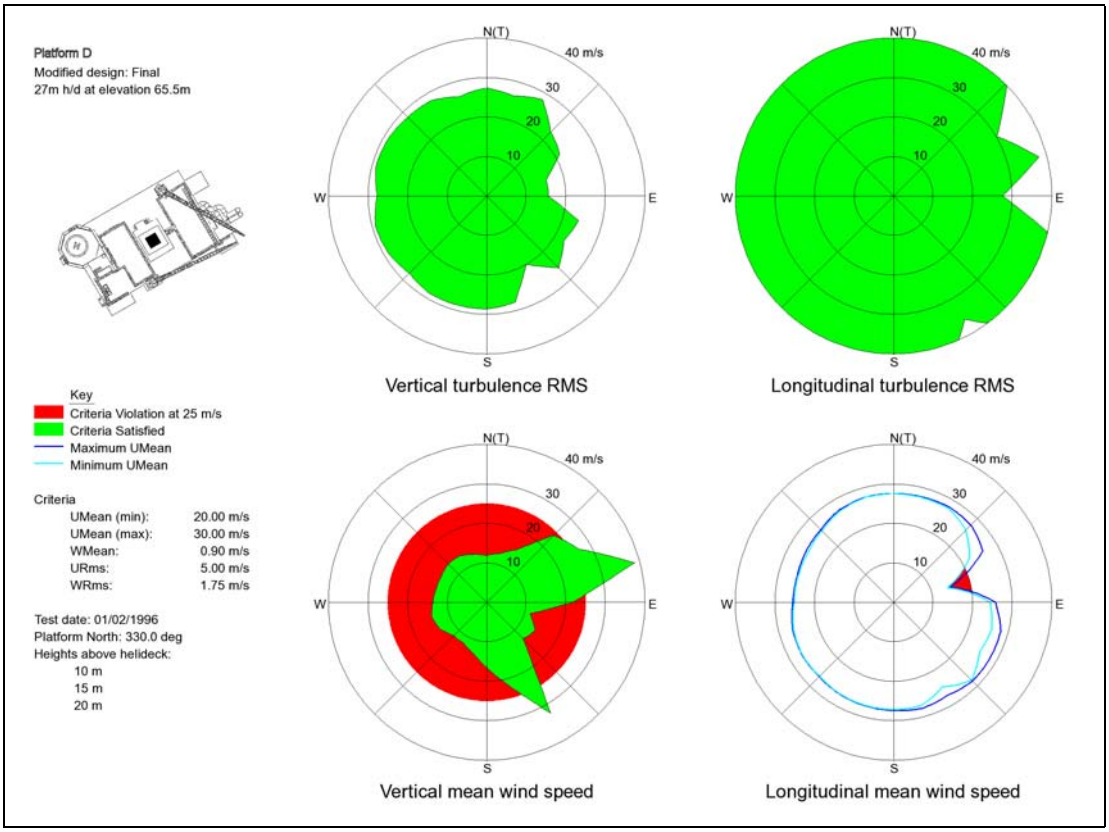

Figure 28 Platform D wind tunnel data

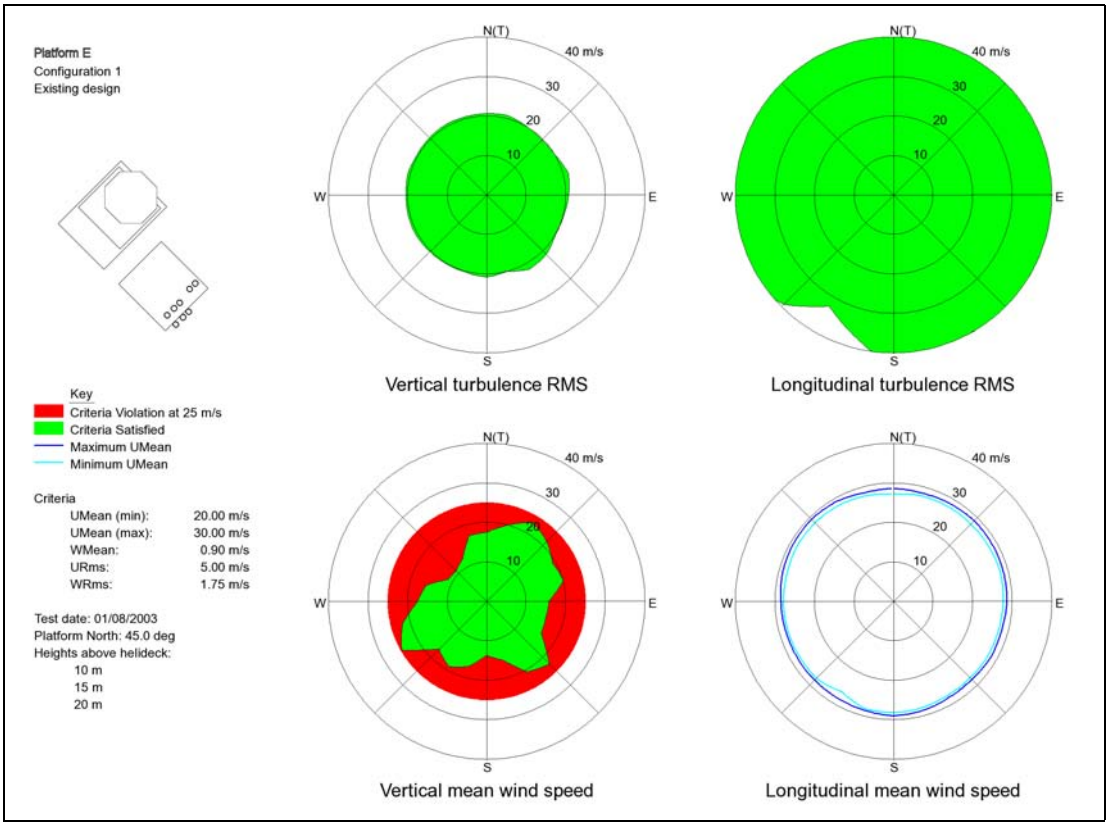

Figure 29 Platform E wind tunnel data

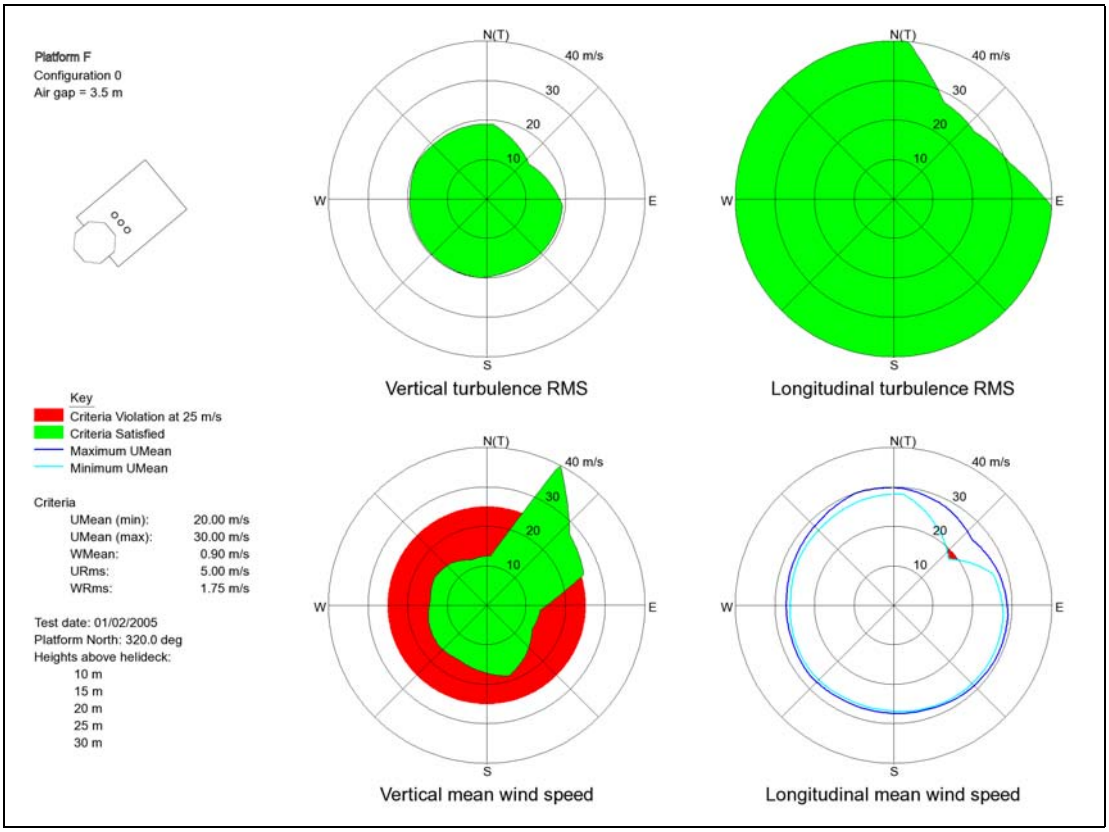

Figure 30 Platform F wind tunnel data

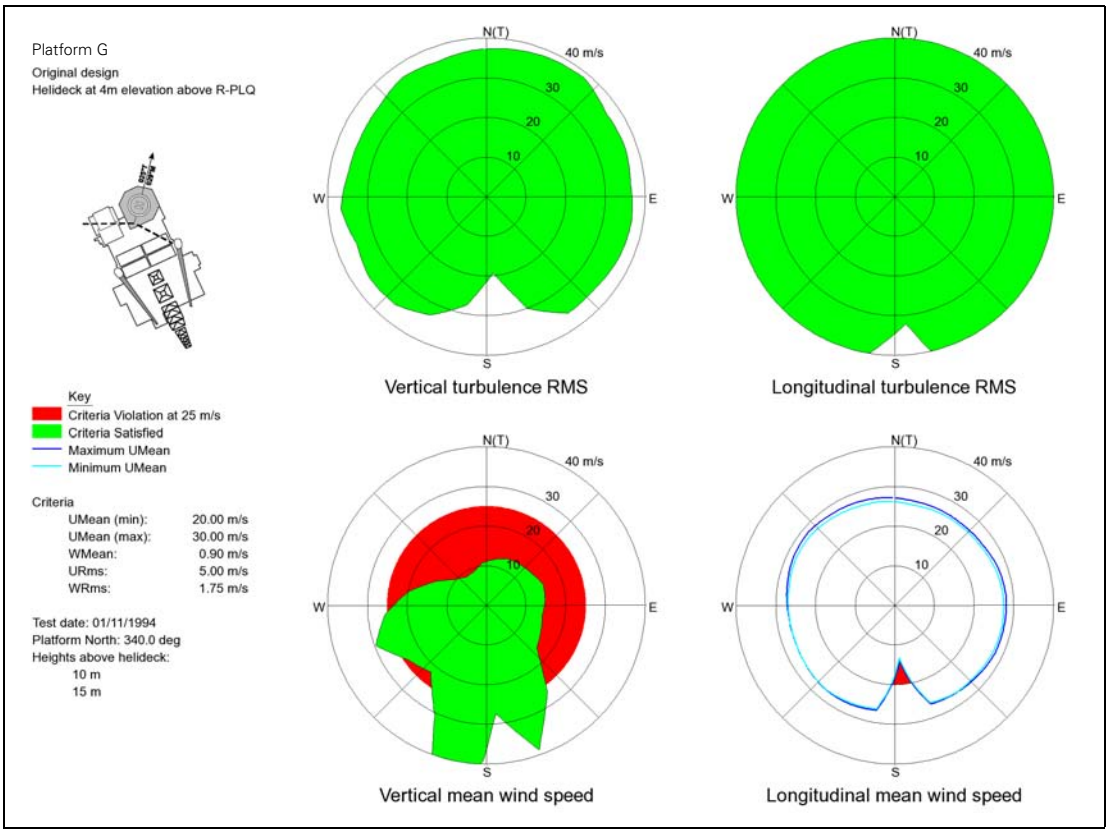

Figure 31 Platform G wind tunnel data

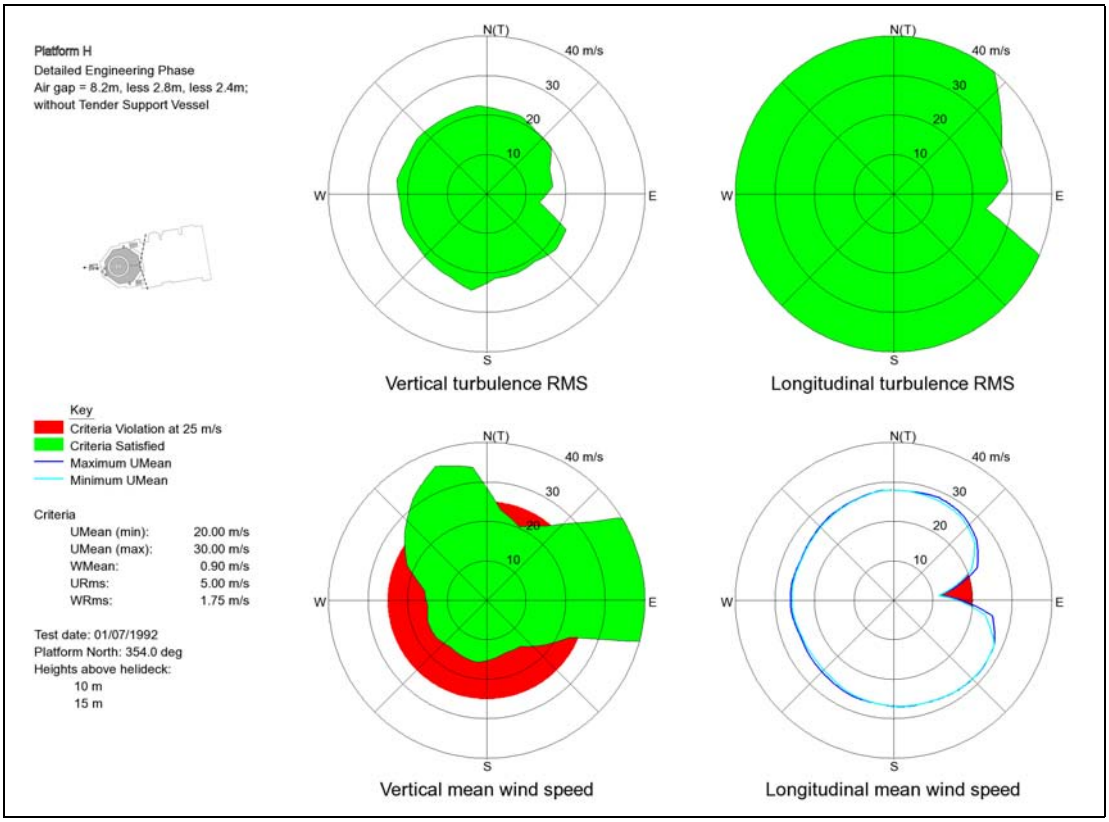

Figure 32 Platform H wind tunnel data

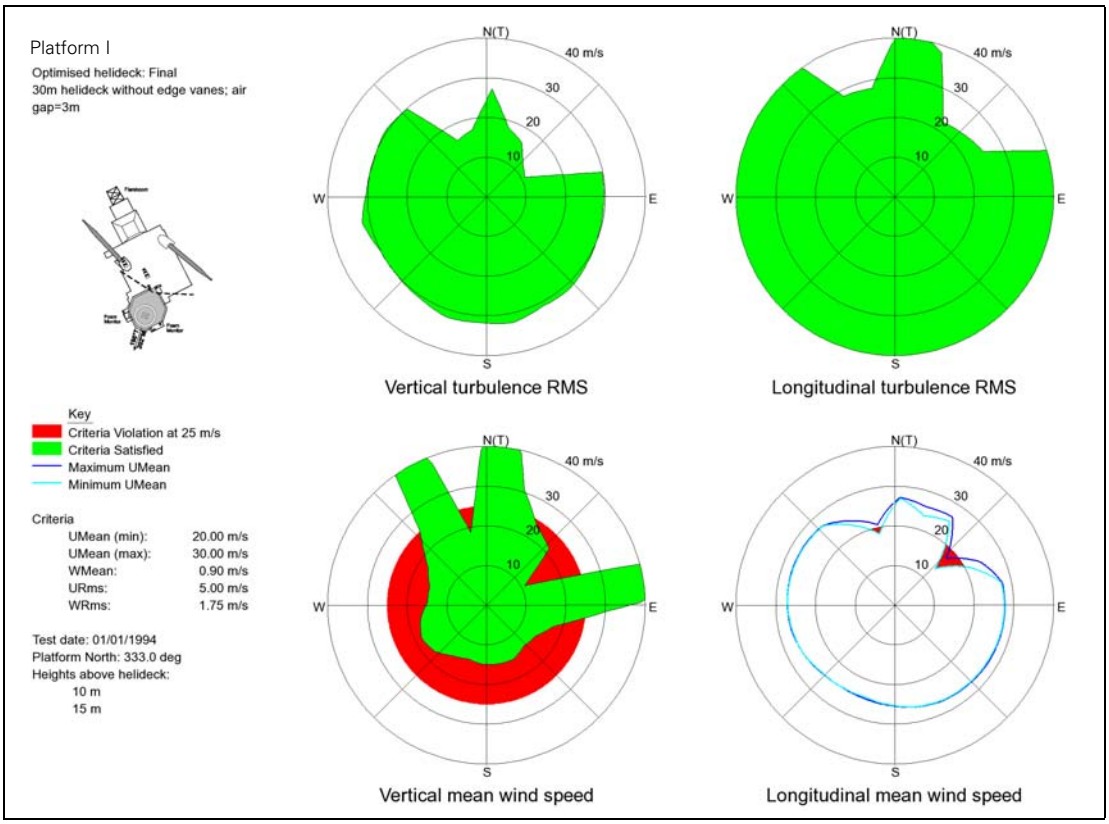

Figure 33 Platform I wind tunnel data

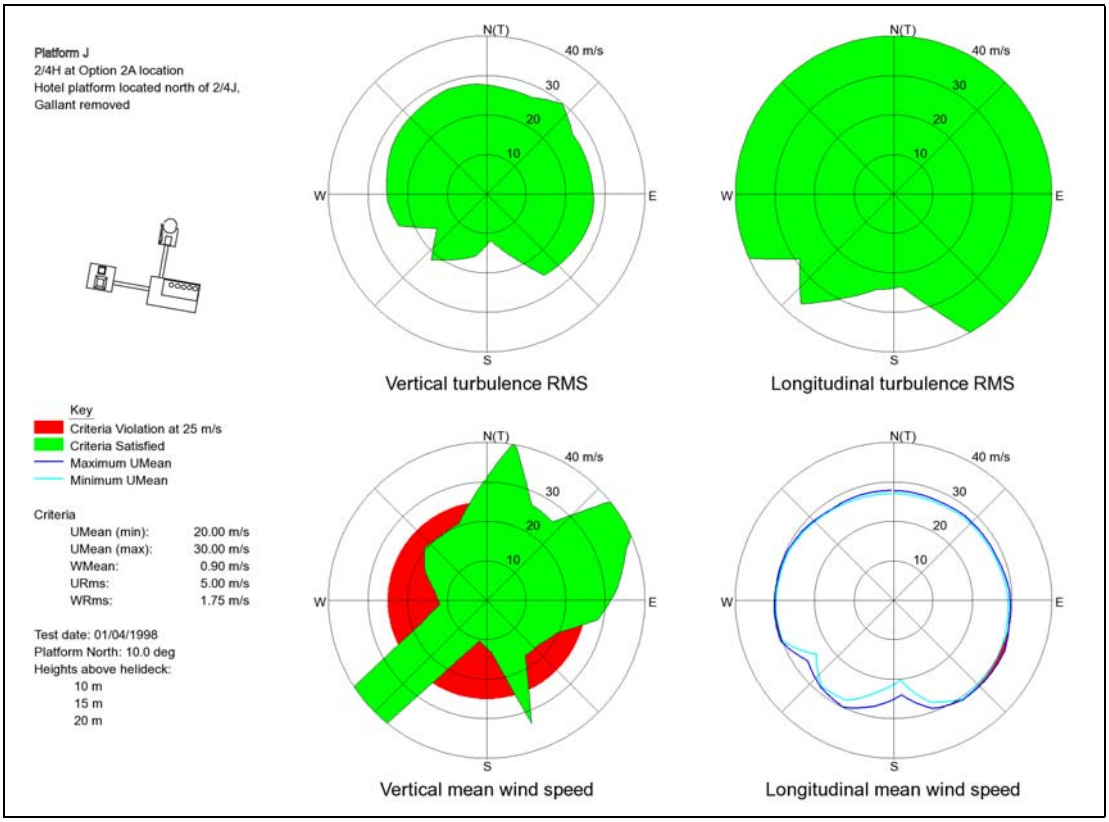

Figure 34 Platform J wind tunnel data

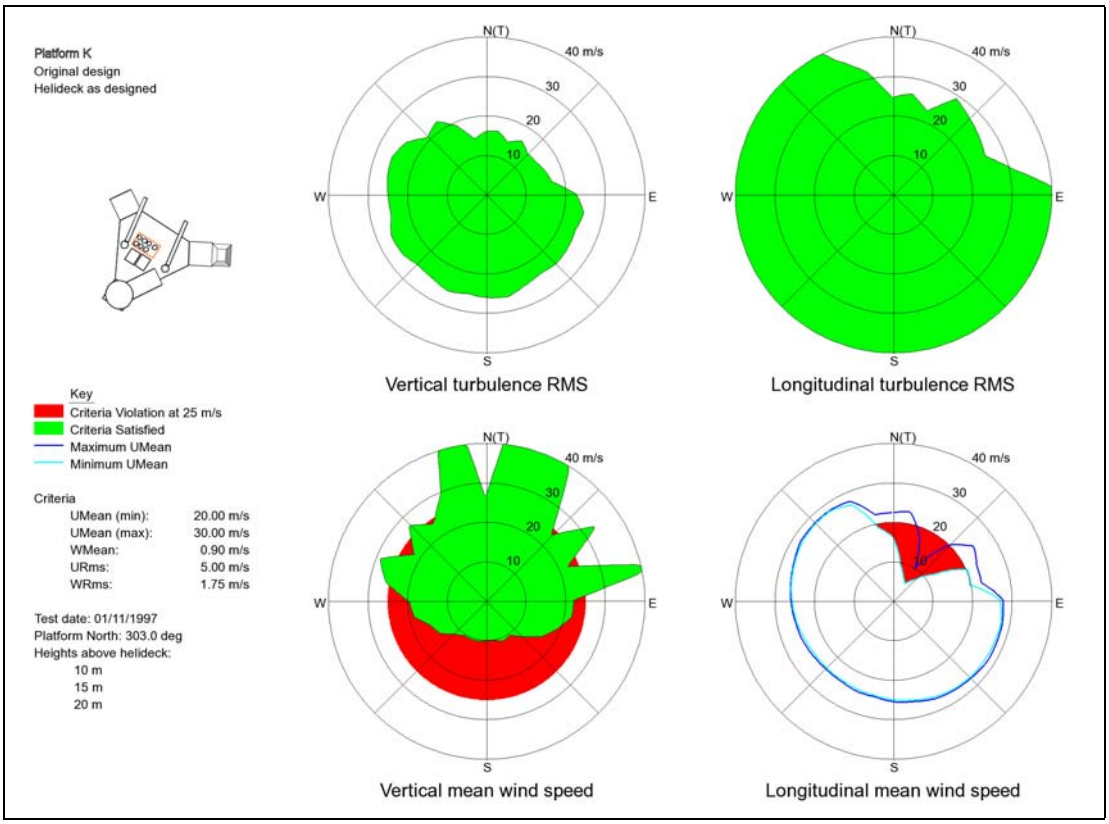

Figure 35 Platform K wind tunnel data

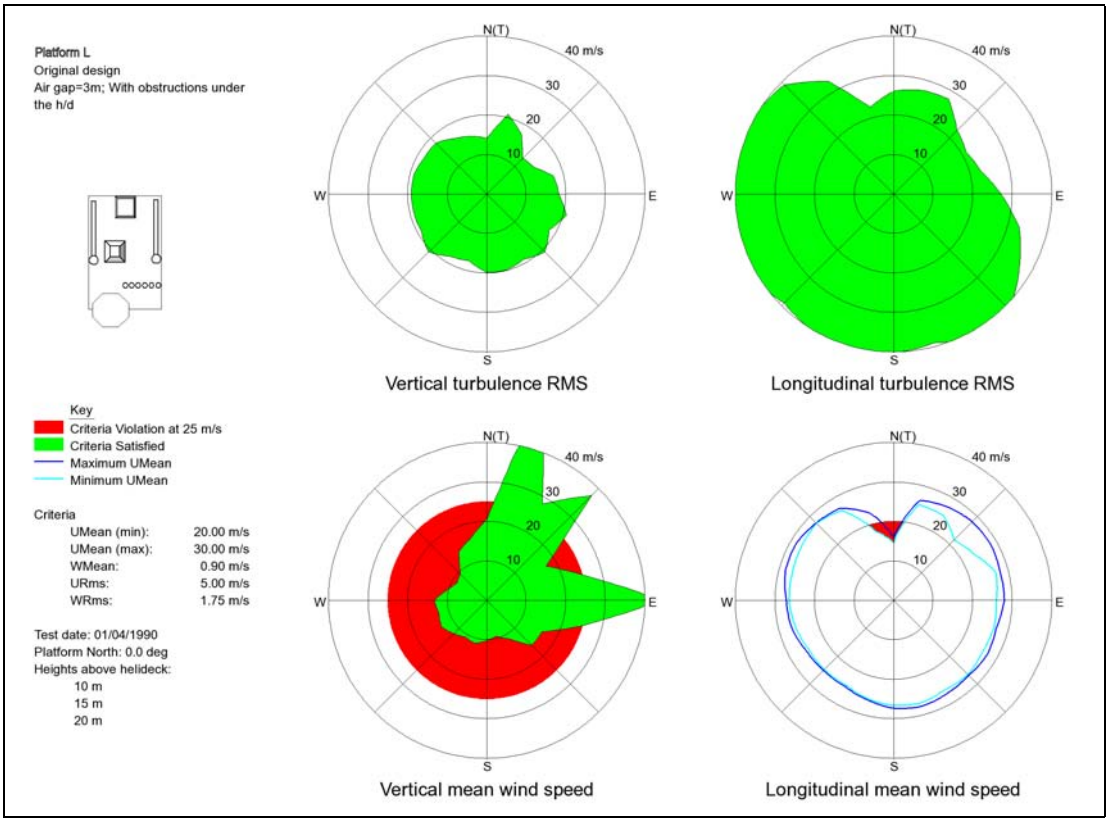

Figure 36 Platform L wind tunnel data

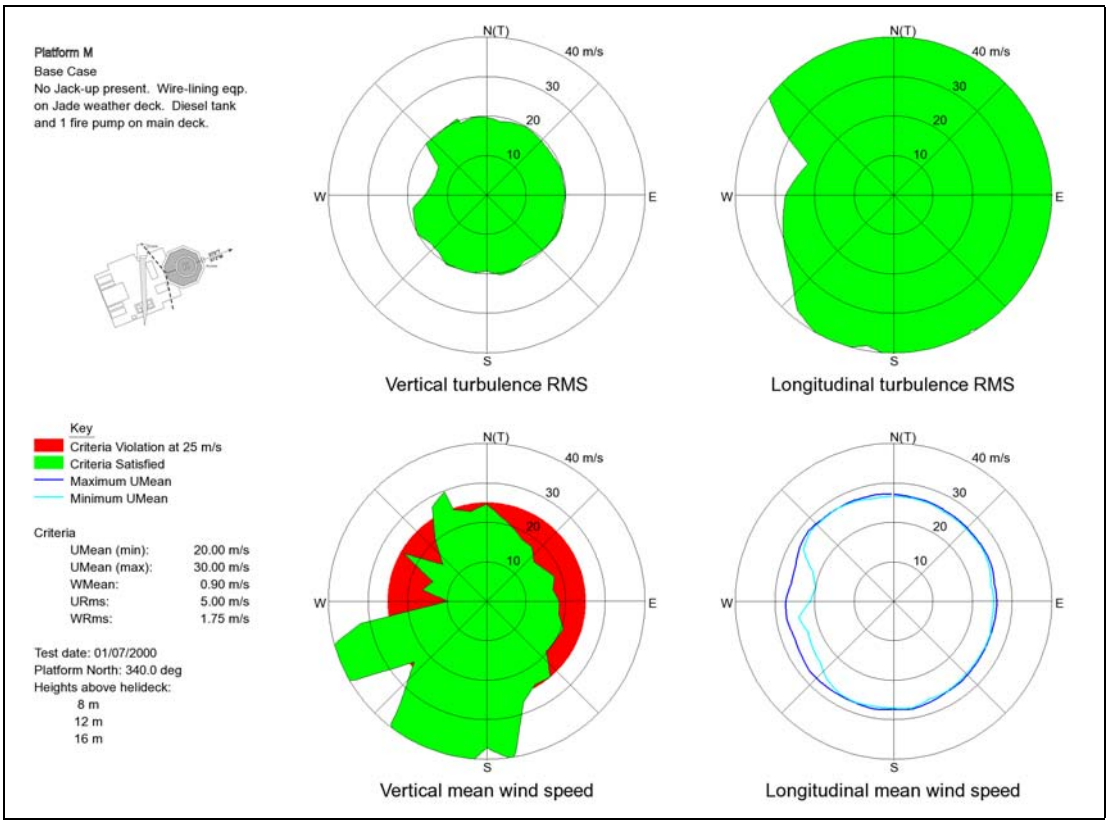

Figure 37 Platform M wind tunnel data

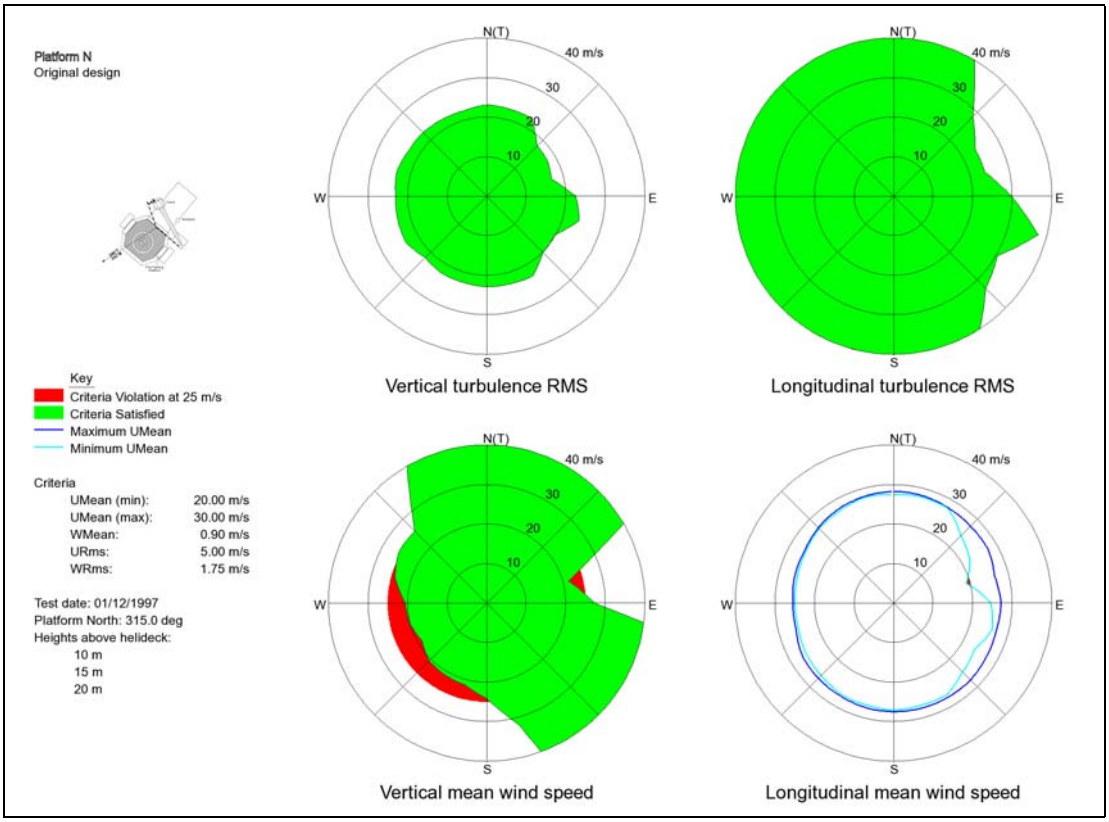

Figure 38 Platform N wind tunnel data

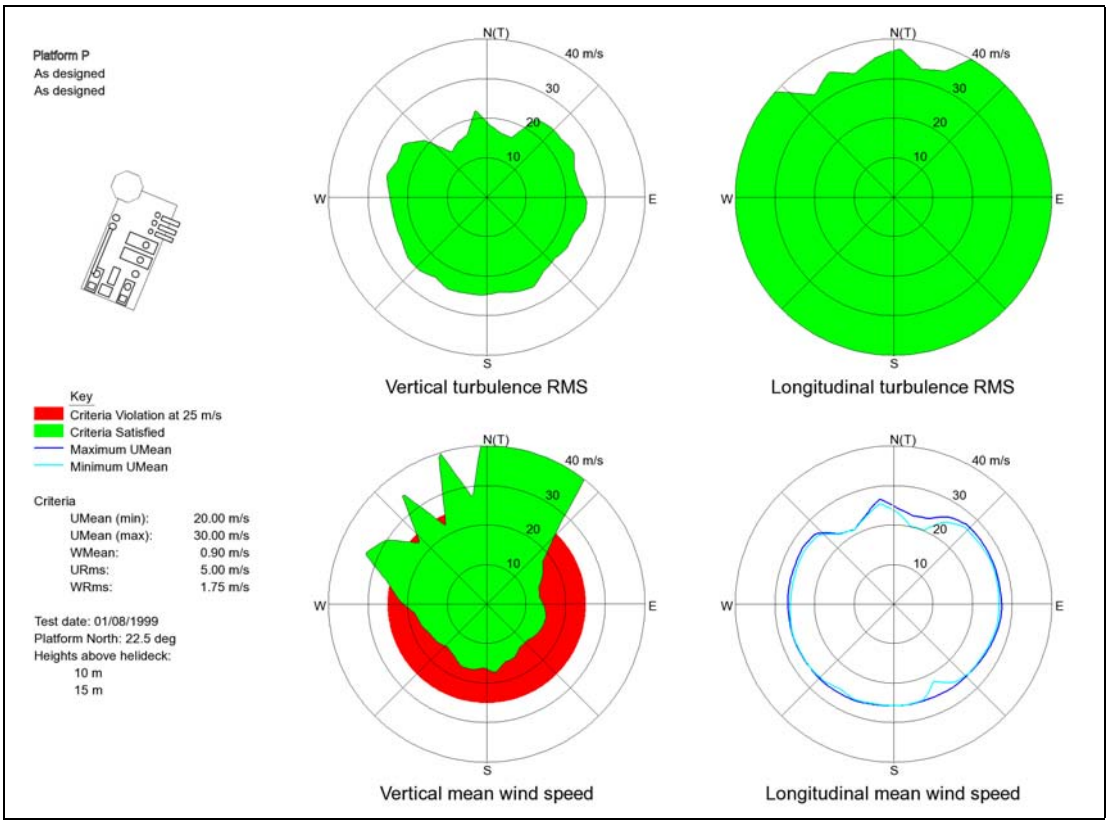

Figure 39 Platform P wind tunnel data

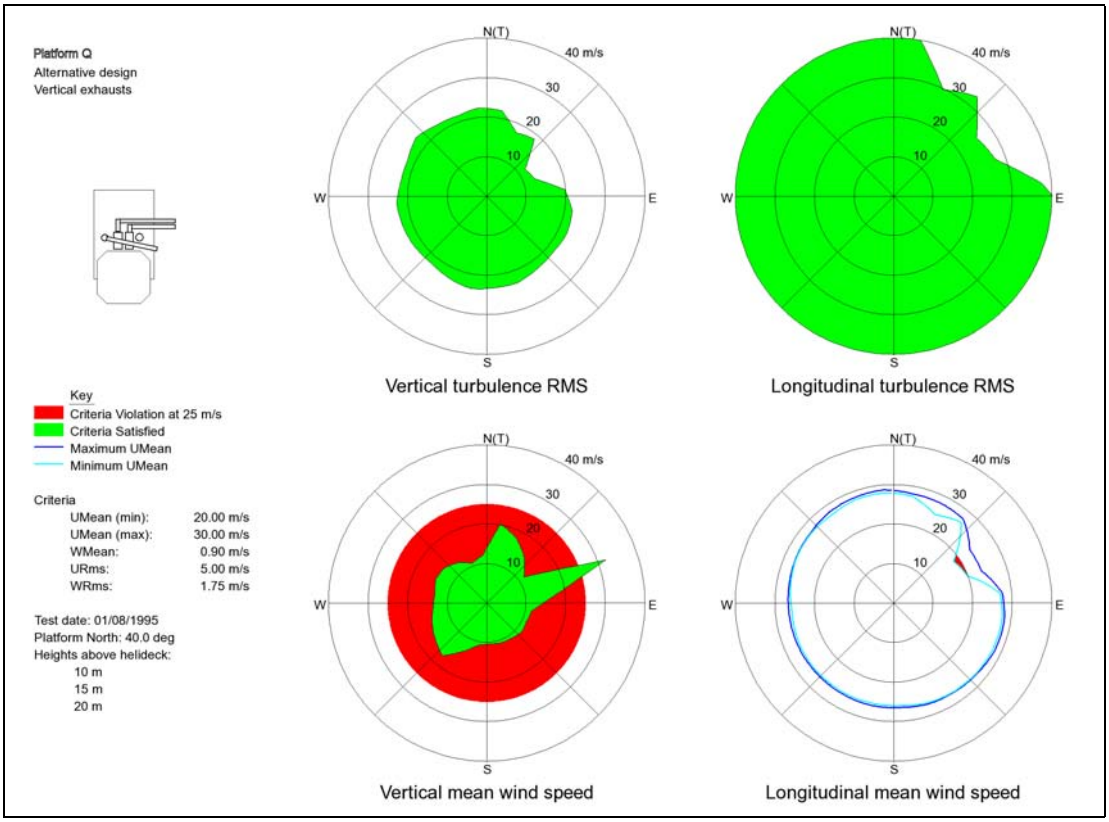

Figure 40 Platform Q wind tunnel data

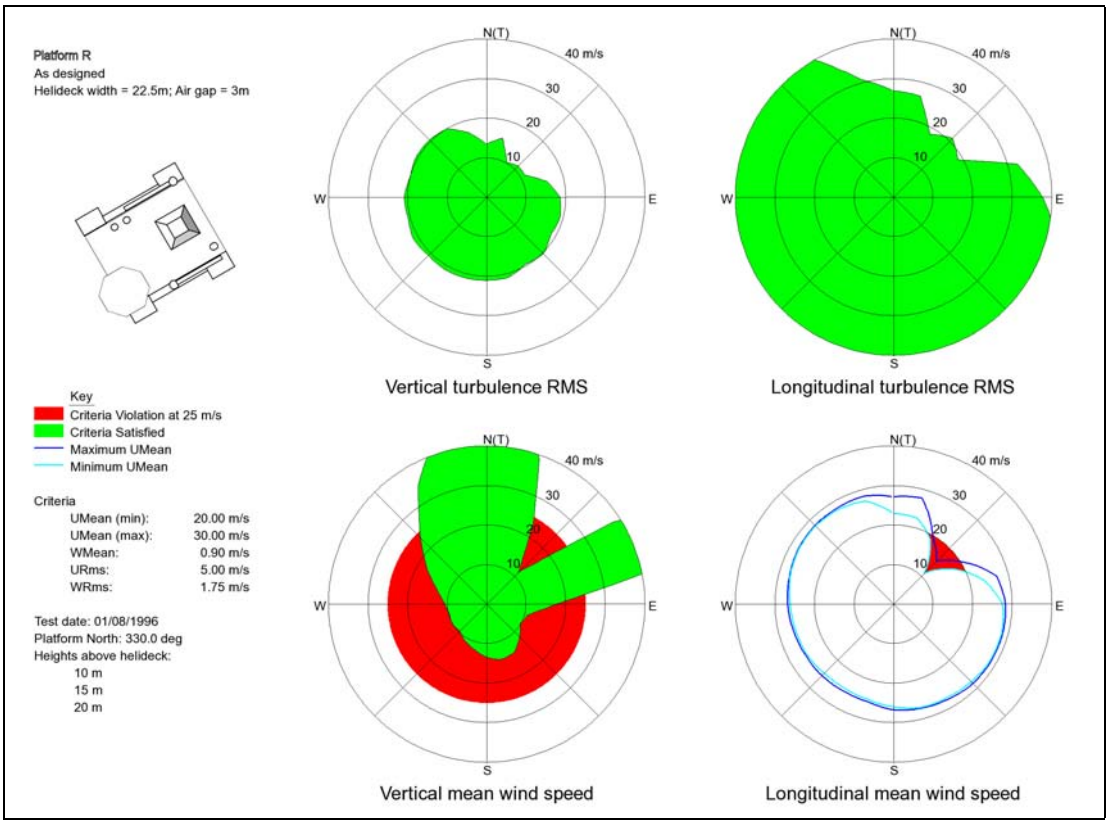

Figure 41 Platform R wind tunnel data

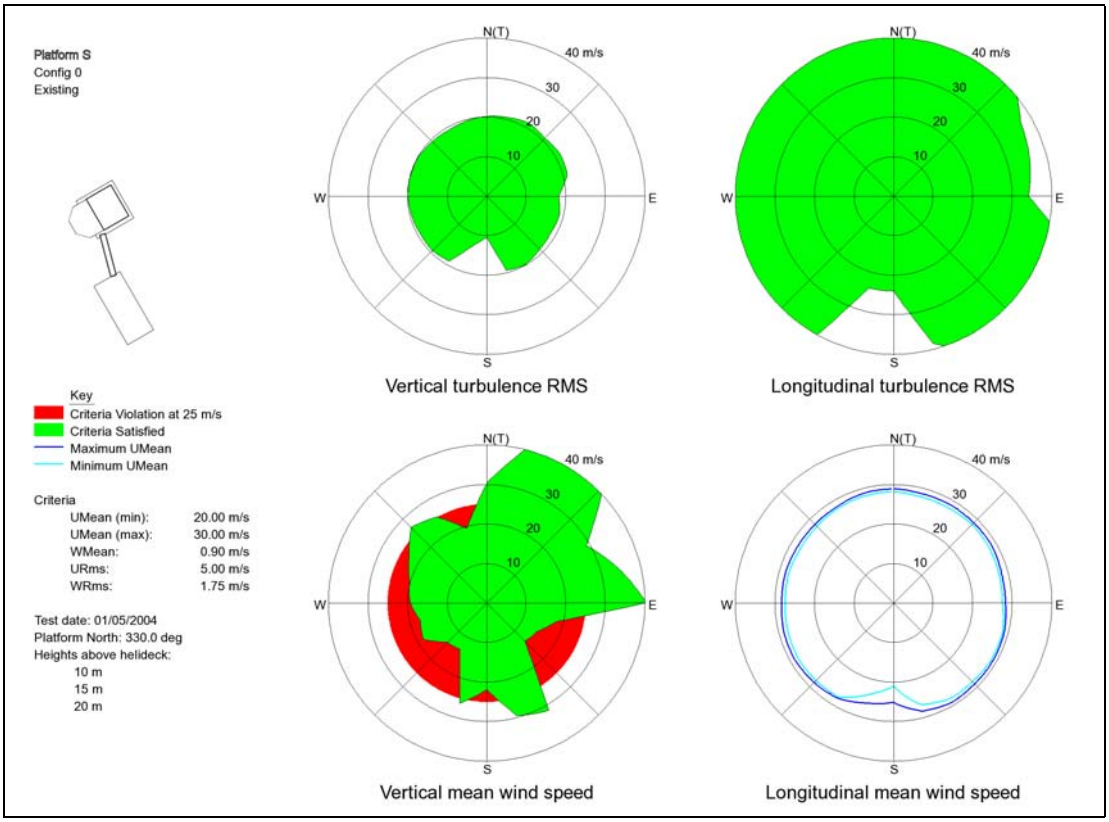

Figure 42 Platform S wind tunnel data

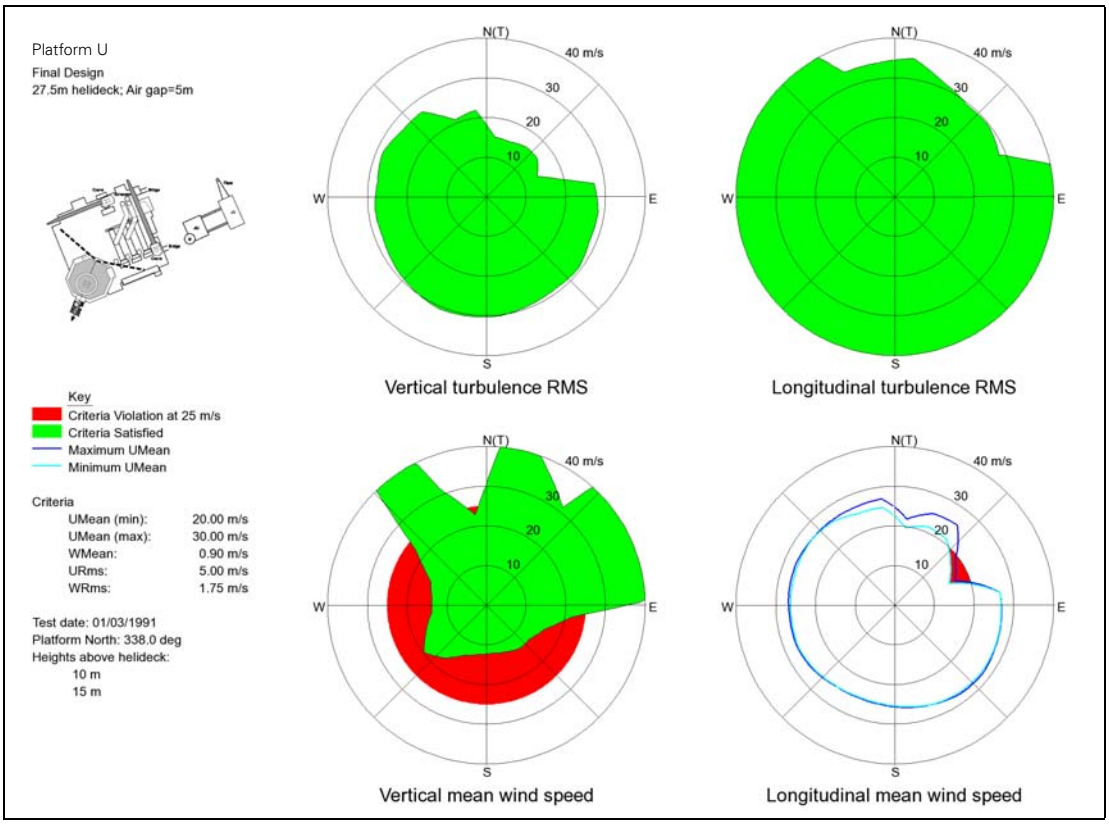

Figure 43 Platform U wind tunnel data

4.2 Results

The charts show that exceedance of the vertical mean wind speed criterion occurs mostly for unobstructed wind directions. This is highlighted in the summary of mean flow values given in Table 4.

Table 4 presents the maximum vertical mean wind speed obtained for the unobstructed and obstructed wind directions[4], together with a brief description of the nature of the obstruction. The table is ranked in order of increasing *obstructed* vertical mean wind speed. Along with the platform name, the table also gives an indication of platform size, and whether it is a single platform or part of a multiple-platform complex. Finally, a Yes/Marginal/No indication is presented relating to whether the longitudinal mean wind speed criterion is violated.

It can be seen that for all but two platforms, the highest vertical mean wind speed occurs consistently for unobstructed wind directions. The exceptions were the small platforms M and J. Only five of the fifteen large/medium single platforms; L, R, A, I and Q, violated the 0.9 m/s criterion in wind directions from the obstructed sector. All but one violates the horizontal flow criterion. This is because large platforms generate large wake flows in the vicinity of the helideck that cause significant reductions in overall mean wind speeds.

4. To avoid placing too much weight on single point data and take into account the effect due to spatial variation, the values in Table 1 are based on averages across three adjacent wind tunnel test wind directions.

Table 4 Summary of the vertical mean wind speed

Platform	Platform size[1]	Single or Multiple platform layout	Wmean (max) for unobstructed wind directions	Wmean (max) for obstructed wind directions	Nature of Obstruction	Violation of longitudinal mean wind speed criterion
U	Large	Single	1.81	0.18	Exhaust stacks	Yes
H	Medium	Single	1.45	0.28	Derrick	Yes
C	Large	Single	2.16	0.45	Derrick	Yes
G	Large	Single	2.43	0.54	Derrick and flare tower	Yes
B	Large	Single	1.17	0.57	Derrick	No
K	Large	Single	2.22	0.63	Exhaust stacks	Yes
F	Medium	Single[2]	1.75	0.75	Exhaust stacks	Yes
N	Large	Single	1.13	0.81	Flare tower	Marginal
D	Large	Single	1.79	0.82	Derrick	Yes
P	Large	Single	1.62	0.88	Exhaust stacks	No
S	Small	Multiple	1.5	0.88	Adjacent platform	No
L	Large	Single	2.4	0.97	Derrick	Yes
R	Large	Single	2.29	1.06	Derrick	Yes
E	Small	Multiple	1.98	1.27	Blockage underneath the helideck	No
A	Large	Single	2.46	1.35	Derricks	Yes
I (Final)	Large	Single	1.55	1.37	Exhaust stacks	Yes
Q (Vertical exhausts)	Medium	Single	2.13	1.58	Flare tower	Yes
M (Base Case)	Small	Single	1.36	1.68	Crane plus blockage underneath the helideck	No
J (2A)	Small	Multiple	0.75	1.75	Adjacent platform	Marginal

1. Large = >80 m (nominal); Medium = 50 to 80 m (nominal); Small = <50 m (nominal)
2. Platform F is actually bridge linked to an adjacent platform. Unlike other multiple installations, however, it is of comparable size to its neighbours and is therefore relatively insensitive to them. For this report therefore, it is classed as single.

It is not clear why the two small platforms M and J are inconsistent with the basic trend. However, in general, smaller platforms will generate less severe wake flows or allow some wake recovery to take place, resulting in generally higher wind speeds at the helideck. This is reflected in the longitudinal mean wind speed criterion, which is complied with for the small platforms. Consequently the high vertical mean flow

components are accompanied by high horizontal flows, which will tend to greatly enhance helicopter lift performance. The precise nature of the flow in individual cases is strongly dependent on the nature and proximity of adjacent structures, which are invariably bridge-linked and close by.

5 Phase 3 – Correlate Wind Tunnel Data with HOMP Archive

5.1 Introduction

In Phase-3 the objective was to correlate the wind tunnel data archive with the helicopter operational data in the HOMP archive to look for evidence of an operational effect of vertical wind flow. In order to accomplish this, pilot workload and rotor torque measurements in the HOMP archive were plotted against the mean vertical component of the flow over the helideck, measured in the wind tunnel at 25 m/s wind speed, by wind direction. It was only possible to do this for platforms that appeared both in the BMT wind tunnel data archive and in the HOMP archive. There were five platforms that met this requirement:

- Platform C
- Platform D
- Platform G
- Platform I
- Platform U

NB: Platforms de-identified – see Section 4.1.

This exercise was limited to 'open' or unobstructed wind directions, so that the results were not contaminated by turbulence caused by upstream structure.

5.2 Results

The plots that follow show the HOMP parameters of pilot workload, maximum 'raw' torque, and maximum increase in 'raw' torque, each plotted against the mean vertical component of wind velocity over the helideck (at a wind speed of 25 m/s and for the same wind direction as the landing), as derived from the corresponding wind tunnel tests. A vertical line on the plots shows the 0.9 m/s criterion. Points to the left of this line will be for wind directions where the criterion is satisfied, whilst those to the right show wind directions for which the criterion is violated. The individual points are colour coded for the actual wind speed in which the landing took place.

Note that the x-axis value for each point plotted is the mean vertical wind component measured during the wind tunnel tests at a wind speed of 25 m/s for the wind direction for the landing, *not* the actual vertical component experienced during the landing. All landings for a particular wind direction in these plots will therefore plot at the same vertical wind component value.

If vertical wind flow is having any operational effect then it would be expected that a trend in one or more of the three operational parameters plotted with vertical flow (at 25 m/s) would be evident in at least one landing wind speed series of points (i.e. points of the same colour).

Plots of workload are given in Figure 44 to Figure 48 for each of the five platforms. Plots of maximum torque and maximum increase in torque are presented in pairs for each platform in Figure 49 to Figure 58.

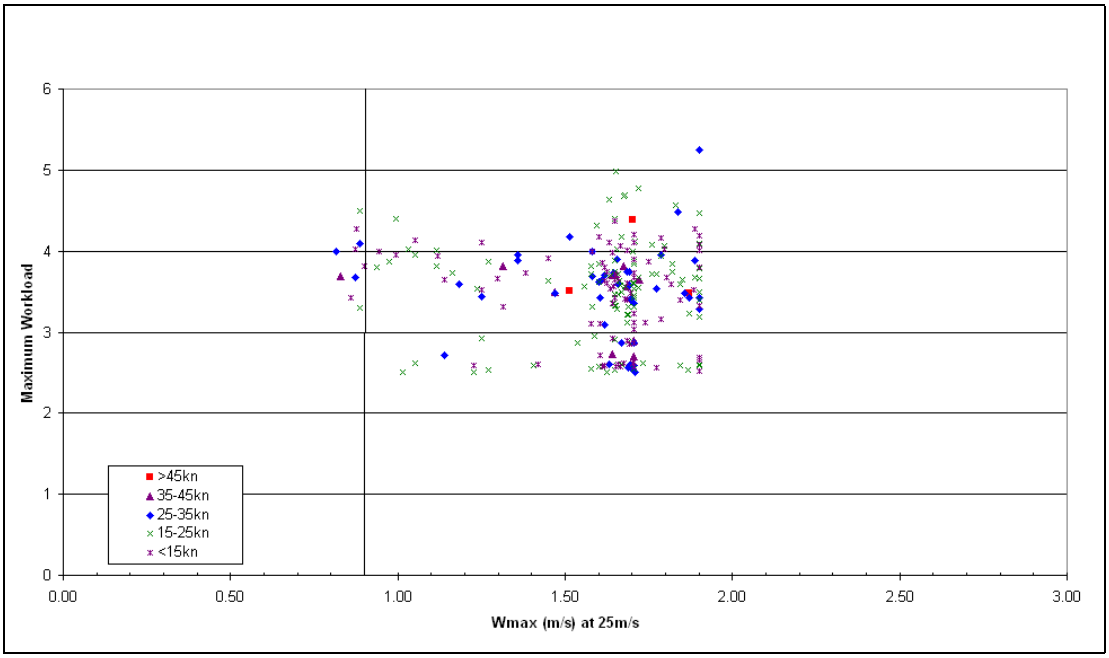

Figure 44 Platform D maximum workload vs mean vertical wind speed at 25 m/s

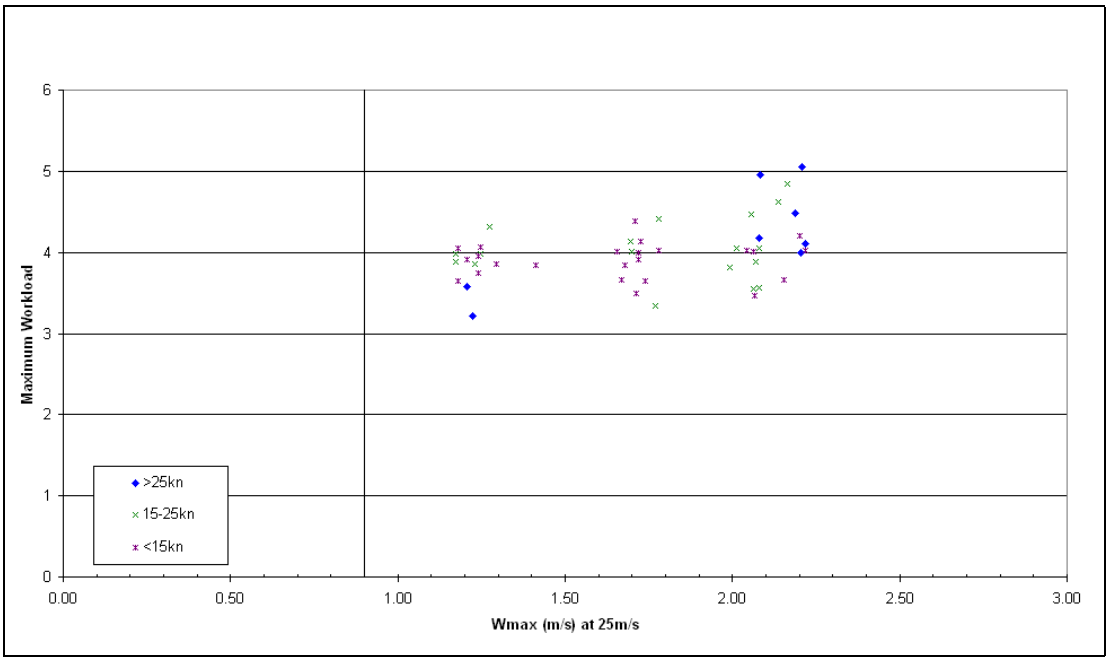

Figure 45 Platform C maximum workload vs mean vertical wind speed at 25 m/s

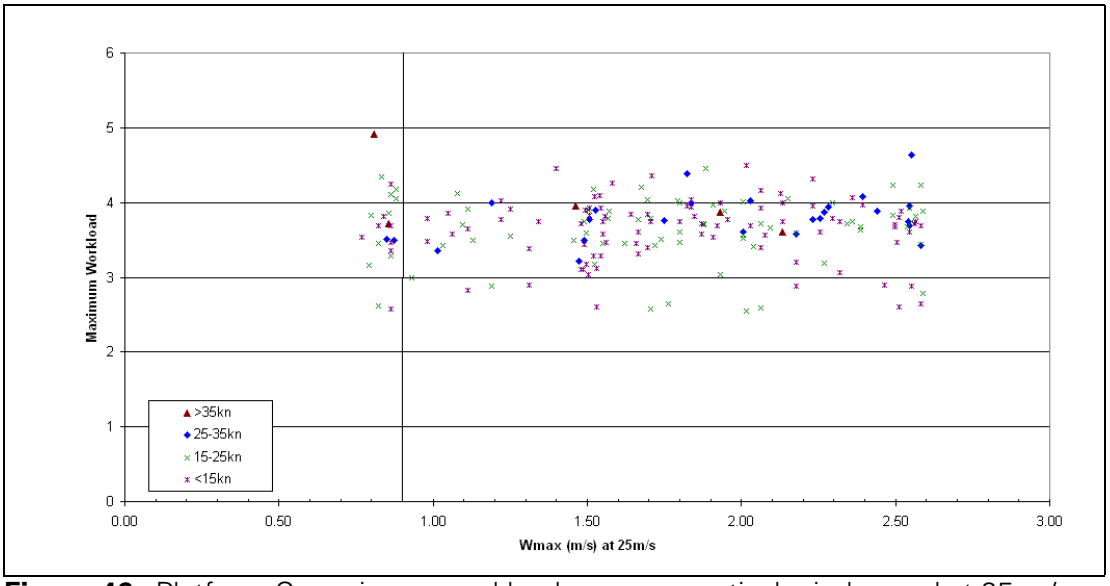

Figure 46 Platform G maximum workload vs mean vertical wind speed at 25 m/s

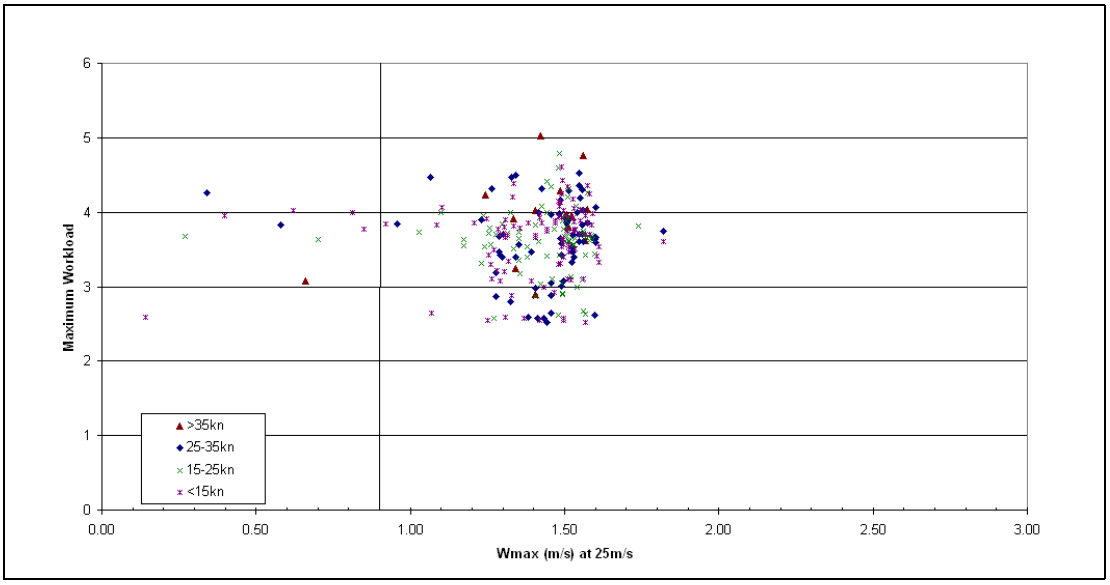

Figure 47 Platform I maximum workload vs mean vertical wind speed at 25 m/s

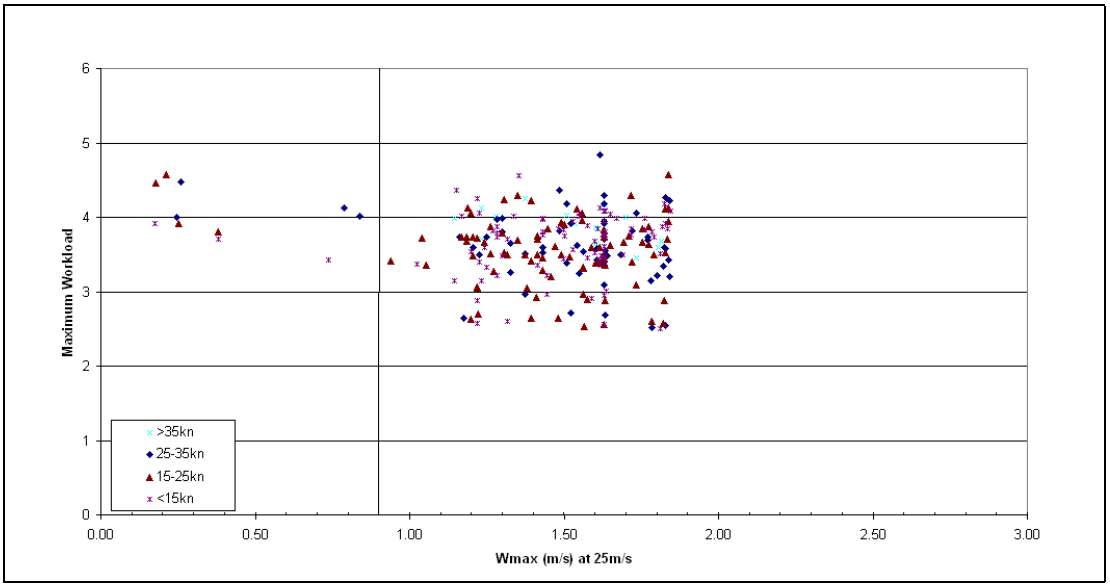

Figure 48 Platform U maximum workload vs mean vertical wind speed at 25 m/s

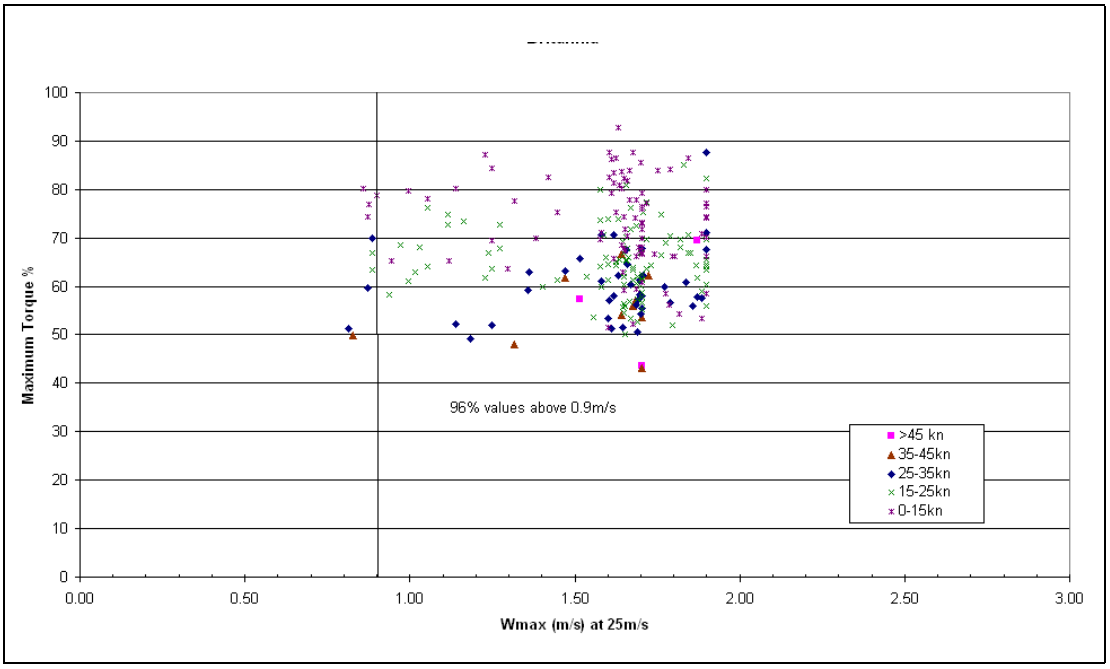

Figure 49 Platform D maximum torque vs mean vertical wind speed at 25 m/s

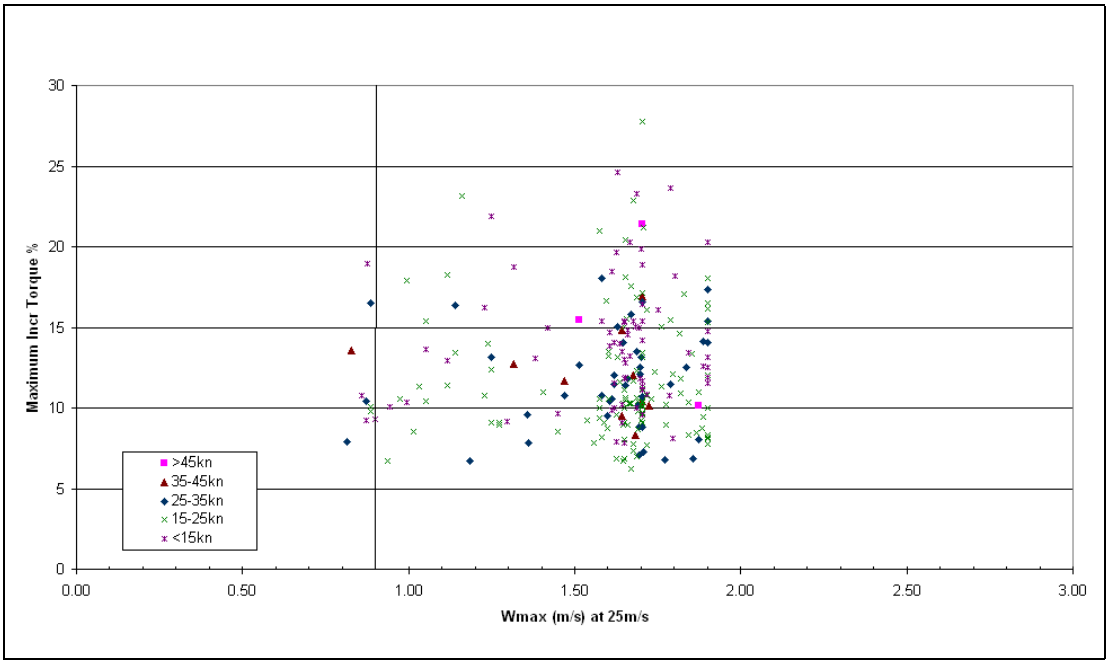

Figure 50 Platform D maximum torque increase vs mean vertical wind speed at 25 m/s

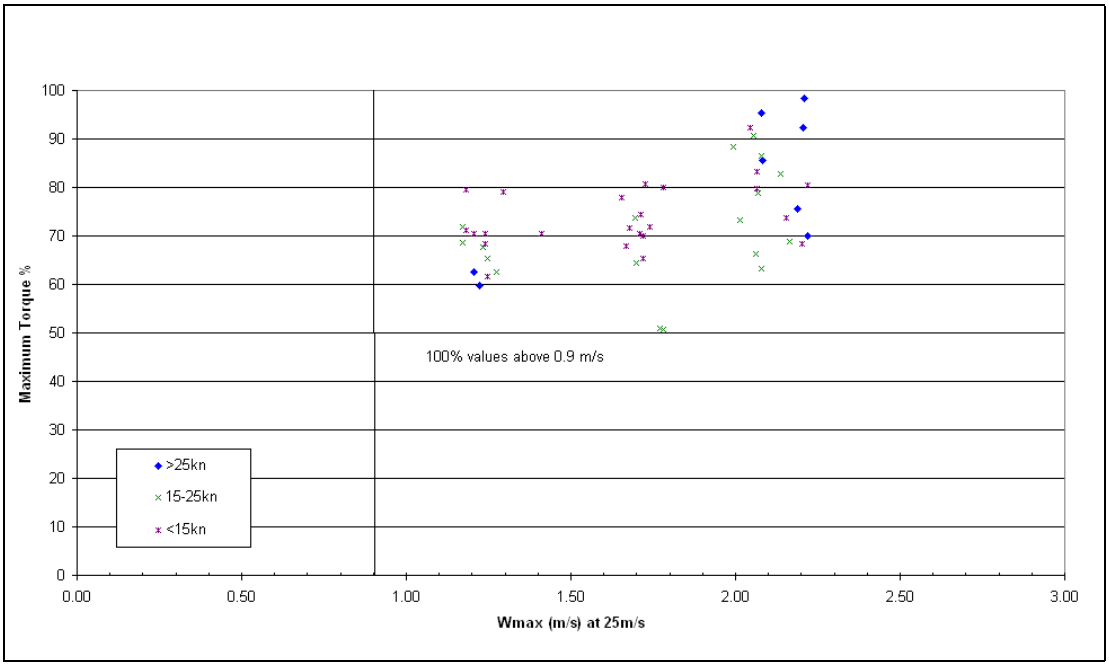

Figure 51 Platform C maximum torque vs mean vertical wind speed at 25 m/s

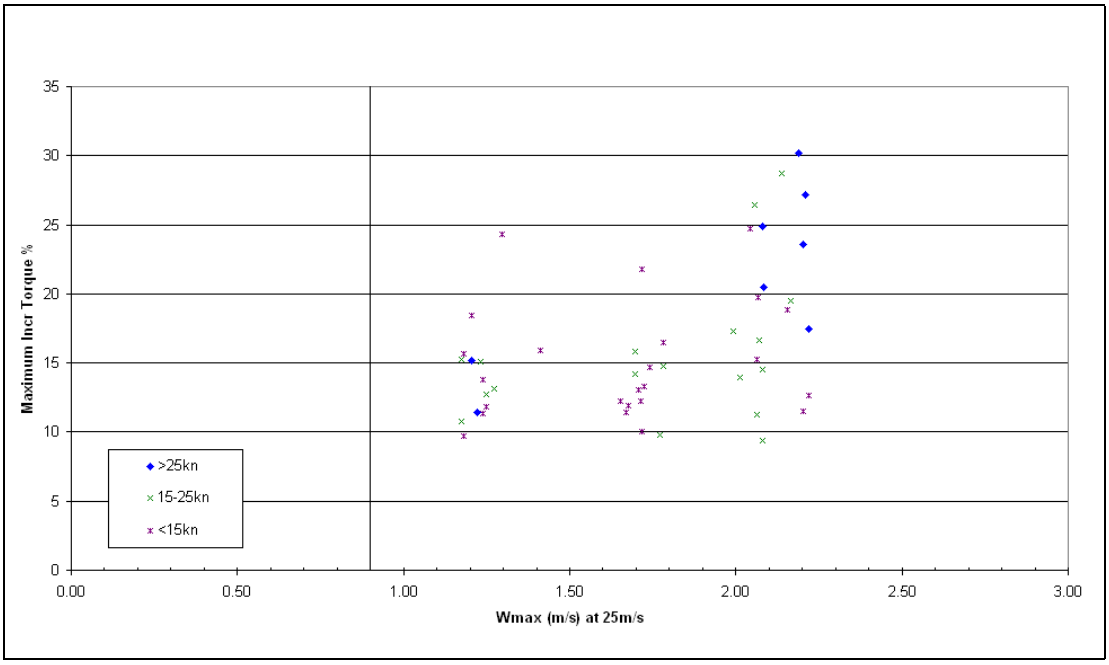

Figure 52 Platform C maximum torque increase vs mean vertical wind speed at 25 m/s

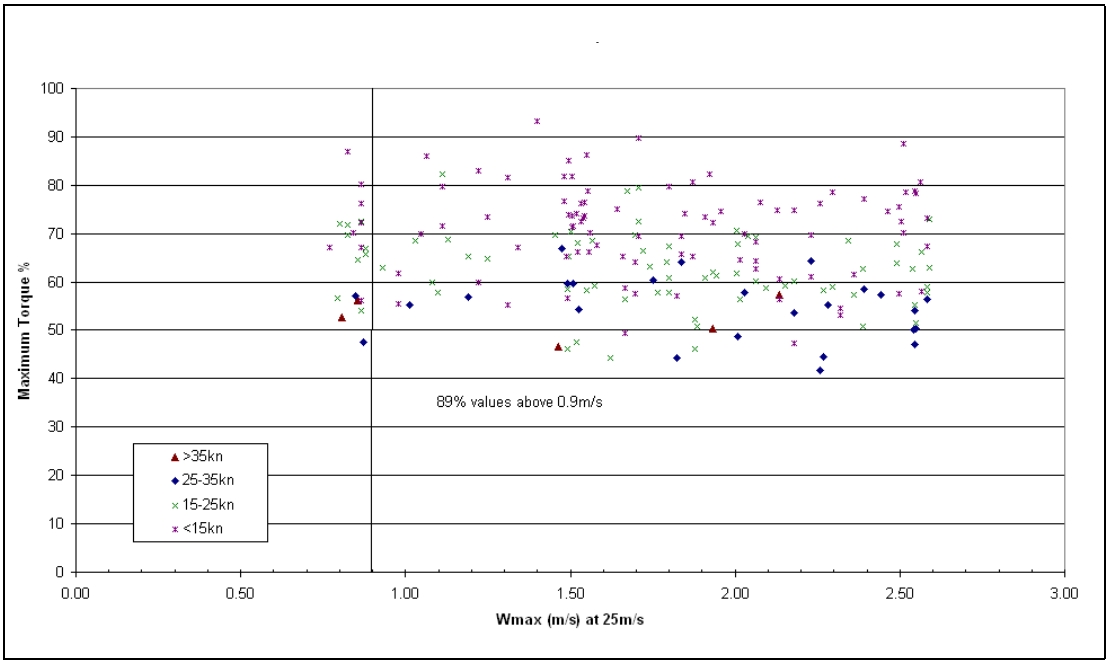

Figure 53 Platform G maximum torque vs mean vertical wind speed at 25 m/s

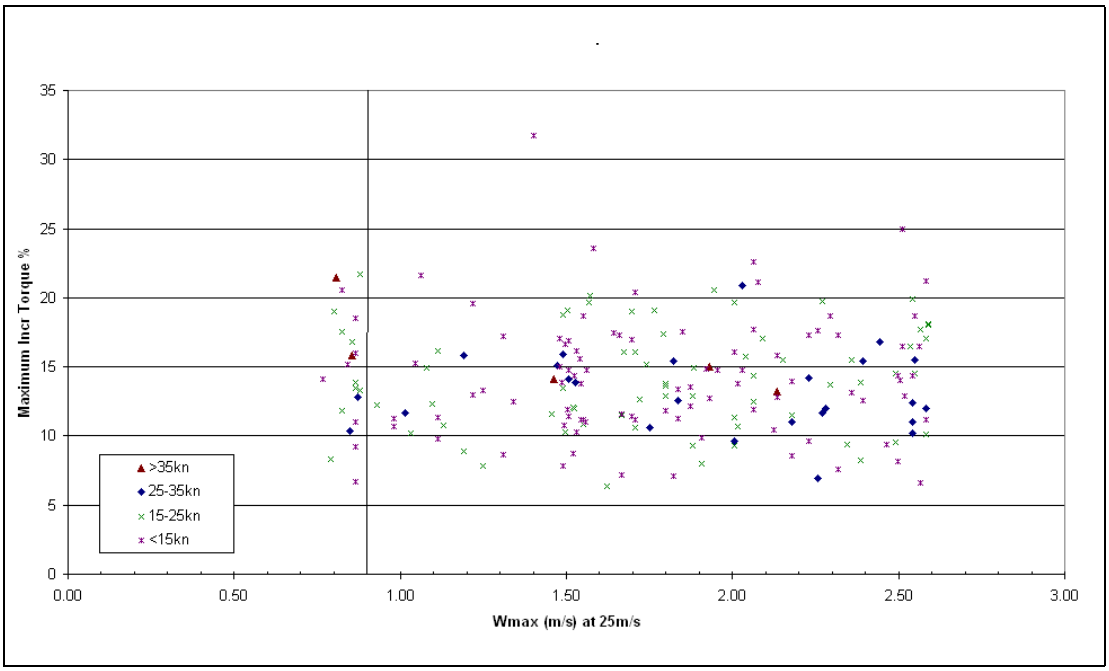

Figure 54 Platform G maximum torque increase vs mean vertical wind speed at 25 m/s

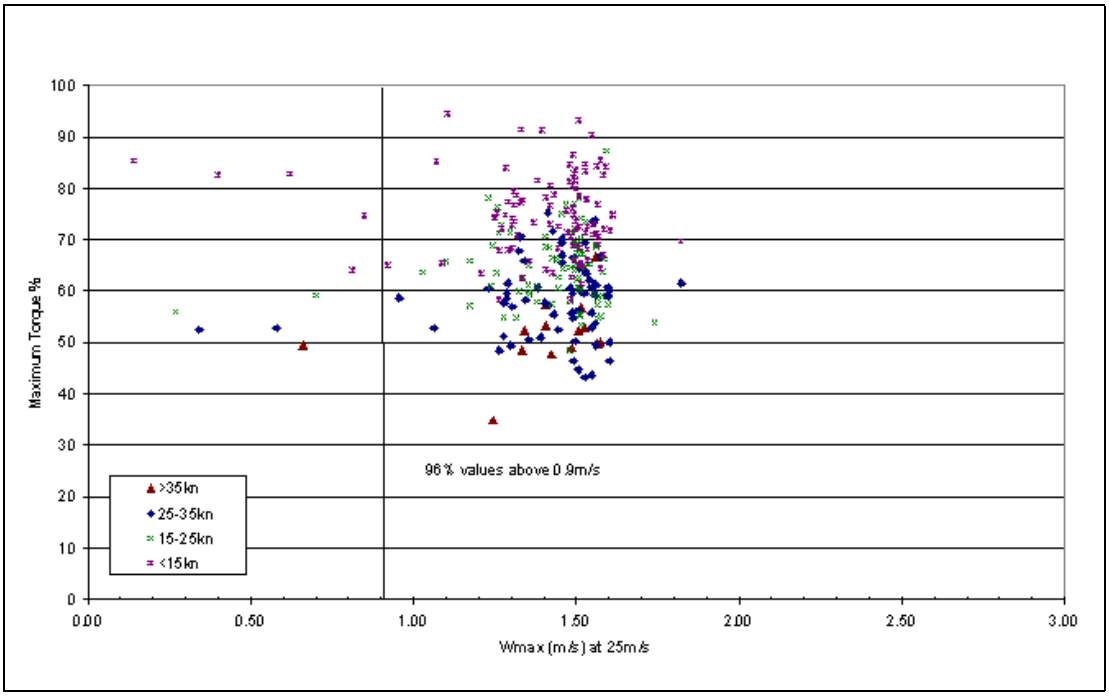

Figure 55 Platform I maximum torque vs mean vertical wind speed at 25 m/s

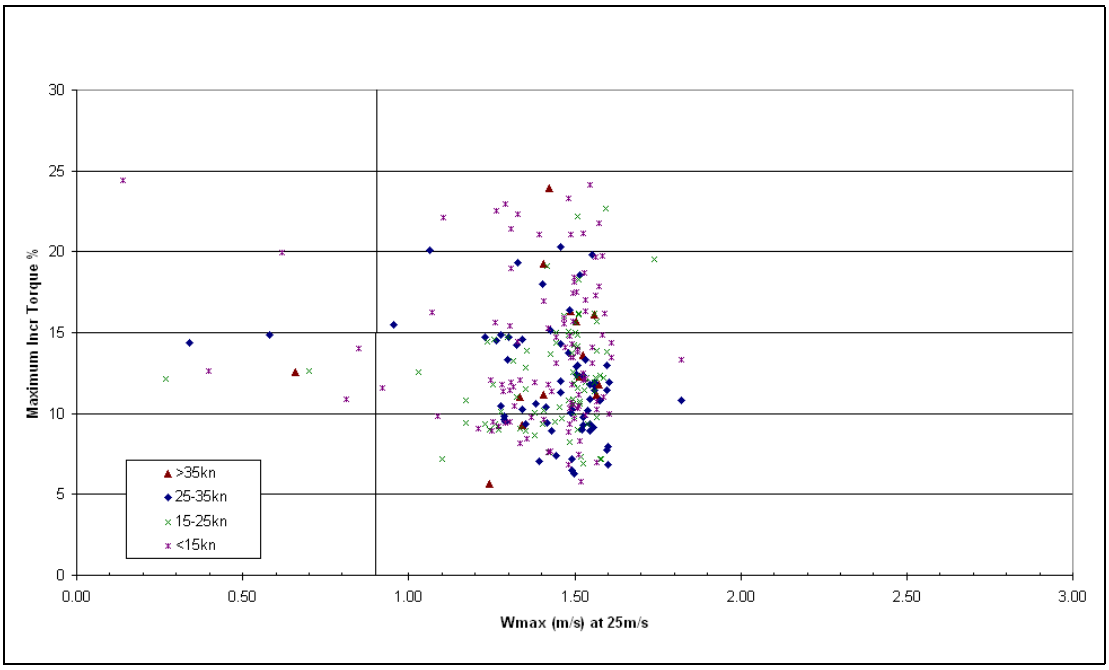

Figure 56 Platform I maximum torque increase vs mean vertical wind speed at 25 m/s

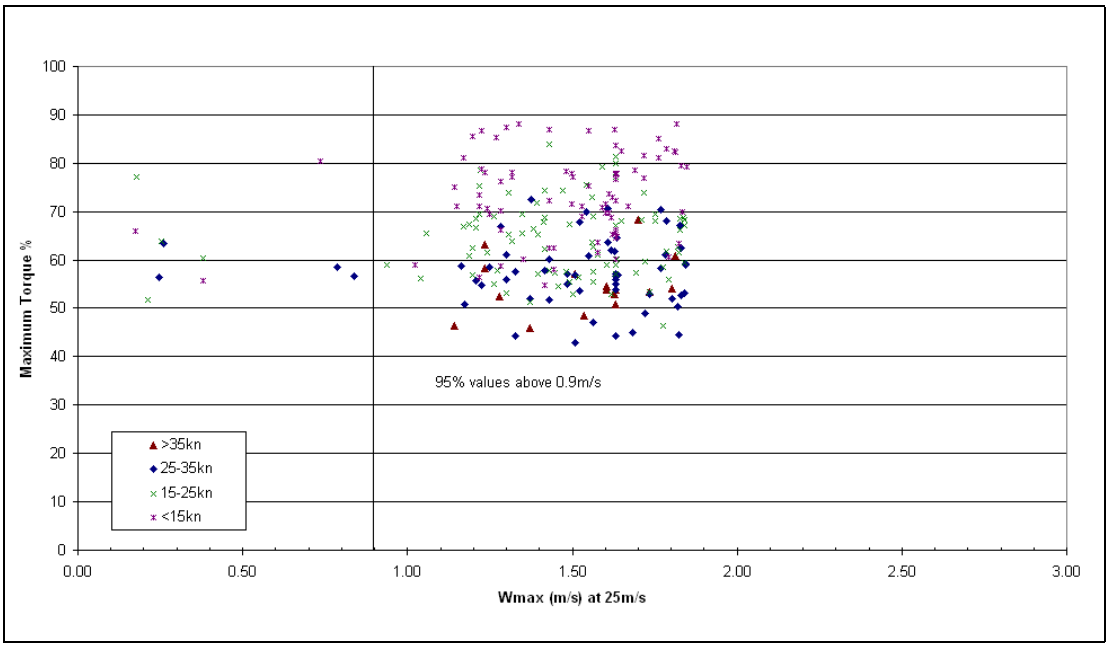

Figure 57 Platform U maximum torque vs mean vertical wind speed at 25 m/s

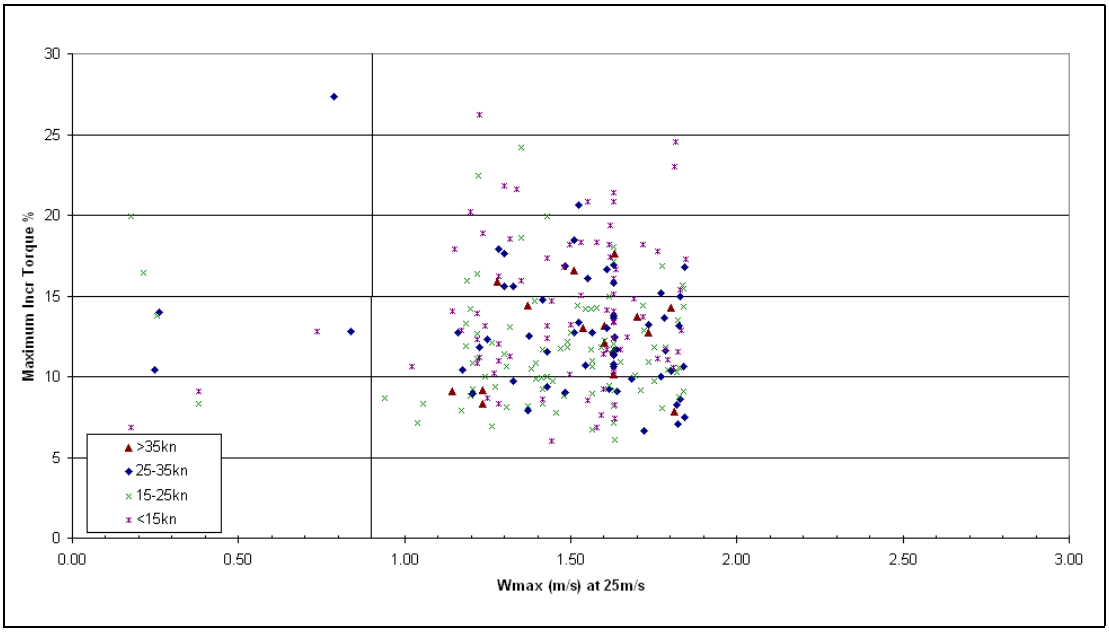

Figure 58 Platform U maximum torque increase vs mean vertical wind speed at 25 m/s

For the 'open' wind directions covered by these plots, just over 96% of landings occur in wind directions where the 0.9 m/s criterion was violated in the wind tunnel tests. Nevertheless, the plots show that there is very little correlation between the vertical component of mean velocity at 25 m/s wind speed and either pilot workload, or the torque parameters (maximum torque and maximum increase in torque over 2s).

There is some slight suggestion for Platform D (Figure 44) and Platform C (Figure 45) that pilot workload increases with the vertical mean velocity, but the effect is very small, and is also probably unreliable for Platform C due to the relatively small number of landings recorded in the HOMP archive. Platforms G, I and U show no such trend.

The lack of any correlation with pilot workload suggests that the existence of high mean vertical velocities in open wind sectors does not cause the pilot any difficulties with control. If spatial variations in the vertical component were causing a control problem, then one would expect such variations to occur during landings in wind directions causing the greatest vertical component over the helideck and that, in turn, this would result in high pilot control activity registering a higher workload. However, this is certainly not evident in the data.

As with workload, there is a slight trend for the highest torque values to occur in wind directions with higher vertical mean velocities on Platform D (Figure 49 and Figure 50) and Platform C (Figure 51 and Figure 52). Again this trend is not seen on the other three platforms. It can be seen that most of the plots exhibit the expected trend of higher torque values in lower wind speeds.

The lack of any correlation with rotor maximum torque or maximum torque increase suggests that the existence of high mean vertical velocities does not cause any helicopter performance problems. Entering a region of high downdraft would be expected to result in a need for increased collective and thus increased torque, but this is not evident in the data. It is presumed that in high wind speeds the effect is not seen because the presence of high horizontal wind components result in a high margin of lift, and small adjustments in collective are sufficient to compensate for any downdraft. In low wind speeds the actual vertical component of velocity and the effect on the helicopter sink or climb rate is small.

Overall it is concluded that there is no evidence of any correlation between the extent of the violation of the 0.9 m/s criterion and either pilot workload or torque.

6 Phase 4 – Helideck Air-Gap Wind Tunnel Tests

6.1 Introduction

The 0.9 m/s criterion has been the main driver for the raising of helidecks, and the maintenance of a good clearance between the helideck and the accommodation block. While it is usually not possible to comply fully with the criterion, wind tunnel tests usually demonstrate a compliance benefit if the helideck height is raised and the clearance increased, and it has therefore often been a key factor in the eventual selection of helideck height in the platform design process.

With the possibility that the 0.9 m/s criterion might be removed from the guidance, there was concern that the pressure on designers to maintain a good helideck air gap might be lost. It was not known whether the application of the new turbulence criterion [5, 8] might take over the role of driving designers towards a similar air gap. Wind tunnel test data in the BMT archive generally did not cover an adequate range of helideck heights to permit conclusions to be drawn on this point.

Consequently, a programme of wind tunnel tests was performed to examine the impact of helideck height on ‘open’ sector wind flow properties over a wider range of heights. A single representative model of a large North Sea platform (Brae-A) was used, and the results interpreted in terms of the helideck height that would have been selected for design if individual flow criteria were the key determinant.

The objectives of the wind tunnel test programme were therefore as follows:

1 To carry out a series of wind tunnel tests on a typical large offshore platform to measure the wind flow over the helideck for a wide range of helideck heights.

2 To compare the results with CAA vertical turbulence and mean speed criteria and with two additional guidelines used by BMT in the assessment of helidecks (see Table 2).

3 To determine how the application of the turbulence criterion might influence the selection of helideck heights in platform design in the absence of a 0.9 m/s vertical mean speed criterion.

6.2 Scope of Work

The scope of work was as follows:

- Refurbish an existing 1:100 scale model of the Brae-A platform (Figure 59) and modify it to enable the helideck height above the accommodation to be varied.
- Measure the longitudinal and vertical mean wind speed and turbulence intensity at 5 m, 10 m, 15 m and 20 m above the helicopter landing spot for the full range of wind direction in 15° steps.
- Carry out the tests for 7 helideck heights (air gap clearances between the helideck and the accommodation block of 0 m – 6 m in 1 m steps).

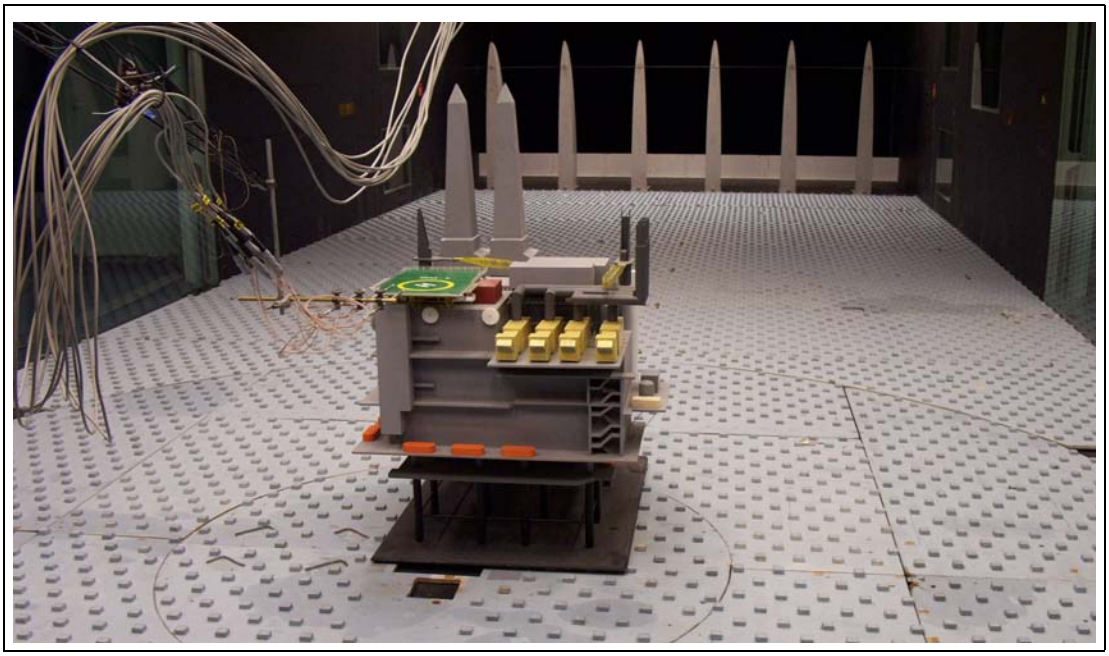

Figure 59 1:100 scale Brae-A wind tunnel model in the BMT Atmospheric Boundary Layer Wind Tunnel

6.3 Presentation of Results

Longitudinal and vertical mean wind speed and turbulence standard deviations were measured at 5 m, 10 m, 15 m, and 20 m above the landing spot of the Brae-A helideck for wind directions 0° to 360° in steps of 15° (where wind direction is relative to platform north defined in Figure 60). The tests were carried out for 7 helideck air gaps from 0 m to 6 m (the air gap on the as-built platform was 3 m).

When a helicopter is in flight over a helideck there is a tendency for the rotor to draw down air from heights well above the rotor height. When on the deck the rotor is approximately 5 m above the helideck. Consequently data measured at the 5 m height are not particularly relevant to an assessment of impact on helicopter performance and so these results are presented in Appendix A for completeness only. Data measured at 10 m, 15 m and 20 m above the deck have much more effect on helicopter performance and handling during the landing or takeoff manoeuvre, and more weight has therefore been given to these results.

The measured data were scaled to a free-stream mean wind speed at helideck height of 25 m/s. The scaled results are plotted in Figure 61 to Figure 72.

The highest vertical mean wind speeds, which form the current basis for helideck design assessment and mitigation, invariably occur for unobstructed or 'open' wind directions, and so the results presented here are for these unobstructed wind directions in the sector 150° to 330°. [5]

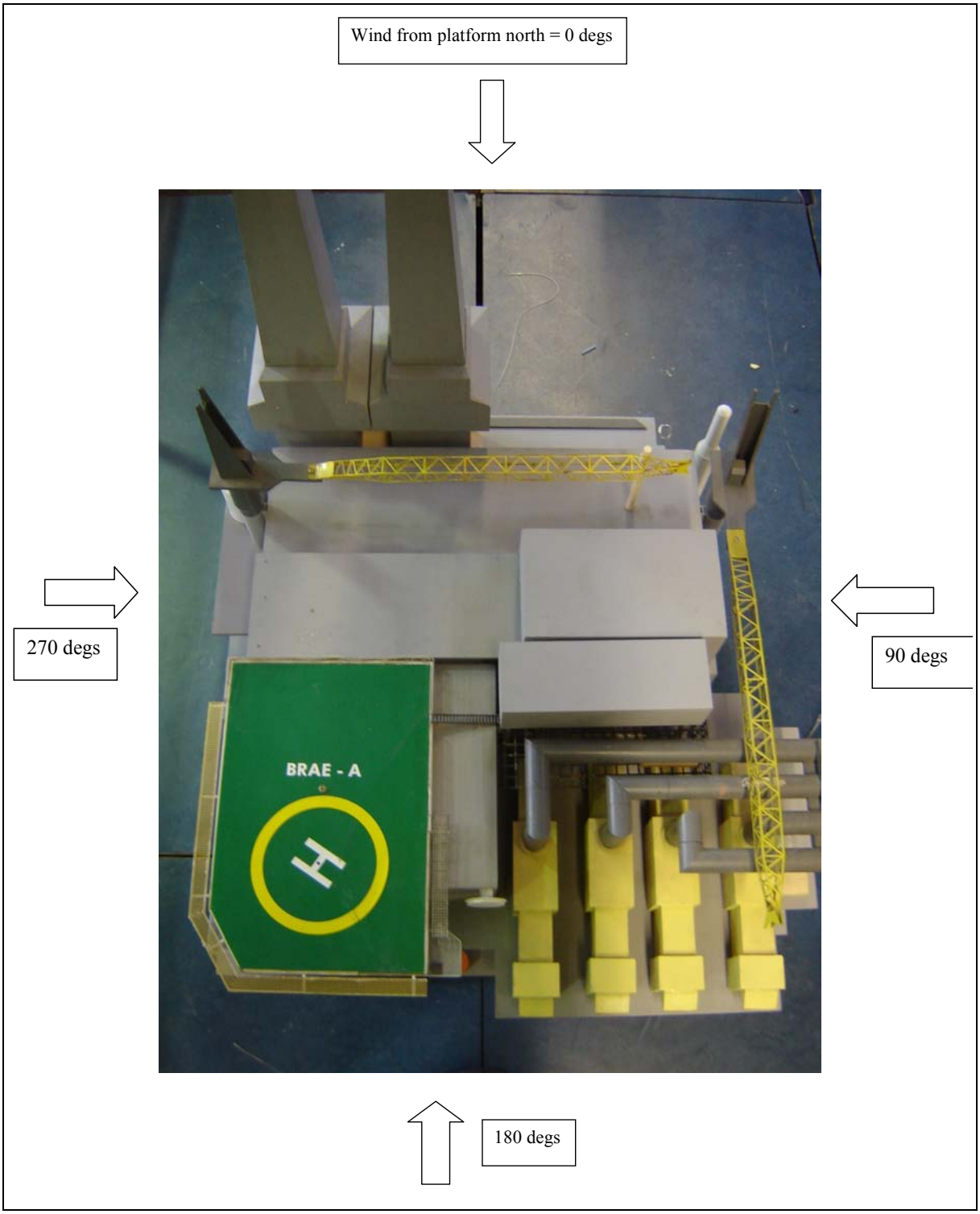

Figure 60 Definition of platform north

5. The results from the wind directions from 330° - 150° are omitted because they do not include large vertical mean flow components, and are also very much influenced by distortions and turbulence specific to Brae-A.

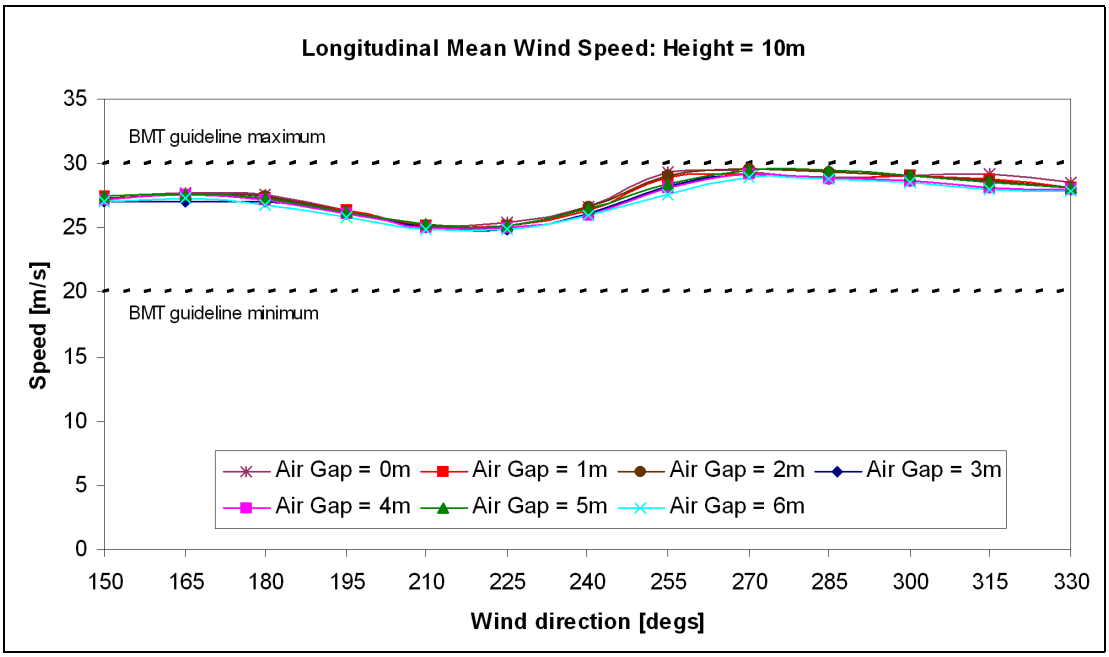

Figure 61 Variation of longitudinal mean wind speed with wind direction in the unobstructed sector at 10 m above the landing spot

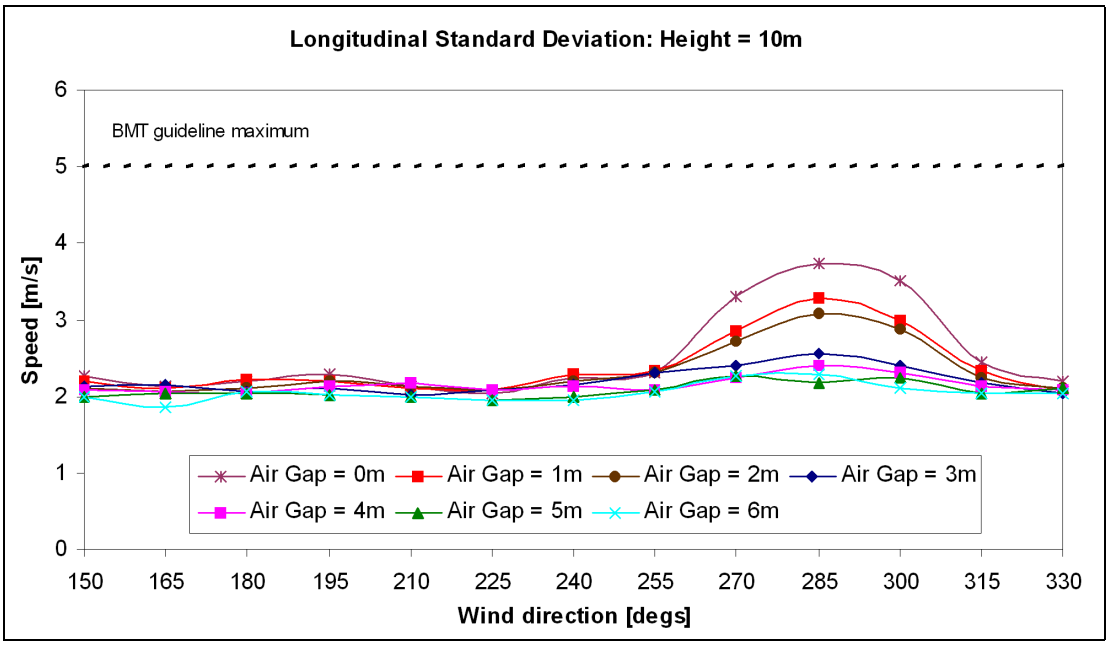

Figure 62 Variation of longitudinal turbulence standard deviation with wind direction in the unobstructed sector at 10 m above the landing spot

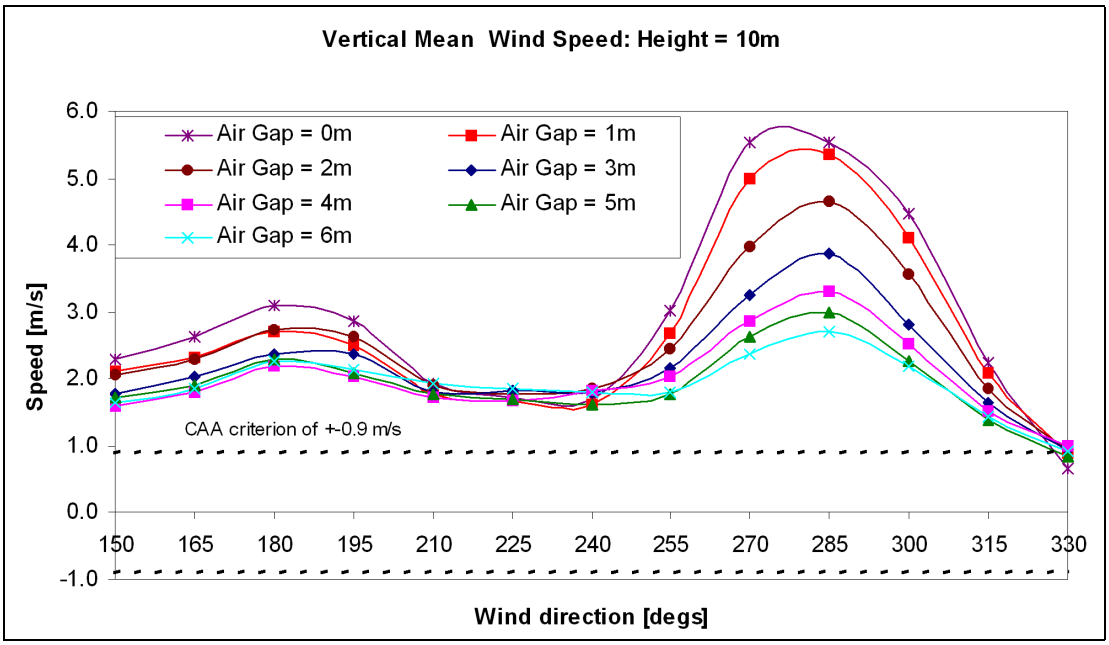

Figure 63 Variation of vertical mean wind speed with wind direction in the unobstructed sector at 10 m above the landing spot

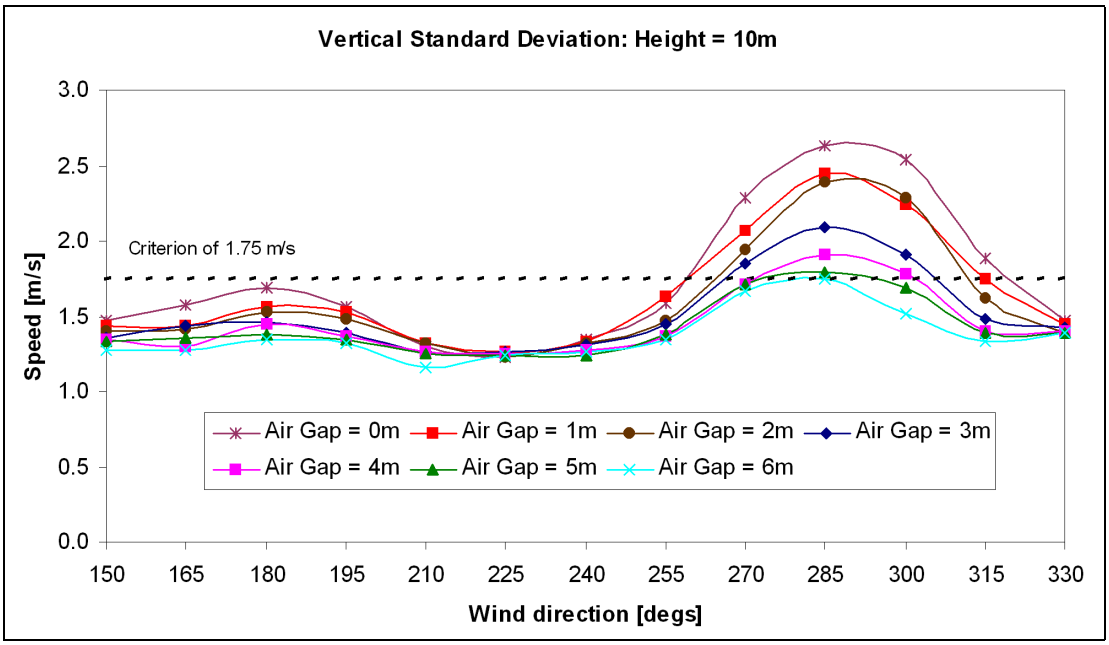

Figure 64 Variation of vertical turbulence standard deviation with wind direction in the unobstructed sector at 10 m above the landing spot

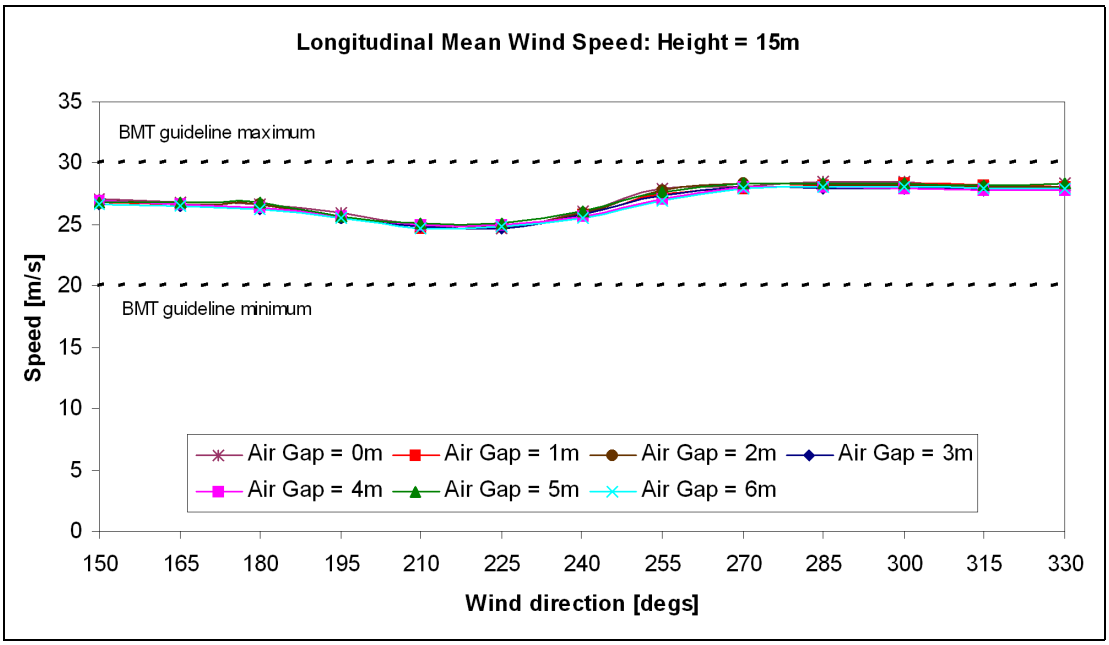

Figure 65 Variation of longitudinal mean wind speed with wind direction in the unobstructed sector at 15 m above the landing spot

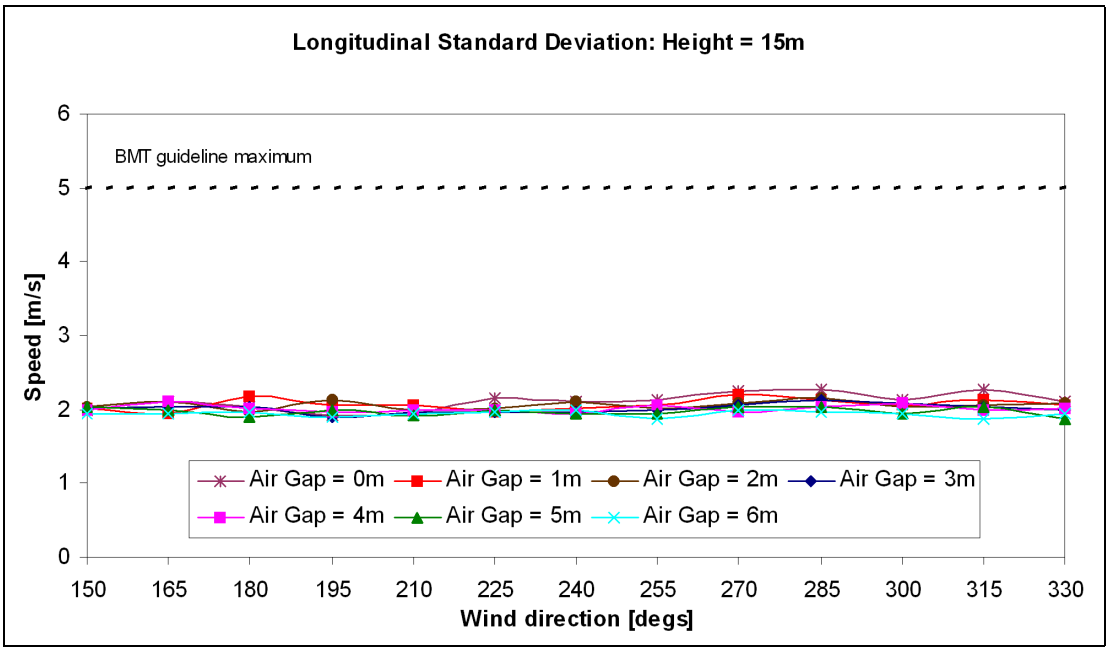

Figure 66 Variation of longitudinal turbulence standard deviation with wind direction in the unobstructed sector at 15 m above the landing spot

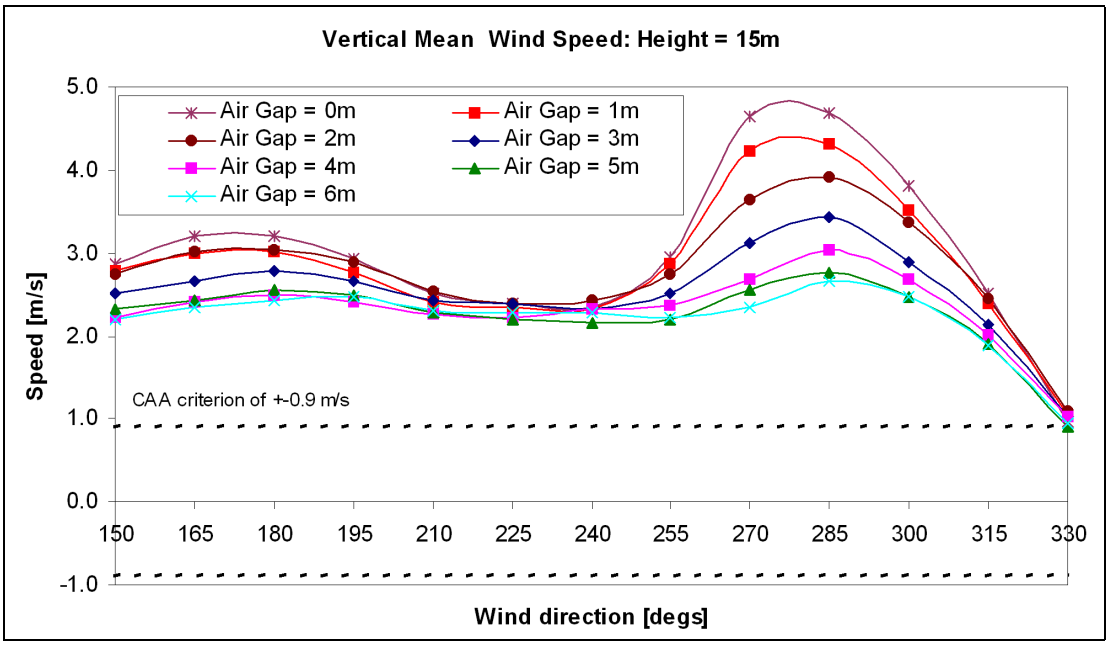

Figure 67 Variation of vertical mean wind speed with wind direction in the unobstructed sector at 15 m above the landing spot

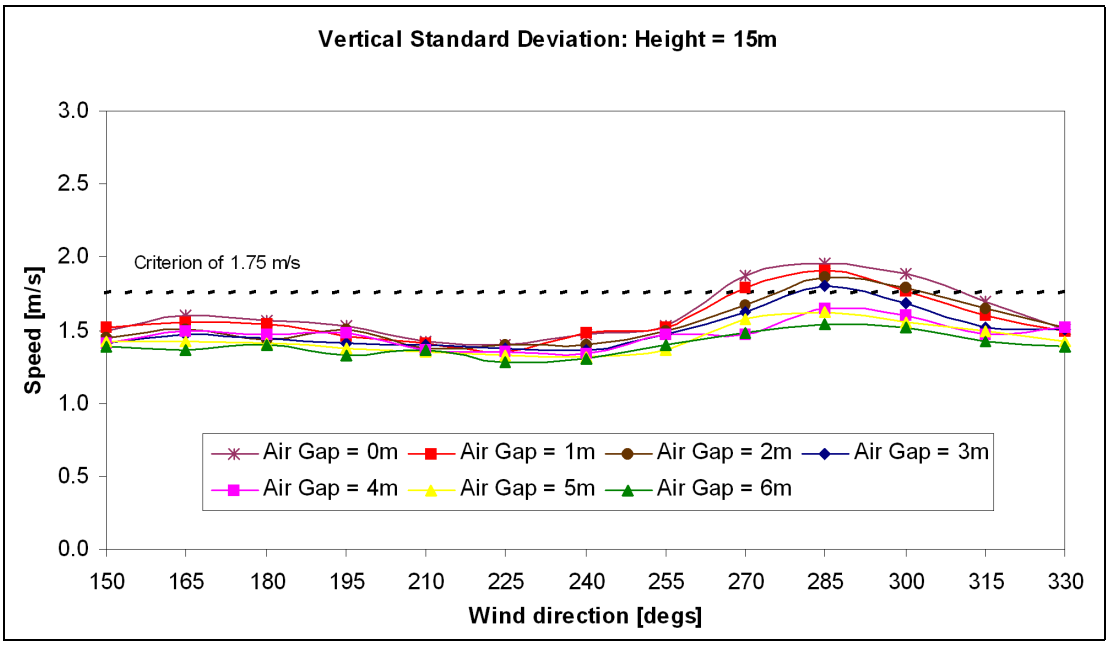

Figure 68 Variation of vertical turbulence standard deviation with wind direction in the unobstructed sector at 15 m above the landing spot

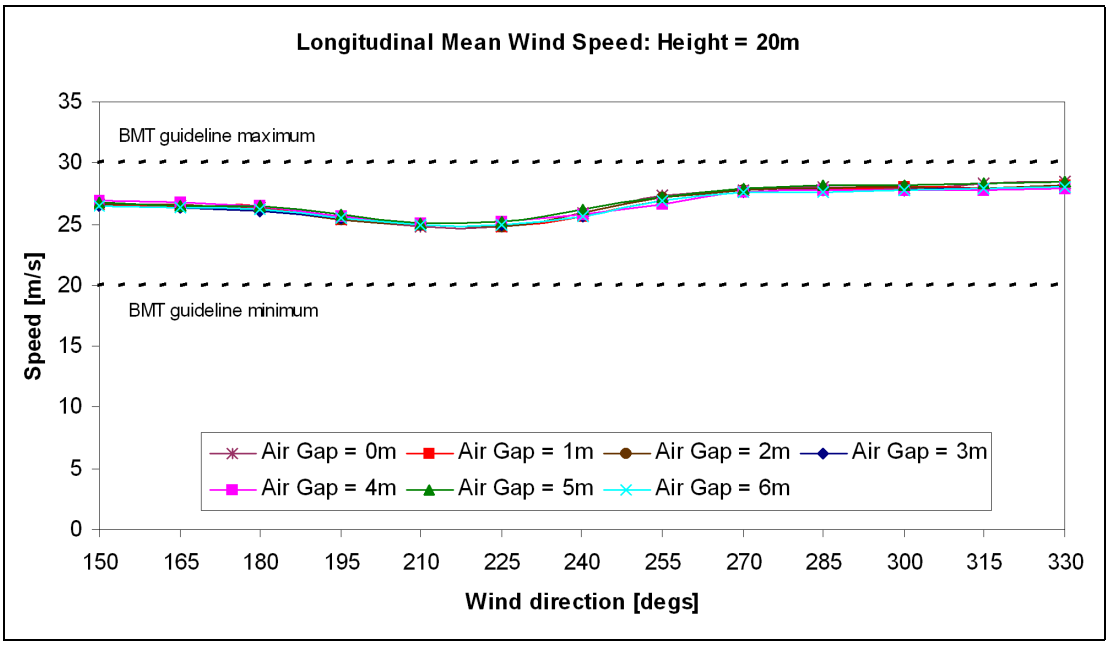

Figure 69 Variation of longitudinal mean wind speed with wind direction in the unobstructed sector at 20 m above the landing spot

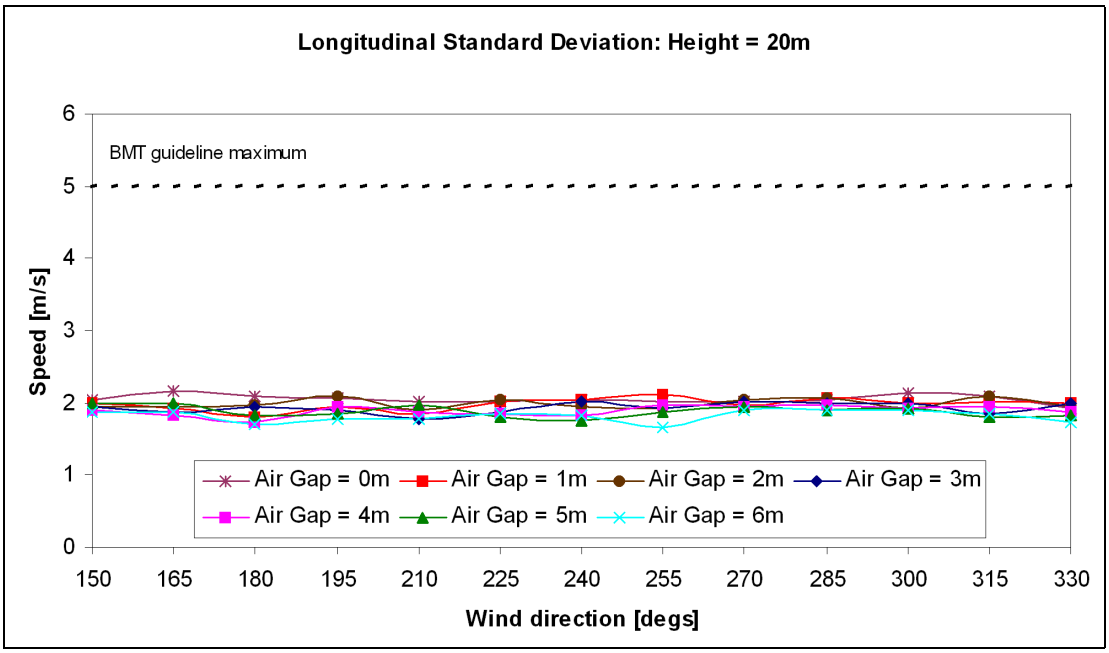

Figure 70 Variation of longitudinal turbulence standard deviation with wind direction in the unobstructed sector at 20 m above the landing spot

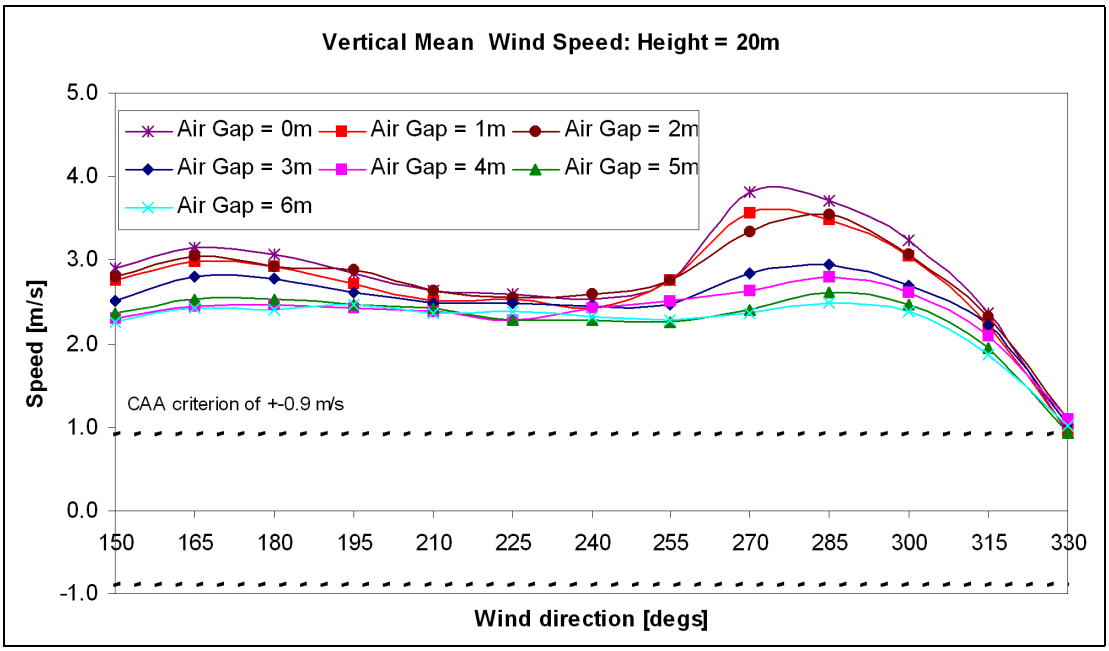

Figure 71 Variation of vertical mean wind speed with wind direction in the unobstructed sector at 20 m above the landing spot

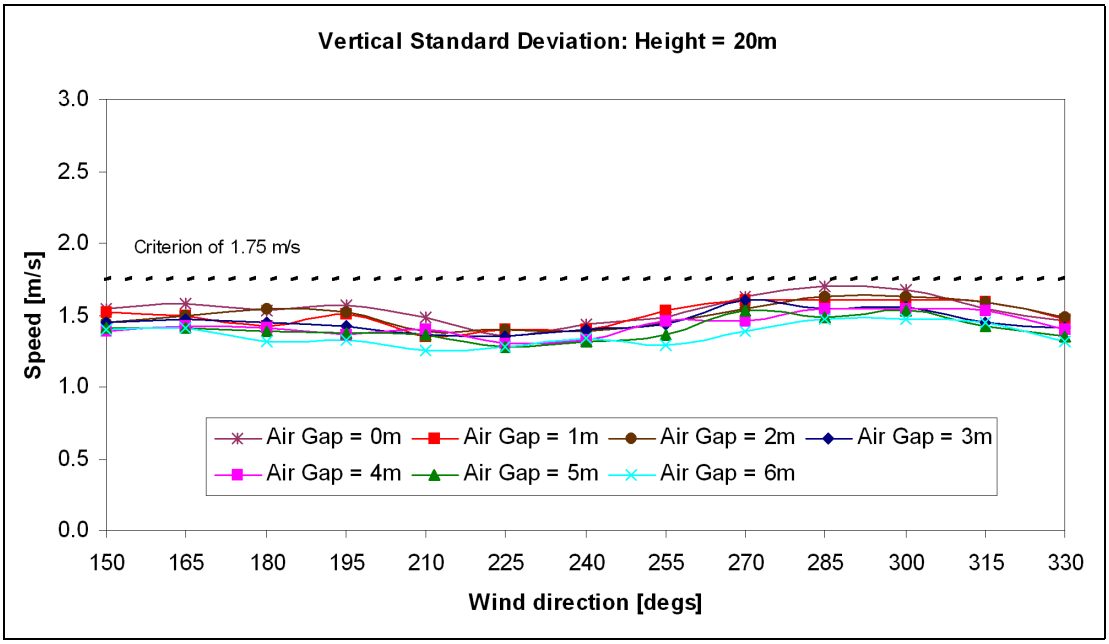

Figure 72 Variation of vertical turbulence standard deviation with wind direction in the unobstructed sector at 20 m above the landing spot

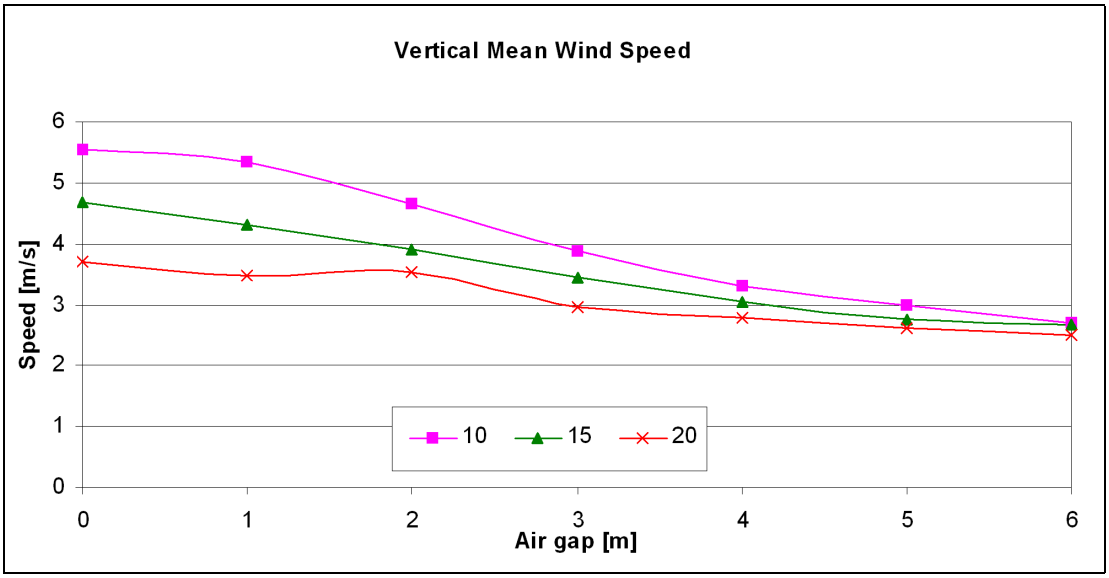

Figure 73 Variation of vertical mean wind speed with air gap for heights above the landing spot of 10 m, 15 m and 20 m for a wind direction of 285°

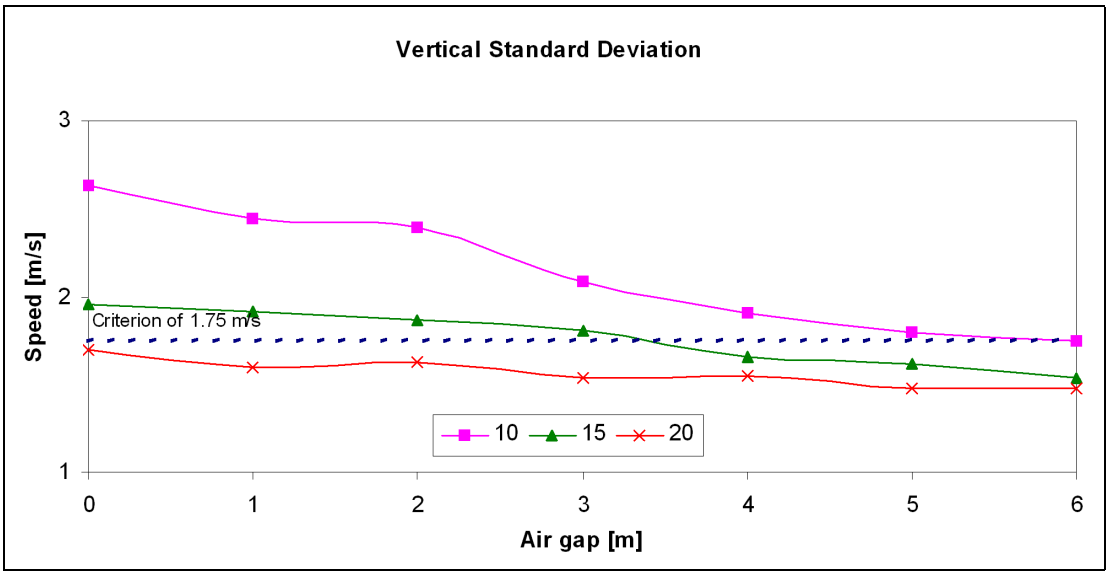

Figure 74 Variation of vertical turbulence standard deviation with air gap for heights above the landing spot of 10 m, 15 m and 20 m for a wind direction of 285°

6.4 Discussion of results

All of the results demonstrate that increasing the helideck air gap improves the flow parameters for all wind directions in the 'open' sector. The wind direction for which the air gap is seen to influence the flow the most is centred on 285°.

Figure 63 shows that the peak vertical mean wind speed at 10 m above the landing spot for the 'open' direction of 285° decreases by over 50% as the air gap is increased. The impact is also highlighted in Figure 73 which shows that, for this particular direction, most of the decrease in vertical mean wind speed is obtained with an air gap of 3 m to 4 m and that further increase of the air gap produces only marginal

improvements. Based on these results an air gap of around 3 m - 4 m would be recommended to the designer.

The effect of the air gap on the vertical turbulence is very similar with peak values of the standard deviation decreasing as air gap is increased. The impact is summarised in Figure 74, which shows that at heights above the helideck of 15 m and 20 m, the sensitivity to air gap is relatively weak but compliance with the 1.75 m/s criterion is achieved for an air gap greater than 3 m. At a height of 10 m above the helideck, the sensitivity to air gap is stronger, and compliance with the 1.75 m/s criterion is not achieved until the air gap is increased to between 5 and 6 m.

The discussion above has mainly been focused on the variation in flow properties with height above the helideck, and the results in the figures have been presented in this way. However, it is also interesting to examine the variation of the flow parameters with absolute height above the roof of the accommodation module, ignoring the actual height of the helideck.

In Figure 75 all of the results for longitudinal mean wind speed for a wind direction of 285° are plotted as vertical profiles relative to the roof of the accommodation module. Figure 76 to Figure 78 present similar results for longitudinal standard deviation, vertical mean wind speed and vertical turbulence standard deviation respectively.

The data in Figure 75, Figure 76 and Figure 78 are seen to fall on unique single lines, which suggests that these parameters are functions of height above the accommodation block irrespective of the proximity of the helideck. In other words, it is the general blockage and distortion of the flow field around bulk of the platform, and particularly the accommodation block, that is influencing the longitudinal mean wind speed and turbulence. As the measurement height above the accommodation block is increased, then the longitudinal mean wind speed and turbulence all approach their free stream conditions. The proximity or otherwise of the helideck has apparently little effect on these parameters.

In contrast, the results for the vertical mean wind speed in Figure 77 show much more scatter and distinct differences depending on the air gap, and thus the proximity of the helideck to the measurement point. For example, at a height above the accommodation roof of 10 m, the vertical mean wind speed varies from 5.5 m/s for 0 m air gap to 1.2 m/s for a 5 m air gap. The results indicate that the vertical mean wind speed is sensitive to the proximity of the helideck and the air gap. This seems intuitively correct, because the horizontal plane represented by the helideck presents an obstruction to vertical flow, and this obstruction will inevitably attenuate the vertical mean component the closer the measurement point is to the helideck surface.

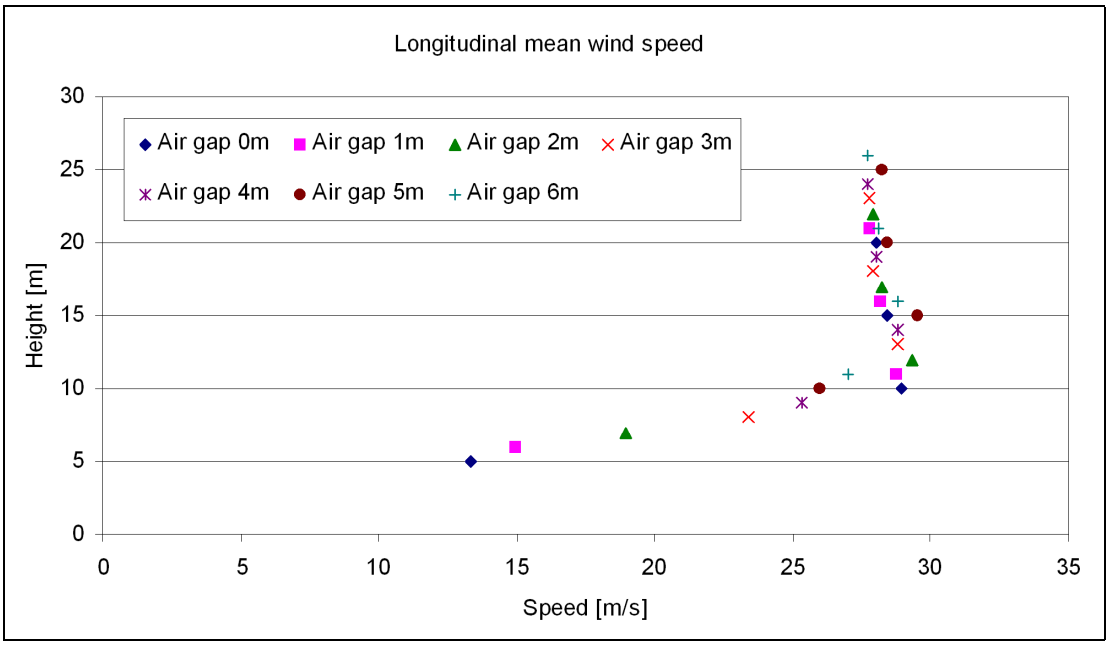

Figure 75 Variation of longitudinal mean wind speed with height above the roof deck for air gaps of 0 m to 6 m and a wind direction of 285°

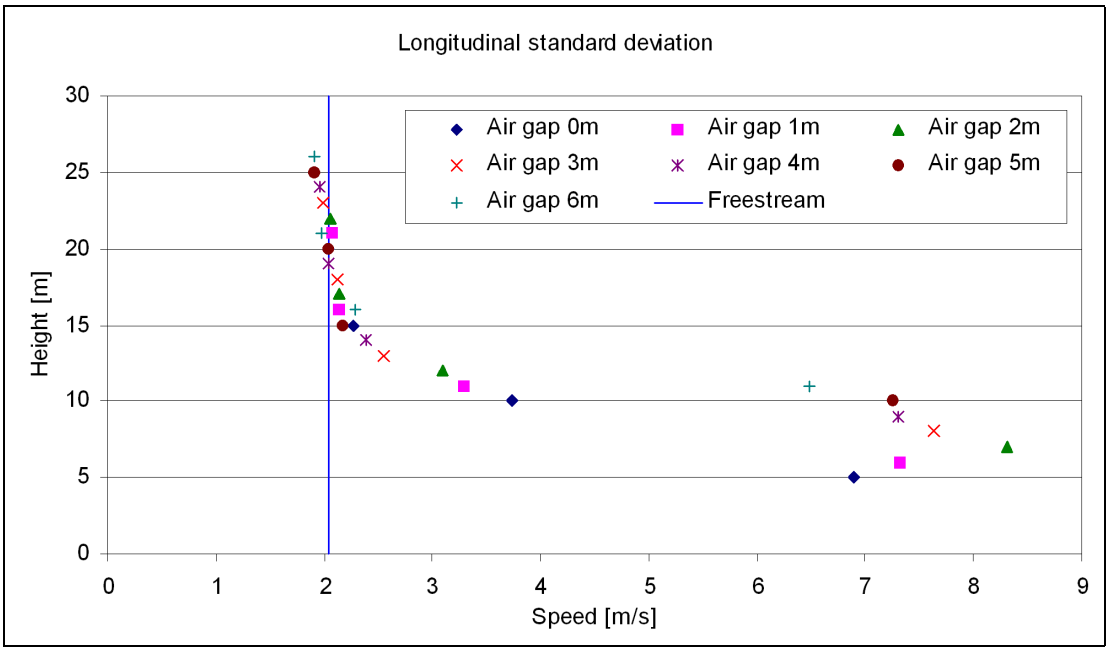

Figure 76 Variation of longitudinal turbulence standard deviation with height above the roof deck for air gaps of 0 m to 6 m and a wind direction of 285°

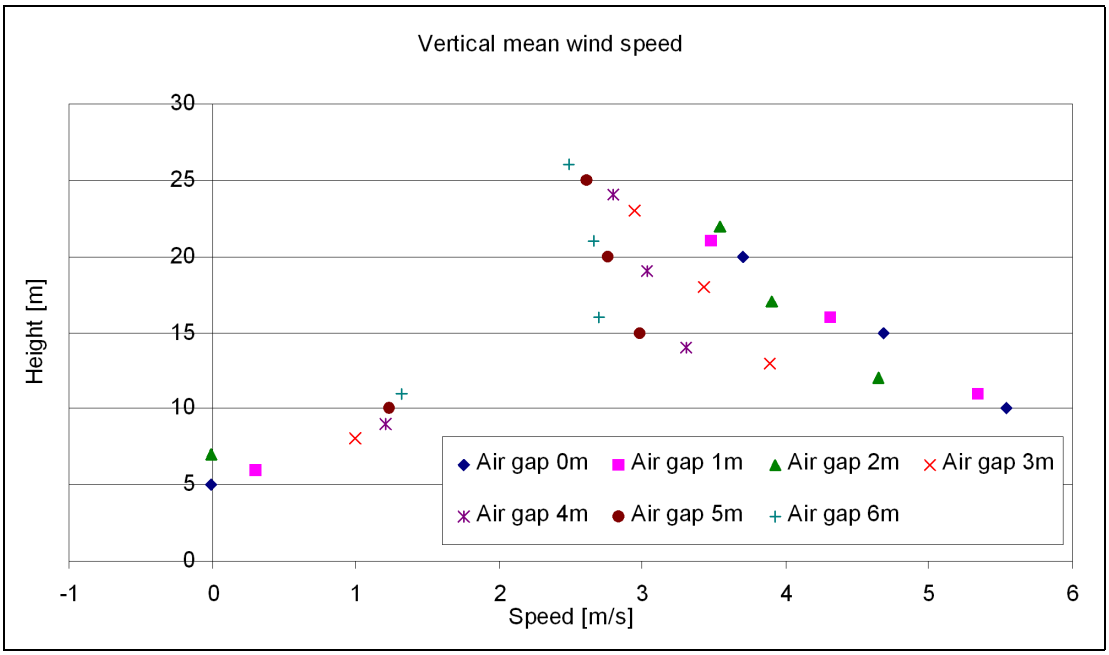

Figure 77 Variation of vertical mean wind speed with height above the roof deck for air gaps of 0 m to 6 m and a wind direction of 285°

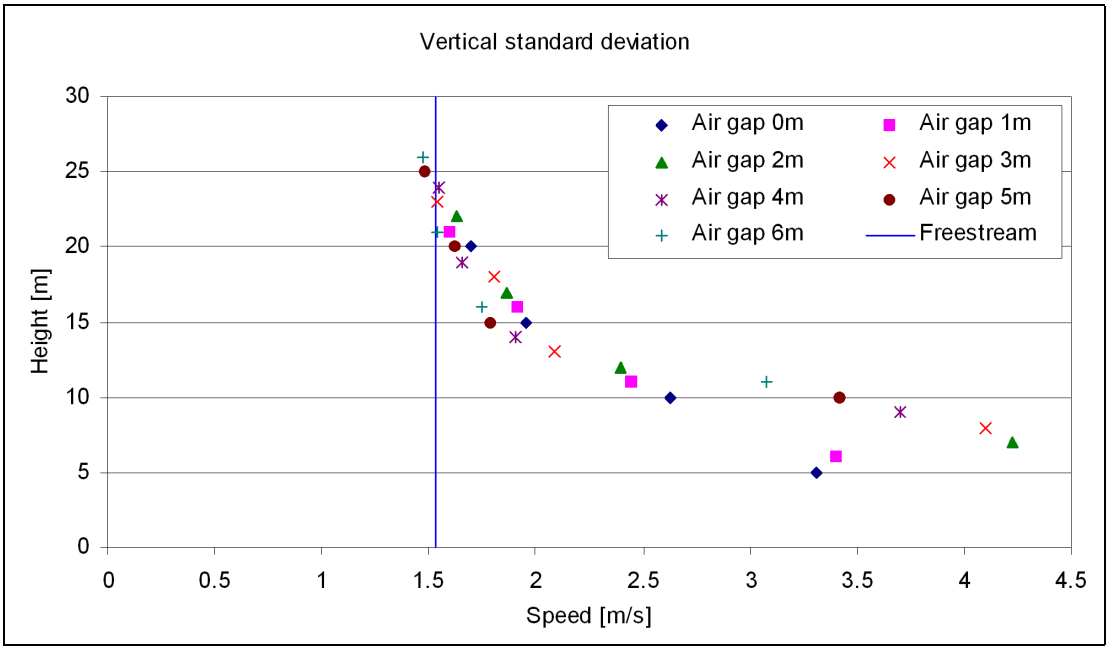

Figure 78 Variation of vertical turbulence standard deviation with height above the roof deck for air gaps of 0 m to 6 m and a wind direction of 285°

It is apparent that one can generally regard the raising of the helideck as simply a means to move the helicopter further away from the turbulent and distorted flow field in close proximity to the accommodation block. In most respects the helideck itself is not influencing the flow field significantly. The exception to this is the vertical mean wind speed, which is clearly attenuated close to the horizontal planar surface of the helideck.

The work described in this section has concerned only one example North Sea production platform, but the key conclusion is that the application of the turbulence criterion to the flow field above the helideck for 'open' wind directions is likely to cause designers to introduce a reasonable air gap under the helideck.

7 Conclusions

The four phases of the study of the 0.9 m/s vertical flow criterion have generated the following conclusions:

7.1 In Phase-1 the HOMP data archive was examined for evidence of high torque events associated with high wind speeds and 'open' wind sectors, which might be indicative of a helicopter performance hazard associated with the vertical component of wind speed. From the results of this phase it is concluded that:

7.1.1 No evidence of high torque events or large torque increase events (over 2 seconds) associated with higher wind speeds and 'open' wind directional sectors was found. (Section 3.4)

7.1.2 Plots of all valid torque data for all 44 platforms for which sketches were available show that torque values are generally higher for lower wind speeds and for winds from sectors that would be expected to feature turbulence caused by the upwind structure of the platform. (Section 3.4)

7.2 In Phase-2 the BMT wind tunnel data archive was analysed to map the occurrence of violations of the 0.9 m/s criterion against wind directions, and thus establish whether the violations could be associated with particular platform features and, in particular, confirm whether violations mainly occur in unobstructed or 'open' wind directions. From the results of Phase-2 it is concluded that:

7.2.1 For large single platforms overall velocity reductions in the wake of obstructions mean that violations of the 0.9 m/s criterion are most likely to occur in winds from the open sectors. In fact, for the 15 medium and large platforms analysed from the BMT database, only five violated the 0.9 m/s criterion in winds from obstructed or 'turbulent' directions. (Section 4.2), and for all 15 the vertical mean wind speed was greatest for winds from the open sectors.

7.2.2 For smaller platforms and multiple platform configurations, where there are less severe wake effects, violations of the 0.9 m/s criterion can occur in winds from all sectors, but are likely to be accompanied by high horizontal wind components with consequent helicopter performance benefits. (Section 4.2)

7.3 In Phase-3 HOMP data on pilot workload and torque were compared with wind tunnel data on 0.9 m/s criterion violations for 'open' wind directions. This was possible for 5 platforms that appeared in both the BMT wind tunnel database and the 16-month HOMP data archive. From this it has been concluded that:

7.3.1 There is no evidence of high torque or torque increase values being associated with high vertical flow components. (Section 5.2)

7.3.2 Similarly, there is no evidence of high pilot workload being associated with high vertical flow components. (Section 5.2)

7.4 Overall it is concluded that violation of the 0.9 m/s vertical mean flow criterion cannot be linked to any helicopter performance (i.e. torque-related), or handling (i.e. pilot workload-related) hazard.

7.5 The highest vertical components of flow almost always occur when the wind is from an 'open' direction for medium and large platforms, or from the obstructed direction on small platforms generating little wake. These are conditions when the horizontal component of flow is likely to be high ensuring that the helicopter has a high margin of lift, and when turbulence levels and associated pilot workload values are likely to be low.

7.6 In Phase 4 of the project a programme of wind tunnel tests was performed to examine the impact of helideck height on 'open' sector wind flow properties over a wider range of heights. A model of a single representative large North Sea platform (Brae-A) was used, and the results interpreted in terms of the helideck height that would have been selected for design if individual given flow criteria were the key determinate. It was concluded that:

7.6.1 Increasing the air gap from 0 m to 6 m systematically reduces the vertical mean wind speed and the turbulence standard deviation. (Section 6.4)

7.6.2 Based on the vertical mean wind speeds at a height of 15 m above the helideck for unobstructed wind directions, an air gap of 3 m to 4 m would be recommended for Brae-A.[6] The results showed that further increase in helideck height provided little additional improvement. (Section 6.4)

7.6.3 A turbulence criterion of 1.75 m/s would result in an air gap of 5 to 6 m being recommended. (Section 6.4)

8 Recommendations

As the criterion cannot be linked to a helicopter performance or handling hazard, it is recommended that consideration be given to removing the 0.9 m/s criterion from the guidance material [1].

It is recommended that the first step should be consultation with the helicopter operators in order to seek their views on the validity or otherwise of the criterion from an operational perspective, and to check whether there may be safety benefits implicit in the criterion that have not been evident during the study.

6. The as-built design has a 3 m air gap.

9 References

[1] *Offshore Helicopter Landing Areas - Guidance on Standards*, CAP 437, Fifth edition published by the CAA, London, August 2005.[7]

[2] *Research on Offshore Helideck Environmental Issues*, CAA Paper 99004, August 2000.

[3] *Review of 0.9 m/s Vertical Wind Component Criterion for Helicopters*, BMT Fluid Mechanics Proposal No. Q/84266q2, 26th January 2005.

[4] *Vertical Wind Component Criterion for Helicopters - Review of Wind Tunnel Data*, BMT Fluid Mechanics Proposal No. Q/84375q2, 18th May 2006.

[5] *Validation of the Helicopter Turbulence Criterion for Operations to Offshore Platforms*, CAA Paper 2008/02 Part 1.

[6] *Final Report on the Helicopter Operations Monitoring Programme (HOMP) trial*, CAA Paper 2002/02, 2002.

[7] *Final Report on the Follow-on Activities to the HOMP Trial*, CAA Paper 2004/12, October 2004

[8] *Helicopter Turbulence Criteria for Operations to Offshore Platforms*, CAA Paper 2004/03.

[9] D Howson email dated 17th March 2005.

[10] BMT Fluid Mechanics Document *homp_full_plots_named_v2.doc*, 21st November 2005.

[11] *Helideck Limitations List (HLL)*, The Helideck Certification Agency, http://www.helidecks.org/.

7. Now at 6th edition.

Appendix A Wind Tunnel Results for Brae-A at 5 m Above the Helideck

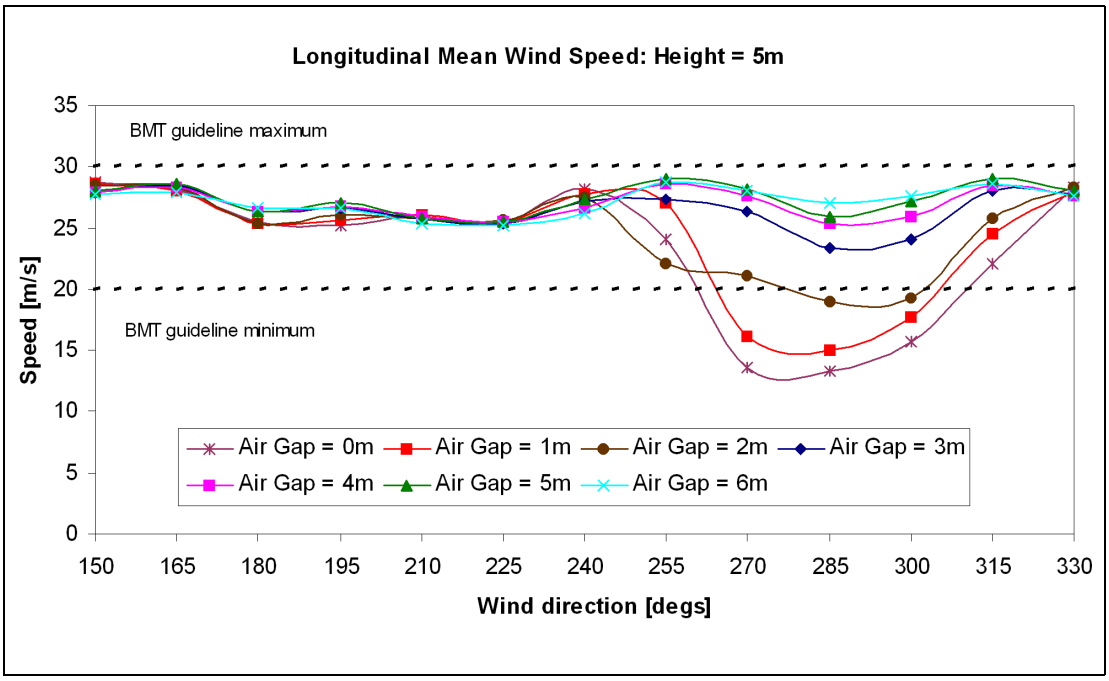

Figure 79 Variation of longitudinal mean wind speed with wind direction in the unobstructed sector at 5 m above the landing spot for a free wind speed of 25 m/s

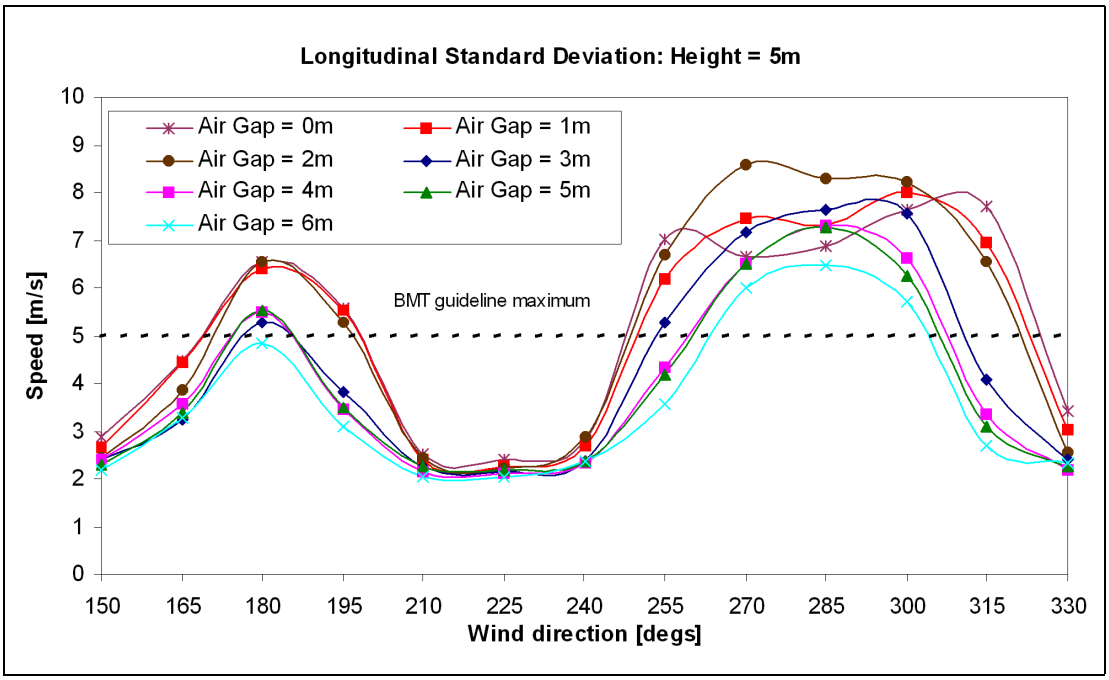

Figure 80 Variation of longitudinal turbulence standard deviation with wind direction in the unobstructed sector at 5 m above the landing spot for a free wind speed of 25 m/s

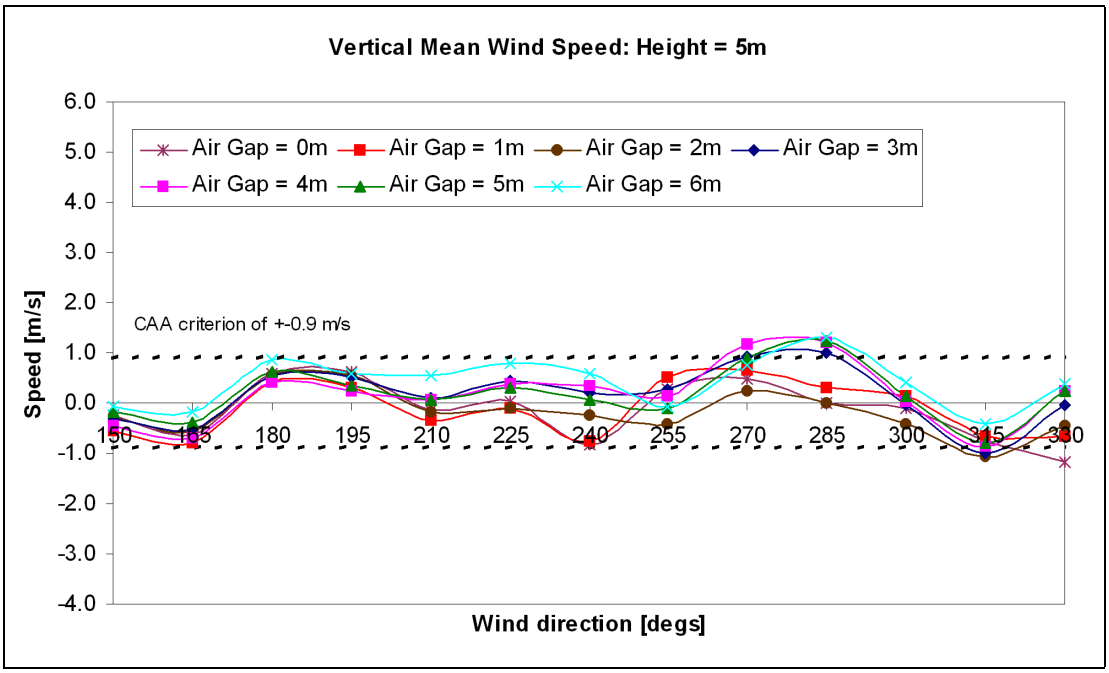

Figure 81 Variation of vertical mean wind speed with wind direction in the unobstructed sector at 5 m above the landing spot for a free wind speed of 25 m/s

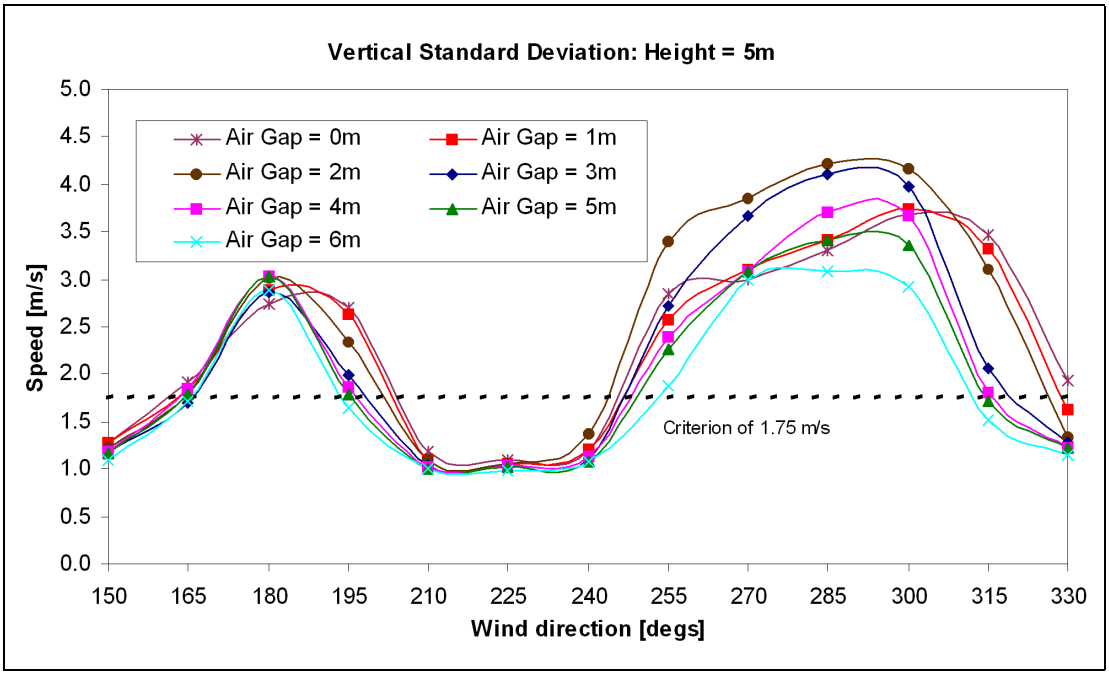

Figure 82 Variation of vertical turbulence standard deviation with wind direction in the unobstructed sector at 5 m above the landing spot for a free wind speed of 25 m/s